eman ta zabal zazu

Universidad del País Vasco

Euskal Herriko Unibertsitatea

FACULTY OF ENGINEERING BILBAO

UNIVERSITY OF THE BASQUE COUNTRY

PROGRESS IN INDUSTRIAL PHOTOGRAMMETRY BY MEANS OF MARKERLESS SOLUTIONS

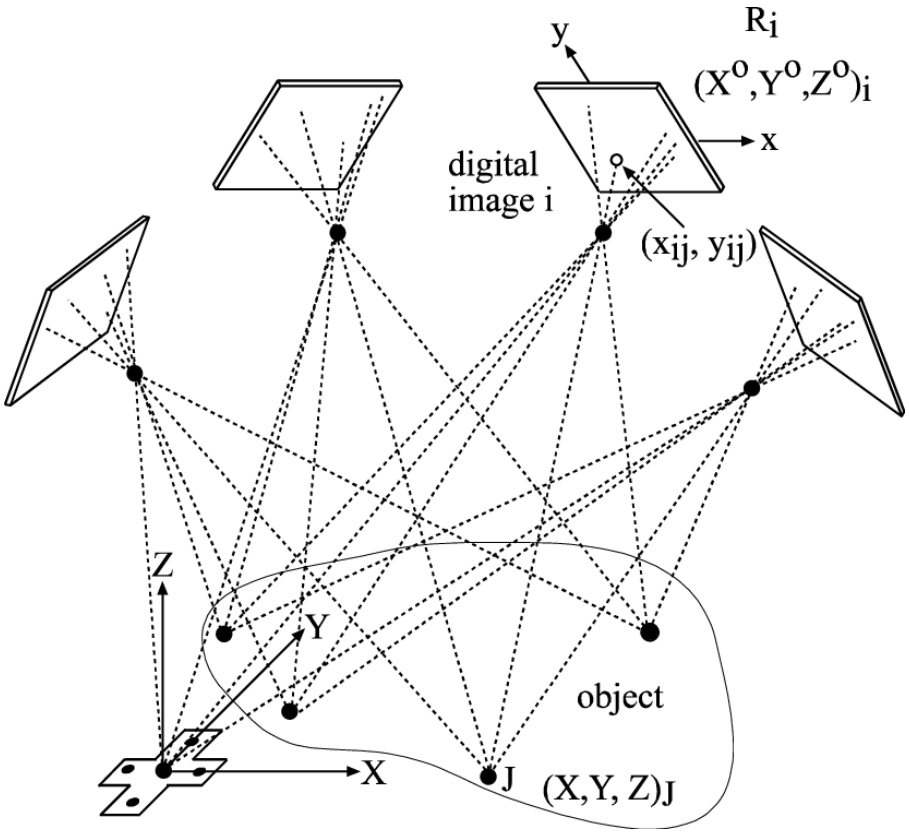

GORKA KORTABERRIA BERRIOZABAL

October 2019

En agradecimiento a tod@s que habeis participado y contribuido en esta tesis y en especial a mi familia que me ha apoyado y animado hasta el final. Muchas gracias por estar a mi lado.

CONTENT

LIST OF FIGURES

LIST OF ABBREVIATIONS

Automatic Guided Vehicle
AGV, 40
Bundle adjustment
BA, 49
Close-range photogrammetry
CRP, 5
Computer numeric control
CNC, 6
Computer-aided design
CAD, 6
Coordinate measuring machines
CMM, 17
Coordinate Measuring Robot
CMR, 29
Coordinate systems
CS, 50
Cross-correlation
CC, 68
Cyber-physical
CP, 3
Degrees of freedom
dof, 18
Depth of field
DOF, 62
Digital image correlation
DIC, 17
Digital Volume Correlation
DVC, 22
Dimensioning and tolerancing
GD&T, 4
Direct linear transformation
DLT, 56
Epipolar geometry
EG, 76
Essential matrix
EM, 75
Feature-based matching
FBM, 32
Finite element method
FEM, 6
First article inspection
FAI, 38
Fundamental matrix
FM, 75
Graphic processing unit
GPU, 23
Indoor Global Positioning system
IGPS, 5
Internet of things
IOT, 3
Kanade-Lucas-Tomasi
KLT, 72
Laser metal deposition
LMD, 39
Laser-tracker
LT, 17
Least Median of Square regression algorithm
Lmeds, 76
Least-square matching
LSM, 73
Maximum permissible error
MPE, 19
Metrology/Measurement Assisted Assembly
MMA, 35
Normalized cross correlation
NCC, 73
Iterative closest point
ICP, 89
Personal computers
PC, 23
Portable measuring coordinate machines
PCMM, 4
Random Sample Consensus
RANSAC, 76
Region of interest
ROI, 68
Scale-invariant feature transform
SIFT, 33
Scanning electron microscope

KEYWORDS

Structure from motion, bundle adjustment, markerless photogrammetry, dense matching, geometric fitting, camera calibration, extrinsic orientation, image processing, feature detectors, space resection, relative orientation, absolute orientation, collinearity equations, optical distortion.

ACKNOWLEDGMENTS

I would like to thank the possibility of having carried out this thesis to all the people who have supported me during these 3 years and who have encouraged me every day to follow up and be able to reach its final delivery and defense. I have felt really wrapped up both technically and emotionally during the different phases of it, which has led me to the materialization and achievement of this study. Thank you …

To TEKNIKER for giving me the opportunity to go on this thesis aligned with the technical activity of the work, for the resources provided and for having taught me what the job is, to have trained myself so much personally, to be a part of my professional growth as well as to show me the methods to carry out this type of studies.

To my TEKNIKER colleagues for helping me technically in the execution of experiments, in the publication of results, as well as in multiple administrative procedures linked to a thesis based on their previous experience. Thanks, Aitor, Unai, Eneko, Jorge, Alberto and others for your teamwork.

To my co-director Alberto Tellaeche, who on the same experience has advised me on the different aspects to follow during the thesis, as well as in achieving accurate results and has given me strength at demotivated moments where it is easy to throw in the towel.

To the University of the Basque Country for being interested in the subject of the thesis, open the doors for their development as well as guiding me throughout the process and present me the guidelines on how to properly monitor the different phases of the thesis.

To my director Rikardo Minguez and the Product Design Laboratory of the University of the Basque Country (UPV/EHU) to follow up, technically support and determine the main line of the thesis. Thanks for the constant support and the continuous words of encouragement that has helped me a lot. It has been a pleasure to share with you this research and you have facilitated me a lot the achieving of established goals.

To my lifelong friends for enduring me again and again after long periods of study, for their understanding, for their words of support in that task, as well as the interest shown in this project.

To my partner, Lucia that after having gone through the same process has understood me perfectly and has helped me to free up time, has given me strength and has helped me to focus the execution of the thesis and take care of the important details that make the difference. Thank you for your understanding and for standing my lower motivation moments.

To my son Markel for being the best thing I have done in this life and for transmitting me his happiness that has given to me strength for this task and other multiple activities. Although he requires a lot of time to take care of him, he gives me back this energy multiplied by many times.

To my family and especially to my parents for giving me an education and affection that allowed me to have the ability to carry out this work and grow both professionally and personally. Thank you for your perseverance and your know-how when I was still a kid and I did not have the criteria to know what I wanted to be at a professional level. For sure, you guided me through the right way.

To my father, who is no longer with us, but I hope that wherever he is, he is proud of me and of my personal and work career. We miss you aita. This thesis is partly also yours.

And last but not least to my family in law who has encouraged me to face this thesis and has looked after my family for long periods during my study.

Thank you very much to all and to each one of those who have collaborated in the different works and phases of the development of the thesis, for being part of it and its results and giving me the necessary strength for its development and achievement. I really have appreciated your collaboration and I hope that in the coming future we will continue in the same line with other research activities of the same nature.

RESUMEN DE LA TESIS

La siguiente **tesis** está enfocada al **desarrollo y uso avanzado de metodologías fotogramétrica sin dianas** en **aplicaciones industriales**. La fotogrametría es una técnica de medición óptica 3D que engloba múltiples configuraciones y aproximaciones. En este estudio se han **desarrollado procedimientos de medición, modelos y estrategias de procesamiento de imagen** que van más allá que la fotogrametría convencional y buscan el emplear soluciones de otros campos de la visión artificial en aplicaciones industriales. Mientras que la fotogrametría industrial requiere emplear dianas artificiales para definir los puntos o elementos de interés, esta **tesis** contempla la **reducción e incluso la eliminación de las dianas tanto pasivas como activas** como alternativas prácticas. La mayoría de los sistemas de medida utilizan las dianas tanto para definir los puntos de control, relacionar las distintas perspectivas, obtener precisión, así como para automatizar las medidas. Aunque en muchas situaciones el empleo de dianas no sea restrictivo existen aplicaciones donde su empleo condiciona y restringe considerablemente los procedimientos de medida empleados en la inspección. Un claro ejemplo es la verificación y control de calidad de piezas seriadas, o la medición y seguimiento de elementos prismáticos relacionados con un sistema de referencia determinado. Es en este punto donde la fotogrametría sin dianas puede combinarse o complementarse con soluciones tradicionales para tratar de mejorar las prestaciones actuales.

Por ejemplo, cuando se lleva a cabo la inspección o control de calidad de piezas mecanizadas que presentan una estructura repetitiva de primitivas geométricas. En estas piezas se requiere medir el posicionamiento 3D de múltiples elementos geométricos tales como agujeros y para ello es necesario colocar en cada agujero una diana con su correspondiente soporte. Estos soportes permiten autocentrar las dianas con los agujeros a caracterizar. Este requisito repercute no solo en el tiempo de preparación de la escena, sino en el coste de la solución ya que es necesario disponer de tantos adaptadores como numero de agujeros. Además del coste de adquisición, estos soportes requieren una calibración previa y en función del tamaño de la pieza su colocación es costosa debido una accesibilidad limitada.

Otra aplicación industrial donde el uso de dianas es limitante consiste en la medición de la pose de piezas con formas complejas o redondeadas. Cuando es necesario medir una pieza de esta índole, el empleo de dianas repercute directamente en el procedimiento de medida. Debido al cambio entre perspectivas o incluso problemas de oclusiones entre perspectivas consecutivas, es necesario colocar un gran número de dianas distribuidas sobre la superficie de la pieza. Sin embargo, incluso con esta distribución de dianas la precisión de medida se reduce debido al ángulo de triangulación entre imágenes. Además, existen casuísticas donde el mesurando no permite colocar dianas sobre su superficie debido a la tipología de la aplicación.

Otro caso habitual en la inspección 3D de piezas consiste en emplear dianas para poder relacionar y fusionar los escaneos parciales de la pieza que son necesarios para digitalizar toda la superficie de la misma. Al proceso de transformar cada medida parcial a un sistema de coordenadas común se le llama registro y se lleva a cabo en base a medir la posición 3D de al menos 3 dianas homologas entre medidas consecutivas. Este requerimiento limita considerablemente la metodología de medida y además restringe la flexibilidad del procedimiento a emplear. Por ello y con el objeto de mejorar la precisión, los sistemas de escaneado 3D se combinan con sistemas fotogramétricos más precisos que miden una red de puntos de referencia. Estos puntos sirven como referencia en cada escaneado parcial ofreciendo mayor flexibilidad y libertad a la metodología. Sin embargo, el empleo de dianas es nuevamente necesario y dificulta el procedimiento de medida además de prolongar la preparación del mensurando.

Por lo tanto, la motivación de la tesis surge de aplicaciones industriales tales como las descritas donde existe margen de mejora de cara a optimizar las soluciones tecnológicas empleadas. Estas emplean diferentes procedimientos y sistemas de medida para obtener un resultado dimensional, pero presentan limitaciones importantes en cuanto a la aplicación e implementación de la fotogrametría en sus diversas configuraciones. Aunque se sabe a priori que el empleo directo de puntos característicos de las imágenes repercute en la precisión de las soluciones debido a la perdida de precisión en su identificación, su uso puede mejorar tanto la rapidez como la flexibilidad de los procedimientos de medida manteniendo un alto nivel en la automatización y una

precisión acorde a la aplicación. Por lo tanto, esta tesis contempla eliminar las dianas artificiales y utilizar la información intrínseca de las imágenes para mejorar las soluciones fotogramétricas orientadas a las aplicaciones industriales citadas previamente. Para ello, se han desarrollado modelos fotogramétricos específicos y se han utilizado algoritmos de procesamiento de imagen avanzados que permitan fusionar la fotogrametría y el campo de la visión.

La investigación en cuestión se ha estructurado en 3 casos de estudio que tratan de mejorar o al menos conseguir soluciones más polivalentes para distintas problemáticas y aplicaciones industriales mencionadas previamente. Además, este estudio comprende una tesis tipo por compendio de publicaciones. Es decir, los casos de estudio analizados y los resultados obtenidos en cada caso se han publicado en revistas científicas relacionadas con la metrología, sensórica y técnicas de medición.

Para tener una mejor visión de las tecnologías existentes, así como del estado del arte de la técnica, la memoria contempla una revisión completa tanto de sistemas industriales como de los métodos empleados en la fotogrametría convencional. En este análisis también se citan las metodologías y algoritmos empleados en cada caso. Además, se ha descrito el flujo general de trabajo y se han añadido en cada paso las distintas contribuciones desarrolladas para los casos de estudio. El objetivo de dicha estructura busca simplificar la lectura de la tesis y encajar las distintas contribuciones, así como su valor añadido en la metodología general.

El contenido de la investigación se presenta y divide de la siguiente manera. El **Capítulo 1** es un resumen de la tesis que explica los diferentes capítulos, estructura y su contenido. El **Capítulo 2** introduce y enfatiza las necesidades de los procesos de fabricación industrial y cómo se solucionan en base a aplicar soluciones fotogramétricas existentes. De hecho, se añade una breve descripción de los enfoques de investigación empleados como alternativa a las metodologías existentes. Además, presenta los

objetivos de la investigación y presenta las hipótesis iniciales para abordar estos objetivos que servirán de base para el apartado de conclusiones y futuras actividades.

El **Capítulo 3** explica y describe el estado del arte de las soluciones fotogramétricas industriales revisando las soluciones y enfoques existentes en detalle. Desde soluciones offline hasta soluciones integradas en procesos de fabricación, se presenta una descripción general y una clasificación de las tecnologías y se sugieren mejoras al respecto, que son algunas de las necesidades que tratan de cubrir los desarrollos de esta tesis. Como el problema fotogramétrico engloba múltiples conceptos y principios para reconstruir la información de objetos 3D, el **Capítulo 4** introduce la descripción principal de los conceptos generales y los pasos de medición/procesamientos necesarios para reconstruir la información 3D a partir de datos de imágenes 2D. De hecho, el flujo de trabajo presentado es común para las estrategias de medición basadas tanto en dianas, así como en el sin marcadores. El objetivo de este apartado no es ofrecer una descripción detallada de cada término y método, sino una descripción general de los problemas y una breve descripción de los aspectos principales acompañados de referencias bibliográficas precisas. Después de presentar el estado del arte y los principales métodos fotogramétricos aplicados en soluciones industriales comunes, el **Capítulo 5** presenta los casos de estudio desarrollados y evaluados mediante la referencia a los artículos científicos publicados. Se describen tres casos de estudio y se ha determinado su alcance, así como su idoneidad, para potenciar las aplicaciones industriales actuales. Para cada caso de estudio, se describe a modo resumen la introducción y los principales resultados obtenidos. La descripción más detallada se encuentra en los anexos o en la web de cara a facilitar la lectura de la tesis.

El próximo **Capítulo 6** trata los resultados y conclusiones principales, ofreciendo una reflexión general de los objetivos alcanzados y previstos inicialmente. Resume la aplicabilidad real de los procedimientos de medición desarrollados y estudiados para casos de uso reales, así como las posibilidades de mejora y los desafíos a resolver en el futuro. El **Capítulo 7** presenta las referencias a los principios y métodos citados anteriormente de cara a facilitar una consulta más profunda al respecto. El objetivo de estas referencias bibliográficas es permitir la búsqueda de información adicional para entender correctamente los conceptos involucrados en cualquier solución fotogramétrica. Con respecto a los estudios de caso, cada uno de ellos ofrece sus propias referencias a casos de estudio complementarios y recientes. Finalmente, el **Capítulo 8** contempla el anexo donde se encuentra las referencias cruzadas y las citaciones de los artículos publicados, así como el contenido de cada publicación. Además, se proporcionan enlaces web interesantes que se centran en los fundamentos fotogramétricos y las capacidades de medición que ofrecen las soluciones industriales disponibles.

<u>En la siguiente lista se muestra un resumen esquemático de la estructura empleada:</u>

- Capítulo 1. Resumen de la tesis y presentación general de la tesis
- Capítulo 2. Contexto general e introducción de necesidades industriales, objetivos, motivación de la tesis y las hipótesis iniciales.
- Capítulo 3. Revisión del estado del arte de la fotogrametría industrial de campo cercano
- Capítulo 4. Resumen de métodos empleados y principales contribuciones
- Capítulo 5. Descripción de casos de estudio publicados y resultados obtenidos

- Capítulo 6. Conclusiones generales y trabajos futuros.
- Capítulo 7. Referencias bibliográficas
- Capítulo 8. Anexos

Los resultados de cada caso de estudio son prometedores y adecuados para las aplicaciones industriales presentadas. Sin embargo, es necesario demostrar con más aplicaciones prácticas la viabilidad de este campo de la fotogrametría de cara a reemplazar las soluciones fotogramétricas existentes con soluciones sin dianas. Las mejoras en términos de precisión, manejo de datos y estrategias de procesamiento de imágenes eficiencia de cómputo, velocidad en algoritmos de procesamiento de datos, estandarización de procedimientos de medición, así como en asignación de incertidumbre repercutirán de manera directa en el alcance e implementación de este tipo de aproximaciones. La simulación de procedimientos de medición, que generalmente no se ofrece como funcionalidad en los sistemas comerciales, es otra mejora sustancial que se puede utilizar para prever la idoneidad del proceso de medición para fines de inspección. Por lo tanto, a medida que las técnicas fotogramétricas continúen desarrollándose día a día, en el futuro próximo aparecerán procedimientos innovadores de procesamiento de datos y soluciones integradas nuevas e inteligentes que cubrirán las necesidades y desafíos de la aplicaciones existentes y futuras.

1 SUMMARY

The main objective of this thesis is to develop and characterize the scope of a novel and edge-cutting approaches based on markerless photogrammetric solutions. Hence, the presented study is focused on going beyond the state of art limitations of industrial photogrammetry avoiding or reducing considerably the employment of artificial targets. Currently, industrial systems appeal to artificial targets (attached or projected to the part surface) in order to carry out the measurements with high automation and confidence level. Nevertheless, some industrial scenarios are demanding markerless approaches to improve manufacturing efficiency. The main advantages arise both on the avoidance of part or scenario preparation and on the simplification of measuring procedures reducing measuring time consumption and consequently the cost regarding measuring services. Current limitations and performed research to overcome these technology barriers are presented in ***Chapter 2***. As stated in the review of industrial solutions in ***Chapter 3***, trending manufacturing sectors are demanding more and more flexible and fast measuring solutions that deal with photogrammetric capabilities both for static and dynamic scenarios.

The content of the research is presented and divided as follows. ***Chapter 1*** is a summary of the thesis explaining the different chapters and their content. ***Chapter 2*** introduces and emphasizes the needs of industrial manufacturing processes and how measuring solutions are required to improve current approaches. In fact, a brief description of focused research approaches is mentioned as an alternative amendment. Moreover, it presents the objectives of the research and layout initial hypothesis to address these goals which will the basis for final conclusion and discussion.

Chapter 3 explains and describes the state of art (SOA) of industrial photogrammetric solutions going through existing solutions and approaches in detail. From offline to in-line approaches, an overview and classification of market technologies are presented and required enhancements suggested which the reference points of this thesis are.

As the photogrammetric problem covers multiple concepts and principles to figure out and achieve 3D object information, ***Chapter 4*** deals with the main description of overall concepts and processing steps which are required to reconstruct 3D object information from 2D imagery data. Indeed, the presented workflow is the same for target-based and markerless measuring strategies. This is not expecting to be a detailed description of each term and method, but an overview of problematic and a brief description of main aspects accompanied with accurate references. Besides, meaningful contribution of this thesis is added in some processing steps as a value-added approach.

After presenting the SOA and the main photogrammetric methods applied in common industrial solutions, developed and assessed case studies are introduced in ***Chapter 5***. Three case studies are described and their scope, as well as suitability, has been determined for empowering current industrial applications. For each case study and introduction and main results are introduced as a summary.

Next ***Chapter 6*** deals with the main results and conclusions giving an overall reflection of achieved objectives regarding planned ones. It summarizes the real applicability of developed and studied measuring procedures for real application as well as possibilities of improvement and challenges to be solved in the coming future.

Previously introduced principles and methods are deeply referenced for a deeper lookup and comprehension in ***Chapter 7***. The goal of these bibliographic references is to enable further information search to check the many concepts involved in any photogrammetric solution. Regarding the case studies, each one is independently referenced with appropriate and recent complementary studies.

Finally, ***Chapter 8*** comprises the annex where the cross-reference and citation of published articles is encountered as well as published peer-reviewed full papers. Moreover, interesting web links are provided focusing on photogrammetric fundamentals and measuring capabilities offered by industrial solutions.

A summary at a glance of the employed structure is defined in the following list:

Chapter 1. Summary of thesis and main chapter presentation.

Chapter 2. Overall context and introduction of industrial needs, objectives, and motivation of the thesis and initial hypothesis

Chapter 3. Review of state of art of industrial close-range photogrammetry

Chapter 4. Overview of materials and methods and main contributions

Chapter 5. Description of published case studies and obtained results

Chapter 6. General conclusions and future work

Chapter 7. Bibliographic references

Chapter 8. Annex

The results of each case study are promising and fit to purpose for presented industrial applications, however, further research is still to go in order to replace target-based photogrammetric solutions with markerless ones. Improvements in terms of accuracy enhancement, data handling and image processing strategies, higher computation efficiency and speed in data processing algorithms, standardization of measuring procedures as well as uncertainty assessment studies are still pendant. Simulation of measuring procedures, which is not usually established, is another key point that can be used to foresee measuring process suitability for inspection purposes. Therefore, as photogrammetric techniques continue developing day by day, edge-cutting data processing procedures and integrated novel and smarter solutions will appear on the coming future covering existing needs and challenges.

2 INTRODUCTION

2.1 General context

The development of this thesis responds to the growing needs of manufacturing processes to produce more efficient and cheaper parts with high-quality requirements. Hence, it deals with "Industry 4.0" trends and challenges [1] that faces this aim by means of integration and smart combination of multiple technologies and knowledge of different applications fields. As it has been stated and demonstrated in recent years, process digitalization and modelling are real key player for future production strategies, and this supposes to monitor and understand each manufacturing process in high detail and fidelity. This encompasses the employment of cyber-physical (CP) production systems, the internet of things (IoT), big data, cloud computing, and the advancing use of digital twins. Each field is, in fact, a demanding challenge which enables to feed other technologies and their interaction in order to enhance manufacturing capabilities and ensure quality control. As process details are registered and monitored, their performance can be studied in real-time detecting and taking decisions when the output is out conformity assessment. Moreover, predictive actions can be established to keep the production between certain quality thresholds and make the best of manufacturing means and systems. Such kind of approaches are possible by means of digital models fed and adjusted by real and reliable data. These models are the virtual representation of the components and systems that take part during production.

Automotive and aeronautics are suitable examples of sectors that are fostering and driving this change. In each case the process requirements are different, but they share a common standard that is the accuracy and quality assurance. It is at this point where metrology arises as a required tool to overcome this need. Whereas traditional inspection was applied as a mean to validate and certificate the quality of produced parts and system, recent metrology goes further. The goal is to be part of the manufacturing value chain integrating measuring and inspection capabilities in the process and reducing rejected parts. The measuring technology is not only used to final part geometry validation, but to other multiple functionalities during the process, such as: part location, part alignment, partial geometric verification, correction of machining programs, self-verification of production means, etc...

The general trends of globalized production and derived challenges for manufacturing metrology [2,3] are presented in Figure 1***. Fast*** measuring technologies, procedures and data processing strategies (Model-based definition) are critical as production processes require minimum stops and dead time periods during manufacturing. Integrated employment of measuring devices on machine or in process, is enabling to speed up measuring strategies with low influence on process output. ***Accuracy*** is being increased both for large parts and micro parts which demands high accuracy measuring systems and procedures, as well as data to information processing. Traditionally contact-based approaches have been the reference in this sense, but the latest technologies are getting closer to micron level accuracies. Simulation of complex measuring procedures is another challenge to be solved in order to predict achievable uncertainties before sensor operation ***Reliability*** is another key aspect of manufacturing technology as traceability must be guaranteed in the life cycle of the product. Therefore,

employed measuring systems have to be calibrated and maintain their best performance during operation. In-line self-checking of these systems is being applied more and more to ensure suitable and accurate measurements and result output. ***Flexibility*** of measuring technologies and extracted information density is also a key parameter in current production. As the production is getting global and the yield of new processes has to be ensured, more flexible metrology is required in terms of sensor adaptability for different scenarios (multi-sensor approaches) and smart data processing (automated management of geometric dimensioning and tolerancing (GD&T)). This is accomplished by means of smart sensors that permit to adapt their performance depending on the process specifications. ***Holistic*** representation deals with digital data representation and analysis, so as to control process quality and define corrective, preventive or even predictive actions. It is closely related to digital twin (virtual models) and fingerprint (virtual codification) aspects which are used to define cyber-physical models corresponding to the process.

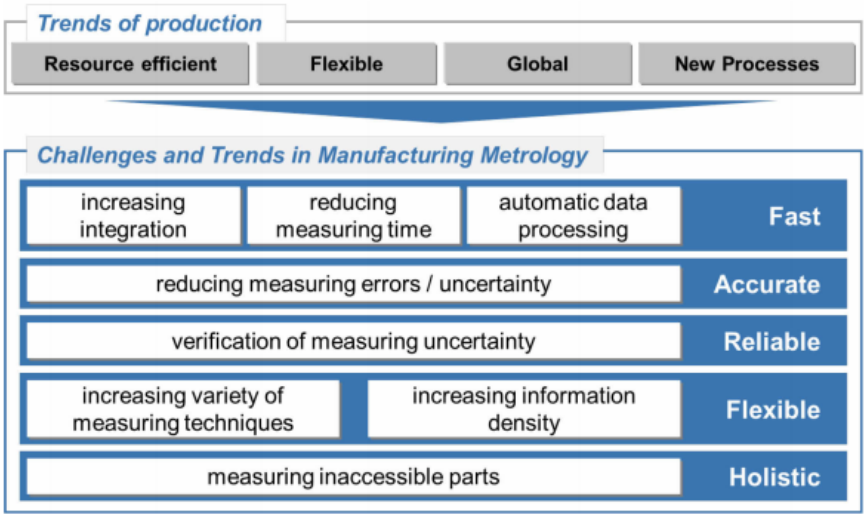

Figure 1. Manufacturing Trends and derived challenges for manufacturing metrology

Hence, measuring technologies have evolved in order to fit these requirements in a fast, accurate and reliable approach. Optical metrology is a major key to play and face this role and it has been demonstrated in last years. Its applicability and extension for many application fields are apparent and the evolution is faster and faster. From initial systems that offered low resolution and data acquisition speed, to current smart sensors, many improvements have been applied. The integration of the measuring system in the production process has adapted the technology to fit their specifications. Therefore, measuring systems have become faster, more flexible and reliable with high automation functionalities in terms of data processing and communication with external systems.

The measuring technology presented in this thesis, in each different set-up, is part of large volume metrology solutions that aim to ensure the dimensional properties of manufactured large parts. When the volume of a part is bigger than 1 m^3 traditional measuring technologies developed for high-tech laboratories do suffer from measuring limitation. Moreover, when the size of a part exceeds certain dimensions, bringing the part to lab facilities is not possible. Therefore, portable measuring coordinate machines (PCMM) are required to characterize the parts in workshop conditions. In this sense, different technologies are available nowadays

comprising multiple measuring capabilities from points-based inspection to surface inspection with measuring ranges of tens of meter, there exist several industrial solutions. A main classification considers two main groups to differentiate between serial kinematic and optical measuring systems (see figure 2). Moreover, another interesting grouping considers centralized and non-centralized systems. Whereas centralized systems are stand-alone devices that can measure a point independently, non-centralized ones combine multiple sensor measurements to estimate the spatial position of a point. Usually, they use mathematical models to combine registered data and estimate useful information. A more detailed description and analysis of existing possibilities are presented in [4,5]. As it is stated in figure 2, photogrammetry is an optical non-centralized measuring technology based on multi-point triangulation similar to indoor Global Positioning System (iGPS) or theodolite technologies.

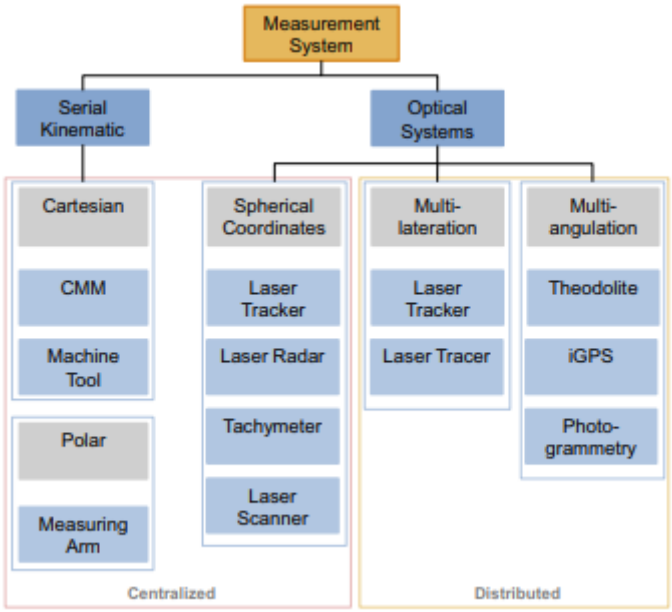

Figure 2. Large scale metrology solutions and classification [4]

Among optical systems, close-range photogrammetry (CRP) is one of the most employed measuring techniques because it deals with many challenges demanded by production trends. In fact, it is one of the measuring techniques that has been developed more in recent years from the point of view of hardware and software functionalities. It ***is really fast*** because it is a non-contact approach based on image acquisition and current image sensors can take images in less than ms. Measuring procedures can be improved in terms of speed moving and positioning automatically acquisition sensors around the measuring scenario and employing accurate known data to improve data processing tasks and achieve precise information. ***Accuracy*** is guaranteed by intrinsic camera calibration strategies and suitable triangulation of surface points with multiple measuring set-ups. Achievable relative accuracy for point-based photogrammetry with targets is 1:200000. Accuracy enhancement is achieved for surface-based approaches combining prior point-based measurement of reference points which are used to stitch all 3D partial scans into a common reference system. The ***reliability*** is ensured by means of the application of standardized guidelines such as the VDI2634 that determines how to check accuracy performance of optical systems comprising mainly photogrammetric systems. At the moment an ISO standard is not yet available but is being developed. Another important aspect that ensures data reliability is the capability of photogrammetry to self-calibrating or even self-

checking of offline calibration. Industrial solutions do offer this functionality guaranteeing the highest accuracy during system operation. More and more ***flexibility*** is another key aspect that measuring system needs to cover. Photogrammetric systems are a good example of reconfigurability and flexibility as the same system can work with different resolutions and measuring areas depending on the requirements. The working range is also adjustable to some limits. Moreover, flexibility is reinforced from the point of view of integrability as many set-ups are designed to be mounted on computer numeric control (CNC) manipulators. This mechanical and electrical integration, as well as system real-time communication, enables to carry out automatic measurements and data processing. A good example of ***holistic*** capabilities of photogrammetry are achievable cloud of points that define the 3D geometry of a part. This representation is indeed the digital definition (digital) of the part and can be used many simulation tasks, such as computer-aided design (CAD) comparison, virtual assembly or finite element method (FEM) model fitting. As-built surface definition is therefore rich information that opens the possibilities of data handling and analysis in comparison to point-based measuring solutions.

2.2 Motivation

Close-range photogrammetry [6–10] is a more and more employed measuring technique nowadays dealing with industrial applications where part dimensional verification, tracking or deformation testing studies are required. It is an optical measuring technique based on 2D images that enable to carry out agile 3D measurements for different working volumes and scenarios. However, as it is common with any measuring technology and procedure, it has some barriers and limitations that can be improved or even completed. One of the main limitations is the need to use artificial targets to carry out the measurement. These targets are employed for different fundamental aspects that are common in point-based and area-based photogrammetry, such as:

- To define the measuring points and geometric characteristics
- To solve extrinsic orientation
- To solve the correspondence problem
- To stitch partial scans
- As known references for automated scanning processes

Hence, industrial photogrammetry is closely related to the employment of artificial targets (active or passive) not only to support listed functionalities but to ensure the highest accuracy. However, in turn, this is a huge limitation in terms of measuring time and measuring procedure flexibility. Therefore, markerless solutions present the opportunity to develop alternative solutions covering these needs.

For example, the preparation of the scene to be measured is a time-consuming task because close-range photogrammetry can be applied to scenarios ranging 1 to 100 m. Thus, locating the artificial targets all around the scene (see Figure 3) is sometimes a demanding task. Industrial photogrammetry is commonly supported by artificial targets that permit to precisely define the points or elements to be measured and to automate extrinsic orientation as well as scaling

obtained results. Although there already exist some approaches that avoid the use of targets based on key natural features, it is not common in industrial applications where accuracy requirements command. This is a huge limitation in any inspection activity in which a grid of repetitive geometries needs to be verified because of the requirement of suitable adapters for each geometry. As the quantity of these repetitive geometric elements increases, as well as the size of the geometric element their, represent, the preparation time and investment for acquiring feasible fixtures increase proportionally. Therefore, a measuring method for avoiding this matter is advisable. ***Chapter 5.1.*** deals with the development of an automatic photogrammetric solution to estimate the XYZ position of multiple drilled holes above a machined surface with a markerless approach.

It combines a feature-based detection image processing approach based on a priori known data and a two-stage bundle adjustment 3D reconstruction process. The measuring procedure has been improved to machined hole detection by means of specific camera networks and camera parameter adjustment avoiding the need for special adapter nor fixture. The measuring process has been reinforced by light sources that ensure high quality and contrast images. Moreover, experimental validation and accuracy assessment are established against certified verification methods.

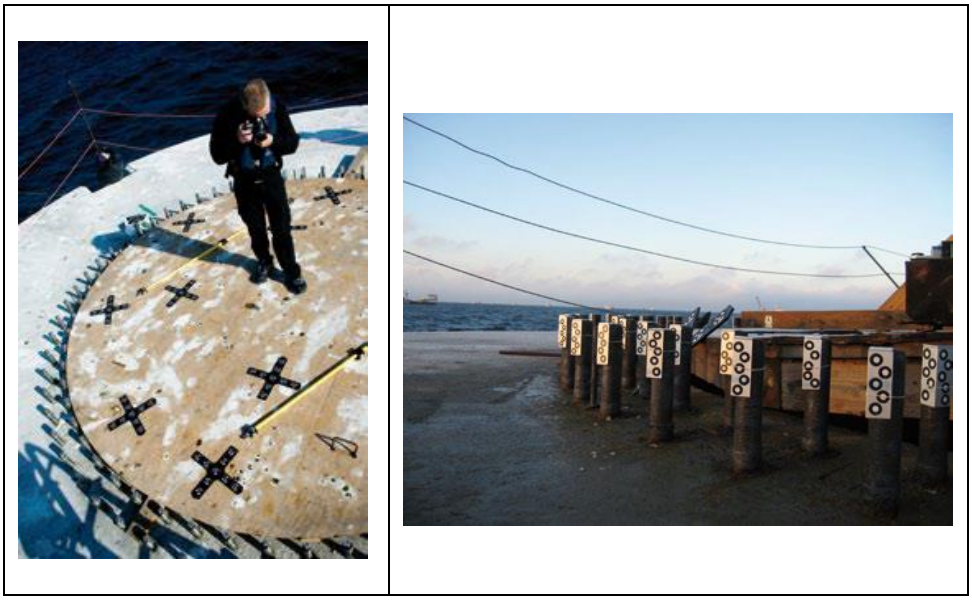

Figure 3. *Close-range photogrammetry with multiple adapters for mounting bolts* [11]

Apart from accuracy issues that recommend using targets, there are other applications where the use of targets brings up some drawbacks. For example, when round parts or complex geometries need to be measured or tracked, many images are necessary to ensure that the photogrammetric camera network will be solved. At least a target needs to be seen by two consecutive images although more views are recommended for accurate point triangulation and correspondence estimation. Consequently, both for a fixed camera or even a hand-held single camera-based approach, such geometries require a high number of image sensors that becomes the measuring system a non-cost-effective solution. Even though a high camera number solution is provided, many times the triangulation of artificial targets is poor or unfeasible which

decreases achievable accuracy and measuring process flexibility. Thus, developing methods that do not require to use targets to define the geometric element to be inspected and avoid the correspondence problem, is a promising research line. In this sense, single or even multiple primitive detections can be faced. ***Chapter 5.2.*** deals with the development and accuracy evaluation of a photogrammetric simulation tool to measure the spatial position of a cylinder based on contour lines. The aim of this study is to arrange a simulation environment for uncertainty assessment and design purposes of this kind of photogrammetric approaches. Traditional methods are based on geometric fitting of measured targets or Best-fit transformation between measured and nominal points. Nevertheless, target arrangement is not feasible for some demanding scenarios such as high solar flux concentration facilities or objects with high occlusions (see figure 4). It is in such kind of measuring scenarios where feature-based modelling can be more suitable than target-based approaches even accuracy loss is expected. Moreover, employed models can detect and carry out the tracking of different geometric elements such as borderlines, circles or cylindrical object. In all cases, a mathematical description of the geometry of interest is required and distances among image rays and mentioned element are minimized to estimate its spatial location and orientation.

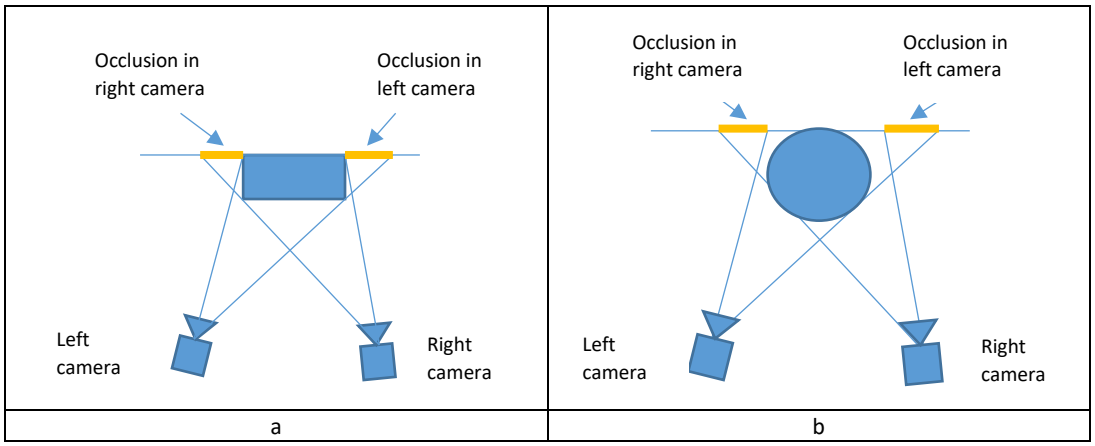

Figure 4. Occlusion problem in stereo view. a) Prismatic part) b) Round part

3D scanning of large complex parts is a common application for area-based photogrammetric scanning systems. The aim is to obtain a representative digital definition of the surfaces that comprise an object by means of a 3D point cloud reconstruction. This is usually accomplished by white light structured or time of flight (TOF) based scanners with referencing targets above the part surface. The limitation arises from time-consuming measuring procedures due to part preparation with reference targets (see figure 5) and the positioning of the measuring system in many locations to scan the whole part. Besides, 3D scanners are many times referenced by previous photogrammetric processes so as to improve achievable point cloud accuracy and increase the flexibility of the scanning stage. However, this technology fusion makes longer the time required for the overall measuring process.

Lately, fields such as topography, cultural heritage or aerial mapping are adopting structure from motion (SFM) approaches and its algorithms for 3D scanning purposes instead of measuring a discrete number of points. The interest comes from the idea of obtaining dense 3D point clouds

only from imagery without the need to use targets. These applications do not aim to get high accuracy data, but for inspection methods like the one studied in this thesis, this requirement must be taken into account. Therefore, establishing the scope of this method is necessary to understand the limits and the applicability of dense matching approaches for verification purposes. ***Chapter 5.3.*** deals with the development of a measuring procedure based on a dense matching approach to scan and verify casting large parts with suitable surface texture. This is carried out by means of SFM procedures with some adaptations. The study considers an approach based on coded targets and another approach based on natural features for the photogrammetric reconstruction. The obtained dense point clouds are compared against a certified method in order to establish the achievable accuracy of this measuring technique both for lab and shop floor conditions.

Figure 5. 3D optical scanning of casting parts with referencing targets[12]

Apart from presenting problems that are tackled in each case study, general drawbacks do condition the employment of artificial targets in industrial environments, such as:

- Target stability→ Adhesive or magnetic targets can move during the measurement due to external effects. If this happens, the accuracy of the measurement is reduced and even the general functionalities of photogrammetric systems can be affected.
- Rejection of target after the measurement→ Depending on the manufacturing process, part or structure inspection demands to remove the targets from previously placed locations. This is a big disadvantage which also makes longer the time consumption of the measuring procedure.
- Dirty above part or structure surface→ In some cases, where the part is inspected before its machining of final manufacturing step, or even when it is in harsh scenarios, available surfaces where the targets are placed require to be cleaned. If this task is not carried out, either magnetic nor adhesive targets can be located above the measurand. Moreover, the targets do also need periodically cleaned to ensure their detection.
- Target random distribution→ Geometric restrictions of photogrammetric models demand non-symmetric and homogeneous target distribution in order to ensure robust image point identification and consequent 3D reconstruction. If this requirement is not fulfilled, obtained information can result in imprecise and messy. Hence, a random

target location is recommended when a high number of control points are required which extends the preparation time of the scene. Later developments do employ smarter algorithms to avoid these problems, but punctual errors or bundle model solving limitations do persist.

- Target size→ A minimum size of a photogrammetric target depends on the camera sensor size, camera parameters and working distance. Usually, the minimum size of a target of 5 pixels is required to detect and identify it, but 10 pixels are recommended to ensure high accuracy. Corresponding dimensions for each application are not always feasible because of a lack of supporting structures or suitable planar surfaces. Hence, the design and employment of specific target dimensions are a huge limitation in industrial case studies.

Considering hosted barriers and the limits of traditional photogrammetry as well as new research opportunities, this thesis aims to study alternative photogrammetric approaches that are not based on targets (named markerless solutions) or at least reduce considerably the maximum number of required ones.

2.3 Objectives

The principal objective of this thesis is to apply novel methodologies based on geometric features to different photogrammetric models in order to study the scope and capabilities of markerless photogrammetric methods. For every case, the aim is to go beyond the current state of the art for this technique and cover existing challenges developing and studying alternative image processing and modelling approaches. In some cases, employed photogrammetric models and workflow are similar to established ones but with improvements in terms of image data detection and extraction strategies, whereas other cases require feature-based models to reconstruct the geometry of interest without the need of traditional target-based geometric fitting approaches. Measuring procedures do also need to be adapted to the specific demands of each application.

The common research point among analyzed case studies is that all of them aim to avoid the use of artificial targets during the measuring process or at least they reduce considerably the amount of them. In some cases, due to ***time–consuming scene preparation*** because of the required high number of targets and locations, other times due to ***occlusion problems*** for the characterization of round forms and even to simplify ***complex scanning procedures and non-cost-effective approaches*** which require a fusion of technologies (photogrammetry, structured light) to tackle the scanning of large parts.

The objective in *Case study 1* (***Chapter 5.1***) is to develop a measuring solution and study experimentally the achievable accuracy measuring the positioning of chamfered drilled holes without employing any target nor adapter for its definition. Industrial verification strategies do usually use them, but in this thesis, the idea is to measure directly the 3D position of these geometric elements with sort scene preparation approaches. The geometry to be measured in this case corresponds to multiple circles which are seen on the images as ellipses. Nominal border point data will be used as a priori data to aid the detection and identification of real border points and estimate their centers. This is carried out by known data 3D space to 2D image plane reprojection based on collinearity equations. Afterwards, 3D spatial position of these geometric elements will be estimated by means of a multi-point triangulation method. In this phase, a two-stage bundle adjustment process will be applied, and the uncertainty of calculated outputs will be assessed.

The objective in *Case study 2* (***Chapter 5.2***) is to develop a model and study the theoretical accuracy of feature-based photogrammetric methods as an alternative to traditional approaches. The objective is to avoid the use of targets and avoid the correspondence problem among camera views for complex geometries such as round objects. The study will consider a cylinder as the geometric element to be measured from a fixed and established camera network which intrinsic camera parameters are known. The contour image point data, extracted from shape-matching image processing approaches, will be used to feed the model and reconstruct the pose of the cylinder according to a world coordinate system. The expected accuracy will be studied by means of statistical Monte-Carlo approaches to assess the applicability of the developed model to industrial applications with large working range. The number of cameras and contour point quality and distribution will be the variables of this study.

The objective in *Case study 3* (***Chapter 5.3***) is to develop a measuring procedure and study the achievable accuracy of dense matching techniques for casting part verification. Both target-

based and target-less approaches will be considered and compared against certified and established measuring strategies. The idea is to assess this imagery-based technique as an alternative to current time-consuming 3D scanning technologies and approaches. Instead of combining a photogrammetric stage with a posteriori scanning process, this approach aims to apply only the photogrammetry as a unique set-up. The difference arises from considered image data. Employed data will be based on natural key points that correspond to interest points and point descriptors extracted from the images. These image points offer natural point codification enabling the automatic surface reconstruction without the need for artificial targets. This data processing strategy will simplify considerably both image acquisition step as well as data processing and dense point cloud reconstruction

2.4 Hypothesis

This chapter describes the main and particular hypothesis that have encouraged this thesis. Current photogrammetric solutions are based on artificial targets (physical or light projected) to ensure high measuring accuracy. The employment of these elements is crucial to achieve state of art accuracy levels (1:200000) in point-based solutions and enable high-density 3D surface reconstruction. However, this approach is at the same time one of the main limitations of photogrammetry as the measuring scenario has to be studied and prepared considering aspects related to the part, measuring technology and measuring conditions. Current solutions do need to locate as many targets (coded and non-coded ones) as required all around the measurand considering image orientation requirements as well as triangulation aspects to guarantee 3D reconstruction and final accuracy.

Whereas image orientation is reinforced by means of coded targets, point triangulation needs to see a point in at least two images (stereo). Besides, the angle between intersecting light rays has to fulfill certain angle ranges to achieve a reliable 3D point reconstruction. In real applications, multi-image triangulation is recommended increasing point accuracy by means of data redundancy. When the part is round or cylindrical, 3D point triangulation is a demanding task because the image perspective changes rapidly between consecutive images which constraints the image acquisition process and requires a huge number of images to characterize the overall measuring scenario. Furthermore, in complex part geometries, occlusion problems arise making harder point triangulation and the correspondence problem establishment.

Depending on the features to be verified, even special adapters are required to carry out the measurements which suppose to purchase or manufacture these accessories for each geometric feature. In the case of 3D surface scanning, targets are also required to bring together all partial scans and ensure an overlapping among each acquisition. The same targets can be referenced with high accuracy combining prior point-based photogrammetry with a posteriori 3D scanning process. This combination is many times advisable as the scanning process becomes more flexible (local referencing) and the point cloud accuracy is enhanced.

Moreover, light-demanding scenarios are usual in industrial workshops where structured light-based solutions are suffering from a lack of contrast of projected fringe-based patterns above the surface. This limitation is faced with more powerful projection systems and more robust projected light color, but even edge-cutting scanning systems do offer better performance in a light-controlled environment. However, this is not many times possible or supposes to carry out the measurement in the nighttime.

Hence, is has been detected that artificial target employment is a huge limitation for photogrammetry in terms of measuring time, measuring process flexibility and measuring solution adaptability to different scenarios. It is at this point where markerless photogrammetry accompanied by advanced image processing strategies can be more suitable and advantageous to overcome detected limitations and develop novel measuring approaches. Thus, ***this thesis emphasizes the suitability of feature-based photogrammetric solutions as an alternative to overcome limitations on existing industrial measuring approaches based on targets***. This means to combine traditional or novel photogrammetric models with feature-based image processing strategies.

In any measuring scenario, the images contain such kind of information that can be used to carry out the measurements combining novel image data processing and optical modelling strategies. Accuracy loss is predicted beforehand, but other mentioned aspects are expected to be improved maintaining fit to purpose uncertainty levels.

Once introduced the main hypothesis, this chapter describes a specific hypothesis for each case study. These hypotheses are the basis for the developed industrial applications that are described in chapter 5. Presented statements will be the reference for final conclusions and discussion.

2.4.1 Case study 1

The hypothesis for ***Case study 1*** is that **natural features** that correspond to common geometric elements like circle or ellipses **can be detected and measured with accuracy** that is fit to purpose based on photogrammetric basics and image processing strategies. This would enable to replace artificial targets with natural primitive direct identification. The main advantage if this development is feasible will be the possibility to measure multiple features from some few images without the need to employ fixtures instead. Traditional methodologies employ them. The main foreseen problem can be the difficulties to detect and extract the features from the images with high definition and contrast. This is necessary to ensure an accurate camera network determination as well as suitable 3D data estimation by means of multi-view triangulation and bundle adjustment approaches.

2.4.2 Case study 2

The hypothesis for ***Case study 2*** is that **contour-based photogrammetric approaches** can be more **suitable** than geometric fitting of 3D points **for pose estimation** of cylindrical elements for large working ranges in harsh environments. The main advantage is that the correspondence among camera views is not required reducing the number of sensors for accurate cylinder position and orientation. A possible problem can arise from challenging contour point detection for real scenery and instabilities of known camera parameters such as intrinsic and extrinsic orientation. Therefore, the theoretical research comprising the scope of such kind of modelling must consider imaging error sources by means of statistical simulation.

2.4.3 Case study 3

The hypothesis for ***Case study 3*** is that **dense matching approach** can be applied to **casting part verification** with **fit to purpose** accuracies employing structure from motion strategies and avoiding time-consuming complex scanning procedures. Although SFM methods have been developed for computer vision applications where accuracy aspects are not so demanding, they can be adapted for industrial filed. The main advantage is that before scanning a casting part with a 3D structured light scanner, a photogrammetric process is usually solved to establish accurate referencing of fixed targets. Therefore, the image data for photogrammetry is already registered and can be applied to dense matching methods. Possibly, the main drawback will

arise from correspondence problem among image views, time-consuming surface point reconstruction and missing data when dense 3D reconstruction is performed.

3 STATE OF THE ART AND BACKGROUND

This chapter introduces available edge-cutting hardware & software photogrammetric solutions in the market classified with several criteria. Moreover, it presents current technology barriers and needs and consequent challenges to overcome these limitations.

3.1 Introduction

The systems based on photogrammetry arise from the need to verify parts of medium and large size [4,13–15] by contactless technologies with a reduced cost and fast response compared to other existing technologies. They seek to complete the measurement performance offered by other PCMM such as Laser-tracker (LT) [16,17] and articulated arms [18] for discrete point number measurement, eliminating the need to touch the surfaces of the elements of interest and/or and enabling measuring multiple points at the same time. Initially, handheld approaches where developed to fill this gap, but stereo systems, as well as structured light 3D scanners [19,20], have widened the applicability of this technology for further industrial fields.

Photogrammetry [9,21] is not a new technology, but it is an emerging technological solution that, together with the evolution of the processing capabilities of PCMMs and vision algorithms, has evolved rapidly in the last decade. From the analog systems of the 80s to the digital systems of this century, the evolution of mono or multi-camera photogrammetric systems has been remarkable, allowing to adapt this measurement technique to different industrial applications and measurement requirements. Although a priori it is a measurement technique that was developed to measure discrete point number, the latest advances at the level of the state of the art are broadening the range of possibilities with digital image correlation (DIC) techniques [22–25] for the measurement of deformations or dense matching that allows the extraction of dense point clouds from information obtained only from the images [26,27]. Therefore, it is a flexible technology that can be configured and materialized in different ways for applications with static needs (3D measurement, quasi-static deformations, and 3D surface measurement) or dynamics (6 dof referencing, multi-point tracking, deformation, vibration). From more or less complex complete systems to accessories based on this technology at a commercial level, many solutions apply photogrammetry as a measurement method and basis. The industrial requirements in order to implement and integrate these means in their production processes as well as in their quality assurance processes are mentioned in the following section.

3.2 Industrial requirements

The integration of this technology for its different setups depends on many factors that industrial processes and their quality control systems require, such as:

Simulation of measuring procedures

Photogrammetric systems can be considered complex measurement systems such as coordinate measuring machines (CMM) or LT where characterizing the different parameters of these systems is very expensive as well as modeling and calibration aspects [16,28]. These complex models allow to simulate [29–31] and predict the behavior of different aspects of the measurement as well as the procedure used for that purpose. Current applications are

requesting more and more that measuring procedures are fit to purpose and to control the precision of measurement for different characteristics of the same object. It is in this scenario where the modeling and characterization of the parameters of the model are critical. Although most of the photogrammetric systems estimate the relative accuracy of measured 3D points, they don't estimate the uncertainty of triangulated 3D points. At the industrial level, there are very few tools that allow to simulate and estimate approximately the accuracy of a specific measurement procedure based on photogrammetry. For example, the Spatial Analyzer software (SA©) together with the VSTARS© software allows to carry out precision studies combining the simulation and modeling capabilities of both tools. The employed camera model is based on VSTARS metric cameras and it is not editable at the moment. While the VSTARS side carries out the photogrammetric simulation, the VSTARS side is used to generate synthetic 2D point data for iterative Montecarlo approach and to represent the estimated 3D point cloud and their error propagation from VSTARS. Based on this point clouds further simulations in SA© environment enable to calculate the uncertainty of specific geometric elements or other characteristics.

There are also more academic tools like Phox© [32] that offer similar possibilities but target more training aims than industrial tools. In this case, the simulation of space resection or even 6 degrees of freedom (dof) positioning among components is feasible apart from 3D point triangulation.

In any case, none of the current solutions can estimate the uncertainty of the intrinsic and extrinsic parameters in a bundle adjustment (BA) approach[33,34]. Neither have they allowed estimating other photogrammetric approaches that are not based on point triangulation for multi-view approaches.

Within this aim, taylor-made solutions based on imaging libraries such as Matlab© or Halcon© are necessary or even own developed functions which are the most flexible solutions for simulation. However, they are a time-consuming option thus most of the times a combination among simulation tools is the right choice.

Some examples of mentioned solutions are mentioned in the following lines. In [35] a photogrammetric simulation of an antenna is shown with SA-VSTARS solution, in [30,36] a simulation based on Matlab© approach is presented and further optimization studies based on different approaches are described in [37–39].

Precise, fast, flexible and simple technologies

The current industry seeks technologies that can replace traditional technologies from the point of view of accuracy and speed, without losing other important aspects such as ease of use, investment cost and system flexibility and/or adaptability for multiple measuring scenarios. Portable measurement technologies initially arose from a need to measure a few control points, but the latest industrial measuring needs have demanded a greater amount of information and a higher density of measured points. This new measurement capacity should not affect the accuracy offered by the technological solution but may limit the speed of measurement and processing due to the high data content. However, the automation level and latest software developments related to data processing are enabling the automatic management of data and its direct use by manufacturing means. In addition, automation allows a non-advanced user to use the technology as well as the measurement procedure without margin for error of use. One of the main advantages of current photogrammetric systems is the adaptability to the measuring

range and required data resolution. Simple calibration and adjustment of optic components can adapt the use of these technologies for a broad measuring application. Furthermore, the current photogrammetric real-time systems control the accuracy of the triangulated points both for measurement tasks as well as referencing, indicating the need for calibration of the equipment if it does not meet supplier specifications. Besides, product robustness for industrial environments has been improved in terms of more stable imaging components.

The measuring speed has also increased with high-speed cameras for deformation or 3D tracking purposes of demanding dynamic scenarios [40,41]. 3D scanning systems based on light projection has also been improved with faster surface point codification light patterns [42,43] and measuring frequency below 0.2 sg. Digital light patterns are faster than previously existing mechanical solutions that have increased considerably the measuring speed for each measuring shot and consequently has reduced the overall measuring time to scan a complete part.

Traceability

The implementation of photogrammetry as a certified solution for quality control tasks depends on the acceptance of reference standards for the production chain. If you intend to use these technologies to validate and certify pieces in a similar way to what has been done with CMM for years, it is necessary to settle rules and procedures that determine how to verify the accuracy of this type of devices and ensure good use of the same. Today there is only one technical guide that defines how to compare the measurement performance of different measurement configurations based on photogrammetry. It is not a standard as such, but in the absence of it is currently the reference used by different technology providers. It is the guide VDI / VDE2634 [44–46] that in fact does not stop being a recommendation but that is extended between the manufacturers and users of Optical 3D measuring systems. This recommendation has several sections. While the Blatt 1 talks about imaging systems with point-by-point probing, the Blatt 2 is focused on optical systems based on area scanning and the Blatt3 defines verification tests for multiple view systems based on area scanning.

As evaluation artifacts, calibrated spheres, length bars, and flat surfaces are used to characterize several performance characteristics of the system and to establish the maximum permissible error (MPE) which is the accuracy parameter that distinguishes accuracy level among industrial systems.

At the moment different committees (ISO, ASTM) and European calls integrated within the H2020 program, seek to complete, improve and develop procedures for this purpose considering the extensive and growing use of this type of measurement systems in many sectors. Some state or art references regarding this issue are presented in [47–49].

Meanwhile, different authors have studied the applicability and scope of this guide to existing optical configurations. In [50] the accuracy of different measuring set-ups has been studied, in [51] a micro-scale system has been characterized form the point of view of accuracy, in [52] the Blatt2 is applied to a mono camera vision system, in [53] a hand-held camera is studied, in [54] a comparison among different reference standards for automotive application is shown and in [55] a comparison between photogrammetric systems against LT technology is presented.

Integrated metrological solutions

The need to take the measurement systems close to the production processes or even integrated into the machines in order to respond to the needs of the emerging production is ever more latent. This new digital paradigm requires that the means of control be in the production chain itself enabling rapid communication between the quality and production of different components. The integrated measurement and inspection solutions allow streamlining the exhaustive control of the processes even in real-time with the aim of taking corrective or preventive actions on the process. Therefore, a greater knowledge of the processes and their behavior is achieved by monitoring them and converting measurements into useful information in order to feed the processes such as automatic assembly, mass production of components, manufacture of parts high added value, etc.

Nowadays the integration of automatic photogrammetric solutions is more and more common in countless industrial applications combining precision positioners with several measuring solutions based on touch probes or non-contact scanning accessories. These accessories are in many cases tracked with stereo or monovision devices [41] targeting to increase the measuring accuracy which increases the cost of the measuring solution. As an alternative, latest approaches called robotic CMMs [56] are arising trying to avoid tracking systems and directly apply the fusion of the positioner pose data and measuring system partial scans by means of accurate calibration strategies and reference point located around the part's fixture. Furthermore, the latest automated cells offer self-monitoring functionalities to assure that the performance of robot metrology solutions is well established and is stable for its operation. For large parts, an add-on photogrammetric sensor can be added to scanning devices to increase the overall accuracy of the fused 3D point cloud up to 10 µm based on established reference marker identification and partial scan transformation. This technology fusion is also common in manually measured use cases. Although the former applications of photogrammetric devices were oriented to manual handling, its integration into different processes or automatic verification cells is a fact these days.

From configurations that combine the measuring head with an angular positioner [57] to more complex systems that mount the measuring heads in a robot's tool center point (TCP) [58,59], the evolution of technology and its integration into productive means has been growing in recent years. These automatic solutions can be prepared and tested offline with virtual software stations that enable to foresee optimum measuring strategy and expected a result.

In addition to the automation of the measurement as well as its optimization through the fusion of technologies, extensive work has been carried out on the automated management and processing of raw data. As more and more data quantity is acquired by novel technologies, smart data processing strategies are required to transform raw data in eligible information for multi-task objectives (GD&T analysis, estimate dimension, color map comparison, a fusion of partial measurements, etc.) with a minimum request for system operators.

Dynamic measurements to study the behavior of structures/components, track components or self-checking

Stereo or multi-view photogrammetric devices allow measuring multiple points (see figure 6) at once with high measuring frequencies. This capability is well-suited to the dynamic evaluation of 3D coordinates, 3D displacement, and surface strain. As the extrinsic orientation among camera projection centers is known, real-time triangulation (up to 2000 images per second) of diverse discrete points is enabled for dynamic measurements. Hence, this functionality is

applied for many purposes such as self-checking calibration of the system, monitoring of a set of control points, live tracking of components against a specific reference (measuring device or fixed component), dynamic referencing [41] between the part and the measuring device as well as for live tracking in 6 dof of measuring hand-held or automated devices. In turn, these accessories (see figure 7) can be touch probes, laser-triangulation systems or even fringe projection sensors. Usually, these functionalities are used by stereo tracking systems or fringe projection 3D scanning system. Dynamic point monitoring is crucial to guarantee that the measuring device is working within its specifications and that calibration of the system is maintained along with its operation. Besides, real-time measuring can be used to detect environmental changes or mechanical instabilities such as movements or vibrations. The goal is to ensure high-quality measuring data verifying continuously calibration status, dynamic referencing of each partial scan and any external environmental drift.

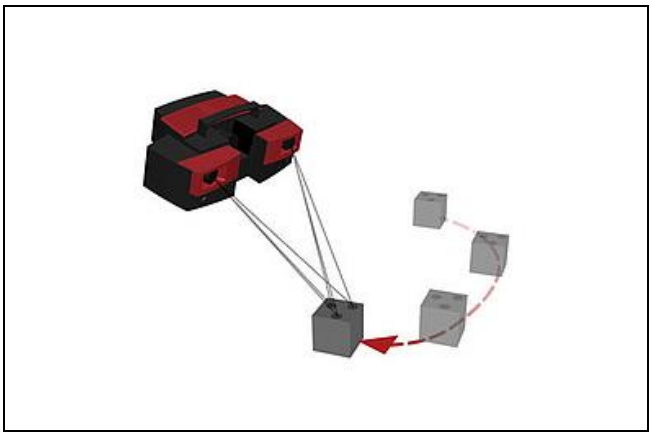

Figure 6. Live tracking of a part with several fixed targets[60]

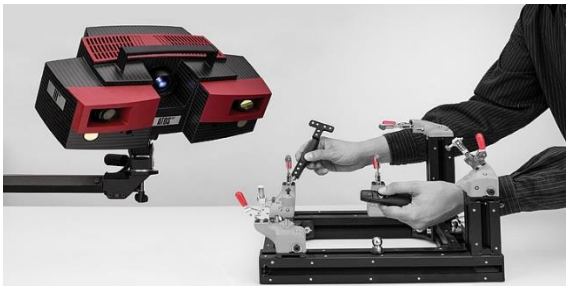

a[60]

b[61]

Figure 7. Optically Tracked touch probes (a) and 3D scanner (b)

Edge-cutting approaches are also permitting to measure dense point clouds in real-time to characterize the 3D deformation of a part or even to align a part based on surface (mesh) data. Whereas the deformation (see figure 8) is established by means of digital image correlation (DIC) based techniques [62–64] part alignment is based on mesh data of high-frequency 3d scanning capabilities.

DIC is a strain measurement technique that works by capturing a series of images of speckled surface pattern throughout a test and processing them afterwards by means of image correlation algorithms. It is a non-contact method where one digital image is mapped onto

another digital image. The images show the specimen that is tested, and the transformation field between the two images is used to retrieve the displacement field on the surface of the specimen. The transformation field is determined by maximizing a correlation coefficient examining pixel intensity array subsets by means of image processing algorithms. A typical system includes a camera system, lighting, and a software package to control image capture and to conduct post-test analysis.

The measurement accuracy of DIC can be affected by many factors, such as the size of the subset are used to match the same point in two images taken at different time points, the step size (i.e., the number of pixels by which the subset is shifted to calculate the strain field) and, if used, the type of data smoothing/filtering adopted. In some cases, laser sources are added to DIC systems creating laser speckle pattern when sprayed treatments on the specimen surface are unsuitable under various testing conditions, for example elevated temperature, microscale, and large deformation.

DIC measurements can be 2D (one camera used), or surface-3D (two cameras used in stereo-vision and located in multiple stations). The full 3D approach (where a 3D imaging device, e.g. an X-ray tomography, is used) is referred to as Digital Volume Correlation (DVC).

Figure 8. Digital image correlation for strain measurement[65]

Hardware and software improvements

Current systems use cameras with higher resolution (up to 12 Mpx) to obtain higher spatial resolution and a more homogeneous definition of the surfaces to be measured as well as greater precision [66]. In addition to increasing the pixel resolution of the cameras, it has also improved its measurement frequency (up to few ms), making it possible to use photogrammetry not only in static scenes but also in dynamic scenes. In fact, the dynamic benefits are increasing allowing to apply this measurement technology in more areas. Other components such as projectors have been adapted to work more robustly using the spectrum of light emission in blue and achieving

better performance in the definition and stability of the points to be measured in industrial demanding scenarios. The internal and external calibration, as well as its stability, is another aspect that is being monitored to ensure that the results obtained are reliable and of high quality. Likewise, if some variation in the parameters is detected, faster self-calibration methods of these means have been developed to minimize dead times of system adjustment. Another aspect that has been improved is the triangulation between the components of the measurement system. While the older systems mediated only with the cameras and therefore the triangulation of the points was conditioned by the common area of view between them, the current systems also triangulate with the projector (more thermally stable technology) obtaining a higher resolution of points, greater accessibility to less accessible geometries as well as a more homogeneous and continuous distribution of points.

In turn, the image processing and algorithms used in the photogrammetric models have evolved according to these hardware improvements in order to speed up the identification of points of interest, strengthen the calibration procedures and obtain the results of interest applying in each case the corresponding model. This last part has also been completed with graphic processing unit (GPU) with greater computational capacity for high-density information management in high-resolution scanners as well as in dense matching solutions.

3.3 Review of industrial Close-Range Photogrammetry

The photogrammetric approaches and capabilities have substantially changed over the last 20 years with the irruption of digital means and high-performance personal computers (PC) in the materialization of this measuring technique. However, the use of photogrammetry in the industry has not meaningfully changed over the last 5 years although new applications and functionalities have arisen. Detailed reviews of industrial close-range photogrammetry state of the art as a previous reference are mentioned in [67] and [68] where hardware, as well as novel measuring functionalities, are described in detail. The further chapters in this SOA aim to update some remarkable topics covered in these reviews and to add new matters and measuring configurations. As well as these authors did, not only photogrammetric point by point solutions are presented but area or surface scanning solution, as well as other novel image analysis approaches trying to broaden camera calibration tasks and dense surface reconstruction. Besides, a general overview of existing solutions is presented both considering existing hardware and software solutions.

3.3.1 Photogrammetric system classification

Photogrammetric techniques can be classified by different parameters, such as measuring range, measuring configuration or even offline or inline performance closely related to application requirements.

In the following lines, industrially employed main classifications are mentioned and described in order to introduce an overall overview of this technology.

A first classification and a common one is based on the measuring scale and how the camera system in handled during the execution of measurements. From this point of view, 3 measuring scales are determined: very close-range (micro) photogrammetry, close-range photogrammetry, far-range photogrammetry (aerial and terrestrial).

Whereas terrestrial photogrammetry means that the camera is employed from ground level image acquisition by means of a photographer, tripod or mechatronic actuator, the aerial use case is carried out mounting the camera on an aircraft (plane, drone, etc.). Therefore, measuring range is limited from few meters to tens of meters for hand-held or tripod-based approaches whereas aerial approaches target large topographic 3D mapping or building as-built 3D modeling. In both cases, hundreds of images are taken and the accessibility and time for image acquisition determine the feasibility of each type of photogrammetric technique. See figure 9 to understand the working range of industrial photogrammetry (1 to 20 m).

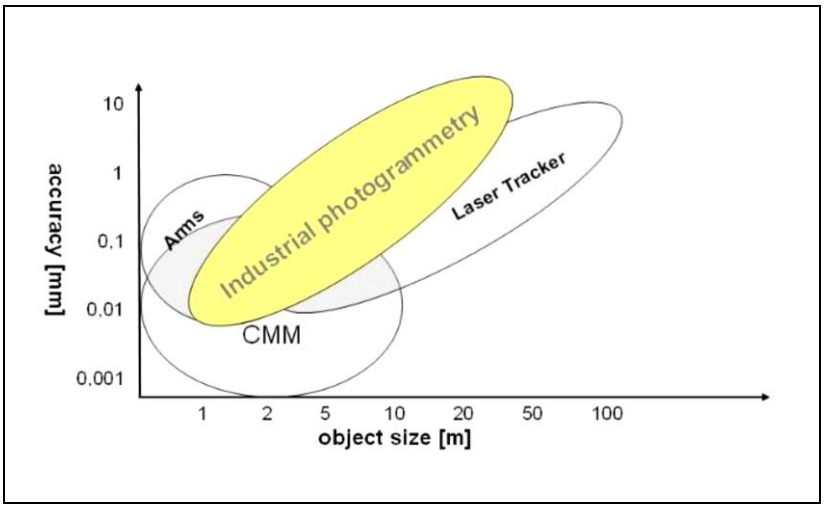

Figure 9. Coordinate measuring machine (CMM) and portable system specifications

Nevertheless, the latest very close range applications require high accuracy for dimensions of few microns or even less [69,70]. This is called small or micro photogrammetry [70–72] where micro-features of small parts are characterized. Some applications go beyond this scale reconstructing 3D surfaces with imagery from scanning electron microscope (SEM) [73–77] achieving resolution of nanometers.

Another system classification is divided into two main groups. The first group aims to solve the geometric inspection of a part against a drawing or a CAD model. Point quantity can be discrete or dense depending on the application. The goal usually is to check selected features of a part against a given tolerance for production control or to measure all features of a new part for 3D reconstruction or reverse engineering. The second group deals with applications more related to analyze the geometric change of a part or structure under certain external conditions.

External loads can be natural effects such as gravity or thermal change but also applied loads to study the behavior of the part against this excitation. These cases are typically related to motion analysis, deformation testing or vehicle dynamics.

Depending on the previously described classification, photogrammetric solutions can be materialized in multiple configurations which a general overview is mentioned in the following chapter. Nevertheless, all set-ups look for reconstructing 3D object information from image data and camera projection modelling.

3.3.2 Photogrammetric hardware solutions

The photogrammetric configurations for different measuring task mainly vary in the number of employed cameras and whether they are fixed or mobile. In this chapter, a description of existing configurations from simplest to more complex is presented.

The simplest set up is based on a camera and known 3D control points which enables to obtain the 6 dof orientation among both elements (see figure 10). This is commonly used to track 6 dof measuring accessories (T-Mac©, T-Scan©, etc.), to verify or correct the positioning accuracy of a robot or even to estimate the relative orientation between a referenced image and an unreferenced one. The algorithm that is implemented to solve this application is called space resection [78–81] and it enables not only to estimate external camera orientation, but also intrinsic calibration if the distribution of control points is suitable. The main drawback of this approach is the achievable accuracy for XYZ translation values because of the high correlation among pitch and yaw angles with planar translation components. An example of this approach is the Metronor © or T-Probe© sensor from Leica© LTs. In both cases, a measuring probe with known targets is tracked in 6 dof for 3D inspection tasks.

a	*b*

Figure 10. Metronor©(a) portable mono camera CMM [82] *and b)hand-held touch T-probe© accessory*[83]

In order to achieve higher triangulation accuracy and therefore less XYZ point uncertainty, stereo solutions or multi-view ones are employed (see figure 11). Stereo systems are usually mounted

on a tripod (NIKON K-CMM©, ZEISS COMET©, GOM ATOS 5©) or manually handled (Handyscan©) while multi-view approaches can be materialized with fixed camera structured or handheld approaches. In any case, the camera intrinsic and extrinsic calibration needs to be solved in order to triangulate target points. Whereas fixed installations can measure in real-time (once this calibration is established beforehand), offline processing solutions are usually self-calibrated and are appropriate for static scenery. The greater the number of cameras is, the higher the achievable accuracy for 3D point determination is obtained but a higher data processing requirement is demanded.

In many applications, stereo systems are used to track a measuring tool (METRASCAN 3D©) or monitor multiple points with high dynamics for motion and/or vibration analysis of a component. Even more, deformation of a surface can be measured analyzing imagery data from a speckled surface based on DIC or a part can be scanned combining structured light with stereo triangulation.

a[84]

b[61]

c[85]

d[86]

Figure 11. Stereo approach for optical tracking (a), 3d scanning (b), motion analysis (c) and deformation purposes (d)

Handheld stereo scanning approaches (Handyscan©, FARO Freestyle3D Handheld Laser Scanner©. Etc.) enable to scan complex part or hardly accessible areas based on multiple partial scans that are stitched among them employing reference markers located around the part or scene to be measured. It is important in this case like in other cases where reference targets are used, that the distance among this points is stable during the scanning process as the accuracy of dynamic referencing of each scan directly depends on this requirement. The technology for

scanning is usually combined with active projection schemes such as laser triangulation or fringe projection (see figure 12).

a[87]

b[88]

Figure 12. Stereo handheld scanner with laser strip projection (a) or structured light (b)

Regarding multi-view fixed frame systems [89], they are used to scan a part for inspection purposes of a figure [90,91] and print afterwards a sculpture based on this 3D measurement. One important aspect of these systems is their self-calibration [92] and also stability [93] for long time periods. They can be complemented with structured light when the texture of the element to be measured is not the proper one and therefore surface point definition must be reinforced externally. Another approach is to use only the texture information of surface points based on dense matching techniques for surface reconstruction. Some few industrial solutions are also oriented to verify the shape and dimension of curved pipes as in [94]. See an example of various configurations in figure 13.

a[95]

b[96]

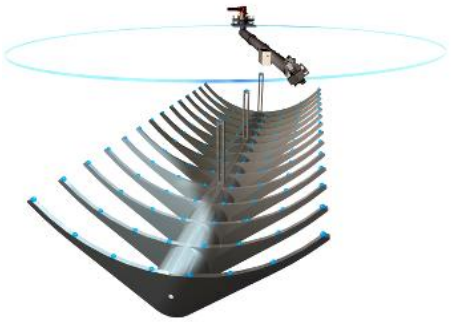

c[97]	d[98]

Figure 13. Fixed multi-view 3d scanning approach (a), measuring cell for tube inspection (b) industrial fixed 3D scanner (c) and customized multi-camera photogrammetric station

Offline multi-view systems (AICON 3D©, TRITOP©, VSTARS©, etc.) are usually based on a high-tech camera or metric camera that is moved around the part to be measured by an operator (see figure 14). From each position, an image is taken with specific procedures and then these image data are processed to obtain 3D coordinates. The XYZ coordinates correspond to artificial targets located above the surface of the part to be checked. These points depict control points for geometric analysis or are used as reference points for further 3D scanning steps (Maxshot©, TRITOP© and GOM 3D scanners). Latest approaches not only enable to solve this photogrammetric problem but based on this output even to reconstruct the surface of the part with dense point clouds. Within this aim, certain surface texture is required to distinguish surface points and their neighborhood points for dense matching reconstruction strategies.

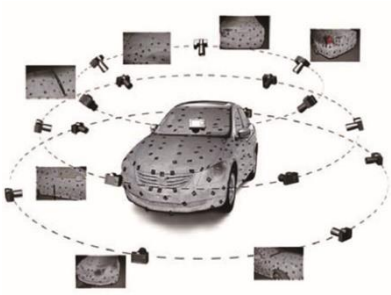

a[99]	b[100]

Figure 14. Offline multi-view approach with hand-held cameras (a, b)

Independently to mentioned configurations, more and more photogrammetric approaches are becoming automatic solutions integrating this measuring capacity in controlled actuators such as robotic manipulators, tables or fixtures. In lab solutions, automatic tables are added to 3D scanners in order to measure without any operator assistance the surface geometry of the part. In in-line use cases (see figure 15), specific measuring cells have been developed as an alternative to traditional CMMs. In some cases, the measuring system is directly attached to an actuator's end-effector and fixed reference points are employed for partial scan fusion whereas other configurations employ this technology for tracking and positioning purposes of touch

probes or scanning 6 dof devices. This kind of integration is targeting to speed up measuring procedures, making more robust photogrammetric solutions with known displacements, enabling automated complex part scanning, automating repetitive measuring tasks, etc.…

	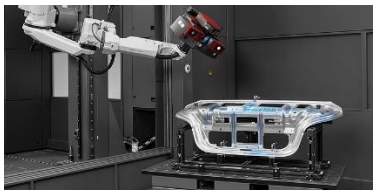	
a[101]	*b*[102]	*c*[103]

Figure 15. Automated photogrammetric solutions

Recently novel measuring set-ups have appeared in the market combining manual and automated employment (hybrid solutions) for specific sectors (for instance dental) and applications (fast scanning of complex parts).

Latest solutions are integrating the measuring technology on the actuator and are taking advantage of the improvement of positioning performance of industrial robots in order to stitch partial scans based on this data fusion. The drawback arises from the accuracy stability requirements from the actuator's side which is not required for previously described solutions. However, the investment is much lower and more and more these solutions called Coordinate Measuring Robot (CMR) are becoming feasible achieving a 100 µm 3D absolute and trackless accuracy (see figure 16).

Figure 16. Example of Coordinate Measuring Robot (CMR)[104]

One of the latest functionalities that have been added to multi-view solutions with light or laser projection (for instance Faro TRACER©), is the capacity to project a light pattern above a scene as a reference for different tasks (see figure 17). For instance, it can be used for part marking

tasks or even as a digital assistant to check if an assembly task or manufacturing process fulfills conformity assessment. It is necessary beforehand to align the part with the digital CAD model in order to take advantage of this virtual inspection assistance.

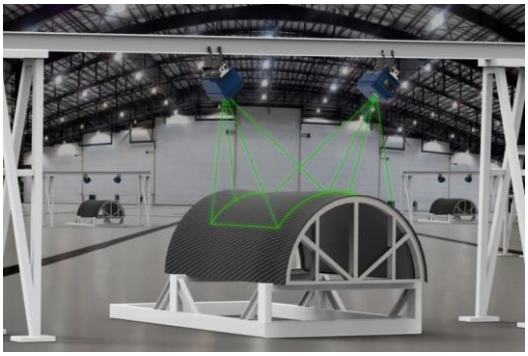

a[105]

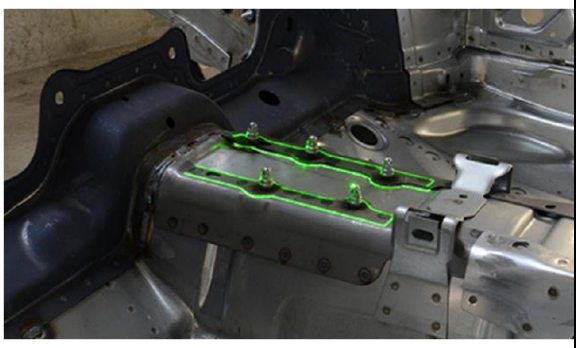

b[106]

Figure 17. Laser (a) and light pattern (b) projection above the part surface for inspection and assembly tasks.

3.3.3 Photogrammetric software and libraries

Photogrammetric software solutions encompass different measuring functionalities depending on the employed hardware approach and covered applications. Indeed, the same hardware configuration can be applied to multiple measuring purposes combining it with specific image processing and photogrammetric solutions. From industrial solutions to academic ones, they enable to measure not only 3D discrete point clouds but to measure dynamic scenarios, real-time data referencing, analyze 3D deformation and motion of components as well as the 3D surface measurement of complex parts. Furthermore, the same software solution can be applied to aerial or close-range applications.

Industrial photogrammetric software packages (TRITOP©, VSTARS©, AICON3D©, etc.) are closely related to technology suppliers and they oblige the user to employ specific hardware set up and even targets. However, there exist some software approaches, which are more flexible (Photo modeler© [107–109], Iwitness© [110–112], etc.) that are opened to different sensor type and configurations. In any case, this software solutions offer the user multiple functionalities integrating high level image data processing algorithms (feature point identification and extraction, Bundle block adjustment, image resection, discrete and triangulation) as well as camera intrinsic calibration or even 3D surface reconstruction based on textured surfaces or projected light patterns above the part to be verified. Apart from measuring capabilities based on image data and photogrammetric models, most of these approaches also consider further 3D data processing functionalities, such as re-alignment of data, geometric element adjustment or even data meshing and edition. Latest software versions are implementing data exchanging options among different approaches in order to standardize data format and analysis in different platforms as well as enable communication among different systems. A suitable example arises from the automation of 3D stereo scanners for in-process quality control purposes. These devices based on software capabilities enable not only 3D

surface scanning and inspection, but real-time live tracking or point or meshes and even CAD-based light pattern projection above the scene for assembly assistance purposes.

Whereas industrial solutions are usually developed for specific solutions, free software libraries (Micmac©, SFM©, etc.), as well as academic GUI approaches [32], offer the possibility to go beyond these functionalities. For example, they enable to generate and foresee the accuracy of 3D scenery based on synthetic images [113,114] or simulate the measuring uncertainty of a camera network located around a 3D part [35]. Moreover, computer vision-based libraries such as Matlab© or Halcon© platforms make possible to develop customized photogrammetric models that can be deeply studied in terms of accuracy and data performance to assure application conformity assessment before sensor materialization. Besides, these libraries speed up customized solution development and validation with high level tested functionalities. A brief comparison of some available industrial tools and their scope is described in [115] whereas a review of open-source applications is presented in [116].

Apart from software for geometric inspection, there exist other solutions that study the 2D and 3D behavior of parts or structures under certain external loads. These software packages (GOM inspect correlation©, Vic-Software©, VIC-2D or VIC-3D©, etc.) enable to study motion, dynamic performance as well as deformation. They are based on image processing algorithms that identify in different image sequences the common points (target points or surface points) among camera views and this manner they can estimate the dynamic behavior of them under the specific test. Some few options are free (and they enable to get closer to this kind of application and understand its limitations

Latest software developments (I-witness Pro-Agilis©, Photomodeler Scanner©, Agisoft Photo Scan©, etc.) are integrating SFM capabilities to traditional photogrammetric software packages in order to broaden imagery data for 3D scanning functionalities. These advanced modules permit not only to calibrate the cameras but also to estimate camera network even without employing physical targets. Furthermore, they are combined with dense matching techniques to reconstruct dense point clouds of textured surfaces. In the market, these solutions are found as 3D image-based scanner or dense matching photogrammetric approaches [117–121].

3.3.4 Automatic camera intrinsic and extrinsic orientation

Camera calibration (intrinsics) as well as camera network calibration (extrinsics) is one of the major issues to be solved in photogrammetric problems. From former solutions that combine manual user assistance to actual systems that automatically carry out self-camera and network orientation, many image processing improvements have been integrated. The automation arises from the employment of coded targets that enable not only to make more robust the correspondence between multiple images and therefore the relative orientation but to scale the output data and speed up BA step. Nevertheless, it supposes to add reference targets above the scene and this task is time-consuming and requires user experience. Hence, avoiding this kind of targets will improve the photogrammetric system performance in terms of time and physical effort. The main drawback comes from accuracy aspects that surely will be decreased (2-3 times) as image processing algorithms are not still good enough as to define natural key points as good reference points. Moreover, acquired image data set and data quality are critical within this aim. Anyway, some software packages have already integrated this as automated target fewer

orientation functionalities and users can take advantage of them considering possible limitations and requirements for a good enough use [112,119,122]. They are based on feature-based matching (FBM) approaches to facilitate fully automatic target-free multi-image network orientation (see the workflow in figure 18). This approach is called SFM photogrammetry [123,124] as mentioned before in this thesis and deals with sparse point cloud reconstruction as well as camera position and orientation determination without a priori data strategy commonly used with target-based approaches.

The image processing workflow follows as:

- Image processing for interest point determination in each image
- Selection of reference image
- Stereo image matching to establish the correspondence among pixels (interest feature points)
- Consecutive resection, triangulation and BA of all image pairs to orient and estimate the coordinates of 3D points in an arbitrary coordinate system with a specific scale.
- Camera self-intrinsic calibration (if required and the geometry is favorable) based on reference feature points

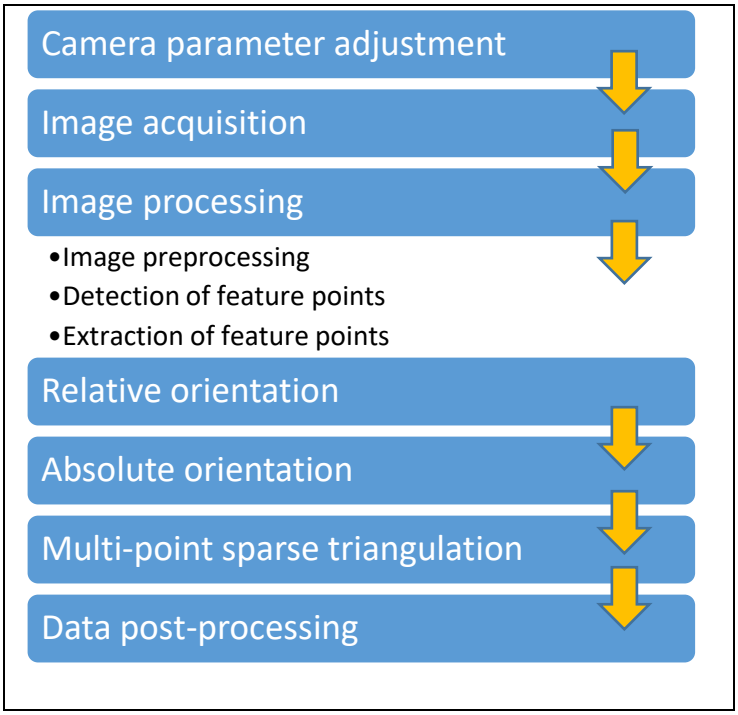

Figure 18. Workflow for 3D object reconstruction from imagery data

Thus, this process can be time-consuming when there are many images. On average, the user should expect that for a 12 – 14 megapixel camera it will take 10-15 seconds per image for the extraction of 50,000 feature points (see figure 19). The matching is carried at generally a few seconds or less per image pair. Thus, a network of ten 14 MPx images, limited to 60,000 feature points per image, is automatically oriented in some 4 minutes on a modern computer.

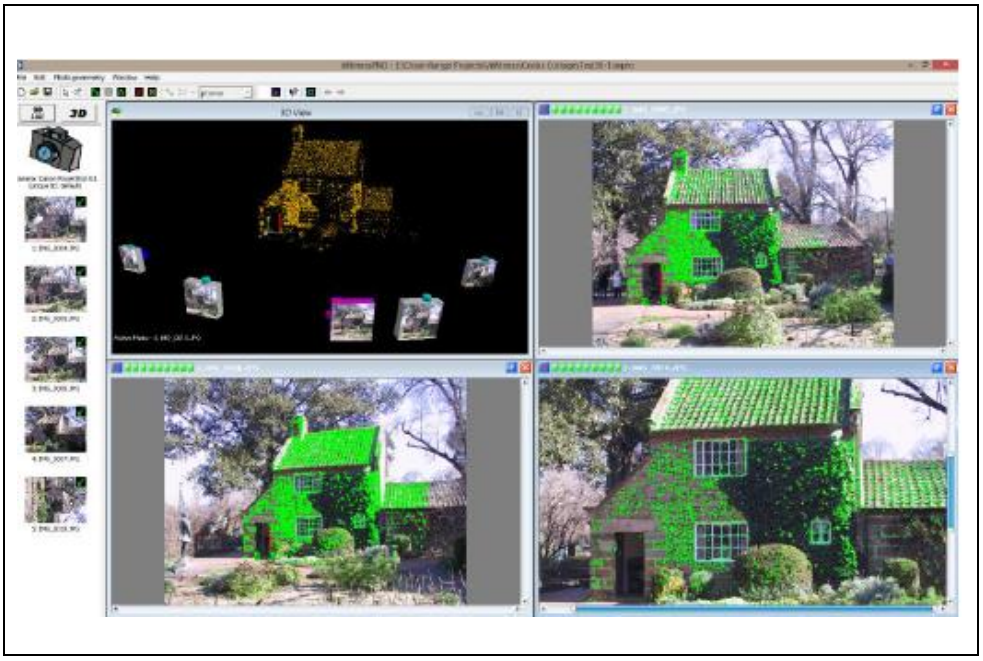

Figure 19. Feature-based camera network orientation (green markers) and sparse point cloud reconstruction (orange markers)

3.3.5 Dense reconstruction

Once the photogrammetric network orientation (stereo or multi-view) has been estimated, the object surface reconstruction via dense image matching or light projection (structured light) can be initiated. In favorable situations, where the scene is texture-rich and the network geometry suitable, it is possible to recover textured 3D surface information to pixel-level resolution without any supporting light projection (see figure 20). Thus, the generated 3D point clouds can be very large, comprising many millions of points. In surfaces where the texture is not available (homogeneous, high reflection surfaces or transparent ones) it is necessary to adapt the surface and project a known light pattern above the part's surface and measure each surface point by means of stereo triangulation.

Whereas fringe projection systems work in real-time, the dense image matching [27] offline process is a time consuming and computationally demanding phase and it can take several minutes to hours to generate the dense 3D point cloud to highest resolution. It is based on semi-global matching algorithms [125] that are well suited and offer a suitable balance between data processing time and accuracy. The core resides on the consecutive stereo matching of image pairs which determine the depth information of each pixel to reconstruct the 3D surface information. Although in photogrammetry other matching approaches have been usually applied (template matching, normalized cross-correlation, epipolar geometry, etc.) these algorithms are not suitable for dense reconstruction as surface point robust description is not fulfilled. This is achieved with robust key feature descriptors based on robust operators such as scale-invariant feature transform (SIFT). The advantage of the semi-global technique (SGM) arises on adding radiometric information of images to stereo matching reducing the computation time and making more accurate the output depth result. A detailed explanation is presented in [126,127]

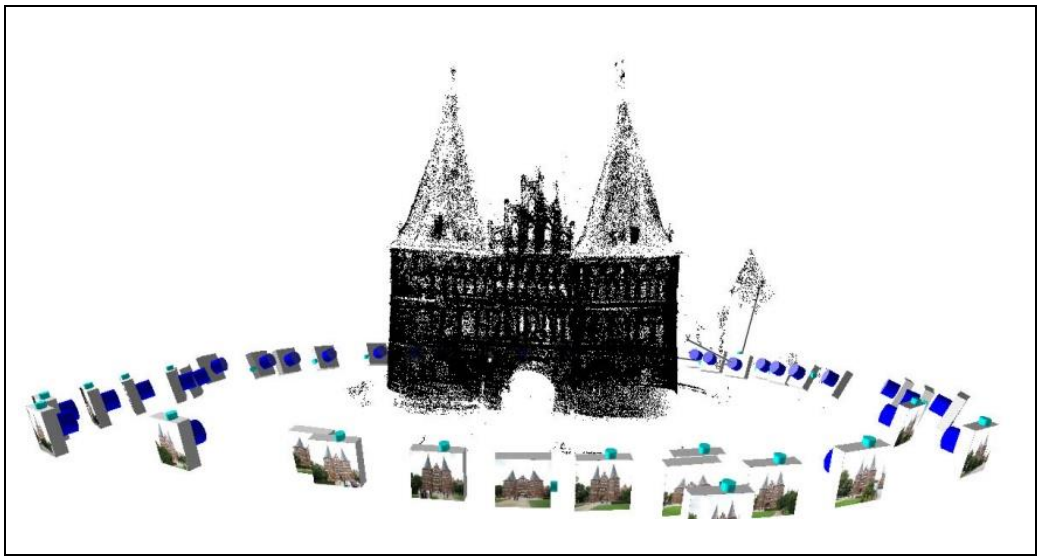

Figure 20. Camera network orientation and dense point cloud reconstruction[128]

Further dense matching algorithms and software versions need to be improved in terms of accuracy and processing speed in order to be considered for industrial applications as an alternative to provide 3D scanning technologies (fringe projection, time of flight, laser triangulation).

3.4 Overview of industrial applications

As photogrammetry has become a very common technique for multi-inspection purposes, there exist multiple industrial applications [6,67,129,130] where it has been tested and implemented as an alternative to other standardized solutions. The main advantage of any photogrammetric configuration is that they can offer non-contact, fast and high data quantity solutions, as well as broad flexibility to adapt for a wide range of measuring scales. These advantages have permitted to replace existing portable technologies with photogrammetric configurations and to go beyond in many cases.

In the following lines, some representative industrial applications are presented in order to show the adaptability of photogrammetry to multiple scenarios and measuring requirements. From static measurements of few points to dense scanning, passing through dynamic applications where the part or structure of interest is under mechanical or thermal load, photogrammetric configurations enable to fulfill many industrial measuring needs. The working scale can also cover a few cms or even measure large components with hundreds of meters.

→ Real-time assistance for assembly tasks

Dynamic referencing of multiple points with real-time photogrammetric approaches can be applied to assembly processed as an assistant and quality control solution. The approach consists on measuring the 3D position of multiple points attached to different objects (fixed one and moving ones) and to estimate in real-time the relative position among them in order to move an bring the parts to their nominal assembly location (see figure 21). This is call

Metrology/Measurement Assisted Assembly (MMA) [131–135]. Some similar applications have been solved until nowadays with LT technologies, combining more than one device for real-time applications. However, there exists an obvious limitation in terms of the number of points that can be measured at once by each system as LT technology only measure a point each time. In this sense, stereo or multi-view photogrammetric approaches present a huge advantage if they can keep on required accuracy and measuring ranges.

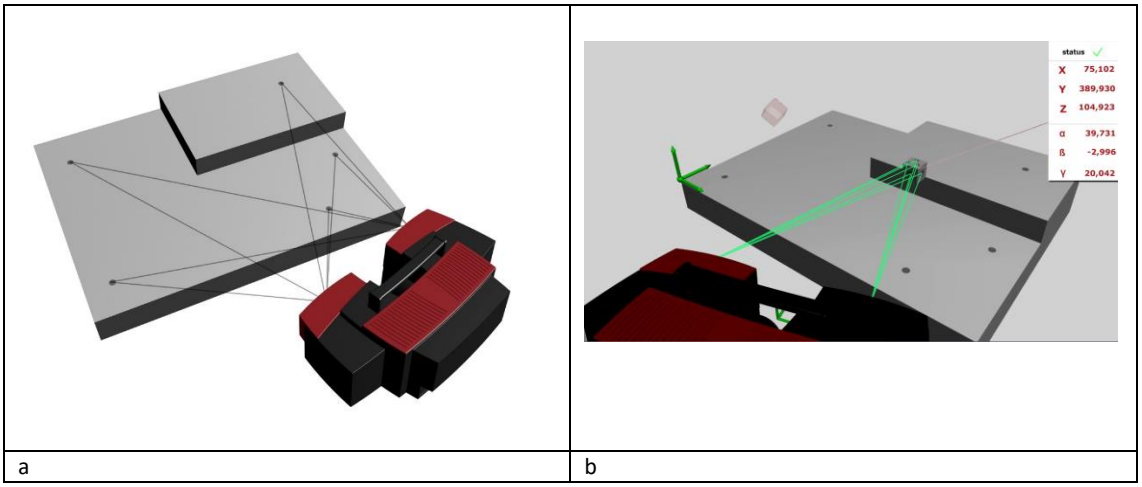

a b

Figure 21. Part positioning assistance according to a fixed reference with multi-point tracking real-time photogrammetry a) Point detection and identification b) 6 dof part monitoring and positioning assistance

→ Deformation analysis

Deformation analysis of static scenes is a common application in industrial photogrammetry to measure how a part geometry is modified under specific mechanical or thermal loads. The approach requires to carry out two independent measurements with or without external loads and then to compare the displacement of the control points. If these points are marked with coded points and a common coordinate system is used for both measurements, the results are directly comparable. If the coordinate system is not fixed between measurements an establishment of a common reference will be necessary to compare obtained results (see examples in figure 22).

This kind of deflection studies can help to improve FEM based simulation and to understand the real behavior of certain parts under specific conditions. For example, it can be used to analyze the deformation of a vacuum vessel or to quantify which the gravity effect above a flexible part is.

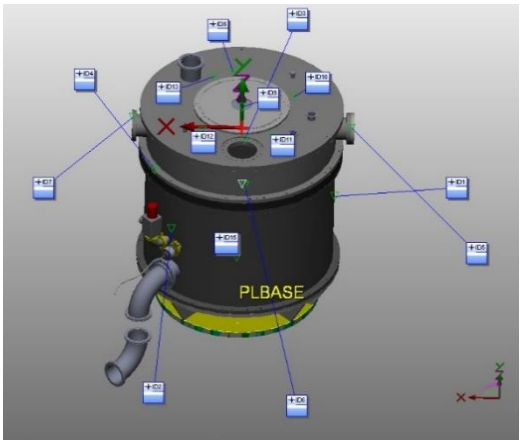

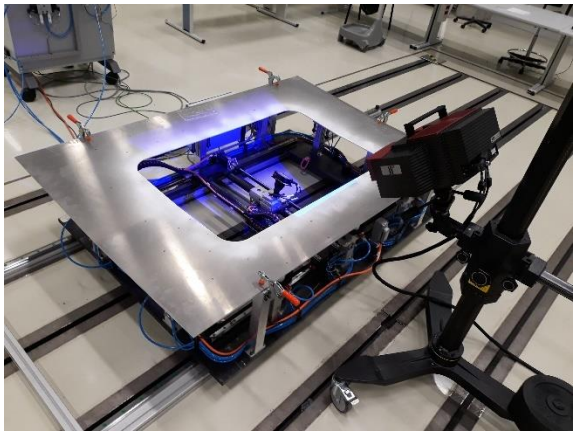

a b

Figure 22. Deformation analysis of vacuum vessel (a) and a flexible part (b)

→ Stability monitoring of large structures

Stereo or multi-view photogrammetric systems enable to monitor the motion and therefore the stability of control points above a rigid structure in order to control its stability through long periods.

If the systems are fixed frames, the drift of 3D points can be directly compared in XYZ coordinate variation, whilst whether the system is not fixed reference points that define the reference frame are required to transform each measurement and allow this data comparison. In figure 23, a hand-held photogrammetric system and reference targets attached to the structure of interest are presented. Usually, other PCMM technologies are employed as certified methods for similar measuring tasks.

An example of a periodic non-fixed solution is presented in [136].

Figure 23. Portable coordinate measuring machines for structural health checking of CERN facilities.

→ Dynamic and vibration performance assessment

High dynamics stereo systems [137] can monitor multiple points with very fast frequencies (up to 4000 Hz) which is useful for dynamic testing of parts and for vibration analysis. If the measuring speed of the system is higher than the required sampling for characterization the vibration modes, this optical approach can be used to acquire a set of consecutive images and by means of motion analysis estimate with is the displacement of each point for applied excitation. In this manner, the vibration of a system can be monitored and quantified as an alternative to existing technologies such as accelerometers or other transducers. Moreover, stereo devices can measure the vibration in a plane or 3D space broadening the applicability of this capability.
In some cases, discrete targets are located above the sample while other times stochastic speckle patterns are printed or projected above the sample surface to increase the number and resolution of available surface points (see figure 24).

An example of the study of wing testing is presented in [138].

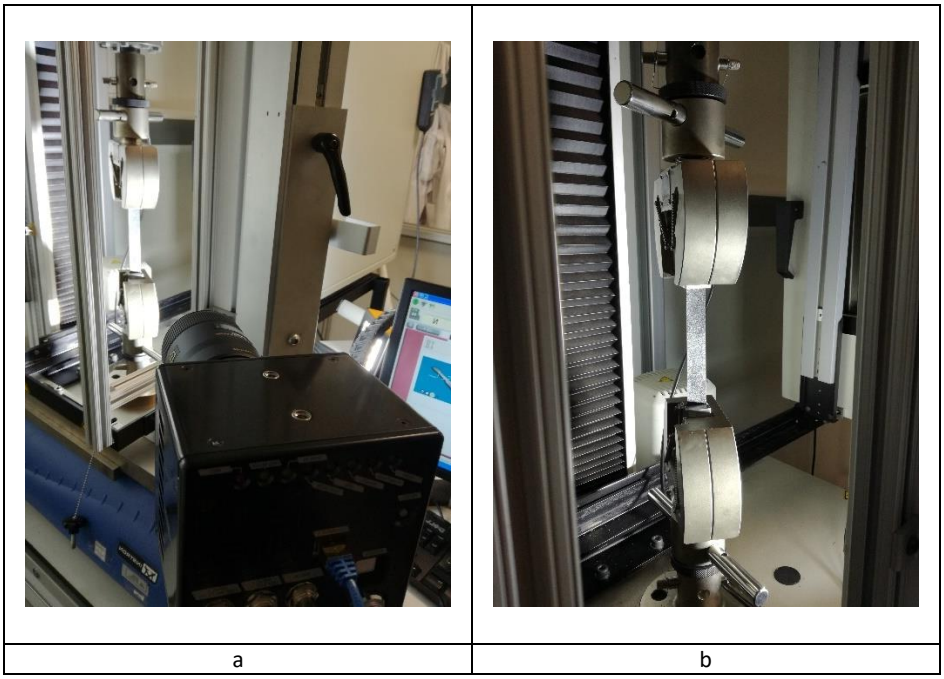

a b

Figure 24. High-speed camera system (a) for traction test with a speckled sample (b)

→ Inspection of solar concentration approaches

Solar concentration approaches are most of the time composed of plane or curved mirror facets mounted on supporting structure that defines the overall shape of the collector. This shape must be controlled during new prototype development and mirror assembly step to assure that real form fits nominal shape and therefore the thermal efficiency of the collector is compliant. Therefore, it is required to measure both geometric shape of all the structure but also the location and orientation of each facet as well as the position of light ray collectors in relation to the collector itself.

Photogrammetry is well-suited to these needs as it enables large scale non-contact measurements of markers located above the collector surfaces [139–142]. Moreover, structure

stability can be analyzed in terms of gravitational and thermal effects and how their variation affects the form of the structure (see figure 25b).

a

b

Figure 25. Calibration of heliostats in a solar plant (a) and cylindrical parabolic concentrator verification (b)

Another approach of photogrammetry deals with supporting structure verification and deformation analysis due to thermal and gravity effects. The solution is called In-line Quality Control for Support Frames of Collector Modules[98]. Other camera-based integrated solutions do calibrate simultaneously the orientation of the heliostats according to fixed references in order to guarantee the tracking of the sun (see figure a).

→ Part inspection and scanning

The most widespread application of the optical measuring system is the inspection and testing of manufactured parts to check if they fulfill their conformity assessment which guarantees afterwards its functionality. From casting parts to machining ones, 3D scanning systems do permit to characterize geometric elements as well as freeform surfaces as part of quality control processes. Moreover, they are well suited to first article inspection (FAI) or even to mass production demands by means of automation of both acquisition and data processing strategies. Resulting sparse point clouds or dense ones do enable to verify part shape and dimensions as well as further data analysis. For example, dense point clouds can be fitted to parametric surfaces by means of reverse engineering and they can also be employed for FEM model validation and adjustment.

Independently to point cloud density, a common procedure to check if the part is fit to purpose is to carry out actual data to CAD comparison as it is shown in figure 26.

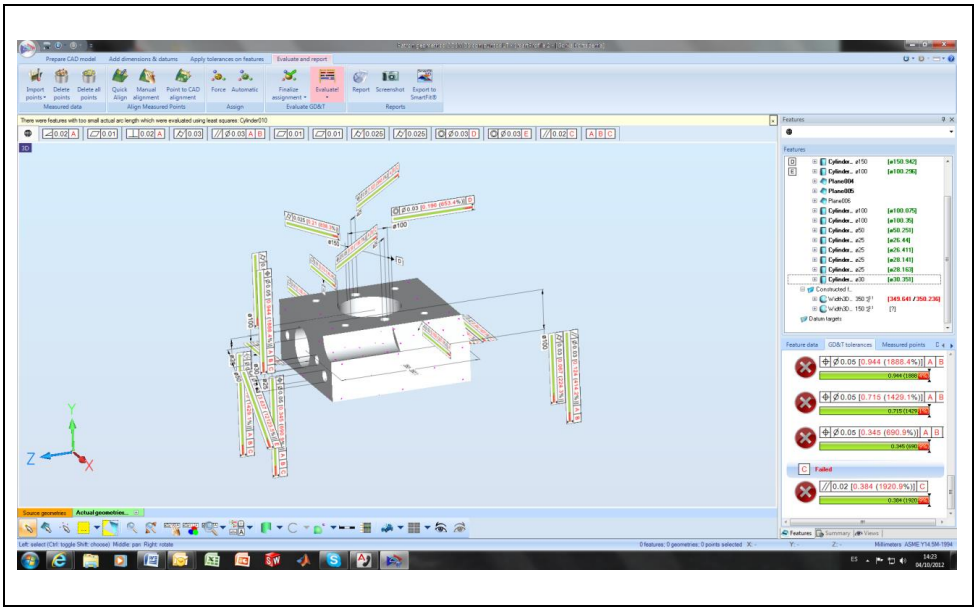

Figure 26. Model-based definition and CAD comparison of surface points

→ Microstructure testing

DIC based approaches can enhance merging manufacturing processes such as laser metal deposition (LMD) additive manufacturing where part geometry is distorted each time a new layer is deposited above the previous one [143]. DIC approach monitors layer deposition process controlling and quantifying material behavior from each deposition to each stabilization. Moreover, it determines surface point deformation and strain from a set of acquired images. The stochastic surface pattern required for image processing algorithms is guaranteed by an external light projection source. In the following figure, part deformation is presented during a phase of the manufacturing process and this result is used to enhance process thermal modelling (see figure 27).

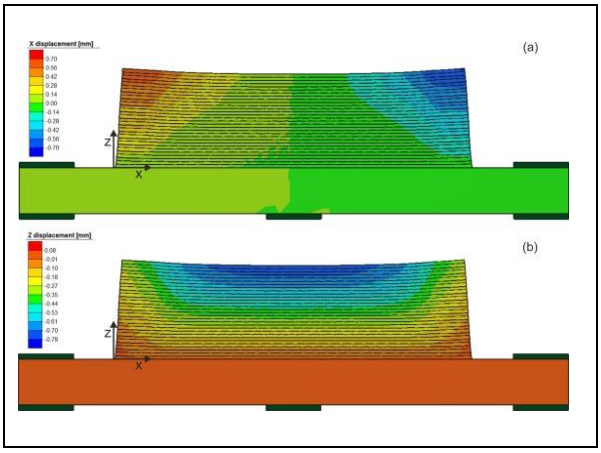

Figure 27. Measurement of in-situ distortions of part geometry

→ Robotic CMM

As mentioned in the classification of photogrammetric configurations, more and more industrial and collaborative robotics are integrating 3D scanning sensors on their end-effector (see figure 28). The goal is to scan a part with high accuracy and flexibility in a few time. Within this aim, former solutions used reference markers located on part supporting fixture in order to transform all the partial scans to a common reference system. This way the robot positioning accuracy is not conditioning the accuracy of the achieved 3D point cloud. Edge-cutting solutions are not using this approach an instead are employing high accuracy robots and their pose positioning values to stitch all partial scan to a common point cloud. Apart from requiring robot accuracy at least during the overall scanning, these solutions are dependent on sense calibration in relation robot base coordinate system. Usually, this is carried out scanning some calibrated geometries in different robot poses which determines the transformation between measuring system coordinate system and robot end-effect point.

Some examples of this kind of measuring solutions are presented below [144].

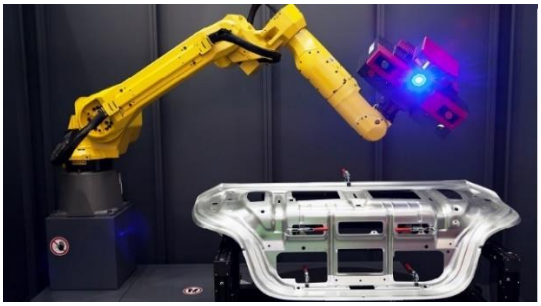

a

b

Figure 28. Robotic CMM with markers all around the fixture (a) and without them (b)[145]

→ Mobile robot and Automatic Guided Vehicle (AGV) localization

Another application of photogrammetry deals with autonomous robot localization [146,147] in relation to known markers located around a workshop. The solution is based on a camera which projects Infra-red (IR) light rays to the environment and receives back the reflection of coded markers located around a workshop. Each marker is coded which enables not only to define the relative position between the marker and the camera, but also the orientation. In this measuring approach, if the camera is attached to a mobile robot, its position and orientation can be controlled in large working areas [148]. The basis for localization estimation is the space resection photogrammetric technique, which estimates where an object is in relation to fixed known marker based on image processing techniques and reprojected image point minimization (see figure 29).

Figure 29. Indoor localization of mobile robots

→ Verification and kinematic calibration of industrial robots

Robot kinematic calibration [149–156] is the process of establishing real kinematic parameters and consequently improving the absolute positioning performance of such systems. Although industrial robots' repeatability can be high, the accuracy is not so. This is due to the lack of identification of real geometric joint and arm dimensions and their relative position. Many methods do already provide robot characterization in terms of kinematic calibration, but most employed methods are based on optical systems such as LT [157,158] or optical CMMs [159,160] (see figure 30 for examples). The calibration process comprises an automatic measurement process which registers a discrete number of robot poses all around its working volume. Once these positions and orientations are measured with external devices, kinematic parameter identification is established by means of iterative minimization strategies. The verification of the adjustment and achieved robot performance is carried out by ISO standards (9283 Robot performance analysis).

a[161]

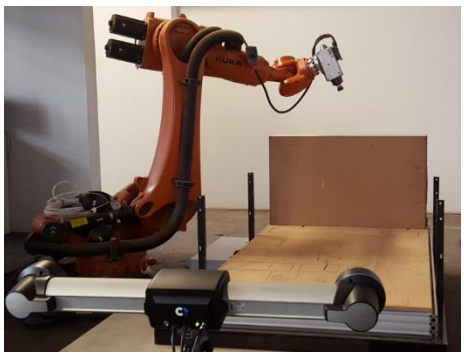

b[162]

Figure 30. Robot calibration approaches a) LT technology b) Optical CMM technology

3.5 Current limitations & barriers

In the following lines, some remarks of current industrial photogrammetric limitations are mentioned from different point of views. Further hardware and software solutions are expected to integrate these missing functionalities to cope with more advanced and flexible solutions.

Simulation:

- Tools for synthetic image generation are missing which could be used to simulate and design the suitability of the image acquisition procedure. Engineering platforms can deal with these issues, but customized solutions need to be prepared and adjusted.
- Lack of industrial simulation tools (SA-VSTARS©) and complexity of turnkey solution development and testing (Matlab©, Halcon©, Phox©) are real. Even more, process optimization from the point of view of the number of cameras and network disposition is still a pendant issue like other complex measuring procedures.
- Available simulation tools require specific measuring setups that not correspond to real procedures and error sources.

Photogrammetric modeling:

- Camera calibration models are not prepared for very wide view angles (fisheye lens) or have view angle limitations.
- Industrial algorithms assuming contour-based photogrammetric measurement are not available for task-specific application requirement. Photogrammetry based on contour-based data is not implemented in commercial solutions.
- Industrial tools are like black boxes which photogrammetric model is not editable at the time being.

Data acquisition & available hardware:

- The addition of dense matching surface reconstruction requires specific image acquisition procedures and parametrization that is not currently defined by equipment manuals.
- High-resolution cameras enable to obtain a higher 3D point resolution but the amount of data that is generated can happen to be memory consuming and big files reduce the yield of data processing software.

Image & data processing

- Smarter and more robust algorithms to solve the image correspondence are required to speed up 3D surface reconstruction approaches where this processing phase conditions further estimations.
- Offline multi-view approaches are time-consuming with a high amount of data which results in reliability decreasing compared with real-time approaches.
- High accuracy automatic image orientation without targets is necessary avoiding target location preparation around the part or the scene to be measured. Another approach could deal with image orientation by means of a fusion of target and markerless methods which would improve the performance of hand-held offline photogrammetric solutions.

- Automated feature-based pattern recognition and therefore triangulation is not a common functionality for industrial software. This should avoid the use of nests to carry out specific geometric element measurement.

Uncertainty assessment

- Accuracy is limited when image resection algorithms are applied because of high parameter correlation among pitch and yaw with planar displacements. Angle measurement restriction can deal with this matter improving achievable accuracy.
- Bundle block adjustment approaches require expert measuring image acquisition procedures to assure model convergence and result achievement below certain threshold values.
- Uncertainty estimation of both intrinsic and extrinsic calibration tasks is missing which directly affects 3D coordinate accuracy.
- Most of the industrial close-range photogrammetric softwares do not offer this functionality as they have not implemented Montecarlo based uncertainty assessment approaches.

General insights

- Although applications dealing with computer vision are using targetless approaches, industrial close-range photogrammetry is based on artificial targets to solve the orientation and triangulation problem, as well as camera calibration with high accuracy.
- Data fusion for multi-modal approaches with several sensor type combination is lacking for industrial application
- Dense reconstruction functionalities. Software packages are adapting to this need.
- Camera and network calibration based on natural features are available, but it must be improved in order to be applied in high accuracy applications.

3.6 Trends and challenges

The trends and challenges of photogrammetric solutions concentrate on developing higher performance systems from the point of view of hardware and software functionalities. This improvement addresses among other higher dynamic applications, accurate markerless approaches for 3D surface reconstruction and multiple feature 3D location, more robust and flexible photogrammetric solutions for integration into production workshops, faster and still higher accuracy solutions with low investment, multi-sensor fusion for advanced applications, higher resolution and point density, etc.

One of the main drawbacks now is still the requirement to use targets for high accuracy approaches both for camera calibration, orientation as well as point triangulation. Although this is partially avoided by means of light projection above the surface, this solution is not flexible for large parts or components. Therefore, smarter image processing algorithms are required not only to increase the accuracy in the triangulation of natural feature points but also for automatic and simultaneous geometric element determination purpose. It is in this scenery where SFM approaches are being fused with traditional photogrammetric solutions aiming to reach high accuracy eliminating the preparation of the surfaces to be studied. Many efforts are still pending to get this goal.

Another main limitation of current systems is the lack of suitable virtual simulation tools fed by synthetic images that could help not only to design a fit to purpose measuring procedure but even to improve it in terms of camera distribution and the number of reference points. Besides, model contemplating contour-based approaches will help to solve different applications such as bin-picking or live tracking of geometric components without markers.

Finally, camera orientation approaches might be improved by known restrictions in order to gain accuracy of specific parameters and minimize the high correlation among camera center rotation and translation among multi-view approaches. The control of restricted degrees of freedom for some parameters could help the photogrammetric user to obtain higher accuracy results as well as simplify the image acquisition procedure.

Some examples of coming research that it is not still integrated into industrial solutions are introduced and mentioned below.

3D thermal mapping

3D thermal mapping means to obtain 3D point clouds with thermal values for each point. It is a fusion of 3D scanning and infra-red (IR) vision to achieve multi-modal data of scenes where there is a need for monitoring both geometric and thermal information. First, a calibration between employed technologies must be solved with and secondly a data mapping is carried to assign thermal data to 3 points or vice versa. It can be very useful in applications where a high correlation between both magnitudes is present. For example, in applications related to energy [163,164] or emerging manufacturing processes based on laser material deposition.

Dense matching of textured surfaces

Dense matching technologies are usually applied in computer vision applications to scan textured parts [27,120,165,166]. However, its adaptation to industrial parts is still a pending issue. Although the latest software packages are adapting this functionality, it is not by far a standard procedure and therefore it must be studied in more detail for industrial part inspection purposes. Aspects such as data resolution, processing time and spatial accuracy of automatic approaches will directly define the scope and adaptability of these techniques for industrial requirements.

Its main novelty arises from feature-based camera calibration and camera network automatic estimation which reduces the achievable accuracy of the photogrammetric problem. As a reference, accuracy of 2-3 times less is achieved compared to traditional photogrammetry based on targets. This accuracy needs to be improved to replace traditional approach and within this aim better image data processing algorithms are required. The time-consuming processing time for large data sets has also to be optimized by fast data handling strategies.

Constrained modelling

In many photogrammetric scenarios, the employed photogrammetric models to solve camera calibration, camera orientation, as well as 3D point achievement, are ill-conditioned due to

restrictions in terms of acquired images or even available 2D data corresponding to control and reference point on the images. This matter directly affects the output results and their uncertainty which may not fulfill the conformity assessment. A possible alternative to improve this limitation is to add restrictions for space resection and bundle block adjustment algorithm in order to make easier and more robust their performance and therefore to obtain more accurate and reliable results. These restrictions can be applied in terms of known camera calibration or camera network orientation values, which would improve camera position and 3D point coordinate estimation.

Simultaneous multiple feature measurement

In many photogrammetric applications there exist a need to measure multiple geometric elements at once and this is accomplished by locating target adapters above the geometries of interest. As the number of these elements increases the number of adapters increase proportionally which means that the investment for hundreds of control point is high as well as the required time to prepare the scene. Another limitation arises from the point of view of part dimension where the location of these adapters becomes a hard task when the accessibility to the part must be supported with extra structures such as ladders or bigger structures. Considering these limitations, novel photogrammetric solutions should enable to replace this inspection procedure with feature-based methods avoiding the need for adapters and maintaining the same accuracy level. Within this aim, image processing algorithms for customized geometry identification based on nominal data and triangulation must be improved. Now, this functionality is lacking in industrial software packages or must be manually assisted which is not efficient for multiple elements. Therefore, CAD data-based optical pointing functionalities, as well as feature detection and multi-point automatic triangulation, will enhance current system capabilities.

Multi-task simulation tools

Although few software packages offer the possibility to roughly estimate the relative accuracy of the bundle block adjustment or even to estimate the uncertainty of the 3D points, the simulation capabilities of current tools are very limited. Moreover, a combination of inspection 3D software and photogrammetric software is required for this which is not convenient from the point of view of the user. Besides, this simulation solution only offers the possibility to estimate the uncertainty of control points defined by targets and they do not integrate other photogrammetric models that are not based in point triangulation (for example contour-based approaches). Further software packages should include this kind of functionalities to fulfill industrial requirements and assure more suitable use of this kind of technologies. An example of a virtual planning environment for automated 3D scanning is the Virtual Measuring Room (VMR©) platform of GOM©, which deals with photogrammetric simulation and robotic scanning offline simulation and robot measuring path programming.

4 MATERIALS AND METHODS

The methodologies employed in this thesis follow the main steps of any photogrammetric solution applying some improvements and modifications in terms of image processing and novel model development to a traditional workflow. These methods are also employed as the basis for remote sensing approaches. It is important to remark and highlight the close relationship between computer vision and photogrammetry and how they share common problems. Principle differences arise from accuracy aspects that are tightened in photogrammetric applications.

In order to understand better what the basis of all case studies are, some general remarks of what is required in each step are mentioned and highlighted in this chapter. The goal is not going in deep detail for each matter, but to explain what it is about and give suitable references in case more detailed analysis from readers is required.

Moreover, the contribution of this thesis is presented in the workflow where meaningful approaches have been developed and adapted as an alternative to usual methods. Although each case study in chapter 5 is solved independently, contributions are introduced in the overall photogrammetric workflow to place each enhancement in its corresponding processing step. The objective is to enable applying these improvements in further solutions where it proceeds. As it is presented below, the thesis has provided new methods to simulate the performance of specific measuring models, it has developed new images acquisition procedures, it has employed a priori CAD data to enhance point detection, it has employed imagery data for surface point reconstruction, etc…

4.1 Fundamentals and description

Photogrammetry is a measuring technique based on images that reconstruct 3D information by means of the triangulation principle. If an object point is seen by two images from different known locations and the correspondence of image points is established, mathematical models permit to intersect this object point and to obtain its 3D information (XYZ coordinates). Hence, two general problems have to figure out, calibration and point triangulation. Whereas calibration comprises intrinsic and extrinsic parameter identification, triangulation faces 3D point reconstruction from homologous image points in several images.

In general, photogrammetry is a science or technology that enables to obtain 3D precise information from 2D image data sets of one (mono), two (stereo) or several views (multi-view). It is based on a camera model which tries to describe how the light behaves when it is projected from the 3D scene to 2D image plane through a camera lens. The fundamentals for any approach deal with camera calibration, point identification and matching, exterior orientation and 3D point triangulation.

The overall problem is also known as SFM which deals with the same matter for 3D scanning, referencing or augmented reality applications based on feature points and matching (FM). Both approaches require to estimate the orientation (poses) of employed calibrated cameras in order to triangulate corresponding points from 2D data sets and reconstruct the 3D information (see figure 31). Whereas photogrammetry is oriented to sparse point cloud estimation, SFM combined with dense matching targets to obtain dense point clouds once the photogrammetric step has been solved based. Many applications (robot navigation, augmented reality, computer vision, autonomous driving) must solve this problem in order to track, scan or characterize 3D scenarios from camera sensor technology.

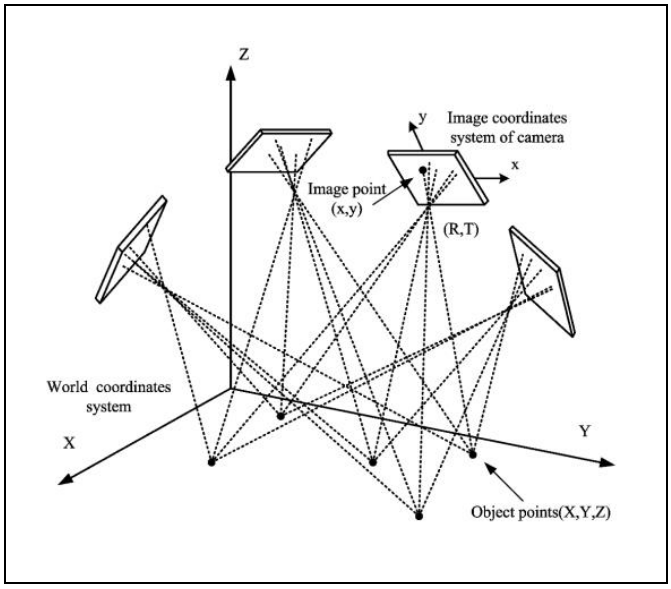

Figure 31. Structure from motion problem[167]

Aiming 3D point and camera motion estimation, the workflow consists of the following steps and workflow:

1. Offline camera intrinsic calibration
2. Preparation of the object and measuring scenario. Target and scale bar positioning.
3. Image acquisition
4. Image processing for detection, identification and extraction of coded and non-coded targets and geometric features through all acquired images. Outlier image point detection and rejection.
5. For each stereo pair of consecutive images, the correspondence among image data points is established. Key points are detected and identified, the image point data is extracted based on different operators and finally, the matching among inlier points is determined. Image point codification is used to automate relative orientation estimation based on coded targets. This correspondence among 2D data sets is saved in a structure that defines the relationship among data points (coded and not coded) and cameras.
6. Based on previously determined image data, the relative pose (camera orientation and location) is estimated according to a previous camera view.
7. Each relative pose is transformed into the first camera view in order to define a common and absolute coordinate system.
8. 3D rough points are estimated by means of triangulation based on absolute camera poses and corresponding matched image points.

9. BA refinement method is applied to estimate camera poses and 3D points that minimize the overall mean error among observed points and reprojected ones for every camera view. If the image data set is well-conditioned, even intrinsic calibration can be solved by BA methods.
10. The 3D scene is scaled up and rigidly transformed to world coordinate system that finally represents the output results (3D points and camera poses).

Whereas offline photogrammetric systems do need to go through all these steps to solve point triangulation, real-time systems carry out the calibration prior to measurements (offline approach) thus they can directly apply triangulation (see the workflow in Figure 32). Anyway, point identification and matching are also required previous to multi-point triangulation.

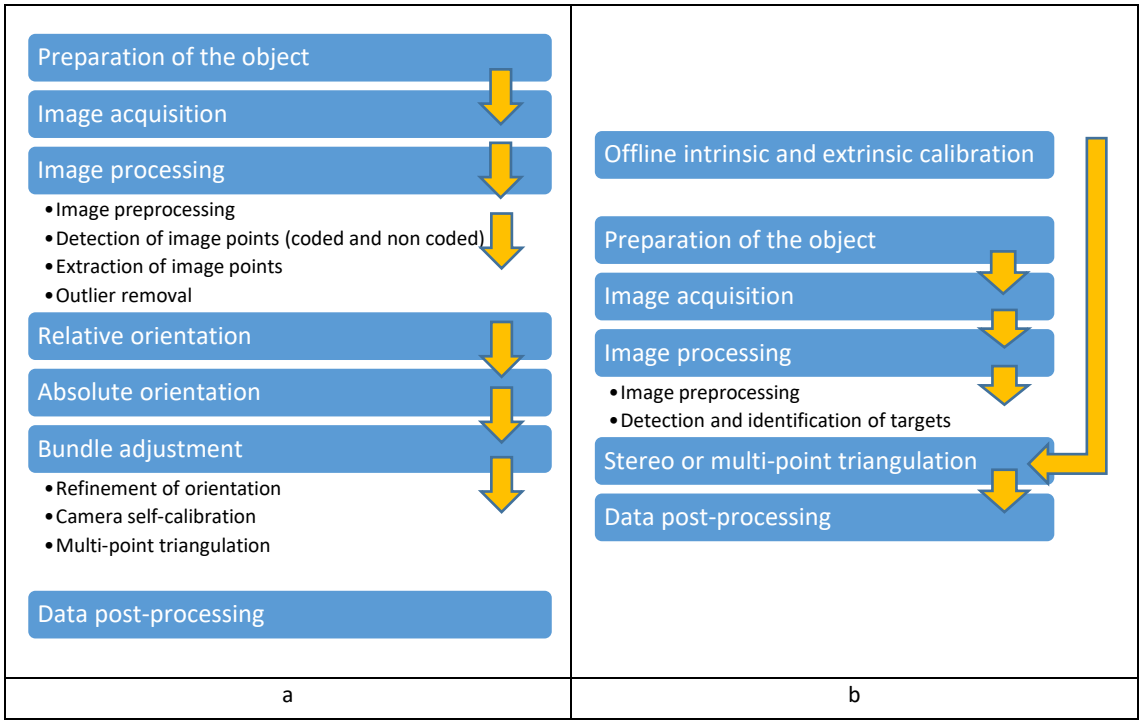

Figure 32. Offline (a) and online (b) photogrammetric workflow

In the case of dense 3D reconstruction applications, the previous result is employed as input data to estimate interactively a dense matched set of points trough all images and compute surface 3D points. However, the camera network and absolute poses are already known, as well as camera intrinsic parameters. The workflow for this use case is similar but the operators and algorithms for surface point determination are different as well as available information quantity management and accuracy aspects in 3D point determination. In fact, although the camera network geometry is well known, accurate and continuous surface data reconstruction strongly depends on rich surface texture and image data similarity from different views. If all these parameters are well-conditioned, even pixel-level resolution can be achieved depicting very large point clouds (millions of points).

4.2 Coordinate systems and data transformation

Defining the different coordinate systems in a photogrammetric approach is important to follow the meaning of employed parameters and to understand which the relationship among them is and how 2D image points are transformed to 3D spatial points. From raw image data in pixel coordinates to metric image points and output object points, the extracted data from imagery is transformed among different coordinate systems which is the basis of photogrammetric modelling. Therefore, a detailed description of each CS is presented as follows:

4.2.1 Pixel coordinate system

The origin of a pixel CS is usually defined in the upper left side of an image (see figure 33), with the axis pointing left to right (columns) and up to down (rows) directions with increasing pixel coordinates. This CS is a method to discretize the image data and use the same criteria for all local image and data sets. Although the column and row number are fixed, the extracted data can deal with sub-pixel accuracy which directly improves the final accuracy of the employed model.

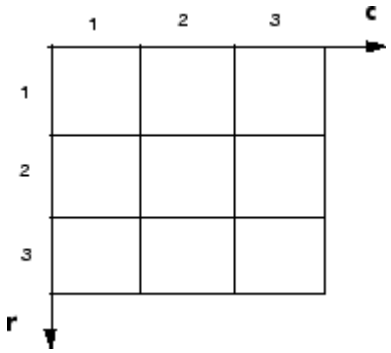

Figure 33. Pixel coordinate system

4.2.2 Image point coordinate system

Once the image data has been detected and extracted in pixel CS, it is usually transformed to image point CS (2D). The employed parameter to convert pixel coordinates to image point is the pixel size in metric units (see figure 34). This is an intrinsic characteristic of each camera and enables represent the data of interest in metric coordinates. Apart from this, it is common to change the origin of the CS to the principal point which corresponds to the intersection of the camera projection axis and image plane. Axis orientation is also modified to make Z axis the one out of the plane, but this rotation depends on employed model criteria.

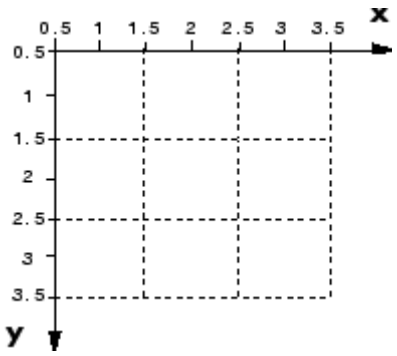

Figure 34. Image coordinate system

4.2.3 Camera coordinate system

Camera CS is a 3D reference system parallel to image CS (see figure 35). In fact, it is similar to an image point CS but with an origin translated the principal distance value in the Z axis. This manner, the image points are converted to 3D space adding a Z coordinate which corresponds to the principal distance parameter (f).

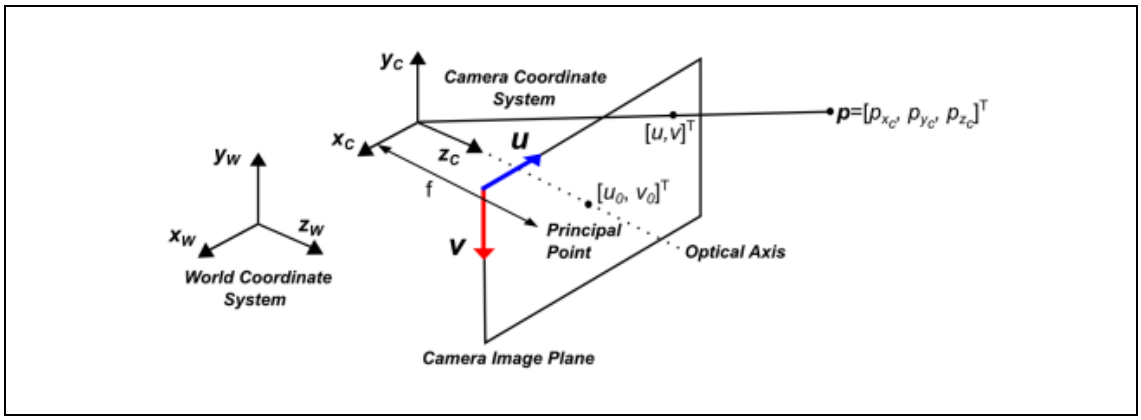

Figure 35.Camera coordinate system

4.2.4 Object or World point coordinate system

The object CS, also called world CS, is the common reference for all image CS and it is the one the output results are referred to (see figure 36). The object CS can be defined with known control points or sometimes it corresponds to a reference camera CS (usually the first). Both camera extrinsics and object 3D point coordinates corresponding to a photogrammetric solution, are expressed in relation to this CS. In order to change this reference, rigid transformation is usually applied based on fitted geometric elements, required control points or even calibrated artifact.

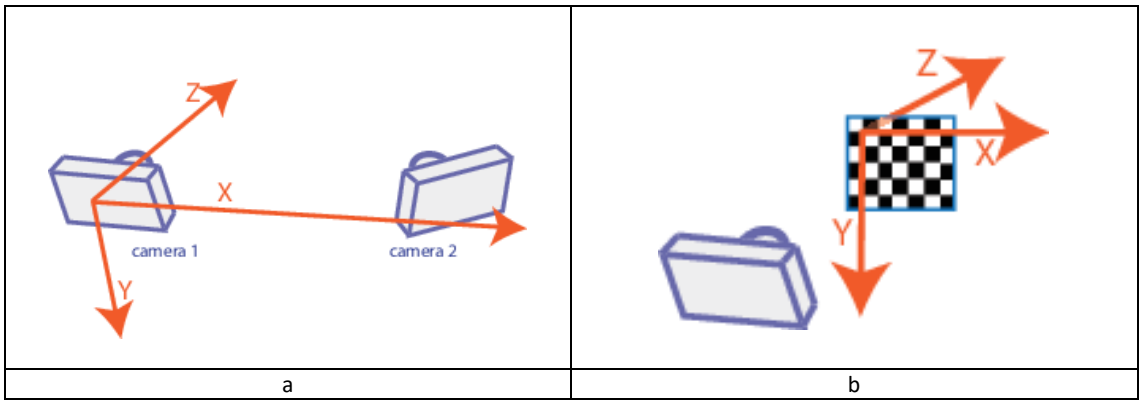

a b

Figure 36. Object coordinate system. Camera-based world CS (a) and Calibration Pattern-Based Coordinate System (b)

4.2.5 Transformation among CS

In order to transform image data from CS to another, as well as to change the CS they are referred to, rigid plane and spatial transformations are applied. A transformation deals with not only the translation of the CS's origin [X_0, Y_0, Z_0] but also with the rotation of the axis ($R=R_x*R_y*Rz$). Whereas plane rigid transformation is based on 3 dof, spatial affine transformation requires to know 6 dof (translation=3 & rotation=3) among the reference and target CS (see equation 2).

Plane transformation and rigid affine 3D transformation are defined as follows (rotation and translation criteria):

$$X = X_0 + R * X \tag{1}$$

$$\begin{bmatrix} X \\ Y \\ Z \end{bmatrix} = \begin{bmatrix} X_0 \\ Y_0 \\ Z_0 \end{bmatrix} + \begin{bmatrix} cos\varphi cos\kappa & -cos\varphi sin\kappa & sin\varphi \\ cos\omega sin\kappa + sin\omega sin\varphi cos\kappa & cos\omega cos\kappa - sin\omega sin\varphi sin\kappa & -sin\omega cos\varphi \\ sin\omega sin\kappa - cos\omega sin\varphi cos\kappa & sin\omega cos\kappa + cos\omega sin\varphi sin\kappa & cos\omega cos\varphi \end{bmatrix} * \begin{bmatrix} x \\ y \\ z \end{bmatrix} \tag{2}$$

Where planar transformation is a simplification of spatial transformation where translation in Z_0=0 and rotations around X (R_w) and Y axis (R_ϕ) are null.

4.3 Central projection camera model and collinearity equations

In many fields such as photogrammetry, augmented reality and computer vision applications it is usual to employ camera sets to measure 3D points from 2D image data. Traditionally the pinhole camera model is used to describe how a 3D world point (P) in the object space is projected towards an image plane defining a 2D pixel point (P'). This model does not consider a lens and assumes that the aperture of that camera is a discrete point (O) (see figure 37). Thus, no geometric lens distortion nor other optical errors in scene focusing and light projection behavior is included. Therefore, these models are usually complemented with lens distortion

parameters (radial, tangential) to characterize in a more realistic manner light performance through a camera lens.

As a mathematical definition of this behavior, collinearity equations are used, which materialize a pinhole camera model considering distortion parameters. Therefore, a pinhole camera model can be compensated for becoming a representative model of how a camera model depicts a 3D scene.

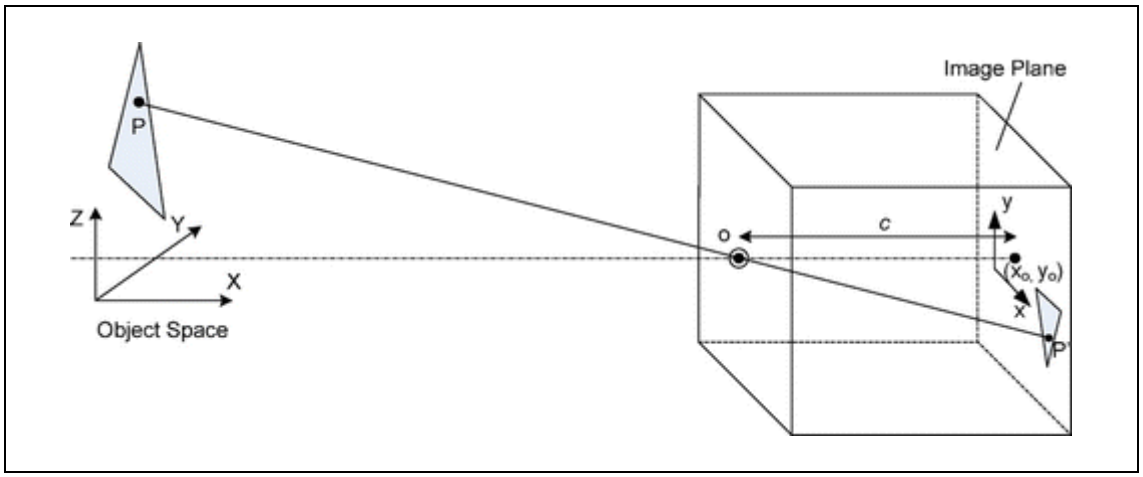

Figure 37. Pinhole camera model and 3D object to 2D image plane projection

The collinearity equations (see equations 3 & 4) are a set of two equations that correspond to the central projection of a 3D world point into a 2D image point. They use the compensated pinhole camera model to approximate how the light is projected from the 3D scene to 2D image plane considering and optical center and real optical aberrations.

$$x - x_0 = -c\frac{m_{11}(X-X_0)+m_{21}(Y-Y_0)+m_{31}(Z-Z_0)}{m_{13}(X-X_0)+m_{23}(Y-Y_0)+m_{33}(Z-Z_0)} + \Delta y \quad (3)$$

$$y - y_0 = -c\frac{m_{12}(X-X_0)+m_{22}(Y-Y_0)+m_{32}(Z-Z_0)}{m_{13}(X-X_0)+m_{23}(Y-Y_0)+m_{33}(Z-Z_0)} + \Delta x \quad (4)$$

Where,

x, y: image point coordinates
x_0, y_0: principal point coordinates
c: focal length
X_0, Y_0, Z_0: projection center coordinates in the reference coordinate system

X, Y, Z: object coordinates in the reference coordinate system
mij = rotation matrix elements (M) between the image coordinate system and reference coordinate system
Δx, Δy = additional parameters corresponding to distortion parameters

Δx and Δy systematic distortion errors are defined in different ways depending on the implementation but some examples are Brown and Fraser models [168]. An example of a

polynomial description of the radial distortion is presented in equations 5 and 6, where r is the radial distance of the pixel from the principal point and x or y are the image coordinates of the corresponding pixels.

$$\Delta x = x\frac{\Delta r_{rad}}{r}; \qquad \Delta y = y\frac{\Delta r_{rad}}{r} \tag{5}$$

$$\Delta r_{rad} = K_0 r + K_1 r^3 + K_2 r^5 + K_3 r^7 \tag{6}$$

It is important to remark that the pinhole camera is representative of wide-angle lens behavior but is not applicable to lenses with a higher view angle such as a fisheye lens. This kind of lenses is usually modeled by adapted polynomial equations that fit better to their working performance and optical aberrations [169–171]. Nevertheless, this kind of lenses is not so common in industrial fields although they are advisable when a large field of views are required with sort working distances.

4.4 Geometric constraints

Geometric constraints are common for any photogrammetric set-up as they describe the theoretical assumptions and mathematical foundations of light ray performance. These constraints are the basis for camera modelling and algorithms solving the correspondence problem n. Hence, the photogrammetric methods are based on these fundamentals to simplify light behavior and projection from 3D space to the image plane. Moreover, they try to avoid geometric ambiguities of central projection principles.

Three main constraints are the basics of photogrammetry: collinearity, coplanarity, and coangularity [172]. Whereas collinearity is considered in every camera set-up, coplanarity and coangularity restrictions are applied among different cameras to set their relative absolute orientation.

Collinear means that several points are lying on the same line. This description applied to photogrammetry describes the central projection of a 3D point to the image plane (2D point) through the camera model projection center. Collinearity equations do define mathematically this behavior (see figure 37).

Coplanar means that several points are lying on the same plane. This is common in stereo pairs where a 3D point, its corresponding 2D image points and both camera projection center are part of the same plane (see figure 38). This is the basis of the correspondence problem and simplifies its resolution by means of epipolar geometry considerations.

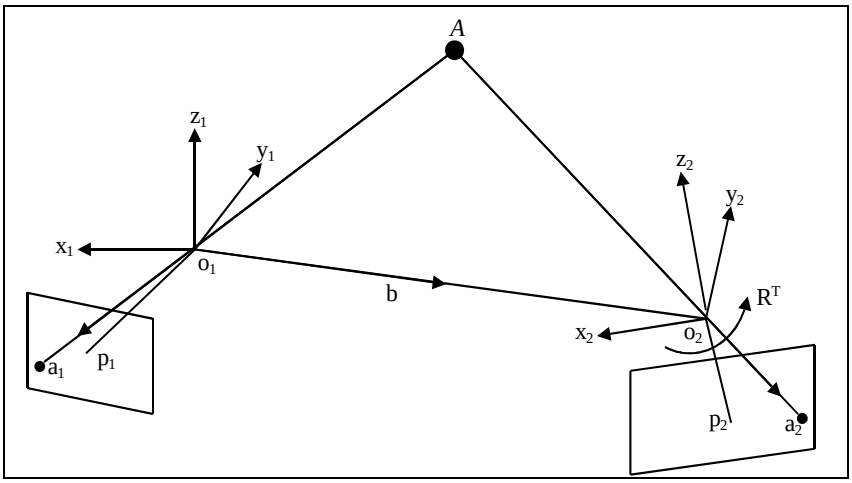

Figure 38. Coplanarity condition in a stereo pair

Coangular means that the angle between two points is the same in different projection planes. Applied to photogrammetry means that the angle between two given points seen from the projection center in the object space is equal to the angle between the images of these points (see figure 39). This restriction is useful to solve space resection problem by means of trigonometric relationships and considerations.

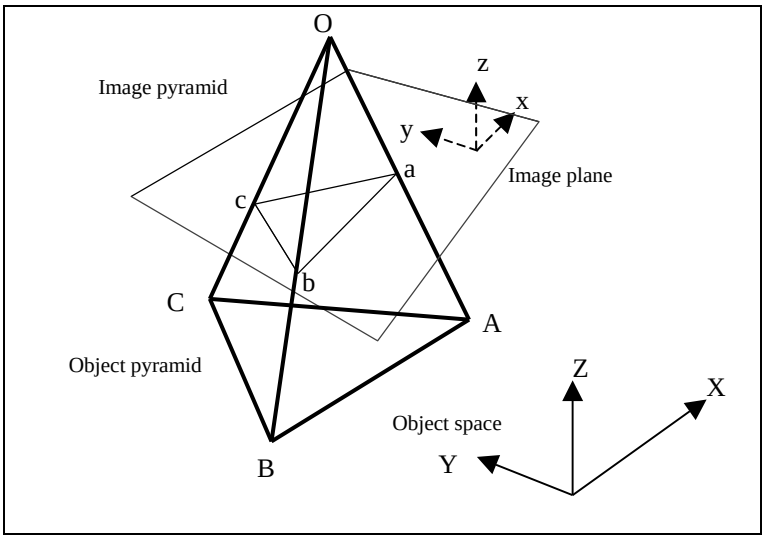

Figure 39. Coangularity condition

4.5 Camera calibration

As mentioned before, SFM methods are based on calibrated cameras which means that the intrinsic parameters, as well as lens distortion parameters, have already been characterized by means of camera calibration procedures. These methods can be applied offline or inline (self-calibration) and there exist multiple algorithms that overcome this issue. A bibliographic review is presented by [173,174]. Whereas offline methods are easy to apply, and algorithms are available, inline methods are more demanding as they try to solve intrinsic calibration all at once

with camera pose and 3D point determination. For it, camera network, as well as point distribution around the 3D scene, needs to fulfill some requirements and many times the BA problem it is ill-conditioned. Images with camera rotation around the optical axis are recommended to solve these matters and ensure accurate intrinsic parameter identification. These turned images do contribute to figuring out calibration ambiguities due to optical aberration symmetry. Thus, although industrial photogrammetric systems offer this self-calibration functionality, they can also be fed by offline calibration results.

Camera calibration deals with the estimation and correction of camera parameters and optical distortions that do not correspond to ideal pinhole camera performance. Therefore, mechanical constructive and assembly imperfections, as well as optical ones, must be modeled and characterized in order to use them and obtain higher accuracy 3D data. There already exist many different models and mathematical approaches (linear and non-linear methods) that aim to identify these parameters. The most usual ones are direct linear transformation (DLT) [175,176], Tsai [177,178], Zhang [179,180] and Faugeras [181] methods. Others are also used based on these ones or combined models.

However, most of them consider similar error parameters for light 3D to 2D projection. A general brief introduction is presented as follows:

The intrinsic parameters of a camera are defined by the focal length (f) and projection center (C) also called projection point (see figure 40). The focal length describes the normal distance between the image plane and the projection center, whereas the principal point determines which the position of the pinhole center point from which all light rays pass through is. In real cases, both the focal length and principal point need to be corrected due to mechanical manufacturing and assembly imperfections.

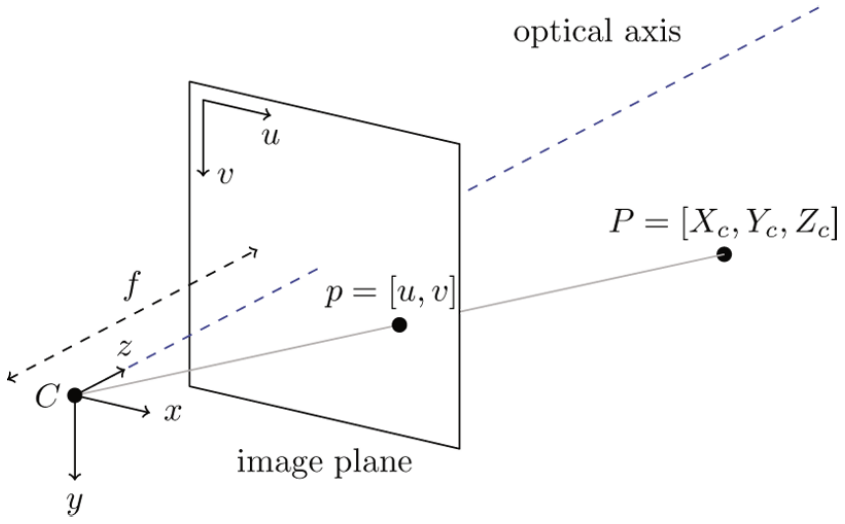

Figure 40. Camera model and intrinsic parameter calibration

Apart from intrinsic camera parameters, there exist other errors related to lens form (radial distortion) and mounting issues (tangential distortion). As the name indicates, each of the errors generates a specific distortion type. Radial distortion (see figure 41) is due to light bending in the lens areas that are far from projection center, whereas tangential distortion (see figure 42)

is because of a misalignment between image plane and lens. Usually, both parts are corrected in collinearity equations as an extra parameter (see equation 3 and 4) which enables to model more realistic 2D and therefore obtaining more accurate 3D points.

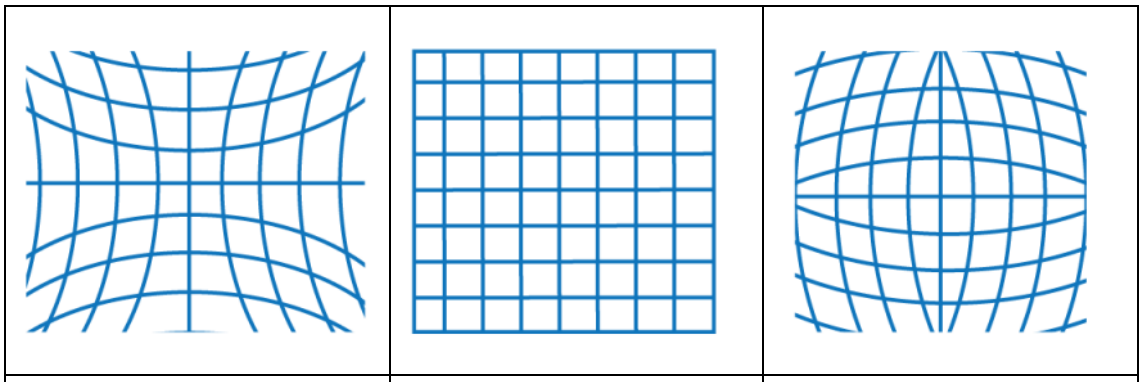

Figure 41. Radial distortion. a) Negative distortion, b) no distortion, c) positive distortion

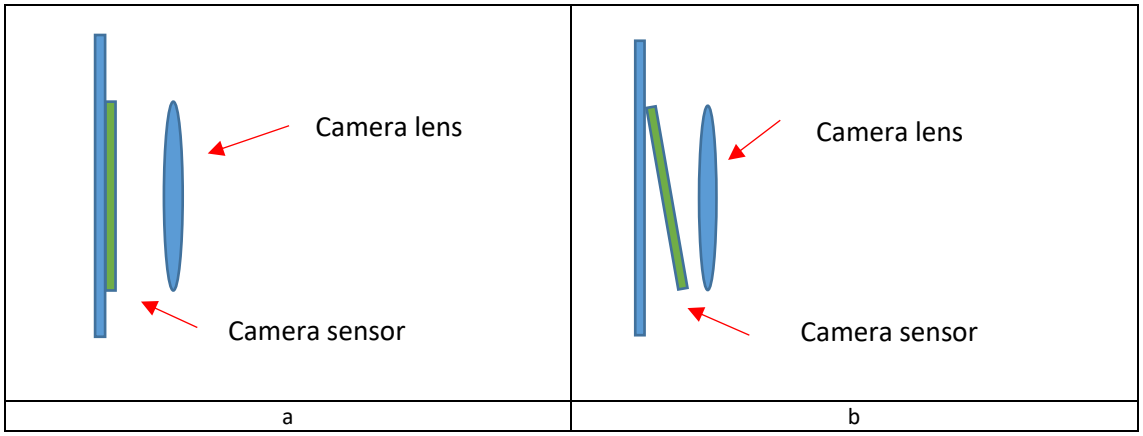

Figure 42. Tangential distortion. a) Zero tangential distortion (sensor and lens parallel) b) Tangential distortion (sensor and lens unparallel)

There exist more complex and complete camera models that consider other optical imperfections as well as specific models for lenses with a high view angle. In this thesis, high tech industrial cameras have been studied which corresponds to described principles and fundamentals.

4.6 Measuring process simulation

The simulation of the measuring process is a demanding task that it is not addressed for many measuring procedures. The simulation in advance of complex measuring procedures is a challenging issue that needs to estimate system reliable performance combining measuring device accuracy (MPE) and measuring scenario restrictions. This capability enables a proper selection not only of the most suitable technology but also designing the measuring procedure and previewing the results that will be obtained during the monitorization. This manner, the acceptance criteria for the measurement is checked before any measuring attempt is carried

out and the feasibility of the measurement is assured. This a priori planning prevents the measuring operator from encountering not previously considered difficulties during the measurement. Another advantage is to design the measurement and to simplify it according to the measuring requirements. The applied methodology that is employed for the simulation comprises these main steps:

- Instrument modeling
- Network definition for target points and instrument location
- Measurement fabrication
- Visibility analysis for the network considering line of sight restrictions and ascertain where measurements can and cannot be taken.
- Parametrization of simulation inputs
- Simulation running
- Uncertainty results analysis

After the results are obtained a new design of the network can be established considering the improvement and optimization of them till measuring requirements are reached. This iteration is sometimes automatic but most of the times requires manual edition based on operator experience.

In order to face the photogrammetric measuring process simulation few industrial tools are available, and their prediction is limited by error source qualitative characterization and implementation. From simulation software for CMMs such as VCMM© (see figure 43) which comprises a full characterization of each influencing parameter to available tools for portable systems, a gap is detected for simulation of photogrammetry. Although academic tools such as Phox© or even the combination of SA© and VSTARS© for simulation do allow to carry out some predictions, they lack the capability of considering multiple critical error sources in photogrammetry. Besides, the uncertainty estimation is focused on point triangulation without considering the uncertainty of intrinsic and extrinsic calibration. Therefore, customized tools or more advanced industrial tools are expected to be developed to fill this need.

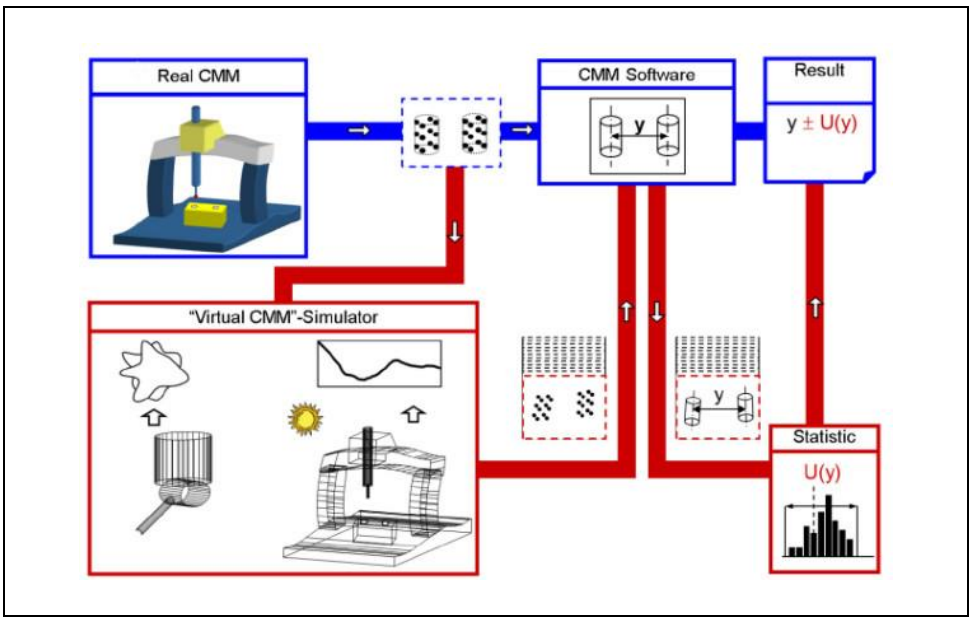

Figure 43. A simulation tool for CMM task-specific measurement and uncertainty assessment

4.6.1 Main contribution

The contribution of the thesis in terms of measuring process deep simulation has been studied in **case study 2** where the pose of the cylinder is estimated with uncertainty values. For this, a Montecarlo based simulation chain has been applied once the geometric model has been developed. This simulation tool is fed by statistical variations of error sources that directly affect the performance and output result of the model. Varying the input values of influencing parameters in each iteration, the probabilistic assessment of the cylinder's pose is established. Studying the standard deviation of the output values distribution it is possible to determine the uncertainty of the cylinder pose which is employed to analyze the conformity assessment of the model in relation to accuracy requirements.

The same approach is applicable to triangulation-based models which is the basis for SA©-VTARS© photogrammetric simulation tool. However, the model is not editable and error source statistical distribution is only applied for image coordinate noise. Hence, the simulation results have to be taken into account as a rough estimation of 3D point uncertainties.

In **case study 1** (see figure 44) the simulation based on Montecarlo applied to LT technology has been employed as an estimation tool quantify the uncertainty of this measuring approach as reference data. As this technology is nowadays established as a certificated method, it is important to control which the accuracy of reference results is. In fact, the described methodology can be used for performance comparison of measuring technologies like LTs, 3D scanners, and photogrammetry-based solutions. All of them are portable CMMs that permit to measure the 3D position of points of a part or structure, so as to carry out the verification and even the monitorization of this kind of components. The differences among them are mainly the accuracy, number of measured points, the measuring speed, range, etc...

A similar simulation but applied to photogrammetry has been employed in **case study 2** (see figure 44) based on point triangulation approach to understand achievable accuracies based on target-based approaches.

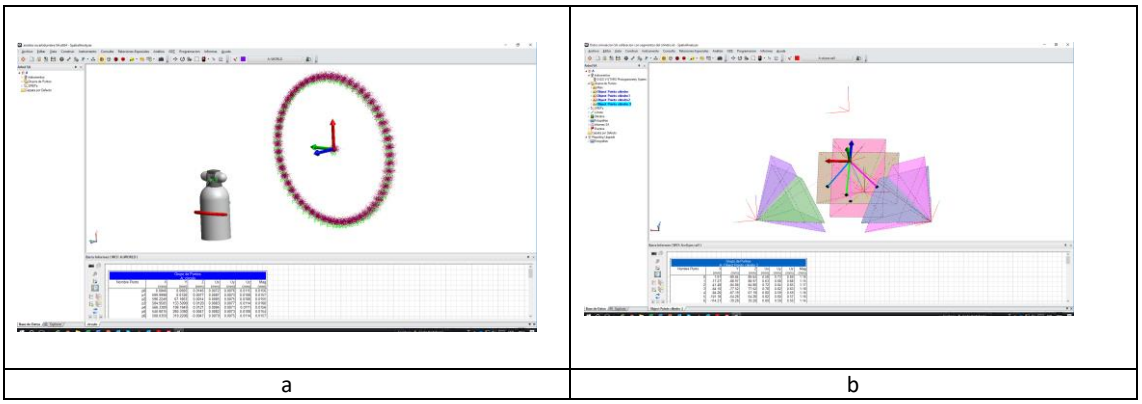

a | b

Figure 44. Uncertainty assessment by means of simulation for point-based approaches in complex measuring procedures. a) LT technology for case study 1 b) Point-based photogrammetry applied to case study 2

4.7 Close-range photogrammetric workflow

Once explained how the camera model is defined, existing geometric limitations, considered lens distortions and mathematical representation of all of it, the traditional photogrammetric workflow is described in more detail to understand which the challenges and limitation of each step and corresponding algorithms are as well as how they are tackled. The simplified workflow is:

1. Offline camera calibration (if required)
2. Preparation of the object
3. Image acquisition
4. Image point detection, identification, and extraction
5. Image matching
6. Relative orientation
7. Exterior orientation
    a. Calibration methods→ space resection, stereo-calibration, self-calibration (BA)
8. Triangulation
9. Scaling and referencing of a 3D scene
10. Output data analysis

4.7.1 Preparation of the object

The preparation of the object and the measuring scenario in photogrammetry is a time-consuming task, especially for large and hardly accessible parts. It supposes to place the artificial targets (coded and non-coded ones, passive or active ones) all around the part considering control points, camera orientation matters, and triangulation aspects. For instance, the criteria for the placement of the coded targets is the following one:

- Minimum 5 common targets between different images. Robustness is improved if they are 8 or more targets
- Size of the target should ensure an approximate image size of 10 pixels (also non-coded targets)
- Do not overexpose or underexpose the reference points
- Keep constant camera settings
- Targets must keep their position
- Camera rotated images are recommended for self-calibration

Besides, specific geometric features do require special adapters to define their location which supposes to acquire or manufacture measuring fixtures to cover such kind of inspection task.

The larger the part is, the more the preparation time is. For example, the preparation of a wind turbine (rather accessible use case) takes approximately one hour of preparation (see figure 45). However, bigger parts or structures can suppose a whole day of preparation. Apart from laying the targets above the object, offline hand-held photogrammetric systems need to place with high stability a calibrated scale bar on the measuring scenario in order to scale up obtained results.

Figure 45. Preparation of the measuring object with targets (coded and uncoded) and calibrated bars

Other aspects that prevent using target are demanding surfaces such as dusty ones, non-alloyed ones or even the ones that irradiate high temperature. In these cases, the placement of targets on the objects is hardly feasible or not enabled which makes more difficult to apply non-contact measuring approaches based on target photogrammetry.

4.7.1.1 Main contribution

The contribution of the thesis regarding object preparation step on a measuring task is straightforward. In fact, all case studies aim to avoid object preparation with artificial targets. In every case, natural features are employed not only for camera orientation estimation but also for 3D object reconstruction. In **case study 1** few targets are used to solve a photogrammetric measurement and to take advantage of camera orientation results which enable to optically detect and estimate the position of specific geometric elements on the images. In **case study 2** contour points of the cylinder are used as input data for the model that estimates the pose of the cylinder. Therefore, targets placed all through the cylinder are not required. Finally, in **case study 3**, both photogrammetry and dense reconstruction are carried out without any target and this approach is compared to traditional one in terms of 3d data reconstruction and achieved accuracy.

Hence, the absence or minimum object preparation is one of the main contributions of the thesis as enables to speed up the measuring processes and put in more flexibility compared to traditionally restricted measuring scenarios.

4.7.2 Image acquisition

Once the scene is prepared, it is necessary to adjust the camera parameters to the lighting conditions of the room where the images are taken. Normally, in a photogrammetric process, the camera adjustment is set on the targets to be measured (maximum aperture and zoom of 10x) combining camera parameters and flash power. Another important parameter is the working distance and depth of field (DOF) which encompass large ranges for industrial lenses. These parameters should be kept constant for the entire measurement to solve the photogrammetric BA.

The identification of the camera with the software is automatic and therefore the parameters related to the sensor (resolution and image dimension) are determined automatically. However, it is necessary to verify these parameters and change them if necessary.

Once the camera and its acquisition parameters have been set-up, the image acquisition process is executed depending on object dimensions, form, and surrounding space. Strictly speaking, usual image acquisition strategies are few and closely related to object form and size. If the object is round or presents 3D geometries, circular strategies are applied whereas the part is rather flat linear strategies do suit. In case the parts are quite small, even images from above of the part can be taken (see figure 46 and VSTARS© reference in annex for more detail). In every case, it is very important to keep constant illumination conditions or at least to set-up a robust camera parametrization to deal with possible variations.

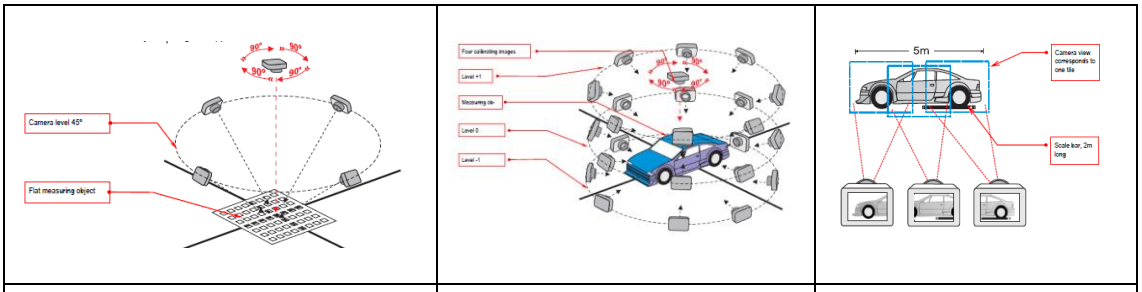

a b c

Figure 46. Shooting methods and strategies a) Camera movement for a flat measuring object b) Camera movement for a 3D object c) Camera movement for a large 3D object

As mentioned in the previous object preparation step, consecutive images do need to ensure an overlapping among the field of views which guarantees the relative orientation and consequently absolute one among all images. Coded targets are usually employed as a reference to solve the correspondence problem among images. At least 5 targets are necessary between image pairs to carry out the relative orientation, but a higher number of coded points is recommended to increase the accuracy.

4.7.2.1 Main contribution

The contribution in terms of image acquisition procedures arises for specific camera adjustments and camera to object orientation. Whereas target-based approaches do require a camera adjustment suitable for target identification, markerless approaches have to deal with focusing on natural geometric features. Not only ensuring a suitable focusing is required, but not to exceed certain angular viewing limits that guarantee better performance of presented

case studies. For instance, **case study 1** requires not to take images of the object with angular orientations higher than 90˚, whereas dense matching strategies do limit point selection for accurate sparse point triangulation (see figure 47).

In the case of camera parameter adjustment, industrial cameras have to be employed as nearly artistic photography tools instead of setting up standard parameters. It is really important to find a well-balanced camera parameter configuration that ensures a good contrast on the images of the natural features of interest. For it, working distance, lens aperture, shutter time, flash intensity (if required) and depth of field optical concepts have to be controlled and adjusted.

With this aim, the combination between the image sensor and lens is studied so as to define the minimum focusing distance, the DOF and the resolution on the features to be measured. Depending on this parameter and the working distance, the features to be determined are more accurately defined. It should be pointed out that, in order to get a more accurate intrinsic calibration, camera parameters remain fixed during the acquisition. The most critical one is the focal distance, but the shutter time and the aperture of the lens remain also fixed throughout the image acquisition process.

When it comes to the image acquisition process, it is necessary to consider what is intended to be measured. Therefore, in addition to photogrammetric aspects, a proper contrast of features of interest and triangulation of surface points should be guaranteed. For this, it is necessary to reach a compromise between a good angle of triangulation and an excessive change of perspective between consecutive images. Thus, high angular views should be avoided and angles ranging from 60 to 110º are recommended. Depending on the relative angle between pairs of images, the accuracy of the photogrammetric method or dense reconstruction stage will be enhanced.

In addition to triangulation, it is important to take care of the internal calibration aspect, for which it is necessary to acquire rotated images on the image plane. Normally 4x 90º rotated images are acquired respectively at the beginning of the measurement. The same criteria for acquiring rotated images during the measurement is strongly recommended to enhance camera self-calibration.

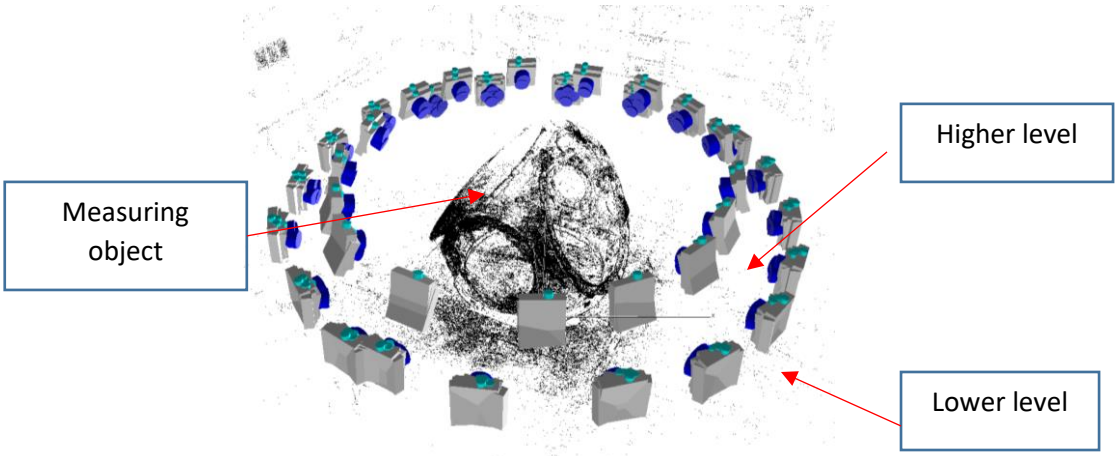

Figure 47. Camera shooting technique around the part.

4.7.3 Point detection, identification and extraction

The first step in any photogrammetric approach after acquiring the image data set is to detect, identify, localize and extract in each image the features that need to be measured and the ones that are used for camera pose determination as well as scaling and absolute referencing purposes. These features can be natural elements such as specific geometric elements (circles, lines, vertices) or key points or artificial points defined by targets (coded or not) or even light projected patterns. Depending on each case, a different image processing algorithm [182] is required which handles to define in pixel coordinates the position of the features in each image with sub-pixel accuracy. Identification is another key matter in photogrammetry where unambiguous point denomination is critical for further matching and triangulation purposes.

Usually, industrial photogrammetric approaches are based on artificial targets (white on black or vice versa) as they ensure a more precise spatial point definition and enable to automate many image data processing stages of the photogrammetric problem. For example, coded targets [183] are used to make more accurate camera intrinsic self-calibration and facilitate camera orientation estimation as the correspondence problem among stereo camera views is directly solved. Hence, image matching tasks are not mandatory. Besides, coded targets which are located in the calibrated scale bars (see figure 48 a) enable to automatically adjust the scale of triangulated points, define control points that are used for rigid transformation of 3D points or to even to automate measuring repetitive tasks for statistic or deformation case studies. Another common use is to employ point codification for eccentric probing real-time identification and tracking (see figure 48 b) for inspection purposes.

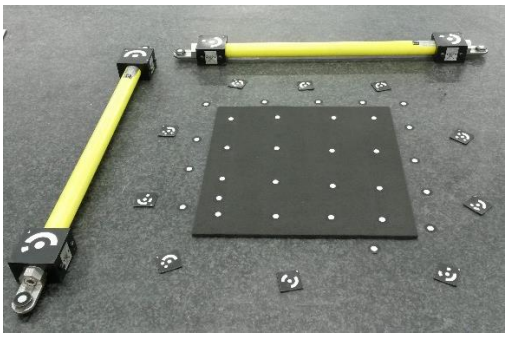

a

b

Figure 48. Codification purposes. a) Calibrated length bars b) Hand-held eccentric probing for surface scanning[184]

The coded targets are detected and unequivocally identified depending on their type of codification which is usually defined by each industrial solution. Their position, as well as orientation in image coordinates, is therefore robustly established reducing ambiguities and outlier data. There exist multiple codification alternatives as seen in figure 49 which aim to robustly define the identification of a point from different viewing angles. Codification patterns are divided into two main groups: coded bar (linear, radial or angular) or dot-based codification. Even numeric codification is available but less employed. Whereas dot-based codification offers a higher range of target codification, some industrial solutions prefer bar-based codification

because of its robustness. Every coded target is composed by characteristic geometry and a coded unequivocal coded patter. The accurate detection and identification of each target depend on aspects such as light condition, high resolution and contrast among background and the features printed on the targets. If these conditions are not fulfilled from different perspectives of the same scenarios, coded point codification and consequently image orientation would fail.

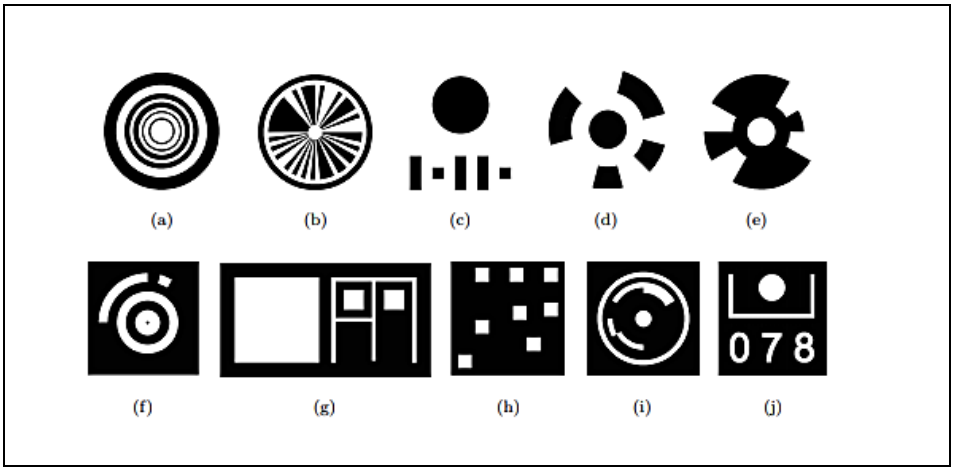

Figure 49. Target codification approaches. a-f & i) Coded bars g,h) Dot codification j) Numeric codification[185]

Systems based on a projection of structured light do also use coded light patterns to solve the correspondence between stereo approaches and permit real-time 3D point cloud triangulation and acquisition. Similar to artificial coded targets, its manufacturer employs a different point codification strategy to assure correspondence between stereo views. Depending on the projected light pattern, aspects such as spatial point resolution as well as data acquisition speed are variable. Whilst initial scanners used to employ mechanical approaches to project a set of fringed patterns above the surface of interest, latest projectors employ digital image codification to achieve the same objective. Besides, improved thermal stability of novel light sources such as blue ones [186,187], has enabled an accurate triangulation between cameras and the projector itself, which enlarges the applicability of these systems to measure more complex geometries and to obtain a more dense point cloud in each capture. Latest approaches are applying fast light pattern codification schemes aiming to fulfill in-line measuring speed requirements. This is achieved reducing the sequential pattern projection strategies and employing one-shot complex patterns based on translational and color information. Other approaches aim to solve limitations with reflective surfaces or shadows based on diffuse structured light or even preparing the surfaces with specific sprays. An overview of common patterns is shown in Figure 50 and deeply described in [188,189].

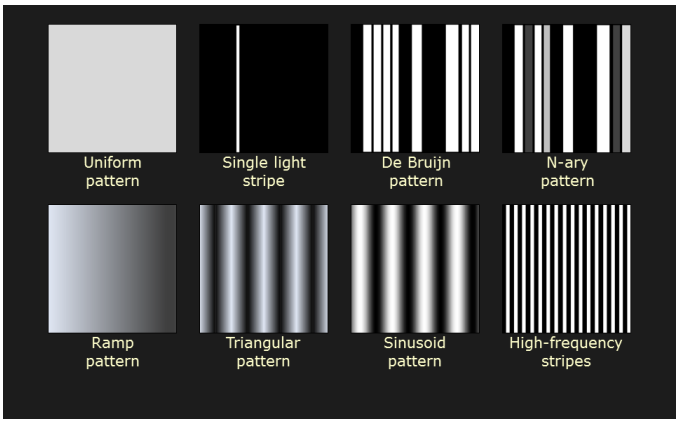

Figure 50. Structured light codification patterns with translational symmetry

In relation to uncoded targets, they are usually round circular points (see Figure 51 a) with a surrounding area that creates a high contrast for the contour points. They can be manufactured with passive or reflective materials to enhance their detection in light-demanding scenarios and provide a precise center of the target. Active targets materialized with light bulbs are also available for special environments. In relation to fixing options, different approaches are offered by industrial providers, such as adhesive targets (point-based or multi-point strips), magnetic targets or even special adapters for specific feature measurement.

Precise center determination is critical for orientation and triangulation processing step and directly affects their achievable accuracy.

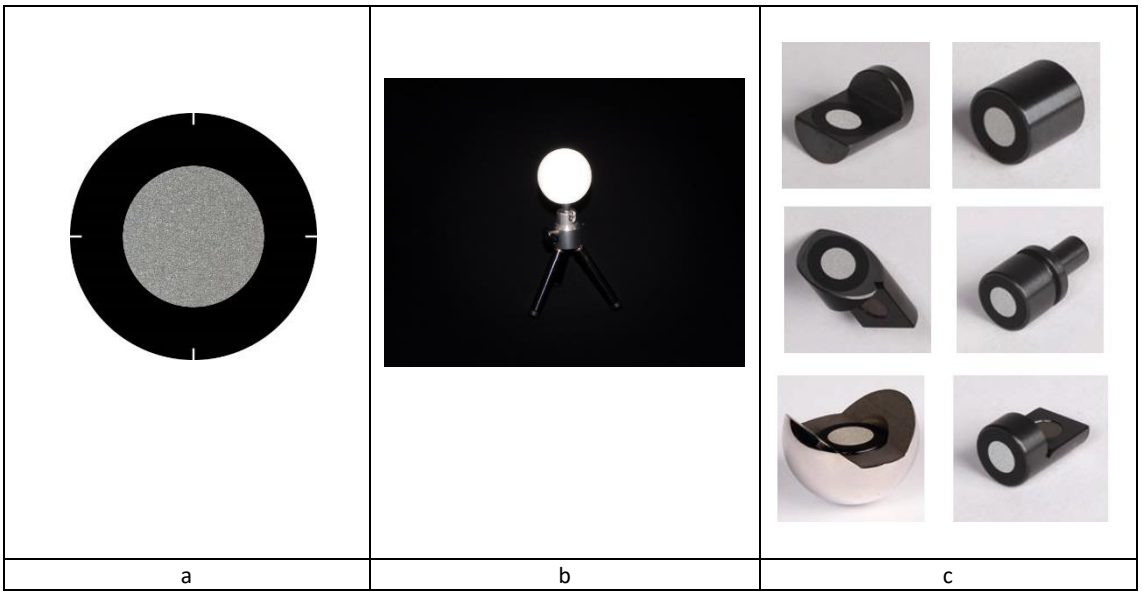

a b c

Figure 51. Type of non-coded targets a) retroreflective adhesive target b) Active spherical target c) Special target adapter

The most common algorithms and operators employed for the detection and extraction of the center for this kind of targets are listed below:

- Centroid method [190]: Measurement of a target by centroid calculation of grey values above a threshold within the measurement window (see figure 52). This method is a

weighted mean of the pixel coordinates in the processing window and it is well suited to symmetric patterns. It works properly even for small features as far as the shape of the targets is not distorted. The achievable accuracy is between 0.03-0.05 pixels for white dots on dark backgrounds.

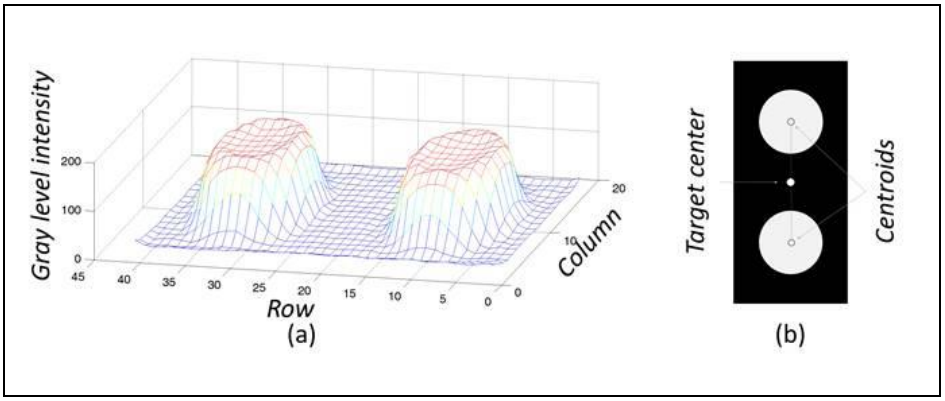

Figure 52. Centroid method

- Ellipse operator [191]: Measurement of a target by determination of the elliptical outline and calculation of a Best-fit ellipse center iteratively (see figure 53). Circular targets are usually imaged as ellipses. The main operators employed in this adjustment are the star operator and Zhou operator[192]. In both cases, good quality and planar targets are required for accurate performance assurance.

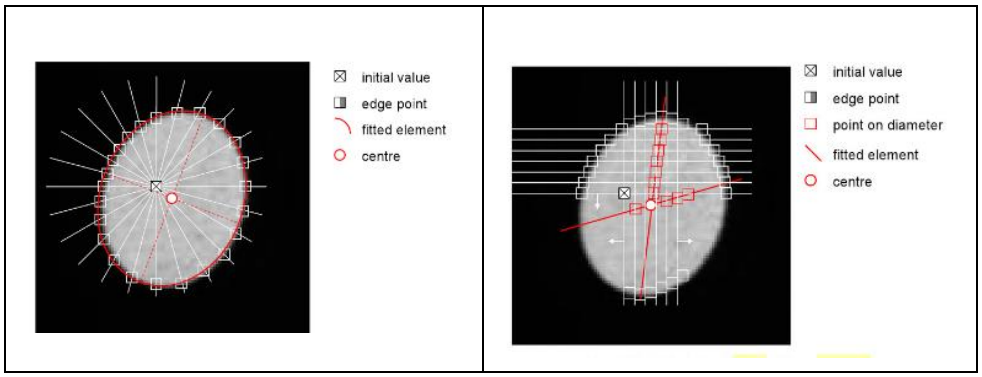

Figure 53. Ellipse operator a) Star operator b) Zhou operator

- Least square template matching [193–195]: Measurement of a target by least-squares matching of a template and a search area (see figure 54). The template is any (small) grey value image employed as a reference for iterative geometric and radiometric transformation between reference and search image. This method is well suited for stereo or multi-view matching purposes which derive in common employment for image processing diverse applications. The achievable accuracy is about 0.08 pixels for standard quality images.

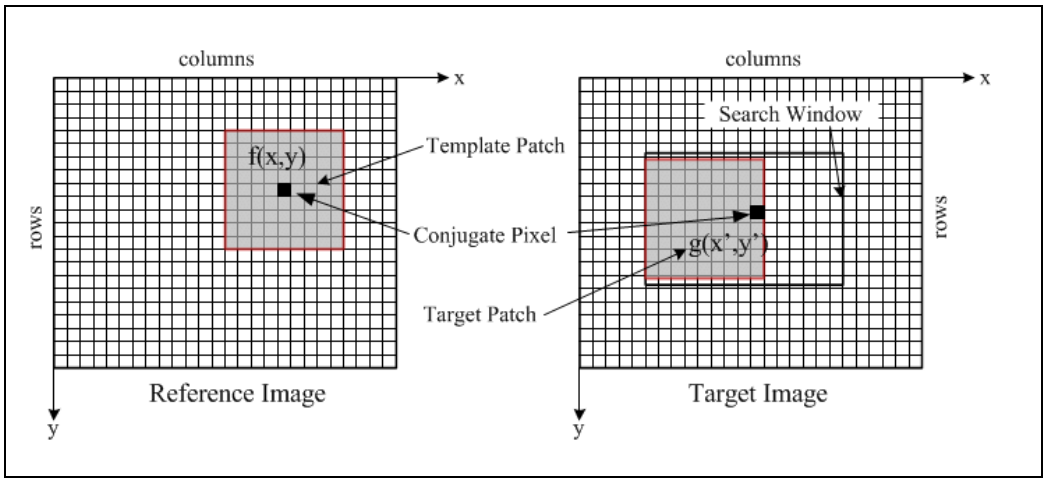

Figure 54. Least square matching method

- Cross-correlation (CC) [196]: Measurement of a target by normalized cross-correlation of a template (reference image) that must be defined as a Template matching of a larger image area. It estimates the similarity between a reference pattern and a target image path (see figure 55). The position of the best agreement is the location of the target. In order to obtain a more accurate target position, further image processing methods based on maxima correlation estimation are required. This method is very robust independent of contrast quality but time-consuming. The achievable accuracy is 0.1 pixels.

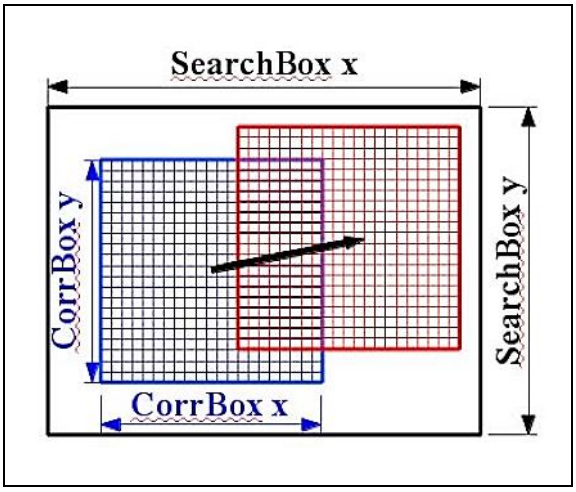

Figure 55. Cross-correlation method

As a practical summary, centroid methods can deal with few pixel (less than 5) target diameters whereas highest accuracy (0.01-0.03 pixels) is achieved by least-square and ellipse operators when the target diameter is at least 8-10 pixels. With bigger targets (>15 pixels), even more accurate (0.005 pixels) ellipse center adjustment can be reached. In real practice, target diameters range from 5-10 pixels with 0.03 to 0.1 pixel accuracy.

Mentioned methods [197,198] are usually automatically processed and many times are subsequently applied to obtain more accurate image point determination. Most of the industrial software also enable manual assistance for the region of interest (ROI) definition and center point automatic estimation.

The overall image processing workflow follows as:

1. Conversion of acquired image data to grey values
2. Binarization of the image with an adaptive threshold for different areas of the image based on neighborhood information (not required for all methods)
3. Detection and localization of targets based on previously described methods. Random identification is assigned
4. Selection of possible targets that correspond to a range of size

Apart from circular target position determination, there are some photogrammetric approaches based on lines that employ other image processing operators to detect and extract related data. In this case, edge operators are necessary to detect, locate and extract contour point information. Common algorithms include the Sobel, Prewitt, Roberts, Canny, and Laplacian of Gaussian methods [199–201].

Regarding natural key points that are used for structure from motion approaches, other operators such as SIFT are used [202–204]. This operator detects and describes local features in an image. Therefore, it transforms image data to sparse key points that present the following characteristics:

- invariant to image translation, scaling, and rotation,
- partially invariant to illumination changes
- robust to local geometric distortion
- robust to changes in illumination, noise, and minor changes in viewpoint
- key point descriptor that aids in consecutive image matching steps

For accurate key point discretization, detection and selection, outliers and redundant low contrast points are rejected during the image processing step. See point selection in figure 56.

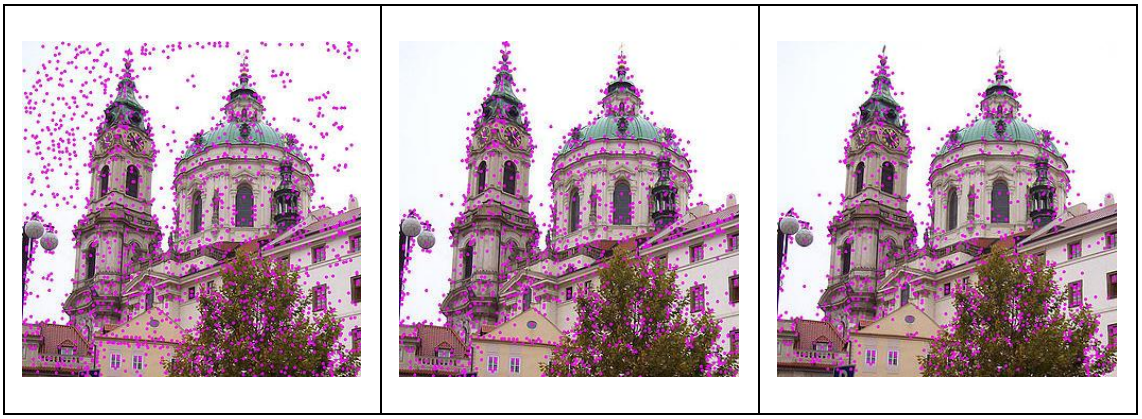

Figure 56. Workflow of SIFT operator for image key points detection, filtering and extraction

In this manner, stereo or multi-view image matching problem and consecutive external orientation based on natural feature points is enabled. Usually, these points correspond to edge points or characteristic points all around an image whilst dubitative image points are filtered.

The operators can be divided into two main families. The ones used as detectors and the ones employed as descriptors [205]. Whereas detection operators (Harris, Moravec, Forstner, Tomasi and Kanade, etc..) do detect and locate geometrically stable features (interest point or corners

mainly) on an image under different transformations, they don't add to these key points any type of codification. Descriptors instead (SIFT and its variants, etc..) are able to detect, extract and also encode natural key points based on neighborhood and radiometric texture information. Usually, 2D vector of pixel information is added to certain points (interest points) enabling their classification. Hence, they are more suitable for matching purposes explained in chapter 4.7.4. As the key points are saved with extra information regarding their surrounding area, they can be used as tie points between image pairs[206].

4.7.3.1 Main contribution

The contribution in this step deal with geometric characteristic detection and extraction based on nominal data exploitation and roughly aligned images. If the photogrammetric session is aligned with the nominal coordinate system, the relationship among acquired images and reference coordinate system is established and consequently, 3D known data can be projected to real images. In this manner, by means of nominal data reprojection, optical probing is enabled above each image to detect and locate the elements of interest.

In the **case study 1**, the border points of the holes which position must be verified are projected on the images defining a ROI where the real hole should be. The pointing accuracy depends on the previous photogrammetric procedure and its output results. The more accurate the definition of the reference coordinate is, the more accurate the pointing of all holes for all images will be. Once the ROI of each geometry is established for each image, an adjustment between real and reprojected nominal border points (see figure 57) is carried out to determine the real center of the holes.

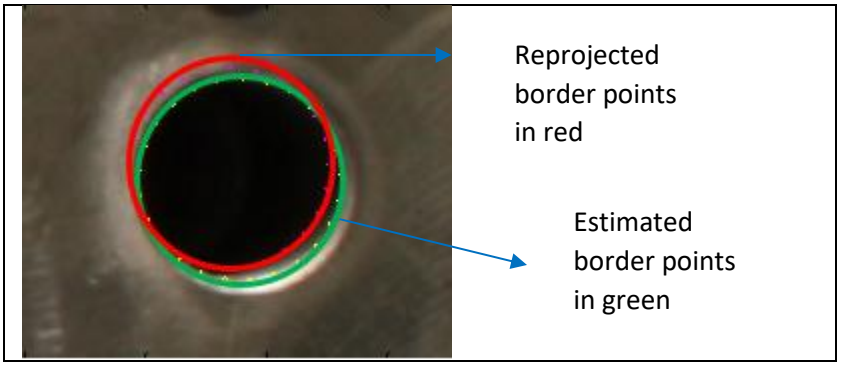

Figure 57. Nominal and estimated border points on the image feature

The data and image processing steps follow as:

- Loading of images
- Photogrammetric measurement result importation (intrinsic and extrinsic calibration)
- Nominal data importation
- 3D data generation for the edge points of each hole from known values
- For each image
    - Image adjustment (from RGB to grey data, edge filtering).
    - ROI determination for each feature
    - Reprojection of edge points from 3D to 2D for each feature

- Sum of the gradient of the evaluated ROI at these edge points for each feature
- Maximization of this function to establish the correction value for the center image coordinates
- Center image coordinate correction
- Result data storage and exportation

It is important to remark that the fitting of the hole centers is less accurate for oblique images where perspective effects appear and make more difficult the location estimation. Therefore, it is advisable to quantify the accuracy of this adjustment to assess if the hole center image coordinate is suitable for subsequent BA and triangulation steps. In the following image (figure 58) a multiple hole identification is presented for one image.

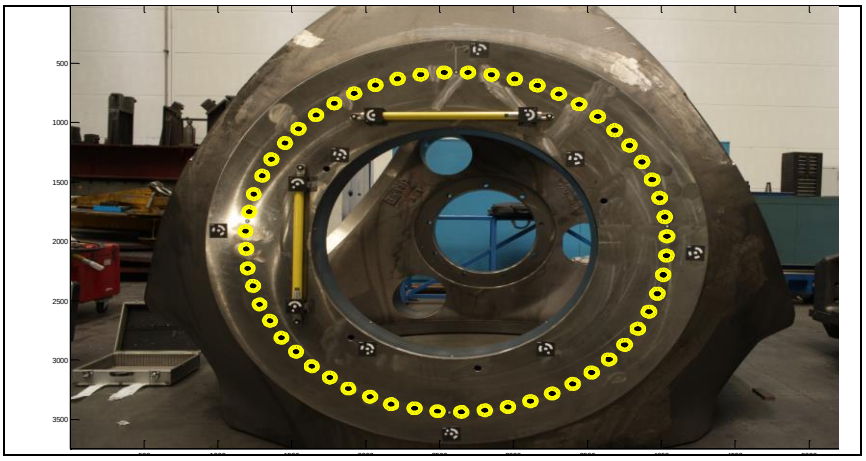

Figure 58. Multiple circular feature identification on an image

4.7.4 Image matching

An image matching process can be defined as the establishment of the correspondence between various data sets (conjugate or homologous points). The matching problem is also referred to as the correspondence problem [207] that aims to identify in an image data set, homologous and unequivocal image points. Solving point correspondence is a common and necessary matter in most of the photogrammetric solutions used in industrial application. The correspondence can be determined between 3D to 2D points (space resection method for extrinsic calibration) or among image points of multiple cameras for multi-view triangulation. Matching approaches are many times employed in the second case whereas image point codification is usually used for automatic point identification and matching purposes.

Once the interest image points have been detected and extracted from the images, a matching process among all views is required (also called object tracking). When the image points are coded targets, this correspondence is automatically established, but for the rest of the image points, the correspondence problem must be solved. The difference among features to be correlated arises from different image point of view, changes of radiometric data or even object movement in the scene relative to the camera set. When the images are consecutively acquired

and the movement of the elements to be detected and matched is not high, other strategies based on motion tracking can be applied.

The correspondence is usually carried out by image pairs (stereo pairs) considering all possible combinations among acquired images (see figure 59). It is important to use only the best matches and not all possible matches. This is mostly due to the ambiguity of multiple matches and employed operators. Hence, there exists a high correlation among matching techniques and methods for interest point extraction.

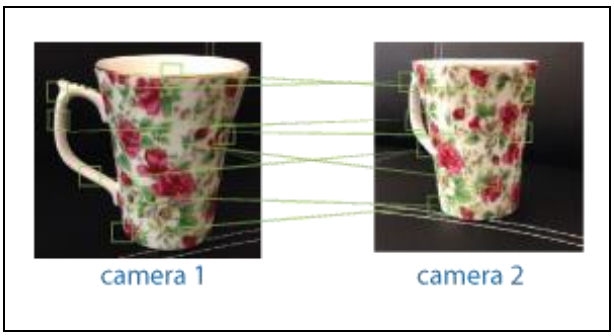

Figure 59. Image matching based on interest points and epipolar geometry in a stereo pair[208]

Fundamentals of correspondence refer to the problem of estimating a set of features in one image that can be identified as the same features in another image. To face this matter, image data processing algorithms are employed based on area-based correlation or feature-based approaches. When the relative movement between image views is limited, even image tracking methods can be applied. The approach is different depending on 2D or 3D matching purposes.

Traditional photogrammetry or even SFM photogrammetry requires point correspondences between images. This is handled by finding corresponding points either by matching features or tracking points from image 1 to image 2. Whereas image tracking methods are suitable for camera views that are close together, for example, Kanade-Lucas-Tomasi (KLT) algorithm [209,210], feature matching algorithms are more flexible and assumes stereo pairs with higher base distance and convergence viewing angle. Common classification of matching methods is the following one:

- Feature-based matching (FBM)
- Matching based on epipolar geometry and known relative orientation
- Area-based matching (Correlation & LSMatching)

FBM is based on interest point detection operators which try to find distinctive image points that can be reasonable candidates for matching purposes. These candidates are expected to be distinctive for their pixel region and maintain similar in corresponding images. In this way, homologous points among image pairs are likely to be found. Typical operators for FBM methods are Moravec and Forstner among others [211–213].

Matching based on epipolar geometry is based on epipolar geometric constraints and known relative orientation between image pairs. Indeed, it is an algorithm that tries to reduce the ambiguities between possible interest points and can be used to discard unreliable points and outliers. The search area for a corresponding point in the stereo pair is limited to the epipolar line. However, the relative orientation is not habitually known in this processing step and therefore is hardly applicable. An improvement of this method is to use more than two images

(called image triples) to enhance robustness and reliability by means of reduction of data processing response-time.

Area-based matching techniques are based on cross-correlation (CC) [214,215] and least-square matching (LSM) [194,195,216,217] algorithms to accurately define the location of homologous points between images. The reliability can be enhanced by geometric constraints such as epipolar geometry.

Robust image matching process simplified workflow is:

1. Detect interest points with detector operators
2. Extract neighborhood features with descriptor operators
3. Match features and reject outliers based on matching methods
4. Feed network orientation or point triangulation models

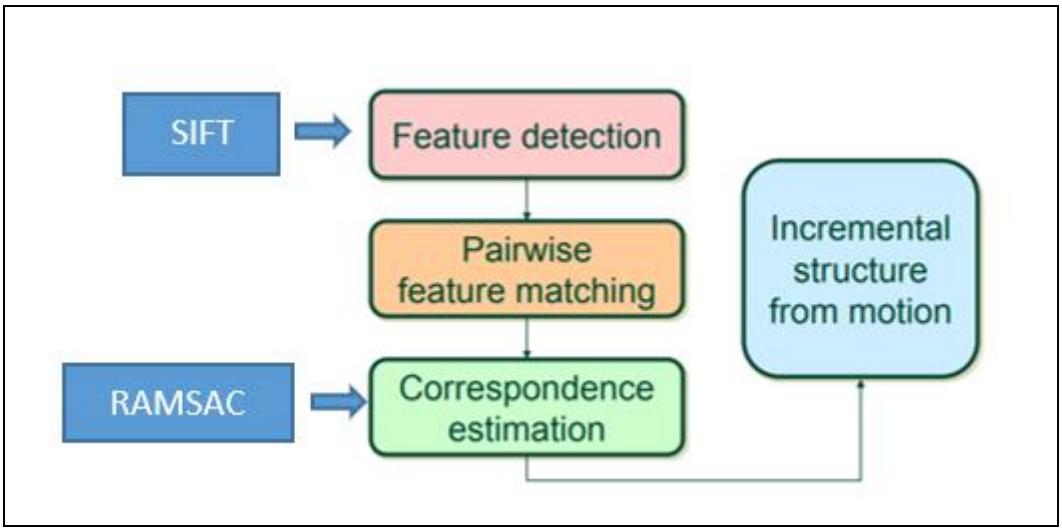

Figure 60. Image processing and data matching for incremental stereo-pairs

In dense reconstruction homologous image point determination is carried out by methods [27,120,126,166], which estimate the stereo and overall correspondence among image data sets. This is based on texture information of the images and image processing algorithms that are capable of establishing the similarity of surface points among multiple image data sets with different depth information. This method is the alternative to other common image matching methods, such as CC or normalized cross-correlation (NCC), which are not suitable for dense point surface reconstructions. SGM is the best approach when pixel-level data recovery is expected as it is based on a pixel by pixel information. Nevertheless, it is a time-consuming technique that needs to be reinforced with advanced image processing strategies (GPU, FGA) [125] that enable to reduce computational demands.

4.7.4.1 Main contribution

The ***contribution*** for matching purposes arises from 2 case studies. In ***case study 1***, as the nominal data is known and referenced in relation to a specific coordinate system, the identification of each hole once the point detection and extraction has been carried out is

straightforward. Hence, the codification of the features of interest comes from a priori structured nominal data which is usually defined in a drawing or even CAD files. In this manner, the correspondence problem and matching tasks required for triangulation purposes are avoided (see Figure 61).

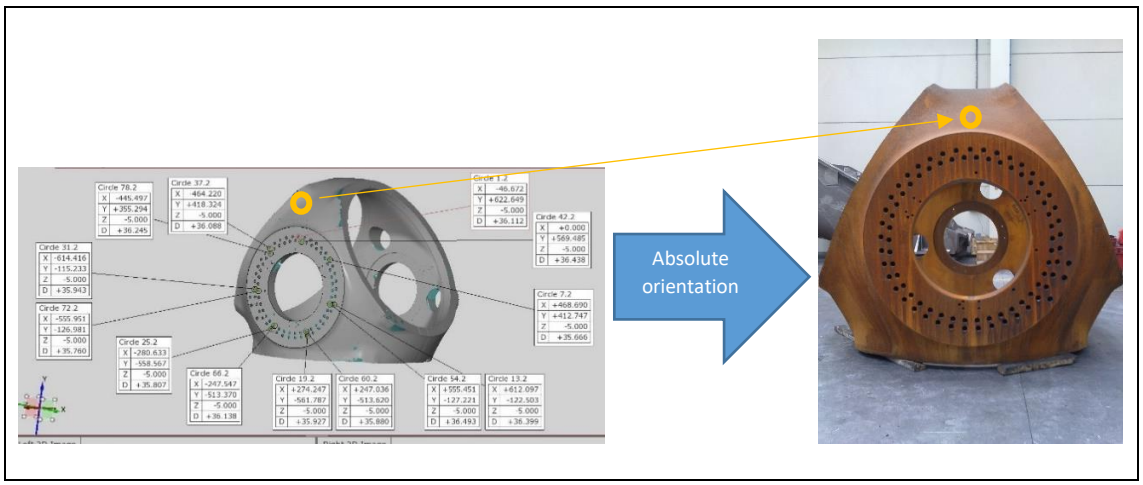

Figure 61. Automatic feature identification based on a priori 3D known nominal data and absolute orientation

The ***contribution of case study 2*** goes even further as the correspondence problem is avoided. The employment of geometric models that estimate directly the pose of elements is a non-exploited approach that offers many advantages where the correspondence problem is demanding. For example, in complex parts or round ones where a slight change of imaging perspective changes considerably the viewing area above the object to be measured. Hence, Best-fit adjustment of geometric elements to the measured contour point in multiple images is an alternative to be considered in such applications. This kind of approaches require known intrinsic and extrinsic calibration to determine the pose of straight lines, circles or even cylinders. In order to figure out the pose estimation contour points of all images and geometrical models that define the geometry of interest are combined with iterative minimization strategies.

For every geometric element, the distances of each light ray (projected form image plane to spatial plane) to the borderlines of the geometry to be measured are estimated and minimized. Linearization of the cost function that defines mathematically the geometric element is required before the iterative adjustment is carried out. This method enables to measure a geometric element only with one image, but more than two images are recommended to improve achievable accuracy (see Figure 62). Moreover, a well-spaced border point distribution is necessary to ensure a suitable geometric element reconstruction.

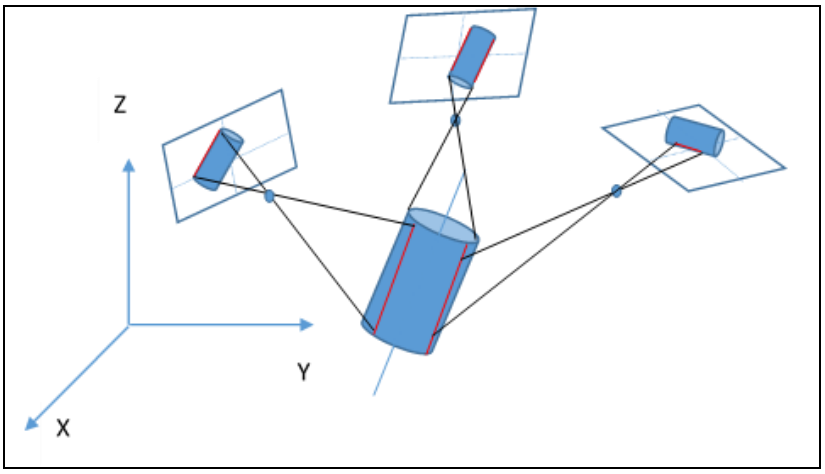

Figure 62. Best-fit adjustment of a cylinder pose based on contour point data in multiple images

4.7.5 Relative orientation

After the image point identification and correspondence is solved among different views, the extrinsic orientation of each image must be computed. As a general rule, this estimation is carried out in two steps (relative orientation and exterior orientation) or simultaneously in one step (Bundle block adjustment or space resection of individual images). This chapter and the following one deal with the orientation matter.

First, the relative orientation among image pairs is settled based on fundamental matrix (FM) [218–221] determination or essential matrix (EM) [222,223]. When intrinsic calibration is known, the FM can be reduced to the EM. Secondly, the absolute orientation is calculated taking as a reference one of the images and estimating the orientation and position of each camera projection center in relation to the absolute reference system. When the absolute coordinate system is fixed to the reference camera, the relative orientation determines at the same time the absolute orientation. However, the absolute coordinate system is usually defined by a 3D object (calibrated artifact or ground points), thus a rigid transformation of camera orientations is required to determine their absolute orientation. This is usually accomplished for stereo system calibration.

Regarding the relative orientation [224–227], it determines the position and orientation of an image in relation to a reference image by means of corresponding homologous points (see figure 64). Geometric constraints such as collinearity and coplanarity are the basic principles of employed mathematical models. Usually, more than five points are used assuring the redundancy and iterative linear (they require initial guess) or non-linear approaches are employed. In stereo systems, this is one of the core challenges to ensure accurate performance of the device. In multi-view systems, consecutive image pair relative orientation is estimated to bring afterward all camera network to a common reference (absolute orientation). The reference is commonly the first image or a coordinate system that is defined by a transformation offset in relation to the first image (see Figure 63).

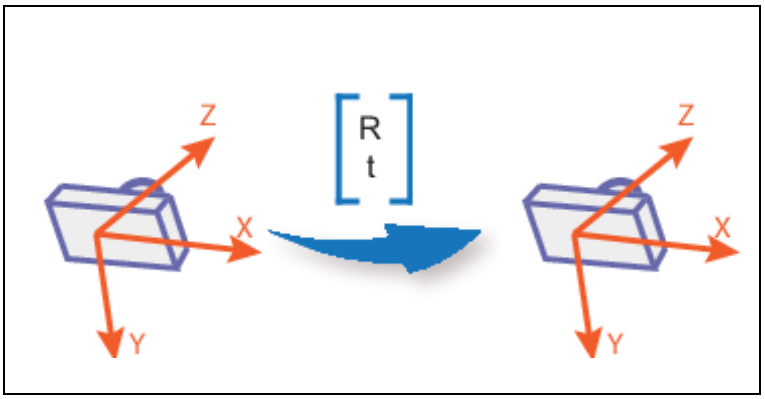

Figure 63. Relative orientation for a stereo pair with corresponding coordinate systems (reference and target)

The fundamental matrix [228,229] describes mathematically the epipolar geometry (EG) [228,230] of the two cameras (see figure 64). It relates a point in one camera to an epipolar line in the other camera by means of their relative orientation. The input data to the estimation of this matrix are the corresponding points (feature points) from a stereo pair and the output is the relative orientation between camera views which is not scaled and usually set to 1 unit. There exist different algorithms that tackle this problem that are conditioned by the reliability among previously estimated matched points. Some of them are even able to assume some percentage of outliers by means of iterative fitting and doubtful point discard.

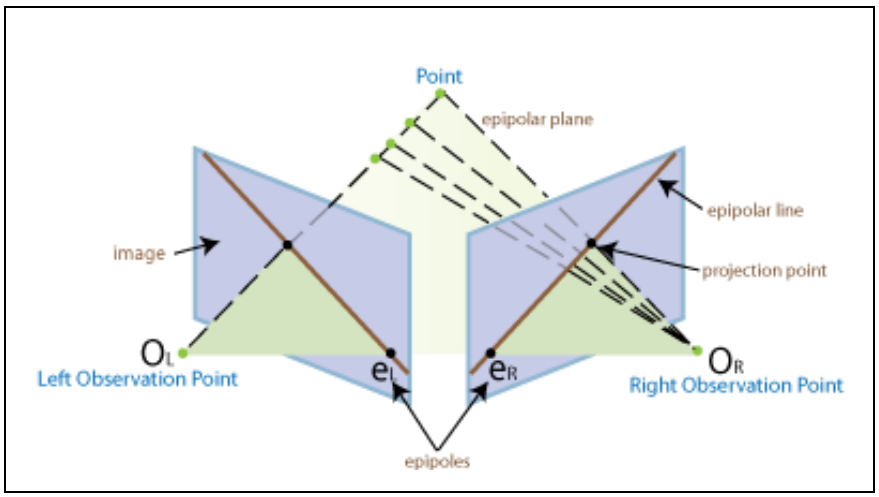

Figure 64. Epipolar geometry for a stereo pair

A wide range of techniques is provided in computing the fundamental matrix such as the seven-point [231], least-squares and eigen analysis linear techniques among others and robust techniques such as M-Estimators, Least Median of Square regression algorithm (LMedS), Random Sample Consensus (RANSAC) and so on [227]. From high-reliability requirement (nearly 100%) of Norm8Point [232] algorithm to fewer reliability methods such as LMedS [233] or even RANSAC [234] methods, the output result is more accurate when the correspondence of feature points is robust.

The methods to estimate the fundamental matrix can be classified into linear, iterative and robust methods. While linear and iterative methods can cope with bad point localization in the image plane due to noise in image segmentation, robust methods can handle with both image

noise and outliers which enables to filter inaccurate matching points. In all cases, the output is the fundamental matrix that defines the epipolar parameters that best suit this stereo correspondence.

Although most of the times the fundamental matrix aims to solve the relative orientation between stereo pairs when this information is known it can be used to facilitate the correspondence problem limiting the search for one of the images to a 2D line. In fact, this approach is very common in stereo devices where the relative orientation is established by means of calibration procedures and real-time triangulation is required by the measuring device according to the 3D scene. Therefore, image processing techniques for photogrammetry are improved by means of epipolar geometry and other strategies. For example, when rectification of images is applied, the correspondence problem is simplified to search a corresponding pixel point in a specific row on the other image.

4.7.6 Exterior orientation

Exterior orientation means to define each camera pose (orientation & translation) according to a common reference system (world coordinate system). In computer vision, the determination of the exterior orientation parameters is known as the “pose estimation” problem which supposes a rigid 6 dof transformation between its camera projection center and world coordinate system. Usually, a camera network is depicted according to a specific camera coordinate system (first image). In order to estimate the exterior orientation of acquired and computed images, two main approaches are employed in photogrammetry. A two-step process based on relative orientation followed by absolute orientation or a simultaneous orientation estimation by means of bundle block adjustment methods. In the case of single images, space resection methods (indirect method) are the reference approaches although there exist other geometric approaches introduced in this review [172].

Apart from the number of steps to solve the exterior orientation, the methods also differ from accuracy aspects depending on their application field[235]. See an overview in figure 65. Whereas computer vision applications are not so demanding, photogrammetric applications do need accurate and reliable methods and therefore output results. Many times, different direct and non-direct methods are combined to fulfill these requirements. Usually, linear methods are

employed for rough parameter estimation that is employed as a priori data for non-linear more accurate approaches.

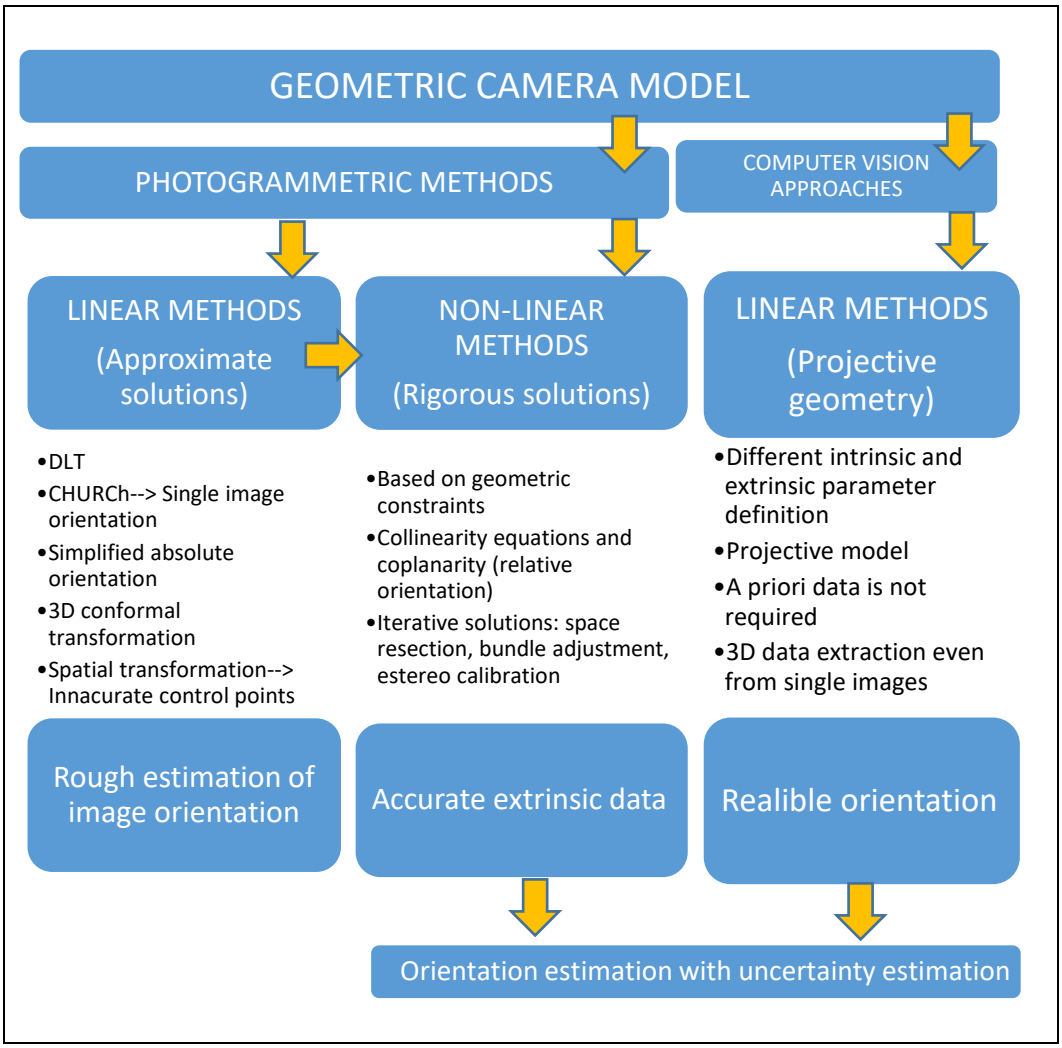

Figure 65. The relationship among different solutions and applications fields for exterior orientation

External orientation means to bring all relative camera poses to a common reference system that is usually in the first camera view of the image data set. It supposes a subsequent transformation among estimated relative orientations of each camera. Once every camera pose is referenced to the first camera view, the main coordinate system of the photogrammetric system is defined in the projection center of the first camera (see figure 66). Nevertheless, this coordinate system is not useful to extract useful 3D points coordinated but it enables to depict

3D points related to camera poses. Thus, once the triangulation step is established, and absolute referencing is settled to 3D points and camera poses to extract meaningful 3D information.

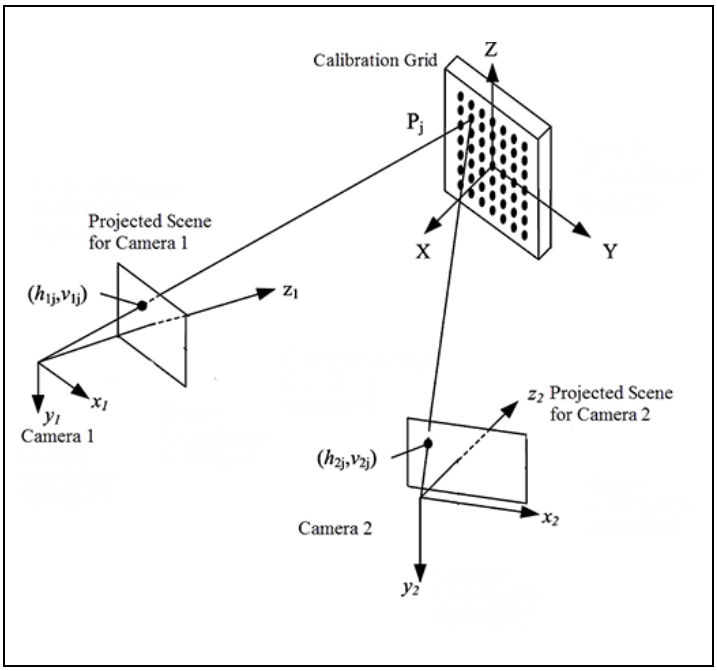

Figure 66. The external orientation of stereo camera set-up

4.7.6.1 Extrinsic calibration methods

The exterior orientation of a photogrammetric set-up (also called extrinsic camera network calibration) can be established by means of different methods. This calibration step is necessary to apply afterwards any model which will triangulate object points. In any case, each camera position and orientation (6 dof), as well as intrinsic calibration, has to be precisely known to solve 3D point XYZ coordinates.

The exterior orientation problem can be classified depending on the image number:

- The orientation of a single image→ Space resection method with known or unknown intrinsic parameters (non-linear collinearity equations and linear methods DLT without a priori data knowledge) can be applied.
- The orientation of stereo pairs→ Separated orientation methods based on space resection or joint orientation methods based on simplified bundle block adjustment or the combination of relative orientation followed by exterior orientation methods can be applied.
- The orientation of multiple images→ Exterior orientation of multiple images is usually simultaneously estimated by means of bundle block adjustment methods.

4.7.6.2 Description of methods

Absolute image orientation problem is solved by indirect methods as direct angle and position determination of the image projection center is not physically accessible. Hence, the employ photogrammetric projection models based on collinearity equations and iterative minimization numerical strategies. In any case, known 3D object points are projected to 2D image planes and corresponding models are fitted minimizing the Euclidean distance between observed image points and theoretically estimated ones. This minimization is iteratively executed until certain convergence threshold values are achieved modifying the image pose parameters to be identified.

The different methods that enable the extrinsic calibration to be solved are the following ones:

- **Space resection (SR)**: It is used to estimate the external orientation parameters (6dof) of a part related to a camera or vice versa comprising three coordinates of a position and the three elements of angular rotation. Normally, a part with calibrated 3D targets (coded or uncoded) is employed as a reference in world coordinates and the camera orientation is determined to minimize the distance among observed and reprojected points in the image plane which correspondence is already known (see Figure 67). A central projection approach is commonly used, and a pin-hole camera model is considered for camera behavior definition.

  The exterior orientation of the camera can be estimated by linear (DLT method, Church) or non-linear (iterative minimization method) approaches. Many times, linear methods are employed for the definition of initialization parameter of non-linear methods such as SR or Bundle Block Adjustment. DLT is linear and an extended case of collinearity equations with an affine transformation without the need to use initial approximate values as SR method. At least 5 non-coplanar known points are required to solve image absolute orientation.

  Existing non-linear methods involve linearization of the collinearity condition and the use of an iterative process to determine the final solution using the least-squares method. The process also requires initial a priori data of the unknown parameters which are roughly known or estimated by less accurate methodologies. At least 3 non-coplanar known points are required to solve image absolute orientation although a higher point number is advisable. Some of these algorithms also permit to estimate the intrinsic parameters at the same time based on a unique image, but this demands to distribute the 3D control points in a non-coplanar set-up and to increase the minimum number of control points.

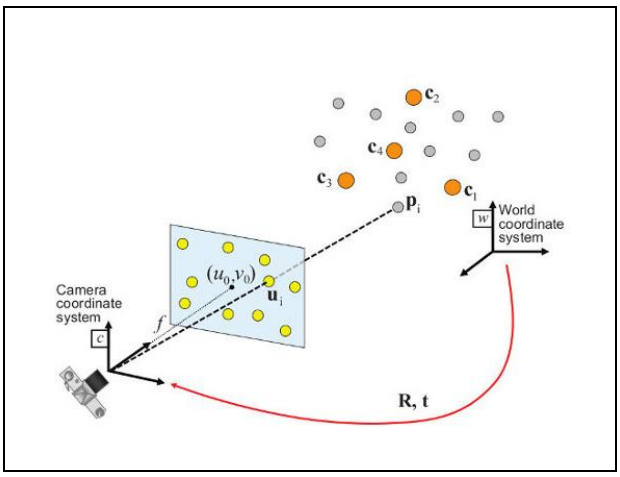

Figure 67. Space resection method to estimate extrinsic calibration (exterior orientation) of a camera view

SR is also commonly used to orientate a unique of a reduced set of images that have been taken after the overall measuring process. It aims to add non-measured points or features to the overall data set without re-estimating the BA. Only spatial triangulation is applied to the image points that appear in these extra images.

- **Stereo calibration**: A stereo calibration determines which are the camera poses regarding a common known artifact which defines the reference World Coordinate System (WCS). Aiming to solve extrinsic parameters, this calibration method minimizes the distance among observed image points and reprojected ones by means of linear least squares considering both cameras of the stereo pair. Therefore, the 3D point triangulation model is established to estimate XYZ coordinates and these points are reprojected to each camera in order to solve this minimization problem. The output is the absolute pose of each camera which enables to triangulate 3D common points between stereo pairs (see figure 68). The App[236] that carry outs this stereo calibration is shown in Figure 56 where each camera view is presented for a specific artifact position and orientation.

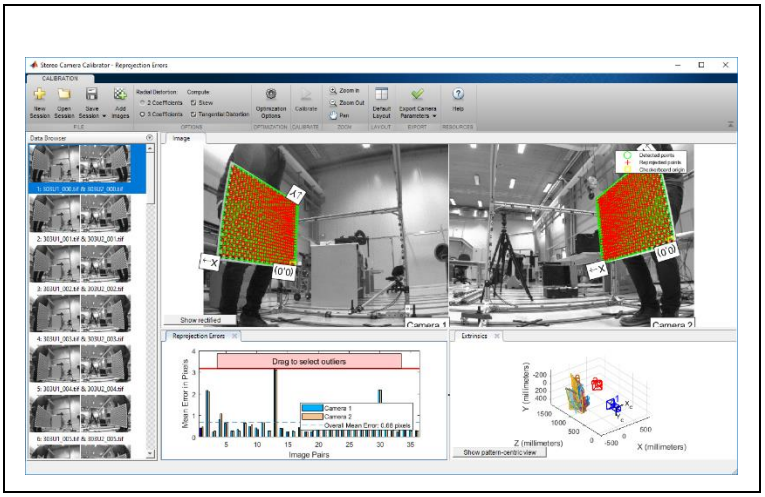

Figure 68. Stereo calibration App for camera extrinsic calibration

Apart from determining extrinsic parameters, this method makes possible to establish intrinsic parameters for each camera, but the uncertainty is higher than using single-camera calibration methods. Moreover, the App can be used to estimate the translation and rotation between the two cameras (relative orientation).

The calibration workflow is the following one:

1. Image pair acquisition with the calibration pattern with angles below a certain threshold
2. Import image pairs to App
3. Calibrate the stereo camera and intrinsic parameters
4. Evaluate calibration accuracy by means of fitting residuals and estimated parameter errors
5. Export the extrinsic parameters

Once absolute orientation parameters are known regarding CS of the pattern, relative orientation among image pairs can also be established. The drawback of this method is that

the absolute orientation is defined according to the calibration artifact that does not correspond to WCS of the photogrammetric system. Therefore, a posteriori absolute referencing of all cameras or points is required by means of a rigid transformation.

- **Self-calibration**: this method is based on the BA algorithm which is used to estimate and refine both extrinsic camera parameters and 3D point coordinates. It is also called as SFM problem in computer vision and it is the generalized case for multi-view stereo calibration. Again, it is an iterative problem that aims to minimize the distances among observed image points and reprojected image points based on estimated model parameters. However, it can be used to solve the extrinsic orientation of multiple cameras and 3D points without a priori knowledge of these parameters (see figure 69). The simplest case is the stereo problem.

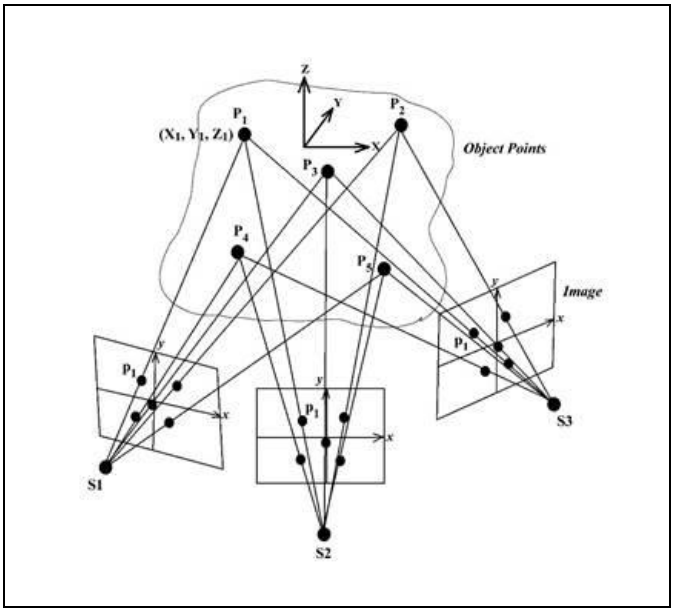

Figure 69. The BA for 3D point and camera pose estimation

In some cases, intrinsic parameters are also determined at the same time, but this problem is many times ill-conditioned. Therefore, it is advisable to estimate intrinsic parameters with other calibration procedures although industrial photogrammetric systems are able to deal with this inconvenience. Thus, BA is the method that handles simultaneously camera self-calibration, image resection and 3D point triangulation based on rough image orientation data. Industrial libraries such as Matlab© offer required functionalities to apply this method handling the following workflow (see figure 70):

1. Acquire images of the scene from all cameras.
2. For each pair of consecutive images, find a set of point correspondences. This means that point detection and matching between image pairs must be solved.
3. Estimate the relative pose of the current view, which is the camera orientation and location relative to the previous view.
4. Transform the relative pose of the current view into the coordinate system of the first view of the sequence.
5. Store the current view attributes: the camera pose and the image points.
6. Reject outlier image points

7. Define correspondence among all camera views and image points
8. Use triangulation to compute the initial 3D locations of the points.
9. Use the BA function to refine the camera poses and the 3-D points.

Also, the absolute orientation corresponds to CS of the reference camera in this calibration method, usually it is necessary to transform this camera poses to the WCS of the 3D object Moreover, a scaling of the data is required as 3D points are also determined by the method but not scaled. One of the advantages is that 3D point Multiview triangulation is also estimated at the same time, which enables to measure a 3D scene with a camera network without knowing a priori where the 3D points and cameras are located in the scene.

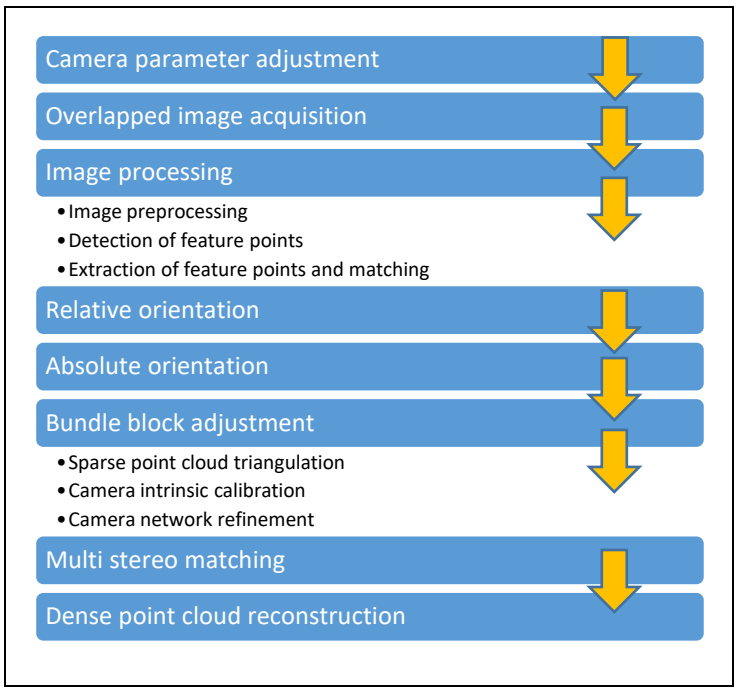

Figure 70. Standard SFM photogrammetry processing workflow.

4.7.6.3 Main contribution

The main contribution in terms of camera orientation establishment is applied in **case study 1**, where a BA[237] tool has been developed to estimate the 3D coordinates of machined holes. As described before, the BA method is applied to estimate simultaneously intrinsic, extrinsic and point triangulation. In this case, camera calibration has not been identified but it has been applied as an offline approach. In relation to extrinsic image orientation and hole position calculation by means of multi-view triangulation, a two-step process has been employed (see Figure 71). This implementation aims to obtain better results than simultaneous estimation due to ill-conditioned Jacobian matrix. Therefore, a bundle method has been developed and its scope for sparse point triangulation has been studied for the case of natural features.

In both estimation steps, constrained BA is employed to reduce the number of parameters to be identified at once. Therefore, firstly, camera orientation has been established as the output of the bundle refinement method, whereas this output has been used as an input for further hole center position triangulation step. Separating the overall parameter identification in two steps increases achievable accuracy of obtained results in comparison to a simultaneous solving of model parameters. This is in fact due to parameter strong correlation and relationship. Hence, such kind of constrained strategies are beneficial when the mathematical problem is ill-conditioned or even when higher parameter identification accuracy is required.

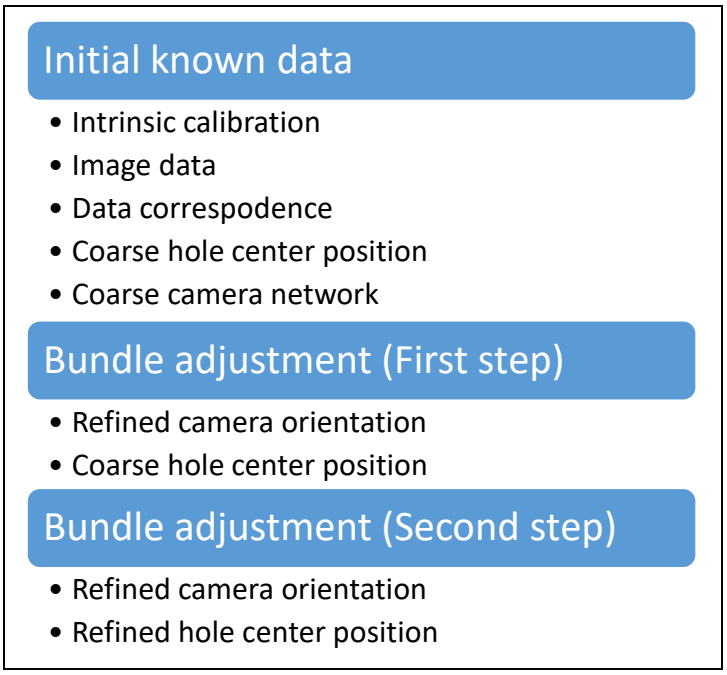

Figure 71. BA approach with a two-step approach

4.7.7 Triangulation

The triangulation [238,239] is the data processing step where 3D information is estimated by spatial intersection computation among multiple oriented camera views (see figure 72). It is usually carried out after the intrinsic and extrinsic camera orientation issue has been resolved or even simultaneously.

At least a stereo pair is necessary to compute 3D data from 2D image points, but a higher number of camera views and image data is recommended to increase the accuracy by means of data redundancy. Moreover, viewing angle limitations between 60° - 120° are commonly established to ensure high output accuracy and a suitable uncertainty.

In many offline photogrammetric solutions, the triangulation is part of a data refinement process called BA [240,241]. As every relative orientation step from one camera view to the following ones contains accumulative residual errors, one approach to reducing this source of inaccuracy is to refine camera orientation and 3D point coordinates at the same time. It is also possible to use this non-linear optimization approach [241,242] to estimate the intrinsic

calibration, but as the model to be solved gains in complexity, the required data conditioning is more demanding and sometimes not affordable.

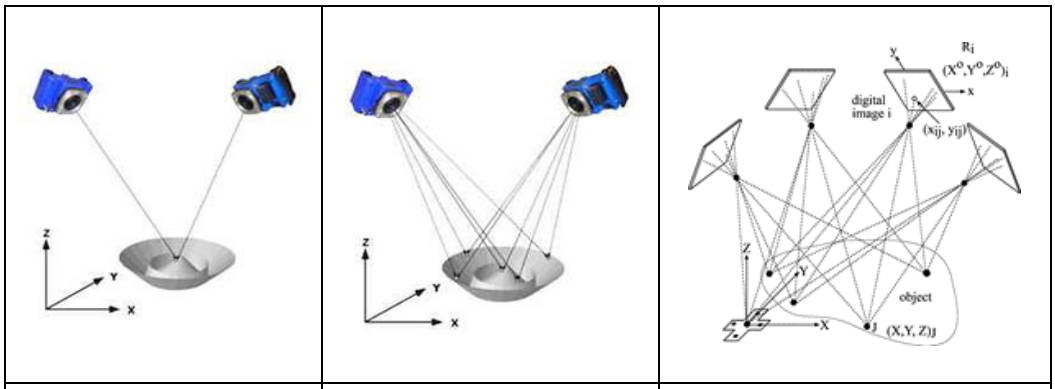

a b c

Figure 72. Spatial triangulation[167] *a) Stereo single point triangulation b) Stereo multipoint determination .c) Multi-view and multi-point triangulation*

In the case of real-time photogrammetric systems, triangulation is carried out for referencing partial 3D scans, to track the 6 dof positioning of a part based of a discrete number of points or even to measure 6 dof positioning of measuring accessories by means of inverse resection (IR). Monitoring based on partial mesh tracking is also appearing in the latest industrial solutions as data computing capabilities are being improved more and more, but it is not the most common solution.

Triangulation is also the basis for the reconstruction of dense point clouds aided by light projection or even based on surface texture data. Whereas light projected solutions support surface point codification with structured light, textured surface already present this intrinsic natural codification. Depending on the approach a different image processing step is required to identify and extract from imagery required point information.

Stereo or multi-view real-time camera systems, which calibration is already known, are capable of triangulating points on-site as the correspondence problem is minimized with coded or reference points among distance is kept fixed during measurements. These systems do also use camera intrinsic parameters that are already characterized by offline calibration strategies. Indeed, the triangulation can be established between cameras or a camera and a light projector. Current, 3D scanning systems have developed thermally more stable projectors with blue light which enables to use them for triangulation without losing the calibration set-up as previous systems did.

Triangulation step is an important part of the dense reconstruction of textured parts where multiple corresponding points among large imagery data sets are intersected together aiming to estimate the 3D coordinates of each surface point. In this case, the overall photogrammetric and 3D data reconstruction problem is an offline process, which takes a long time. This type of 3D data reconstruction requires a previous, robust and reliable image matching process required to guarantee a suitable multi-point triangulation based on natural textured surface points.

4.7.7.1 Main contribution

On the one hand, the main contribution of the thesis for point triangulation has been described in chapter 4.7.6.3 where a bundle approach applied in two steps is used to estimate multiple hole center position presented in **case study 1**. In order to apply this sequential two-step method, previously a sensitivity study of the BA model has been employed so as to understand the robustness of the algorithm regarding available measured data set. As the simultaneous orientation and point coordinate estimation is not well conditioned, a two-step process has been established.

On the other hand, **case study 2** deals with cylinder pose determination by means of best-fit fitting of each geometrical model. It is not indeed a triangulation strategy as traditionally applied in target-based photogrammetry, but this approach directly estimates the position and orientation of an element that it is a usual post-processing step for point-based methods. Hence, it is a straightforward alternative to measure the pose of different geometric elements without adjusting a geometric element to 3D point coordinates.

Apart from previous contributions, **case study 3** deals with dense point cloud reconstruction of texturized objects based on dense matching techniques (see Figure 73). Specially applied to casting parts. Although industrial software packages do offer this functionality, a suitable performance in terms of data quantity and accuracy is not guaranteed if a proper measuring procedure is not applied beforehand. Hence, this case study has demonstrated the capability of dense matching techniques to accurately reconstruct surface points corresponding to industrial parts.

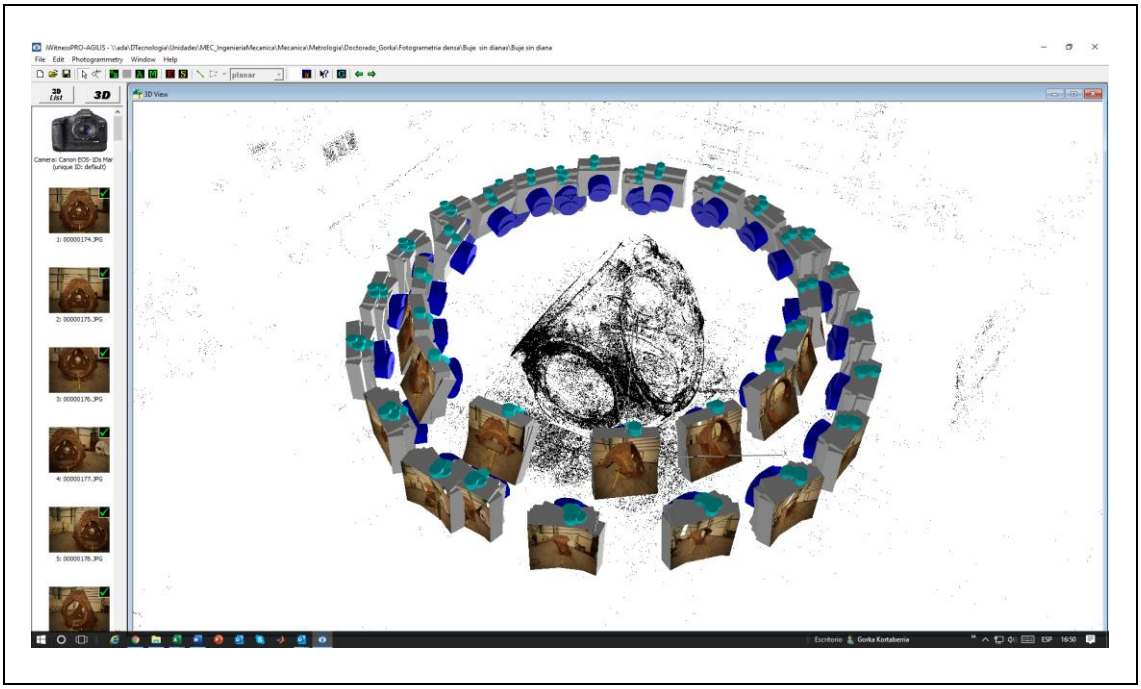

Figure 73. Representation of dense point cloud reconstruction based on dense matching techniques

4.7.8 3D object scaling and referencing

The absolute orientation relates image or model coordinates to the world coordinate system. It corresponds to the correct position, orientation and scale of a 3D scene with respect to a world coordinate system. It requires known control data (ground points) in order to transform the estimated orientations and XYZ point coordinates to the target coordinate system. At least, the nominal and measured coordinates of 3 corresponding points are required to estimate the translation and rotation between reference and measuring CS. Once this transformation is calculated, it is applied both to camera extrinsic orientation and 3D point coordinates and the results are shown in WCS. A higher number of points enables redundancy with Best-fit least square estimation methods. The correspondence between measured and control points is again a need to apply properly the spatial transformation.

When only 3 control points are available geometric alignments can be applied such as the 321 method where a point is selected to define the origin of the target coordinate system. Next, a point through which the X axis will pass is defined, and finally, a third point is selected to define the XY plane and therefore the direction of the Y or Z coordinate axis which blocks all degrees of freedom

Many times, this spatial transformation is automated and integrated into industrial solutions by means of coded targets which nominal coordinates in the target coordinate system are already known. For example, SR methods for single or stereo image orientation employ calibrated chessboard and bundle block adjustment methods do use calibrated known cross-bars within this aim (see figure 74). This type of points are also employed for 3D data scaling purposes as the scale of SFM approaches is a priori arbitrary.

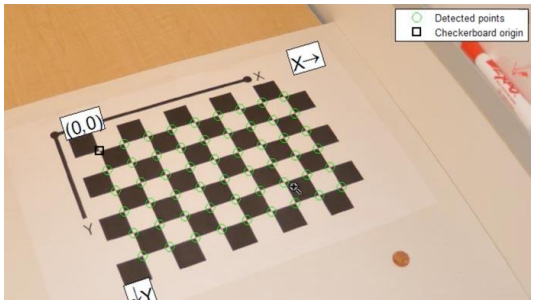

a[243]

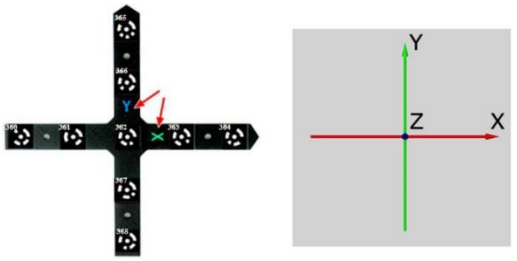

b[244]

Figure 74. Calibrated artifacts for absolute orientation establishment

In any case, absolute referencing enables to transform the measuring system output data to a WCS system which deals with the real representation of acquired and processed 3D points (see figure 75).

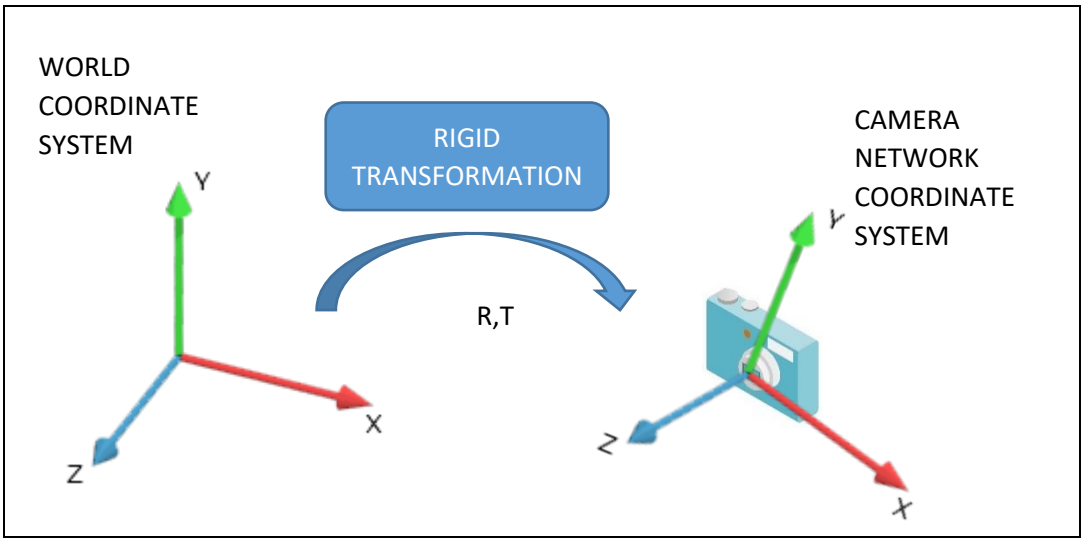

Figure 75. The transformation between the camera network and world coordinate system

4.7.9 Output data analysis

Once the photogrammetric model has been solved, the 3D output data is usually processed for further analysis, such as: fitting of geometric elements, identification of feature-based adapters, real-time element tracking, surface comparison of measured data against nominal values, static or dynamic deformation analysis of measured part, etc..

Depending on the required analysis the 3D points are converted to specific data formats which enable to carry out specific quantitative studies. These processing tasks comprise point by point analysis, point cloud to mesh conversions, reverse engineering or even point to CAD surface point comparison. In each case, the XYZ coordinates of estimated points are the necessary raw data for such kind of quantitative evaluation.

The first step in any data processing approach is to transform the 3D output into the WCS by means of an alignment procedure (see chapter 4.7.8). Sometimes, previously determined absolute orientation of the measuring systems already depicts the data in this target coordinate system. However, most of the times further alignments are required. Depending on the measured data type, different alignment methods are applied. From geometric alignment based on RPS or 3-2-1 methods to Best-fit alignment methods, several procedures are established as typical rigid transformation (scale is fixed) approaches.

Secondly, the transformed points are processed to extract the required information for further analysis. The range of processing procedures is rather extent depending on inspection requirements and dynamic request.

While discrete point clouds are usually employed for geometric inspection such as part quality assurance or static deformation monitoring, dense point clouds are used for surface comparisons against nominal CAD data or even for reverse engineering purposes. Recent real-

time applications do also use measured cloud of points for dynamic inspection demands, such as partial scan fusion based on reference points, point cloud stitching based on iterative closest point (ICP) transformations, 6 dof positioning tracking or dynamic deformation analysis of parts under external loads.

In figure 76 and 77, different applications of data processing are presented for offline applications.

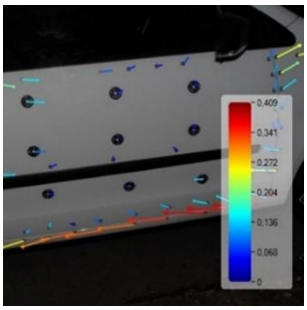		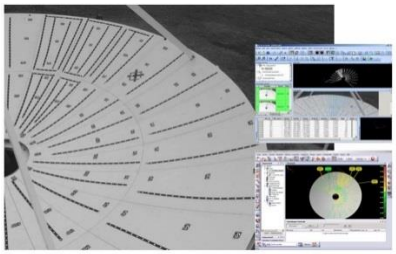
a[245]→ Static deformation Linearis 3D	b[246]→ feature based geometric adapters DPA inspect	c[247]→ surface form and position verification Accurex

Figure 76. Off-line data processing examples with discrete point clouds

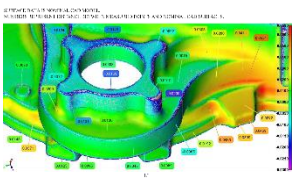		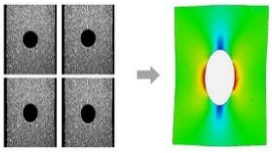
a[248]→ CAD comparison actual versus nominal	b[249]→ Reverse engineering workflow	c[86]→ DIC analysis

Figure 77. Off-line data processing examples with dense point clouds

5 CASE STUDIES

This chapter contains a summary of researched case studies and obtained results for each approach. A brief introduction and obtained main results are presented in each case and cross-references of published papers are included where a deeper description of each application is explained. Moreover, a link to each article is added for annex chapter. The reason for including the papers at the end of this thesis instead of doing it chapter 5 follows reading clearance and flow. In all case studies, markerless photogrammetric solutions are established based on geometric feature point identification or even specific photogrammetric models based on geometric element direct adjustment.

Whereas Case study 1 and 3 highlight measuring approaches based on image processing novel strategies, Case study 2 also presents a non-traditional photogrammetric model that deals with geometric element direct fitting without 3D coordinate adjustment.

5.1 Case study 1

DESCRIPTION: this study is focused on employing image data processing to extract by a photogrammetric approach the centers of machined holes without any artificial marker or target. Indeed, the main objective is to avoid the need to use an adapter to locate a marker centered on each hole for multiple holes simultaneous positioning determination. This goal is handled by replacing these adapters with image processing techniques and procedures that are able to detect, identify and extract each hole's geometric center based on nominal data and photogrammetric network prior establishment. Once camera intrinsic and extrinsic calibration has been determined by industrial solutions regarding a specific coordinate system, these results enable to carry out further photogrammetric processing steps. Nominal data is projected from 3D space to image plane and based on this data the border of the holes is estimated comparing measured and theoretical contour points. After calculating most suitable centers in image coordinates for each hole, a simultaneous positioning of every hole is established by means of BA approaches and triangulation approaches (see Figure 78). Apart from avoiding the need for an adapter for each feature, this method is suitable for the detection and measurement of other geometric elements defined by discrete nominal points.

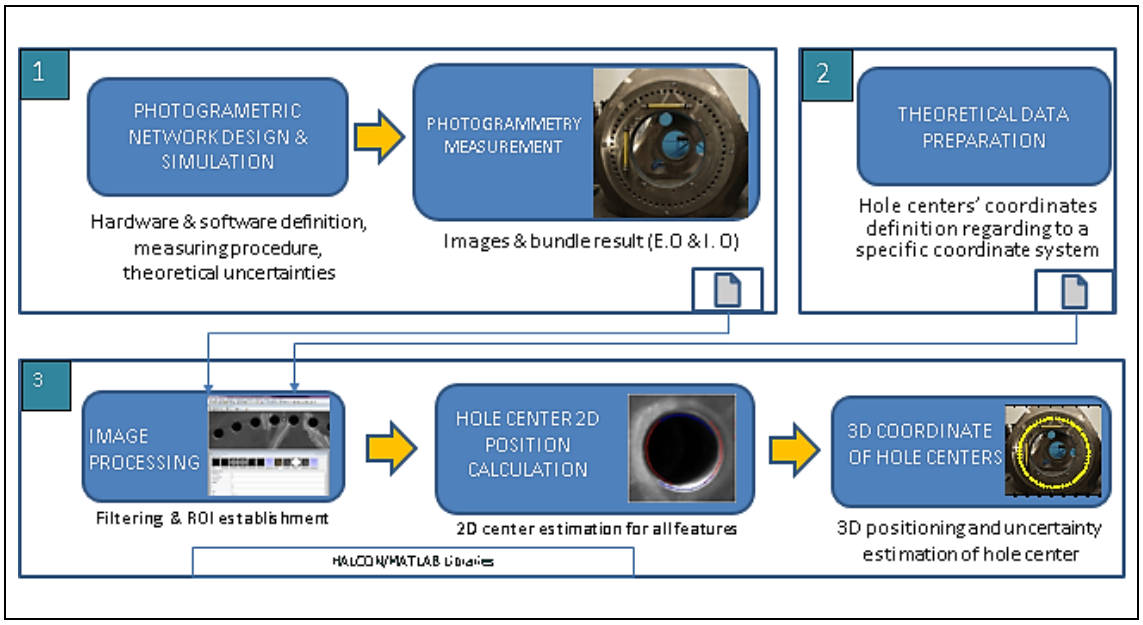

Figure 78. Solution scheme for multiple hole positioning estimation

MAIN RESULTS & CONCLUSIONS: the obtained results show that fit to purpose accuracies can be obtained in relation to part functionality and manufacturing tolerances. Moreover, more accurate image processing algorithms could even increase this accuracy for more demanding applications with similar verification requirements. The accuracy for the researched case study is ± 0.124µm/m and it is below 1mm that is a common specification for the inspection and validation of wind hubs. An improvement of photogrammetric approaches accuracy, CAD-based a priori nominal data employment, as well as pattern-based image processing algorithms, are promising fields that could improve industrial solutions capabilities.

Even though a similar approach can be applied to other repetitive geometric patterns which are nominally defined in relation to a specific coordinate system. Optical probing of required geometric elements seems to be an advantageous procedure to measure at once a high amount of identical geometries. The achievable accuracy in comparison to target-based approaches is worse (typically 25 µm/m) but the measuring procedure is faster as part preparation is simplified and cheaper as target adapters are eliminated to define the geometries of interest. Therefore, this measuring procedure presents improvements in measuring process flexibility and execution time reduction which could add value to inspection service where large parts have to be verified including a high number of repetitive geometries.

LINK TO PUBLISHED ARTICLE → Cross-reference

LINK TO ANNEX → Paper nº1

5.2 Case study 2

DESCRIPTION: this case study deals with 5 dof positioning tracking needs of a cylindrical element. It is based on contour-based points of the cylinder and a distance minimization approach between observed contour points, which define tangential light rays, and the monitored cylinder axis. Usual approaches do use characterized targets located on the geometric element or even distributed targets all around the element to estimate the position and orientation of the element. In both cases, the targets define the discrete points that are triangulated by means of BA approaches in order to calculate afterwards the geometric positioning of the element (Best-fit adjustment of 3D coordinates). If the nominal coordinates of the identified and measured points are known, Best-fit alignment approaches directly can be applied to derive cylinder position and orientation. If these points are not characterized a priori, a best-fitting of the cylindrical element can be accomplished in order to estimate its pose. In any case, a demanding difficulty arises from point distribution around and observability all around the element. Occlusion problems have to be handled from different camera views with corresponding limitations in terms of viewing optimal angles, point correspondence among the camera network and resulting accuracy loss. As an alternative to solve this barrier, the presented study doesn't require point triangulation which facilitates geometric element tracking based directly in contour points and mathematical modelling of the element of interest.

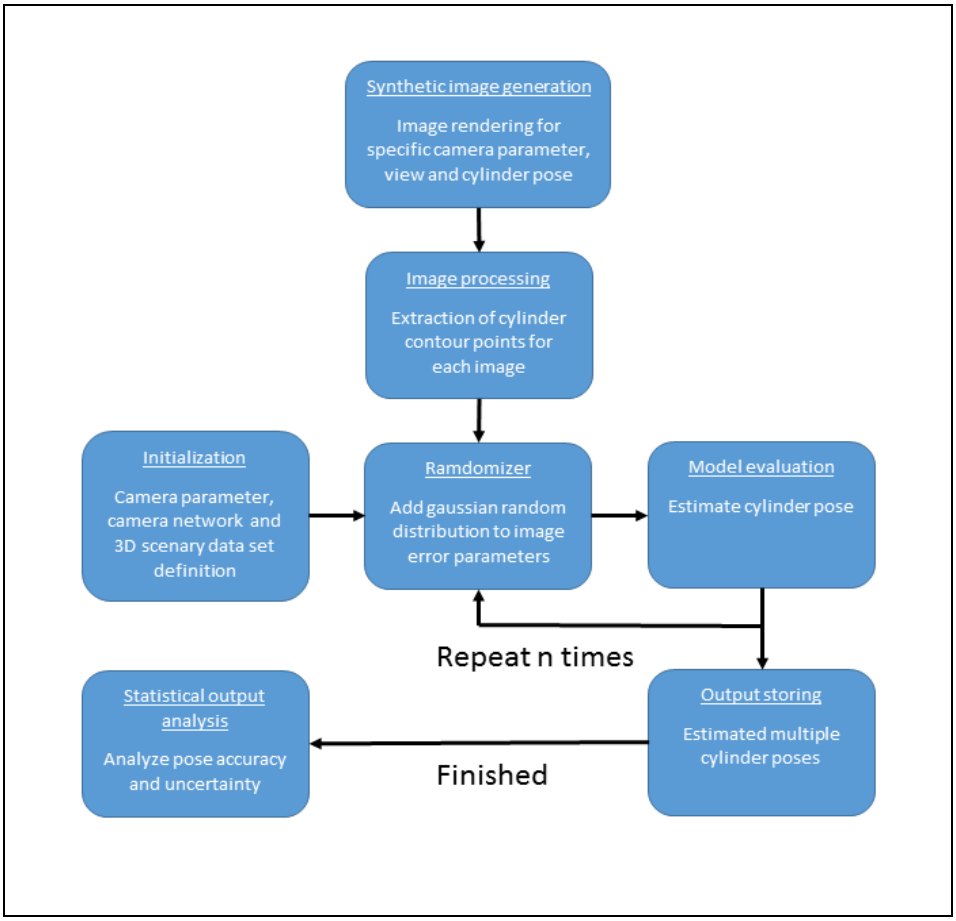

Figure 79. Solution scheme for the simulation of the pose of a cylindrical element

MAIN RESULTS & CONCLUSIONS: the preliminary results obtained in the simulation are promising from the point of view of achievable accuracy and model robustness in terms of contour point number and distribution. Hence, it has been demonstrated that this method is suitable and flexible for described purposes. These results are based on statistical Montecarlo simulation approaches which aim to establish the relationship of the model's error sources with output estimation (see Figure 79). The simulation comprises a known camera network calibration, camera parameter uncertainty, and multiple positioning scenarios to foresee the performance of the model for close-range application with large working ranges. Synthetically created and extracted image data from virtual images is the basis for this study. Achieved results where accuracy of 1/1000 and 1/20000 and uncertainties up to 15 mm for large working ranges are obtained, show the applicability of this photogrammetric approach against traditional target-based approaches in terms of fit to purpose accuracy and flexibility. Hence, this kind of photogrammetric models based on contour data are a suitable approach for similar scenarios where target set up above the object surface is not recommended or enabled. From the point of view of tracking functionalities, this method and its simulation do permit to foresee the performance of the model for critical poses.

LINK TO PUBLISHED ARTICLE → Cross-reference

LINK TO ANNEX → Paper nº2

5.3 Case study 3

DESCRIPTION: this research deals with dense point cloud reconstruction based on imagery data and photogrammetric modelling (See workflow in figure 80). It is commonly known as the structure form motion problem which is divided into two main steps. Photogrammetric network characterization and dense point cloud reconstruction based on surface point texture information. It is a solution that arises from application fields, such as heritage and topography, and which is an alternative to other large area scanning solutions such as LIDAR technology. In this specific case, the scope of this scanning approach has been deeply studied to understand the suitability for industrial requirements. In fact, the dimensional inspection of oxidized parts has been analyzed both in lab and workshops environments against established measuring procedures. Apart from reconstructing surface points form imagery data, the need for locating coded targets all around the part and its significance in terms of accuracy and processing time has been determined. This capability applied to industrial parts is a possible alternative of simplifying current 3D massive inspection methods that are carried out in two main steps. An initial photogrammetric phase which deals with reference point network characterization and a posteriori 3D scanning phase, based on structured light technologies, which uses this previous referencing step to bring all partial scans to a common coordinate system.

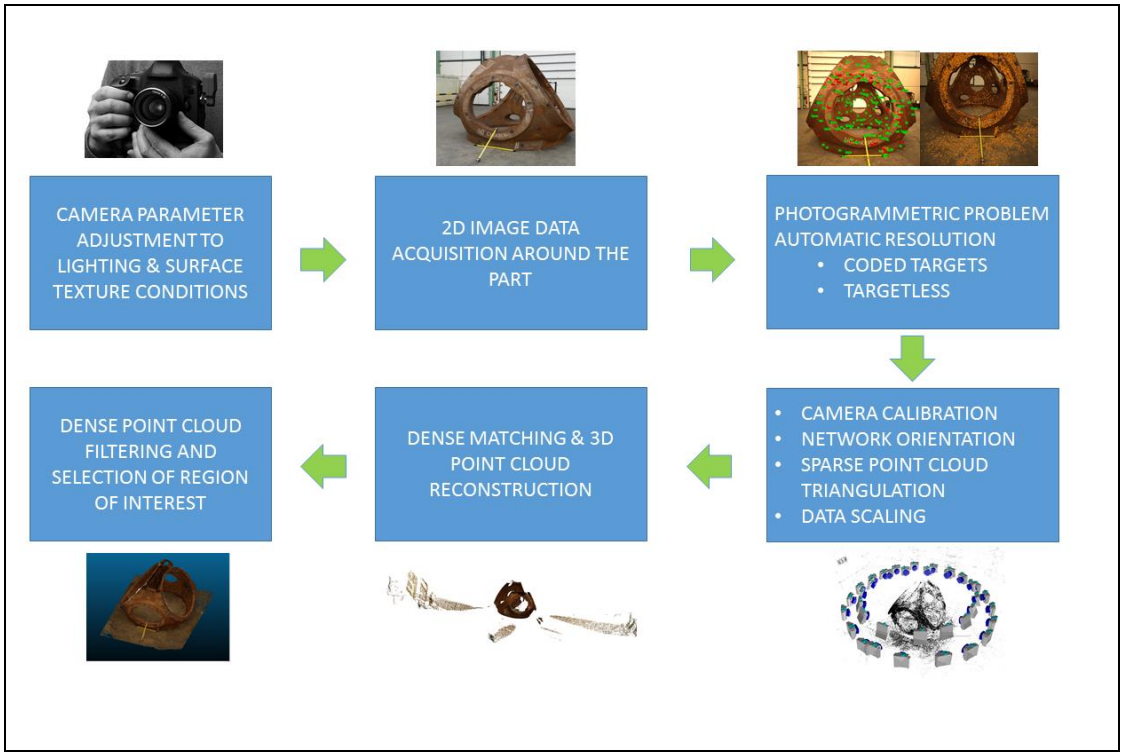

Figure 80. Solution scheme for dense surface matching and reconstruction

MAIN RESULTS & CONCLUSIONS: the results obtained from experimental validation with traditional inspection schemas demonstrate that this scanning method based on texturized image data is suitable 3D surface reconstruction and fulfills overall manufacturing inspection

requirements. Relative accuracies without employing coded targets for camera orientation are 1/27000 for the worst case, which is 2 to 3 times worse than using then. Hence eliminating coded targets for the photogrammetric steps is still a risky approach in terms of photogrammetric problem accurate solving, but it is a promising research line going beyond current photogrammetric solutions. Regarding 3D dense reconstruction, the oxidized surface of foundry parts are well suited to this inspection technology and therefore is a novel procedure for this aim. One drawback of the implementation of this measuring technique arises from data processing computation and time requirements. Currently, an offline processing schema is applied which takes long computation times which supposes a disadvantage in comparison to real-time scanning solutions. However, the data acquisition time is considerably reduced (to the half) as the method is simplified only to the photogrammetric phase avoiding a posteriori scanning step. Hence, an application-based evaluation of cons and pros is necessary to assess the applicability of this measuring technique in industrial applications.

LINK TO PUBLISHED ARTICLE → Cross-reference

LINK TO ANNEX → Paper nº3

6 CONCLUSIONS

Close-range photogrammetry is a promising measuring technique which is constantly and currently evolving due to advances in image processing algorithms, sensor data and optical modelling. These improvements are enabling to apply this measuring technique to a very wide range of industrial and non-industrial applications. Moreover, advantageous properties of this technique such as adaptability, accuracy, and measuring speed among others are replacing established procedures for vision-based approaches. From static scenarios to dynamic ones, different photogrammetric set-ups and solutions do meet with measuring requirements and they even achieve state of the art performance as good as traditional implemented methods.

Aeronautic and automotive sectors are involving more and more these technologies to their production facilities in different steps of the manufacturing process. Not only for quality control inspection but for in-process part qualification and process drift detection. Other application fields related to part manufacturing are also demanding this kind of technologies to overcome inspection and validation specifications.

The need for more advanced solutions which can avoid the use of artificial adapters or projected light patterns is a real need in the current industry. Moreover, novel photogrammetric models and their performance assessment analysis is critical to replace point triangulation-based solutions. In any case, the avoidance of preparation of the part or scene with artificial targets is a real demand nowadays comprising yield improvement of complex system manufacturing and assembly processes.

Traceability and achievable accuracy are one of the main aspects that have to be improved with this technology reinforcing existing standards and calibration methods. As real-time technologies are more and more employing for in-line inspection requirements, reliability of acquired data, as well as monitored data traceability, is critical. Hence, more complete standards based on ISO criteria is required to standardize the use and health check of this growing market. Simulation of measuring procedures and suitable design of camera networks is another key point that has to be evolved and set-up for technology users. At the moment, few tools are offering this capability which limits the in advance knowledge and suitability of photogrammetric methods for each measuring purpose.

In relation to the results achieved in the different case studies, several conclusions and reflections arise. A common conclusion is that ***markerless photogrammetric approaches*** comprising measuring methods and procedures can be ***fit to purpose in industrial applications*** although they come from the computer vision field where accuracy specifications are not such demanding. The validation criteria as for any other measuring technology or procedure is the conformity assessment of the manufacturing process tolerance. Therefore, if the accuracy of studied methods or similar ones that avoid the use or artificial markers is under specifications,

it is suitable for industrial measuring applications although approaches were not focused in industrial fields in their conception. Computer vision fields were fostering such kind of developments instead. However, the developments of each field can feed and improve others.

In the presented work, the suitability of each development for each case study has been demonstrated and discussed. Main conclusions are listed as follows:

1. **Improved image processing strategies** have been developed which enable to extract raw data from natural primitives on the imagery. Data extraction has been facilitated by a priori data employment strategies. The quality of imagery data is many times good enough to fed photogrammetric models instead of using artificial targets.
2. Although **markerless approaches** are less accurate than target-based ones, their accuracy is **under compliance** in studied applications.
3. **Simulation** of measurements and uncertainty assessment is advisable to study the compliance of the photogrammetric model and the measuring procedure for each application. Not only for 3D coordinate **uncertainty estimation** but for **sensitivity analysis** of photogrammetric solutions.
4. **Feature-based models** can be **suitable** for direct measurement of standard geometric elements and they can afford hard to reach of large dimension element measurement which needs to be covered by several cameras and corresponding FOVs. Moreover, such kind of models do add flexibility and robustness to the camera network design.
5. The employment of **natural features** appearing on the images can **simplify measuring approaches** and increase their efficiency. Although data processing can be challenging and time-consuming, the measuring process duration is shortened considerably. Moreover, data processing strategies can be automated by means of scripts and smart algorithms.

Regarding each case study, specific conclusions are included as follows.

Case study1. **Multiple feature simultaneous measurement** brings the opportunity to measure the 3D positioning grids of repetitive geometric features **with faster and cheaper procedures than traditional photogrammetric solutions**. In this case, the positioning of chamfered drilled holes has been successfully inspected. The need for adapters or artificial targets is neglected as raw imagery data is taken in advantage for the photogrammetric solution improvement. This approach comprises a two-step bundle adjustment model and data processing schema. Within this aim a priori data has been successfully employed. Although CAD-based information has been employed in this research, image processing approaches based on reference image definition and pattern-based matching could be employed instead. However, this is not a functionality of industrial offline photogrammetric approaches (optical CMM) or at least it is not automatic (manually guided). Moreover, bundle block adjustment considering this natural point is not provided which limits the possibility to avoid artificial targets. The economic advantage avoiding the use of a wide range of adapters and reduction of time consumption required to the preparation of the scenery set-up is substantial, enabling novel measuring approaches and more efficient manufacturing control processes. Moreover, target rejection from measurand surface disappears as target employment is avoided. Exploitation of this research will follow fixed and self-calibrated multi-camera systems which will permit to develop flexible monitoring systems for in-situ structure inspection and perform quality control.

Case study2. **Contour point-based photogrammetric** approaches enable to measure the spatial pose of geometric elements **eliminating** the need for artificial targets and demanding processing steps such as point **triangulation and correspondence**. Correspondence problem, as well as occurring occlusions and triangulation limitations, are discarded as the geometric element is not fitted by means of distributed points located on each surface. Traditional photogrammetry has to deal with these issues, but restrictions do appear in some applications. Especially, round objects that have to be located/tracked in large working volume, which supposes huge perspective differences, can benefit from feature-based **flexible models**. Possibly, the best compromise would be to use hybrid models taking advantage of the output target-based and markerless approaches. For example, camera calibration and network tasks could be solved by means of few artificial points whereas feature-based models could deal with tracking requirements. One of the main drawbacks instead, is the limitation in terms of measurable degrees of freedom for each geometric element. In most of the case the rotation of the element around its geometric axis is not quantifiable because of lack of sensitivity of this modelling regarding this parameter. However, a combination of geometric elements can overcome this problem. Nowadays industrial software and hardware packages do not offer such kind of model as an alternative to point-based photogrammetric models. Some of them make possible to figure out the photogrammetric problem based on triangulation of straight lines, but the basics and fundamentals are the same as point-based triangulation. Hence, photogrammetric software tools with hybrid modelling will enhance the scope and range of applicability. From the point of view of hardware, the employment of filters and imaging sensor sensitivity for certain spectrum bandpass could facilitate further image processing demands. Although this study has been applied on a single geometric element, the approach can be adapted to multiple features by means of image segmentation techniques. Moreover, such kind of approaches can be suitable for large part characterization with several cameras that measure a segment of the element of interest.

Case study3. Dense reconstruction based on **SFM photogrammetry** of textured parts is a promising field even for industrial applications instead of applying it only to heritage or topographic mapping tasks. It has the capability to achieve fit to purpose dense point clouds with suitable measuring procedures which are required for quality control purposes. Therefore, it could substitute LIDAR or 3D scanners for such applications. Furthermore, it could **replace** or be complementary to existing 3D scanning technologies, which comprise demanding scenario set-up and non-cost-effective technology combination to succeed in large part scanning tasks. The objective is to reduce initial investment costs using cheap cameras and to decrease inspection service costs simplifying **complex measuring procedures**. Another advantage arises from achievable point density and color information which opens the range of output point cloud employment not only for inspection tasks but for 3D digital visualization and as-built augmented reality solutions.

Regarding disadvantages or possible improvements, the dense image matching process is computationally and time intensive and it can take several minutes to hours to generate the dense 3D point cloud to highest resolution. Hence, the development of high-efficiency algorithms and data computation strategies are necessary to speed up result extraction of output results. For sure this limitation will decrease in the coming years with the

development of computer processing capabilities. Another aspect to be enhanced is the continuity and homogeneity of the obtained dense point cloud. As data processing is an offline approach and is time-consuming, the suitability of achieved surface cannot be checked during measurements, which diminish the reliability of this technique in terms of data quality. Considering accuracy issues, more robust and accurate image processing algorithms for feature detection and matching are required which will permit to get more accurate point clouds and consequently the use of this photogrammetric approach for more demanding industrial scenarios. Even, going further with machined parts and surfaces could be a future target although is not compatible with textured surface information. Future exploitation depends on the acquired data real-time employment based on smarter and high-efficiency data handling algorithms. Videogrammetry methods could take advantage of this method and speed enhancement could enable the development of in-process solutions for example for casting part quality control.

Finally, during the execution of this thesis other missing photogrammetric aspects have been also detected and studied but they are out of the scope of this research. For example, simulation tools to design which the suitable measuring or calibration procedure is or even the study of vision technologies fusion aiming progress in existing approaches. Thermal 3D mapping is an example of dense matching with assigned temperature maps and technology. Moreover, constrained modelling is a promising field that could improve current industrial solution capabilities related to extrinsic calibration matters. Algorithms can be enhanced by parameter restriction or a priori data employment increasing their robustness and accuracy. This all leads to new edge-cutting solutions that will be implemented in the coming future driving more flexible, robust and precise photogrammetric solutions.

7 BIBLIOGRAPHIC REFERENCES

1. Schleich, B.; Wärmefjord, K.; Söderberg, R.; Wartzack, S. Geometrical Variations Management 4.0: Towards next generation geometry assurance. *Procedia CIRP* **2018**, *75*, 3–10, doi:10.1016/j.procir.2018.04.078.

2. Majstorovic, V.; Stojadinovic, S.; Jakovljevic, Z.; Zivkovic, S.; Djurdjanovic, D.; Kostic, J.; Gligorijevic, N. Cyber-Physical Manufacturing Metrology Model (CPM3) - Big Data Analytics Issue. *Procedia CIRP* **2018**, *72*, 503–508, doi:10.1016/j.procir.2018.03.091.

3. Berthold, J.; Imkamp, D. Looking at the future of manufacturing metrology: Roadmap document of the German VDI/VDE Society for Measurement and Automatic Control. *J. Sensors Sens. Syst.* **2013**, *2*, 1–7, doi:10.5194/jsss-2-1-2013.

4. Schmitt, R. H.; Peterek, M.; Morse, E.; Knapp, W.; Galetto, M.; H??rtig, F.; Goch, G.; Hughes, B.; Forbes, a.; Estler, W. T. Advances in Large-Scale Metrology ??? Review and future trends. *CIRP Ann. - Manuf. Technol.* **2016**, *65*, 643–665, doi:10.1016/j.cirp.2016.05.002.

5. Muelaner, J. E.; Maropoulos, P. G. Large volume metrology technologies for the light controlled factory. In *Procedia CIRP*; 2014; Vol. 25.

6. Luhmann, T. Close range photogrammetry for industrial applications. *ISPRS J. Photogramm. Remote Sens.* **2010**, *65*, 558–569, doi:10.1016/j.isprsjprs.2010.06.003.

7. Luhmann, T.; Robson, S.; Kyle, S.; Boehm, J. *Close-Range Photogrammetry and 3D Imaging*; 2nd ed.; De Gruyter Textbook, 2013; ISBN 9783110302783.

8. Van Den Heuvel, F. A.; Kroon, R. J. G. A.; Le Poole, R. S. DIGITAL CLOSE-RANGE PHOTOGRAMMETRY USING ARTIFICIAL TARGETS. *Int. Arch. Photogramm. Remote Sens.* **1993**, *29*, 222–222.

9. Luhmann, T. Close range photogrammetry for industrial applications. *ISPRS J. Photogramm. Remote Sens.* **2010**, *65*, 558–569, doi:10.1016/j.isprsjprs.2010.06.003.

10. Gillies, D. Close Range Photogrammetry. *Photogramm. Rec.* 2015, *30*, 318–322.

11. Turbines, W.; Surfaces, M. Application Example : Quality Control Mobile Optical Coordinate Measuring Technology Used in Offshore Wind Turbines Setup. **2009**, 1–6.

12. Foundry modernization with optical 3D metrology solutions | GOM Available online: https://www.gom.com/news/latest-news/foundry-modernization-with-optical-3d-metrology-solutions.html (accessed on Sep 4, 2019).

13. Estler, W. T.; Edmundson, K. L.; Peggs, G. N.; Parker, D. H. Large-Scale Metrology – An Update. *CIRP Ann. - Manuf. Technol.* **2002**, *51*, 587–609, doi:10.1016/S0007-8506(07)61702-8.

14. Franceschini, F.; Galetto, M.; Maisano, D.; Mastrogiacomo, L. Large-scale dimensional metrology (LSDM): From tapes and theodolites to multi-sensor systems. *Int. J. Precis. Eng. Manuf.* 2014, *15*, 1739–1758.

15. Muelaner, J. E.; Maropoulos, P. G. Large volume metrology technologies for the light controlled factory. In *Procedia CIRP*; 2014; Vol. 25, pp. 169–176.

16. Conte, J.; Santolaria, J.; Majarena, A. C.; Brau, A.; Aguilar, J. J. Identification and kinematic calculation of Laser Tracker errors. *Procedia Eng.* **2013**, *63*, 379–387, doi:10.1016/j.proeng.2013.08.190.

17. Muralikrishnan, B.; Phillips, S.; Sawyer, D. Laser trackers for large-scale dimensional metrology : A review. *Precis. Eng.* **2015**, 1–16, doi:10.1016/j.precisioneng.2015.12.001.

18. Acero, R.; Brau, A.; Santolaria, J.; Pueo, M. Verification of an articulated arm coordinate measuring machine using a laser tracker as reference equipment and an indexed metrology platform. *Meas. J. Int. Meas. Confed.* **2015**, *69*, doi:10.1016/j.measurement.2015.03.023.

19. Vagovský, J.; Buranský, I.; Görög, A. Evaluation of measuring capability of the optical 3D scanner. *Procedia Eng.* **2015**, *100*, 1198–1206, doi:10.1016/j.proeng.2015.01.484.

20. Li, F.; Stoddart, D.; Zwierzak, I. A Performance Test for a Fringe Projection Scanner in Various Ambient Light Conditions. *Procedia CIRP* **2017**, *62*, 400–404, doi:10.1016/j.procir.2016.06.080.

21. Heipke, C.; Madden, M.; Li, Z.; Dowman, I. Theme issue “State-of-the-art in photogrammetry, remote sensing and spatial information science.” *ISPRS J. Photogramm. Remote Sens.* **2016**, *115*, 1–2, doi:10.1016/j.isprsjprs.2016.03.006.

22. Kujawi, M. Measuring structural displacements with digital image correlation. *SPIE* **2013**, *2*, 3–6.

23. Orteu, M. A. S. J. J.; Schreier, H. W. *Image Correlation for Shape, Motion and Deformatio Meaurements. Basic Concepts, Theory and Applications*; Springer.; 2009; ISBN 9780387787466.

24. Roberts, B. C.; Perilli, E.; Reynolds, K. J. Application of the digital volume correlation technique for the measurement of displacement and strain fi elds in bone : A literature review. *J. Biomech.* **2014**, *47*, 923–934, doi:10.1016/j.jbiomech.2014.01.001.

25. Pai, P. F.; Ramanathan, S.; Hu, J.; Chernova, D. K.; Qian, X.; Wu, G. Camera-based noncontact metrology for static / dynamic testing of flexible multibody systems. *Measiurement Sci. Technol.* **2010**, 14pp, doi:10.1088/0957-0233/21/8/085302.

26. Toschi, I.; Capra, A.; De Luca, L.; Beraldin, J.-A.; Cournoyer, L. On the evaluation of photogrammetric methods for dense 3D surface reconstruction in a metrological context. *ISPRS Ann. Photogramm. Remote Sens. Spat. Inf. Sci.* **2014**, *II-5*, 371–378, doi:10.5194/isprsannals-II-5-371-2014.

27. Rothermel, M.; Wenzel, K. SURE - Photogrammetric Surface Reconstruction from Imagery. *Proc. LC3D Work.* **2012**, 1–21.

28. Conte, J.; Santolaria, J.; Majarena, A. C.; Acero, R. Modelling, kinematic parameter identification and sensitivity analysis of a Laser Tracker having the beam source in the rotating head. *Meas. J. Int. Meas. Confed.* **2016**, *89*, 261–272, doi:10.1016/j.measurement.2016.03.059.

29. Becker, T. .; Özkul, M. .; Stilla, U. . Simulation of close-range photogrammetric systems for industrial surface inspection. *Int. Arch. Photogramm. Remote Sens. Spat. Inf. Sci. - ISPRS Arch.* **2011**, *38*, 179–183.

30. Hastedt, H. Monte-carlo-simulation in close-range photogrammetry. *Int. Arch. Photogramm. Remote Sens. Spat. Inf. Sci.* **2004**, *35*, 18–23.

31. Shih, T. Y. A photogrammetric simulator for close-range applications. *Photogramm. Eng. Remote Sensing* **1996**, *62*, 89–92.

32. Luhmann, T. Learning photogrammetry with interactive software tool PhoX. *Int. Arch. Photogramm. Remote Sens. Spat. Inf. Sci. - ISPRS Arch.* **2016**, *41*, 39–44, doi:10.5194/isprsarchives-XLI-B6-39-2016.

33. Lourakis, M. I. a.; Argyros, A. a. Sba. *ACM Trans. Math. Softw.* **2009**, *36*, 1–30, doi:10.1145/1486525.1486527.

34. Triggs, B.; Mclauchlan, P.; Hartley, R.; Fitzgibbon, A.; Triggs, B.; Mclauchlan, P.; Hartley, R.; Fitzgibbon, A.; Adjustment, B.; Synthesis, a M.; Triggs, B.; Zisserman, A.; International, R. S. *Bundle Adjustment – A Modern Synthesis To cite this version : Bundle Adjustment — A Modern Synthesis*; 2000; ISBN 3540444807.

35. Buffa, F.; Pinna, a.; Sanna, G. a Simulation Tool Assisting the Design of a Close Range Photogrammetry System for the Sardinia Radio Telescope. *ISPRS Ann.*

Photogramm. Remote Sens. Spat. Inf. Sci. **2016**, *III-5*, 113–120, doi:10.5194/isprsannals-III-5-113-2016.

36. Tushev, S.; Sukhovilov, B. Photogrammetric system accuracy estimation by simulation modelling. *2017 Int. Conf. Ind. Eng. Appl. Manuf.* **2017**, 1–6, doi:10.1109/ICIEAM.2017.8076464.

37. Dunn, E. Development of a practical photogrammetric network design using evolutionary computing. *Photogramm. Rec.* **2007**, *22*, 22–38, doi:10.1111/j.1477-9730.2007.00403.x.

38. Indu, S.; Chaudhury, S.; Mittal, N. R.; Bhattacharyya, a Optimal Visual Sensor Placement using Evolutionary Algorithm. *Natl. Conf. Comput. Vision, Pattern Recognition, Image Process. Graph.* **2008**, 1–5.

39. Olague, G.; Others Design and simulation of photogrammetric networks using genetic algorithms. *Proc. 2000 Meet. Am. Soc. Photogramm. Remote Sens. (ASPRS 2000), Vol.* **2000**.

40. Santos, C. A.; Costa, C. O.; Batista, J. A vision-based system for measuring the displacements of large structures: Simultaneous adaptive calibration and full motion estimation. *Mech. Syst. Signal Process.* **2016**, *72-73*, 678–694, doi:10.1016/j.ymssp.2015.10.033.

41. J.F Larue, M Viala, D. Brown, and C. M. Dynamic Referencing in 3D Optical Metrology for Higher Accuracy in Shop Floor Conditions. *Creaform Fr. Fr.* **2016**.

42. Cuesta, E.; Suarez-Mendez, J. M.; Martinez-Pellitero, S.; Barreiro, J.; Alvarez, B. J.; Zapico, P. Metrological evaluation of Structured Light 3D scanning system with an optical feature-based gauge. *Procedia Manuf.* **2017**, *13*, 526–533, doi:10.1016/j.promfg.2017.09.078.

43. He, W.; Zhong, K.; Li, Z.; Meng, X.; Cheng, X.; Liu, X. Accurate calibration method for blade 3D shape metrology system integrated by fringe projection profilometry and conoscopic holography. *Opt. Lasers Eng.* **2018**, *110*, 253–261, doi:10.1016/j.optlaseng.2018.06.012.

44. Kuş, A. Implementation of 3D optical scanning technology for automotive applications. *Sensors* **2009**, *9*, 1967–1979, doi:10.3390/s90301967.

45. Galantucci, L. M.; Bari, P.; Bari, P. Accuracy Issues of Digital Photogrammetry for 3D Digitization of Industrial Products. *Rev. Int. Ing. Numer.* **2006**, *2*, 29–40.

46. Guidi, G. Metrological characterization of 3D imaging devices. **2013**, 87910M, doi:10.1117/12.2021037.

47. Phillips, S.; Krystek, M.; Shakarji, C.; Summerhays, K. Dimensional measurement traceability of 3D imaging data. *Three-Dimensional Imaging Metrol.* **2008**, *7239*, 72390E, doi:10.1117/12.816498.

48. Dury, M. R.; Woodward, S. D.; Brown, S. B.; McCarthy, M. B. Surface finish and 3D optical scanner measurement performance for precision engineering. *Proc. - ASPE 2015 Annu. Meet.* **2015**, 419–423.

49. Title : Traceable metrology for optical CMMs and quantitative microscopy in industry. **2017**, 2–4.

50. Luhmann, T.; Wendt, K. Recommendations for an Acceptance and Verification Test of Optical 3-D Measurement Systems. *Int. Arch. Photogramm. Remote Sens.* **2000**, *XXXIII*, 493–500.

51. Sims-Waterhouse, D.; Piano, S.; Leach, R. Verification of micro-scale photogrammetry for smooth three-dimensional object measurement. *Meas. Sci. Technol.* **2017**, *28*, doi:10.1088/1361-6501/aa6364.

52. Eiríksson, E. R.; Wilm, J.; Pedersen, D. B.; Aanæs, H. Precision and Accuracy Parameters in Structured Light 3-D Scanning. *ISPRS - Int. Arch. Photogramm. Remote Sens. Spat. Inf. Sci.* **2016**, *XL-5/W8*, 7–15, doi:10.5194/isprsarchives-XL-5-W8-7-2016.

53. Kersten, T.; Przybilla, H.-J.; Lindstaedt, M. Investigations of the Geometrical Accuracy of Handheld 3D Scanning Systems. *Photogramm. - Fernerkundung - Geoinf.* **2016**, *2016*, 271–283, doi:10.1127/pfg/2016/0305.

54. Tiscareño, J.; Santolaria, J.; Albajez, J. a. Measurement procedure for application of white light scanner in the automotive sector. *Procedia Manuf.* **2017**, *13*, 565–572, doi:10.1016/j.promfg.2017.09.094.

55. Martin, O. C.; Robson, S.; Kayani, A.; Muelaner, J. E.; Dhokia, V.; Maropoulos, P. G. Comparative Performance between Two Photogrammetric Systems and a Reference Laser Tracker Network for Large-Volume Industrial Measurement. *Photogramm. Rec.* **2016**, *31*, 348–360, doi:10.1111/phor.12154.

56. De Sousa, G. B.; Olabi, A.; Palos, J.; Gibaru, O. 3D Metrology Using a Collaborative Robot with a Laser Triangulation Sensor. *Procedia Manuf.* **2017**, *11*, 132–140, doi:10.1016/j.promfg.2017.07.211.

57. Li, J.; Chen, M.; Jin, X.; Chen, Y.; Dai, Z.; Ou, Z.; Tang, Q. Calibration of a multiple axes 3-D laser scanning system consisting of robot, portable laser scanner and turntable. *Optik (Stuttg).* **2011**, *122*, 324–329, doi:10.1016/j.ijleo.2010.02.014.

58. Chromy, A. High-accuracy volumetric measurements of soft tissues using robotic 3D scanner. *IFAC-PapersOnLine* **2015**, *28*, 318–323, doi:10.1016/j.ifacol.2015.07.054.

59. Rao, M. R.; Radhakrishna, D.; Usha, S. Development of a Robot-mounted 3D Scanner and Multi-view Registration Techniques for Industrial Applications. *Procedia Comput. Sci.* **2018**, *133*, 256–267, doi:10.1016/j.procs.2018.07.032.

60. ATOS | GOM Available online: https://www.gom.com/metrology-systems/atos.html (accessed on Sep 4, 2019).

61. MetraSCAN 3D | Handheld [Optical CMM 3D Laser Scanner] by Creaform Available online: https://www.creaform3d.com/en/optical-3d-scanner-metrascan (accessed on Sep 4, 2019).

62. Sause, M. G. R. Digital image correlation. *Springer Ser. Mater. Sci.* **2016**, *242*, 57–129, doi:10.1007/978-3-319-30954-5_3.

63. Pan, B. Digital image correlation for surface deformation measurement: Historical developments, recent advances and future goals. *Meas. Sci. Technol.* **2018**, *29*, doi:10.1088/1361-6501/aac55b.

64. Sutton, M. a. Digital Image Correlation for Shape and Deformation Measurements. *Springer Handb. Exp. Solid Mech.* **2008**, 565–600, doi:10.1007/978-0-387-30877-7_20.

65. Digital Image Correlation | Trilion Quality Systems | GOM Certified Partner Available online: https://trilion.com/ (accessed on Sep 4, 2019).

66. GOM5 new hardware Available online: http://metrology.news/5th-generation-gom-optical-sensors-enables-large-measuring-volume-scanning.

67. Bösemann, W. INDUSTRIAL PHOTOGRAMMETRY - ACCEPTED METROLOGY TOOL OR EXOTIC NICHE. **2016**, *XLI*, 12–19, doi:10.5194/isprsarchives-XLI-B5-15-2016.

68. Bösemann, W. Industrial photogrammetry: challenges and opportunities. **2011**, *8085*, 80850H, doi:10.1117/12.889170.

69. Percoco, G.; Guerra, M. G.; Sanchez Salmeron, A. J.; Galantucci, L. M. Experimental investigation on camera calibration for 3D photogrammetric scanning of micro-features for micrometric resolution. *Int. J. Adv. Manuf. Technol.* **2017**, *91*, 2935–2947, doi:10.1007/s00170-016-9949-6.

70. Percoco, G.; Sánchez Salmerón, A. J. Photogrammetric measurement of 3D freeform millimetre-sized objects with micro features: An experimental validation of the close-range camera calibration model for narrow angles of view. *Meas. Sci. Technol.* **2015**, *26*, doi:10.1088/0957-0233/26/9/095203.

71. Galantucci, L. M.; Guerra, M. G.; Lavecchia, F. *Proceedings of 3rd International Conference on the Industry 4.0 Model for Advanced Manufacturing*; Springer International Publishing, 2018; ISBN 978-3-319-89562-8.

72. Guerra, M. G.; Volpone, C.; Galantucci, L. M.; Percoco, G. Photogrammetric measurements of 3D printed microfluidic devices. *Addit. Manuf.* **2018**, *21*, 53–62, doi:10.1016/j.addma.2018.02.013.

73. Cornille, N.; Garcia, D.; Sutton, M. A.; Mcneill, S. R. Automated 3-D Reconstruction Using a Scanning Electron Microscope SEM Imaging Considerations Calibration Procedure. *SEM Conf. Exp. Appl. Mech. Charlotte* **2003**, 2–4.

74. Tafti, A. P.; Kirkpatrick, A. B.; Alavi, Z.; Owen, H. A.; Yu, Z. Recent advances in 3D SEM surface reconstruction. *Micron* **2015**, *78*, 54–66, doi:10.1016/j.micron.2015.07.005.

75. Zolotukhin, A. A.; Safonov, I. V; Kryzhanovskii, K. A. 3D Reconstruction for a Scanning Electron Microscope. **2013**, *23*, 168–174, doi:10.1134/S105466181301015X.

76. Roy, S.; Meunier, J.; Marian, A. M.; Vidal, F.; Brunette, I.; Costantino, S. Automatic 3D reconstruction of quasi-planar stereo Scanning Electron Microscopy (SEM) images *. **2012**, 4361–4364.

77. Eulitz, M.; Reiss, G. 3D reconstruction of SEM images by use of optical photogrammetry software. *J. Struct. Biol.* **2015**, *191*, 190–196, doi:10.1016/j.jsb.2015.06.010.

78. Easa, S. M. Space resection in photogrammetry using collinearity condition without linearisation. **2017**, *6265*, 39–49, doi:10.1179/003962609X451681.

79. Luhmann, T. Precision potential of photogrammetric 6DOF pose estimation with a single camera. *ISPRS J. Photogramm. Remote Sens.* **2009**, *64*, 275–284, doi:10.1016/j.isprsjprs.2009.01.002.

80. Merritt, E. L. Space Resection. *Photogramm. Eng.* **1949**.

81. Shih, T. Y.; Faig, W. A SOLUTION FOR SPACE RESECTION IN CLOSED FORM. **1979**.

82. Metronor SOLO | Industrial Available online: http://www.metronor.com/industrial/products/solo/ (accessed on Sep 4, 2019).

83. Laser Tracker 6DoF Technology to improve Automated Solutions - PDF Available online: https://docplayer.net/54619844-Laser-tracker-6dof-technology-to-improve-automated-solutions.html (accessed on Sep 4, 2019).

84. A History of Metrology - Design Engineering Available online: https://www.design-engineering.com/features/metrology-1004024832/ (accessed on Sep 4, 2019).

85. GOM ARAMIS SRX 3D Measurement System Provides Dynamic Evaluation – Metrology and Quality News - Online Magazine Available online: https://metrology.news/gom-aramis-srx-3d-measurement-system-provides-dynamic-evaluation/ (accessed on Sep 4, 2019).

86. Digital Image Correlation (DIC) | Trilion Quality Systems Available online: https://trilion.com/digital-image-correlation/ (accessed on Sep 4, 2019).

87. HandySCAN 3D | Professional Portable Metrology-Grade [3D Laser Scanner] Available online: https://www.creaform3d.com/en/portable-3d-scanner-handyscan-3d?gclid=EAIaIQobChMIsb36vaa35AIVD853Ch1_Dw6vEAAYASAAEgJ_vPD_BwE (accessed on Sep 4, 2019).

88. Best handheld 3D scanners 2019 - 3D scanner reviews and buying guide Available online: https://www.aniwaa.com/best-handheld-and-portable-3d-scanner/ (accessed on Sep 4, 2019).

89. Tiwari, R. S. Fixed-Frame Multiple-Camera System for Close-Range Photog ram metry. **1976**, *42*, 1195–1210.

90. Kottner, S.; Ebert, L. C.; Ampanozi, G.; Braun, M.; Thali, M. J.; Gascho, D. A Mobile, Multi Camera Setup for 3D Full Body Imaging in Combination with Post-Mortem Computed Tomography Procedures. *Proc. 7th Int. Conf. 3D Body Scanning Technol. Lugano, Switzerland, 30 Nov.-1 Dec. 2016* **2016**, 53–60, doi:10.15221/16.053.

91. Garsthagen, R. An Open Source, Low-Cost, Multi Camera Full-Body 3D Scanner. *Proc. 5th Int. Conf. 3D Body Scanning Technol. Lugano, Switzerland, 21-22 Oct. 2014* **2014**, 174–183, doi:10.15221/14.174.

92. Fraser, C. S.; Veress, S. a Self-Calibration of a Fixed-Frame Multiple-Camera System. *Photogramm. Eng. Remote Sens.* **1980**, *46*, 1439–1445.

93. Habib, A.; Detchev, I.; Kwak, E. Stability analysis for a multi-Camera photogrammetric system. *Sensors (Switzerland)* **2014**, *14*, 15084–15112, doi:10.3390/s140815084.

94. Tube inspection system Available online: http://www.accurexmeasure.com/tubeinspect-p8.htm.

95. Xangle 3d Scanning & Photogrammetry in Montréal Available online: https://xangle3d.com/ (accessed on Sep 4, 2019).

96. TubeInspect | Hexagon Manufacturing Intelligence Available online: https://www.hexagonmi.com/products/photogrammetry/tubeinspect (accessed on Sep 4, 2019).

97. POLYRIX Available online: http://www.polyrix.com/ (accessed on Sep 4, 2019).

98. QFoto - CSP Services Available online: http://www.cspservices.de/products-services/measurement-systems/qfoto (accessed on Sep 4, 2019).

99. DigiMetric Photogrammetry--Shining 3D Tech Co.,Ltd Available online: http://en.shining3d.com/digitizer_detail-3553.html (accessed on Sep 4, 2019).

100. Dedicated Shopfloor Photogrammetry Solution – Metrology and Quality News - Online Magazine Available online: https://metrology.news/dedicated-shopfloor-photogrammetry-solution/ (accessed on Sep 4, 2019).

101. ATOS accessories | Accessories for 3D scanners from GOM - Zebicon Available online: https://www.zebicon.com/en/metrology-systems/accessories/atos-accessories/ (accessed on Sep 4, 2019).

102. ATOS ScanBox Series 7 - Big Zero Technology Available online: http://www.bigzerotechnology.com/Products/GOM/ATOS-ScanBox-Series-7/58 (accessed on Sep 4, 2019).

103. CUBE-R [3D Scanning CMM] for Automated Quality Control | Creaform Available online: https://www.creaform3d.com/en/metrology-solutions/cube-r-automated-quality-control (accessed on Sep 4, 2019).

104. Absolute Accuracy Coordinate Measuring Robot Launched – Metrology and Quality News - Online Magazine Available online: https://metrology.news/absolute-accuracy-coordinate-measuring-robot-launched/ (accessed on Sep 4, 2019).

105. Works, H. I.; Projector, L. Laser Projection for Streamlining Production and Assembly Available online: https://www.qualitymag.com/ext/resources/files/white_papers/FARO/0817-WhitePaper-FARO-LaserProjection3.pdf (accessed on Sep 4, 2019).

106. 3D Augmented Reality Using Laser Projection – Metrology and Quality News - Online Magazine Available online: https://metrology.news/3d-augmented-reality-using-laser-projection/ (accessed on Sep 4, 2019).

107. Hernán-Pérez, a. S.; Domínguez, M. G.; González, C. R.; Martín, a. P. Using iphone camera in photomodeler for the 3D survey of a sculpture as practice for architecturés students. *Procedia Comput. Sci.* **2013**, *25*, 345–347, doi:10.1016/j.procs.2013.11.041.

108. Green, J. Underwater archaeological surveying using PhotoModeler, VirtualMapper: different applications for different problems. *Int. J. Naut. Archaeol.* **2002**, *31*, 283–292, doi:10.1006/ijna.2002.1041.

109. Lynnerup, N.; Andersen, M.; Lauritsen, H. P. Facial image identification using Photomodeler®. *Leg. Med.* **2003**, *5*, 156–160, doi:10.1016/S1344-6223(03)00054-3.

110. Stamatopoulos, C.; Fraser, C. S. Automated Target-Free Network Orienation and Camera Calibration. *ISPRS Ann. Photogramm. Remote Sens. Spat. Inf. Sci.* **2014**, *II-5*, 339–346, doi:10.5194/isprsannals-II-5-339-2014.

111. Jazayeri, I.; Fraser, C.; Cronk, S. Automated 3D object reconstruction via multi-image close-range photogrammetry. *Int. Arch. Photogramm. Remote Sens. Spat. Inf. Sci.* **2010**, *XXXVIII*, 3–8.

112. Fraser, C. Advances in Close-Range Photogrammetry. *Photogramm. Week 2015* **2015**, 257–268.

113. Piatti, E. J.; Lerma, J. L. Virtual Worlds for Photogrammetric Image-Based Simulation and Learning. *Photogramm. Rec.* **2013**, *28*, 27–42, doi:10.1111/phor.12001.

114. Piatti, E. J.; Lerma, J. L. Generation of true ortho-images based on virtual worlds: Learning aspects. *Photogramm. Rec.* **2014**, *29*, 49–67, doi:10.1111/phor.12053.

115. Photogrammetric software comparison Available online: https://en.wikipedia.org/wiki/Comparison_of_photogrammetry_software (accessed on Sep 4, 2019).

116. Bartoš, K.; Pukanská, K.; Sabová, J. Overview of Available Open-Source Photogrammetric Software, its Use and Analysis. *Int. J. Innov. Educ. Res. www.ijier.net* **2014**, *2*, 62–70.

117. Moons, T.; Vergauwen, M.; Van Gool, L. 3D reconstruction from multiple images. **2008**, 1–10.

118. Brito, J. H. Autocalibration for Structure from Motion. *Comput. Vis. Image Underst.* **2017**, *157*, 240–254, doi:10.1016/j.cviu.2016.12.007.

119. Fraser, C.; Jazayeri, I.; Cronk, S. A feature-based matching strategy for automated 3D model reconstruction in multi-image close-range photogrammetry. *Am. Soc. Photogramm. Remote Sens. Annu. Conf. 2010 Oppor. Emerg. Geospatial Technol.* **2010**, *1*, 175–183.

120. Haala, N. Multiray Photogrammetry and Dense Image Matching. *Photogramm. Week '11* **2011**, 185–195, doi:10.1177/004057368303900411.

121. Peterson, E. B.; Klein, M.; Stewart, R. L. *Whitepaper on Structure from Motion (SfM) Photogrammetry: Constructing Three Dimensional Models from Photography*; 2015; ISBN 5306231810.

122. Zhu, Z.; Stamatopoulos, C.; Fraser, C. S. Accurate and occlusion-robust multi-view stereo. *ISPRS J. Photogramm. Remote Sens.* **2015**, *109*, 47–61, doi:10.1016/j.isprsjprs.2015.08.008.

123. Peterson, E. *Whitepaper on Structure from Motion (SfM) Photogrammetry : Constructing Three Dimensional Models from ... Whitepaper on Structure from Motion (SfM) Photogrammetry : Constructing Three Dimensional Models from Photography Research and Development Office*; 2016; ISBN 5306231810.

124. Micheletti, N.; Chandler, J. H.; Lane, S. N. Structure from Motion (SfM) Photogrammetry Photogrammetric heritage. *Br. Soc. Geomorphol.* **2015**, *2*, 1–12.

125. Hirschmüller, H. Semi-Global Matching – Motivation, Developments and Applications. *Proc. Photogramm. Week* **2011**, 173–184, doi:10.1017/S0029665110001813.

126. Hirschm, H. Stereo Processing by Semi-Global Matching and Mutual Information. **2007**, *30*, 1–14, doi:10.1109/TPAMI.2007.1166.

127. Bethmann, F.; Luhmann, T. Semi-global matching in object space. *Int. Arch. Photogramm. Remote Sens. Spat. Inf. Sci. - ISPRS Arch.* **2015**, *40*, 23–30, doi:10.5194/isprsarchives-XL-3-W2-23-2015.

128. 写真計測ソフトウェア『iWitnessPRO』 – 株式会社アイティーティー Available online: https://www.ittc.co.jp/blog/2018/04/10/agilis/ (accessed on Sep 4, 2019).

129. Fraser, C. ADVANCES IN CLOSE-RANGE PHOTOGRAMMETRY Prof . Clive Fraser Evolution 1 : film to digital Evolution 2 : Manual to automatic image meas . & orientation Evolution 3 : Manual Feature Extraction & Graphical Output to Automatic 3D Point Cloud Generation. **2015**, 7–11.

130. Luhmann, T.; Robson, S.; Kyle, S.; Harley, I. *Close range photogrammetry: Principles, methods and applications*; 1st ed.; Whittles Publishing, 2006; ISBN 1870325508.

131. Schmitt, R.; Witte, A.; Janßen, M.; Bertelsmeier, F. Metrology assisted assembly of airplane structure elements. In *Procedia CIRP*; 2014; Vol. 23.

132. Marguet, B.; Ribere, B. Measurement-Assisted Assembly Applications on Airbus Final Assembly Lines. *SAE Aerosp. Autom. Fasten. Conf. Exhib.* **2003**, 3–6, doi:10.4271/2003-01-2950.

133. Maropoulos, P. G.; Muelaner, J. E.; Summers, M. D.; Martin, O. C. A new paradigm in large-scale assembly-research priorities in measurement assisted assembly. *Int. J. Adv. Manuf. Technol.* **2014**, *70*, 621–633, doi:10.1007/s00170-013-5283-4.

134. Muelaner, J.; Martin, O.; Kayani, a.; Maropoulos, P. Measurement Assisted Assembly and the Roadmap to Part-To-Part Assembly. *7th Int. Conf. Digit. Enterp. Technol.* **2011**, 11–19.

135. Mei, Z.; Maropoulos, P. G. Review of the application of flexible, measurement-assisted assembly technology in aircraft manufacturing. *Proc IMechE Part B J Eng. Manuf.* **2014**, *228*, doi:10.1177/0954405413517387.

136. Penicka, J. M.; Gwekoh, R.; Wesling, S.; Knight, K.; Mietsner, K. Photogrammetric Approach to Monitor Radiation Safety System at APS *. *U.S. Dep. Energy* 11357.

137. Dynamic stereo meauserement Available online: https://www.dantecdynamics.com/docs/products-and-services/dic/F-Q-450.pdf (accessed on Sep 4, 2019).

138. Ryall, T. G.; Fraser, C. S. Determination of Structural Modes of Vibration Using Digital Photogrammetry. *J. Aircr.* **2002**, *39*, 114–119, doi:10.2514/2.2903.

139. Fernández-Reche, J.; Valenzuela, L. Geometrical assessment of solar concentrators using close-range photogrammetry. *Energy Procedia* **2012**, *30*, 84–90, doi:10.1016/j.egypro.2012.11.011.

140. Pottler, K.; Lüpfert, E.; Johnston, G. H. G.; Shortis, M. R. Photogrammetry: A Powerful Tool for Geometric Analysis of Solar Concentrators and Their Components. *J. Sol. Energy Eng.* **2005**, *127*, 94, doi:10.1115/1.1824109.

141. Shortis, M. R.; Johnston, G. H. G. Photogrammetry: An Available Surface Characterization Tool for Solar Concentrators, {P}art {I}: Measurement of Surface. *J. Sol. Energy Eng.* **1996**, *118*, 146–150, doi:10.1115/1.2870886.

142. Shortis, M. R.; Johnston, G. H. G.; Pottler, K.; Lüpfert, E.; Commission, V. Photogrammetric Analysis of Solar Collectors. *Int. Arch. Photogramm. Remote Sens. Spat. Inf. Sci.* **2008**, *37*, 81–88, doi:10.1.1.150.8074.

143. Biegler, M.; Graf, B.; Rethmeier, M. In-situ distortions in LMD additive manufacturing walls can be measured with digital image correlation and predicted using numerical simulations. *Addit. Manuf.* **2018**, *20*, 101–110, doi:10.1016/j.addma.2017.12.007.

144. De Sousa, G. B.; Olabi, A.; Palos, J.; Gibaru, O. 3D Metrology Using a Collaborative Robot with a Laser Triangulation Sensor. *Procedia Manuf.* **2017**, *11*, 132–140, doi:10.1016/j.promfg.2017.07.211.

145. Metrology Integrator Delivers Universal Metrology Automation – Metrology and Quality News - Online Magazine Available online: https://metrology.news/metrology-integrator-delivers-universal-metrology-automation/ (accessed on Sep 4, 2019).

146. Debski, A.; Grajewski, W.; Zaborowski, W.; Turek, W. Open-source Localization Device for Indoor Mobile Robots. *Procedia Comput. Sci.* **2015**, *76*, 139–146, doi:10.1016/j.procs.2015.12.327.

147. Oh, J. H.; Kim, D.; Lee, B. H. An Indoor Localization System for Mobile Robots Using an Active Infrared Positioning Sensor. *J. Ind. Intell. Inf.* **2014**, *2*, 35–38, doi:10.12720/jiii.2.1.35-38.

148. Stargazer for robot localization Available online: https://www.robotshop.com/uk/hagisonic-stargazer-rs-robot-localization-system-eu.html (accessed on Sep 4, 2019).

149. Elatta, a Y.; Gen, L. P.; Zhi, F. L.; Daoyuan, Y.; Fei, L. An Overview of Robot Calibration_2004_china. *Inf. Technol.* **2004**, *3*, 74–78.

150. Chen-Gang; Li-Tong; Chu-Ming; Xuan, J. Q.; Xu, S. H. Review on kinematics calibration technology of serial robots. *Int. J. Precis. Eng. Manuf.* 2014, *15*.

151. Cheng, F. S. Calibration of Robot Reference Frames for Enhanced Robot Positioning Accuracy. *Robot Manip.* **2008**, 96–112, doi:10.5772/6200.

152. Majarena, A. C.; Santolaria, J.; Samper, D.; Aguilar, J. J. An overview of kinematic and calibration models using internal/external sensors or constraints to improve the behavior of spatial parallel mechanisms. *Sensors (Switzerland)* **2010**, *10*, 10256–10297, doi:10.3390/s101110256.

153. Conrad, K. L.; Yih, T. C. Robotic Calibration Issues: Accuracy, Repeatability and Calibration. *8th Mediterr. Conf. Control Autom.* **2000**, 17–19.

154. Klimchik, A.; Furet, B.; Caro, S.; Pashkevich, A. Identification of the manipulator stiffness model parameters in industrial environment. *Mech. Mach. Theory* **2015**, *90*, doi:10.1016/j.mechmachtheory.2015.03.002.

155. Motta, S. T. Robot Calibration: Modeling Measurement and Applications. *Ind. Robot. - Program. Simul. Appl.* **2006**, 107–130.

156. Elatta, a Y.; Gen, L. P.; Zhi, F. L.; Daoyuan, Y.; Fei, L. An Overview of Robot Calibration.pdf. *Inf. Technol.* **2004**, *3*, 74–78.

157. Abderrahim, M.; Khamis, a.; Garrido, S.; Moreno, L. Accuracy and Calibration Issues of Industrial Manipulators. *Ind. Robot. - Program. Simul. Appl.* **2006**, 131–147, doi:10.5772/56969.

158. Nubiola, A.; Bonev, I. A. Absolute calibration of an ABB IRB 1600 robot using a laser tracker. *Robot. Comput. Integr. Manuf.* **2013**, *29*, 236–245, doi:10.1016/j.rcim.2012.06.004.

159. Möller, C.; Schmidt, H. C.; Shah, N. H.; Wollnack, J. Enhanced Absolute Accuracy of an Industrial Milling Robot Using Stereo Camera System. *Procedia Technol.* **2016**, *26*, 389–398, doi:10.1016/j.protcy.2016.08.050.

160. Filion, A.; Joubair, A.; Tahan, A. S.; Bonev, I. A. Robot calibration using a portable photogrammetry system. *Robot. Comput. Integr. Manuf.* **2018**, *49*, doi:10.1016/j.rcim.2017.05.004.

161. Robot Calibration (Laser Tracker) - RoboDK Documentation Available online: https://robodk.com/doc/en/Robot-Calibration-LaserTracker.html (accessed on Sep 4, 2019).

162. Robot Calibration (Optical CMM) - RoboDK Documentation Available online: https://robodk.com/doc/en/Robot-Calibration-Creaform.html (accessed on Sep 4, 2019).

163. Borrmann, D.; Afzal, H.; Elseberg, J.; Nüchter, A. Mutual calibration for 3D thermal mapping. *IFAC Proc. Vol.* **2012**, 605–610, doi:10.3182/20120905-3-HR-2030.00073.

164. Yu, S.; Kim, J.; Lee, S. Thermal 3D modeling system based on 3-view geometry. *Opt. Commun.* **2012**, *285*, 5019–5028, doi:10.1016/j.optcom.2012.08.013.

165. Oreifej, O.; Cramer, J.; Zakhor, A. Automatic Generation of 3D Thermal Maps of Building Interiors. *ASHRAE Trans.* **2014**.

166. Remondino, F.; Spera, M. G.; Nocerino, E.; Menna, F.; Nex, F. State of the art in high density image matching. *Photogramm. Rec.* **2014**, *29*, 144–166, doi:10.1111/phor.12063.

167. What is Photogrammetry? – Geodetic Systems, Inc Available online: https://www.geodetic.com/v-stars/what-is-photogrammetry/ (accessed on Sep 4, 2019).

168. Luhmann, T.; Fraser, C.; Maas, H. G. Sensor modelling and camera calibration for close-range photogrammetry. *ISPRS J. Photogramm. Remote Sens.* **2016**, *115*, 37–46, doi:10.1016/j.isprsjprs.2015.10.006.

169. Kedzierski, M.; Fryskowska, A. Precise Method of Fisheye Lens Calibration. *Proc. ISPRS-Congress* **2008**, *XXXVII*, 765–768.

170. Mundhenk, T. N.; Rivett, M. J.; Liao, X.; Hall, E. L. <title>Techniques for fisheye lens calibration using a minimal number of measurements</title>. *Intell. Robot.*

Comput. Vis. XIX Algorithms, Tech. Act. Vis. **2003**, *4197*, 181–190, doi:10.1117/12.403762.

171. Kedzierski, M. Precise Calibration of Fisheye Lens Camera System and Projection Model. *Am. Soc. Photgrammetry Remote Sens. Annu. Conf.* **2006**, 3–8.

172. Grussenmeyer, P.; Khalil, O. Al Solutions for Exterior Orientation in Photogrammetry: a Review. *Photogramm. Rec.* **2009**, *17*, 615–634, doi:10.1111/j.1477-9730.2002.tb01907.x.

173. Luhmann, T.; Fraser, C.; Maas, H. G. Sensor modelling and camera calibration for close-range photogrammetry. *ISPRS J. Photogramm. Remote Sens.* 2016, *115*, 37–46.

174. Fraser, C. S. Automatic Camera Calibration in Close Range Photogrammetry. *Photogramm. Eng. Remote Sens.* **2013**, *79*, 381–388, doi:10.14358/PERS.79.4.381.

175. Abdel-Aziz, Y. I.; Karara, H. M. Direct Linear Transformation from Comparator Coordinates into Object Space Coordinates in Close-Range Photogrammetry. *Photogramm. Eng. Remote Sens.* **2015**, *81*, 103–107, doi:10.14358/PERS.81.2.103.

176. Hatze, H. High-precision three-dimensional photogrammetric calibration and object space reconstruction using a modified DLT-approach. *J. Biomech.* **1988**, *21*, 533–538, doi:10.1016/0021-9290(88)90216-3.

177. Tapper, M.; Mckerrow, P. J.; Abrantes, J.; Science, C. Problems Encountered in the Implementation of Tsai's Algorithm for Camera Calibration. **2002**, 27–29.

178. Tsai, R. Y. An efficient and accurate camera calibration technique for 3D machine vision. *Proc. IEEE Comput. Vis. Pattern Recognit. Conf.* **1986**, *1614*, 364–374.

179. Zhang, Z.; Member, S. A Flexible New Technique.pdf. **2000**, *22*, 1330–1334.

180. Z. Zhang, Camera calibration with one-dimensional objects, IEEE Trans.Pattern Anal. Mach. Intell. 26 (7) (2004) 892–899.

181. Ghosh, P. K.; Mudur, S. P. Three-Dimensional Computer Vision: A Geometric Viewpoint. *Comput. J.* **2012**, *38*, 85–86, doi:10.1093/comjnl/38.1.85.

182. Parker, J. R. (Jim R. .; Terzidis, K. Algorithms for image processing and computer vision. **2011**.

183. Joon Ahn, S.; Rauh, W. CIRCULAR CODED TARGET FOR AUTOMATION OF OPTICAL 3D - MEASUREMENT AND CAMERA CALIBRATION. *Int. J. Pattern Recognit. Artif. Intell.* **2001**, *15*, 905–919.

184. Escáner 3D / para CMM / láser / óptico - MetraSCAN 3D series - Creaform - Vídeos Available online: https://www.directindustry.es/prod/creaform/product-54710-469750.html (accessed on Sep 4, 2019).

185. KAZE Features Available online: http://www.robesafe.com/personal/pablo.alcantarilla/kaze.html (accessed on Sep 4, 2019).

186. Cuesta, E.; Suarez-Mendez, J. M.; Martinez-Pellitero, S.; Barreiro, J.; Alvarez, B. J.; Zapico, P. Metrological evaluation of Structured Light 3D scanning system with an optical feature-based gauge. *Procedia Manuf.* **2017**, *13*, 526–533, doi:10.1016/j.promfg.2017.09.078.

187. Kersten, T. P.; Lindstaedt, M.; Starosta, D. Comparative geometrical accuracy investigations of Hand-Held 3D scanning systems - An update. *Int. Arch. Photogramm. Remote Sens. Spat. Inf. Sci. - ISPRS Arch.* **2018**, *42*, 487–494, doi:10.5194/isprs-archives-XLII-2-487-2018.

188. Salvi, J.; Pagès, J.; Batlle, J. Pattern codification strategies in structured light systems. *Pattern Recognit.* **2004**, *37*, 827–849, doi:10.1016/j.patcog.2003.10.002.

189. Webster, J. G.; Bell, T.; Li, B.; Zhang, S. Structured Light Techniques and Applications. *Wiley Encycl. Electr. Electron. Eng.* **2016**, 1–24, doi:10.1002/047134608x.w8298.

190. Matsuoka, R. Measurement precision and accuracy of the centre location of an ellipse by weighted centroid method. *ISPRS Ann. Photogramm. Remote Sens. Spat. Inf. Sci.* **2015**, *2*, 111–118, doi:10.5194/isprsannals-II-3-W4-111-2015.

191. Matsuoka, R. Oscillation of the measurement accuracy of the center location of an ellipse on a digital image. *Int. Arch. Photogramm. Remote Sens. Spat. Inf. Sci. - ISPRS Arch.* **2014**, *40*, 211–218, doi:10.5194/isprsarchives-XL-3-211-2014.

192. Luhmann, T. (Thomas); Robson, S. (Engineering professor); Kyle, S. (Engineering professor); Boehm, J. (Engineering professor) *Close-range photogrammetry and 3D imaging*; ISBN 9783110302691.

193. Tjahjadi, M. E.; Handoko, F. Precise wide baseline stereo image matching for compact digital cameras. *Int. Conf. Electr. Eng. Comput. Sci. Informatics* **2017**, *4*, 181–186, doi:10.11591/eecsi.4.1015.

194. Gruen, A. Least squares matching : a fundamental measurement algorithm. **2015**.

195. Berger, M. The framework of least squares template matching. **1998**.

196. Roncella, R.; Romeo, E.; Barazzetti, L.; Gianinetto, M.; Scaioni, M. Comparative analysis of digital image correlation techniques for in-plane displacement

measurements. *2012 5th Int. Congr. Image Signal Process. CISP 2012* **2012**, 721–726, doi:10.1109/CISP.2012.6469731.

197. Shortis, M. R.; Clarke, T. A.; Short, T. A comparison of some techniques for the subpixel location of discrete target images. *Proc. SPIE 2350, Videometrics III,* 239–250, doi:10.1117/12.189136.

198. Jiandong, Z.; Liyan, Z.; Xiaoyu, D. Accurate 3D Target Positioning in Close Range Photogrammetry with Implicit Image Correction. *Chinese J. Aeronaut.* **2009**, *22*, 649–657, doi:10.1016/S1000-9361(08)60154-5.

199. Rashmi; Kumar, M.; Saxena, R. Algorithm and Technique on Various Edge Detection : A Survey. *Signal Image Process. An Int. J.* **2013**, *4*, 65–75, doi:10.5121/sipij.2013.4306.

200. Shrivakshan, G. T. A_Comparison_of_various_Edge_Detection_Techniques_used_inImage_Processing_IJCSI-9-5-1-269-276_September_2012. **2012**, *9*, 269–276.

201. Kaur, S.; Singh, I. Comparison between Edge Detection Techniques. *Int. J. Comput. Appl.* **2016**, *145*, 15–18, doi:10.5120/ijca2016910867.

202. Mayer, H. Issues for image matching in structure from motion. *Int. Arch. Photogramm. Remote Sens.* **2008**, *37*, 21–26.

203. Govender, N. Evaluation of feature detection algorithms for structure from motion. *Proc. 3rd Robot. Mechatronics Symp. (ROBMECH 2009)* **2009**.

204. El-Gayar, M. M.; Soliman, H.; Meky, N. A comparative study of image low level feature extraction algorithms. *Egypt. Informatics J.* **2013**, *14*, 175–181, doi:10.1016/j.eij.2013.06.003.

205. Remondino, F. Detectors and descriptors for photogrammetric applications. *Int. Arch. Photogramm. Remote Sens. Spat. Inf. Sci.* **2006**, *32*, 49–54.

206. Dense Image Matching Available online: https://www.gim-international.com/content/article/dense-image-matching-2 (accessed on Sep 4, 2019).

207. Andrade-cetto, J.; Kak, A. C. Object Recognition. *Encycl. Multimed.* **2008**, 674–674, doi:10.1007/978-0-387-78414-4_578.

208. Structure from Motion - MATLAB & Simulink Available online: https://www.mathworks.com/help/vision/ug/structure-from-motion.html (accessed on Sep 4, 2019).

209. Lucas, B. D.; Kanade, T. An Iterative Image Registration Technique with an Application to Stereo Vision. *Robotics* **1981**, *81*, 674–679, doi:10.1109/HPDC.2004.1323531.

210. Galuk, Y. P.; Nickolaenko, a. P.; Hayakawa, M. Amplitude variations of ELF radio waves in the Earth–ionosphere cavity with the day–night non-uniformity. *J. Atmos. Solar-Terrestrial Phys.* **2018**, *169*, 23–36, doi:10.1016/j.jastp.2018.01.001.

211. Wan, W.; Peng, M.; Xing, Y.; Wang, Y.; Liu, Z.; Di, K.; Teng, B.; Mao, X.; Zhao, Q.; Xin, X.; Jia, M. A performance comparison of feature detectors for planetary rover mapping and localization. *Int. Arch. Photogramm. Remote Sens. Spat. Inf. Sci. - ISPRS Arch.* **2017**, *42*, 149–154, doi:10.5194/isprs-archives-XLII-3-W1-149-2017.

212. Rodehorst, V.; Koschan, a Comparison and Evaluation of Feature Point Detectors. *Proc. 5th Int. Symp. Turkish-German Jt. Geod. Days " Geod. Geoinf. Serv. our Dly. Life"* **2006**, 8, doi:10.1016/S0003-2670(03)00175-2.

213. Stylianidis, E. A New Digital Interest Point Operator For Close-Range Photogrammetry. *Int. Arch. Photogramm. Remote Sens. Spat. Inf. Sci.* **2003**, *XXXIV*, 319–324.

214. Das, N. S.; Arunvinthan, S.; Giriprasad, E. Target Detection Based on Normalized Cross Co-relation Target Detection Based on Normalized Cross Co-relation. **2016**.

215. Feng Zhao; Qingming Huang; Wen Gao Image Matching by Normalized Cross-Correlation. **2006**, II–729–II–732, doi:10.1109/icassp.2006.1660446.

216. Bethmann, F.; Luhmann, T. Least-squares Matching with Advanced Geometric Transformation Models. *Photogramm. - Fernerkundung - Geoinf.* **2011**, *2011*, 57–69, doi:10.1127/1432-8364/2011/0073.

217. Li, Z.; Wang, J. Least squares image matching: A comparison of the performance of robust estimators. *ISPRS Ann. Photogramm. Remote Sens. Spat. Inf. Sci.* **2014**, *II-1*, 37–44, doi:10.5194/isprsannals-ii-1-37-2014.

218. Shen, J.; Hu, M.; Yuan, B. A robust method for estimating the fundamental matrix. *Int. Conf. Signal Process. Proceedings, ICSP* **2002**, *1*, 892–895, doi:10.1109/ICOSP.2002.1181200.

219. Huang, J. F.; Lai, S. H.; Cheng, C. M. Robust fundamental matrix estimation with accurate outlier detection. *J. Inf. Sci. Eng.* **2007**, *23*, 1213–1225.

220. Zhang, Z. Determining the epipolar geometry and its uncertainty a review, International Journal of Computer Vision. *Int. J. Comput. Vis.* **1998**, *27*, 161–198.

221. Luong, Q. T.; Faugeras, O. D. The fundamental matrix: Theory, algorithms, and stability analysis. *Int. J. Comput. Vis.* **1996**, *17*, 43–75, doi:10.1007/BF00127818.

222. Bergamini, M. L.; Ansaldo, F.; Bright, G.; Francisco, J. Fundamental Matrix : Digital camera calibration and Essential Matrix parameters. **2016**, *1*.

223. Armangué, X.; Salvi, J. Overall view regarding fundamental matrix estimation. *Image Vis. Comput.* **2003**, *21*, 205–220, doi:10.1016/S0262-8856(02)00154-3.

224. Läbe, T.; Förstner, W. Automatic Relative Orientation of Images. *Proc. 5th Turkish-German Jt. Geod. Days* **2006**, 6 pp.

225. oz, A. Relative Orientation. *Photogramm. Rec.* **1966**, *5*, 198–200, doi:10.1111/j.1477-9730.1966.tb00869.x.

226. Heipke, C. Automation of interior, relative, and absolute orientation. *ISPRS J. Photogramm. Remote Sens.* **1997**, *52*, 1–19, doi:10.1016/S0924-2716(96)00029-9.

227. Stewénius, H.; Engels, C.; Nistér, D. Recent developments on direct relative orientation. *ISPRS J. Photogramm. Remote Sens.* **2006**, *60*, 284–294, doi:10.1016/j.isprsjprs.2006.03.005.

228. Takimoto, R. Y.; De Castro Martins, T.; Takase, F. K.; De Sales Guerra Tsuzuki, M. Epipolar geometry estimation, metric reconstruction and error analysis from two images. *IFAC Proc. Vol.* **2012**, *14*, 1739–1744, doi:10.3182/20120523-3-RO-2023.00098.

229. Luhmann, T.; Fraser, C.; Maas, H. ISPRS Journal of Photogrammetry and Remote Sensing Sensor modelling and camera calibration for close-range photogrammetry. *ISPRS J. Photogramm. Remote Sens.* **2016**, *115*, 37–46, doi:10.1016/j.isprsjprs.2015.10.006.

230. Goldman, Y.; Rivlin, E.; Shimshoni, I. Robust epipolar geometry estimation using noisy pose priors. *Image Vis. Comput.* **2017**, *67*, 16–28, doi:10.1016/j.imavis.2017.09.006.

231. Feng, S.; Kan, J.; Wu, Y. An improved method to estimate the fundamental matrix based on 7-point algorithm. *J. Theor. Appl. Inf. Technol.* **2012**, *46*, 212–217.

232. Sur, F.; Noury, N.; Berger, M.-O. Computing the Uncertainty of the 8 point Algorithm for Fundamental Matrix Estimation. **2012**, 96.1–96.10, doi:10.5244/c.22.96.

233. Zhang, Z.; Loop, C. Estimating the fundamental matrix by transforming image points in projective space. *Comput. Vis. Image Underst.* **2001**, *82*, 174–180, doi:10.1006/cviu.2001.0909.

234. Tegolo, D.; Bellavia, F. noRANSAC for fundamental matrix estimation. **2011**, 98.1–98.11, doi:10.5244/c.25.98.

235. Grussenmeyer, P.; Khalil, O. Al SOLUTIONS FOR EXTERIOR ORIENTATION IN PHOTOGRAMMETRY: A REVIEW. *Photogramm. Rec.* **2002**, *17*, 615–634, doi:10.1111/j.1477-9730.2002.tb01907.x.

236. Estimate geometric parameters of a single camera - MATLAB Available online: https://www.mathworks.com/help/vision/ref/cameracalibrator-app.html (accessed on Sep 4, 2019).

237. Hartley, R.; Zisserman, A. *Multiple view geometry in computer vision*; ISBN 0521540518.

238. Hartley, R. I.; Sturm, P.; K-c, R.; Box, P. O. Triangulation [CVIU]. *Image (Rochester, N.Y.)* **1996**, *68*, 957–966.

239. Schenk, T. Towards automatic aerial triangulation. *ISPRS J. Photogramm. Remote Sens.* **1997**, *52*, 110–121, doi:10.1016/S0924-2716(97)00007-5.

240. Granshaw, S. I. Bundle Adjustment Methods in Engineering Photogrammetry. *Photogramm. Rec.* **1980**, *10*, 181–207, doi:10.1111/j.1477-9730.1980.tb00020.x.

241. Gong, Y.; Meng, D.; Seibel, E. J. Bound constrained bundle adjustment for reliable 3D reconstruction. *Opt. Express* **2015**, *23*, 10771, doi:10.1364/oe.23.010771.

242. Result, A. G. IL (x) Mx. **2000**, *XXXIII*.

243. Camera Calibration with MATLAB - Video - MATLAB & Simulink Available online: https://www.mathworks.com/videos/camera-calibration-with-matlab-81233.html (accessed on Sep 4, 2019).

244. Orientation cross to determine the coordinate system (XYZ). | Download Scientific Diagram Available online: https://www.researchgate.net/figure/Orientation-cross-to-determine-the-coordinate-system-XYZ_fig4_331377530 (accessed on Sep 4, 2019).

245. Photogrammetry by Linearis3D Available online: http://www.linearis3d.com/ (accessed on Sep 4, 2019).

246. DPA Inspect – Close Range Photogrammetry for on the spot error analysis, without long production downtime or time-consuming equipment transport Available online: http://www.accurexmeasure.com/dpa-inspect.htm (accessed on Sep 4, 2019).

247. DPA PRO - Mobile 3D industrial measurement systems for difficult applications. Available online: http://www.accurexmeasure.com/dpa-pro.htm (accessed on Sep 4, 2019).

248. Weblet Importer Available online: https://www.geoform.com/wp-content/uploads/2014/02/colormap-sample3-e1393278048671.png (accessed on Sep 4, 2019).

249. Reverse Engineering Services - Variational Technologies Pvt. Ltd. Available online: https://www.3dlasertracker.com/reverse-engineering-services.html (accessed on Sep 4, 2019).

8 ANNEX

In this chapter cross-references and citations of published articles are presented as well as their full content.

ARTICLE Nº1 (CASE STUDY1)

- Kortaberria, Gorka & Olarra, Aitor & Tellaeche, Alberto & Minguez, Rikardo. (2017). Close Range Photogrammetry for Direct Multiple Feature Positioning Measurement without Targets. Journal of Sensors. 2017. 1-10. 10.1155/2017/1605943. →https://www.hindawi.com/journals/js/2017/1605943/cta/

Hindawi
Journal of Sensors
Volume 2017, Article ID 1605943, 10 pages
https://doi.org/10.1155/2017/1605943

Hindawi

Research Article

Close Range Photogrammetry for Direct Multiple Feature Positioning Measurement without Targets

Gorka Kortaberria,[1] Aitor Olarra,[1] Alberto Tellaeche,[2] and Rikardo Minguez[3]

[1]*Mechanical Engineering Unit, IK4-Tekniker, Eibar, Spain*
[2]*Smart and Autonomous Systems Unit, IK4-Tekniker, Eibar, Spain*
[3]*Department of Graphic Design and Engineering Projects, UPV/EHU, Bilbao, Spain*

Correspondence should be addressed to Gorka Kortaberria; gkortaberria@tekniker.es

Received 9 March 2017; Accepted 24 April 2017; Published 29 May 2017

Academic Editor: Carlos Ruiz

The main objective of this study is to present a new method to carry out measurements so as to improve the positioning verification step in the wind hub part dimensional validation process. This enhancement will speed up the measuring procedures for these types of parts. An industrial photogrammetry based system was applied to take advantage of its results, and new functions were added to existing capabilities. In addition to a new development based on photogrammetry modelling and image processing, a measuring procedure was defined based on optical and vision system considerations. A validation against a certified procedure by means of a laser-tracker has also been established obtaining deviations of ±0.125 μm/m.

1. Introduction

The component analyzed in this article is part of several wind turbine models and from an operational point of view is one of the most critical, together with other components such as shovels and lift towers [1]. The machining of these finished parts requires a periodical accuracy check which guarantees dimensional quality so as to obtain a suitable operation performance.

The hub which is usually made of cast iron or steel is the component of the rotor that joins the blades with the rotation system and constitutes the center of the rotor.

1.1. Review of Current Approaches. The approach presented in this article aims to solve the limitations for measuring the positioning [2, 3] of multiple holes/drills in a large part like a wind hub. Normally the tolerance for positioning is 1 mm for each hole center in relation to a general reference (e.g., a machined diameter), but tighter tolerances are also required depending on the hub model. The standardized actual solution for assuring that the part fulfills the manufacturing acceptance interval [4] is based either on laser-tracker technology [5] or on close range photogrammetry solutions [6]. Although other inspection devices are available (articulated arms, stereo-systems, CMMs, etc.) for 3D inspection [1, 7], specifications such as dimension of the parts as well as required accuracy limit their feasibility for machined part inspection. While casting parts up to 3-4 m require assuring enough material (tolerances around ±15 mm) for further processing, machined parts require tighter tolerances for finished surfaces.

Laser-tracker devices are the most widespread portable CMMs for machined part inspection and validation. Nevertheless, recently appearing vision based systems (photogrammetry, stereo-systems) are also used for some specific measuring tasks (see Figure 1). For example, for cast part validation, the use of white light scanners [8] is very extended, but their uncertainty [9, 10] for machined parts is not suitable and in most of the cases surface preparation is required before the measurement, extending the time schedule for the overall measuring process. Other systems like 3D scanners [11–14] are also used for this cast part validation, but the limitation for finished geometries is similar. The only technology apart from laser-tracker that is accepted by standardized procedures for machined part inspection is the close range photogrammetry.

FIGURE 1: Standard procedures for machined part geometrical verification (from Zebicon & Modern Machine Shop).

Nevertheless, due to its versatility the laser-tracker technology has been historically the reference device.

One of the main drawbacks of these types of measuring devices is the huge amount of time employed for verifying the positioning of multiple (more than 300) repetitive features such as the holes where the blades are fixed. This is mainly due to the measuring strategy that is required to measure these features. For each of the elements, it is necessary to use fixtures [15] that allow the correct scanning of the feature using the laser-tracker in a dynamic mode (interferometric mode). In some cases, this approach is avoidable (static mode), but when the positioning tolerance is narrow, it is the recommended methodology for the verification and First Article Inspection (FAI) validation of machined parts.

Another disadvantage is the inaccessibility to the part when the size of the measurand is greater than a few meters (2 meters). In this case, the operator needs to access the elements to be verified. This lack of ergonomy also increases the time for the overall measuring time which is the main reason for the research presented in this paper.

In the last years, there is a clear tendency to manufacture bigger and bigger parts for more powerful energy generation [16]. Therefore, managing these obstacles will be more challenging in the following years. With the aim of avoiding these problems, some optical methods can be applied to reduce the time for the verification and increase the flexibility of the measuring procedure. Some approaches are still based on new adapters' design and validation. Nevertheless, some of the solutions do not provide enough accuracy for machined features and others require as many adapters (see Figure 2) as features to be measured; accordingly they are not cost-effective. Undoubtedly, the evolution of these optical techniques will result in an improvement of the capacity to detect, assess, and locate natural features in 3D with high accuracy, but at present, this function is not supported by commercial devices high accuracy requirements.

The research presented in this article puts forward an alternative measuring method and technique to solve the limitations that are mentioned in the above part of the Introduction. The following approach is based on a combination of close range photogrammetry and image processing techniques in addition to previously known data that

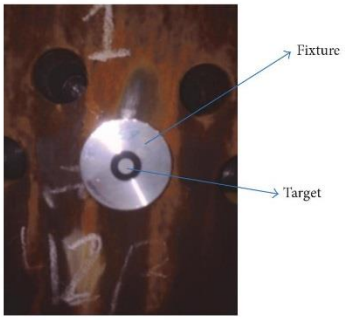

FIGURE 2: Adapter and target for hole center determination with photogrammetric approaches.

defines the nominal position of the features to be measured (see Figure 3). This alternative approach consists of avoiding the employment of targets to speed up the measuring process. The validation against other certified results will determine the scope of this new development.

1.2. Background and Motivation. The capacity to carry out this approach is based on previously acquired knowledge according to photogrammetry and image processing techniques found in libraries in software tools like Labview® or Halcon®. On the one hand, the large experience of users of photogrammetric devices and on the other hand a contrasted trajectory in vision based solutions are gathered to take the most from both technologies. This combination makes it possible to get further functionalities based on image data advanced processing. Besides, tests carried out in laboratory conditions were promising not only according to accuracy, but also in relation to time saving.

Another point for this research was some previous comparison tests between commercial close range photogrammetry and laser-tracker based methodology. The result for the highest positioning differences between both techniques was around 0.05 mm. Along with this comparison, a rejected

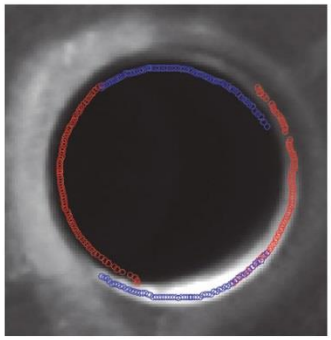

FIGURE 3: Natural feature identification by means of image processing.

and rusted wind hub with holes were scanned with a white light scanner to compare also the results against this type of portable coordinate measuring machine (PCMM). Nevertheless, the result of this method was not good enough for comparison due to a lack of clear data regarding the edge of the holes. Thus, this other comparison only tried to extend the comparison between cutting-edge techniques for other dimensions and geometric tolerances of the hub.

1.3. Overview. This article is organized as follows: firstly an introduction of the aim of the study is presented together with a review of the current measuring methods, then followed by a description of the developed solution, and procedure is shown as well as the obtained results, and finally some conclusions of the research and future trends and challenges regarding this field are mentioned.

2. Method

This section describes the developed solution to combine it with standardized procedures in order to improve the overall measuring process for wind generation part dimensional verification. The root of the solution is based on an industrial photogrammetric system (TRITOP® from GOM, Braunschweig, Germany) which obtains the intrinsic and extrinsic parameters of the image network employed for the approach. The resulting data of this system is combined with the nominal data of the features to be measured to reproject them in the acquired images. Once the images are processed and the centers of the features are detected in image coordinates, these coordinates are transformed into spatial coordinates applying the photogrammetric model previously solved. In this way, the positioning of these features is determined without using any target and this speeds up the duration of the verification method.

Apart from the developed procedure, and to validate the proposed solution, other aspects such as lighting, accuracy, and traceability were analyzed not only in simulation but also experimentally.

2.1. Developed Solution. The developed procedure (see scheme in Figure 4) is a hybrid solution between photogrammetric data and image processing tools integrated in a Matlab architecture/platform. First, the photogrammetric data is obtained by means of a commercial portable CMM called TRITOP. This device is composed of a professional reflex camera (CANON EOS-1ds Mark III®), a wide aperture nonmotorized lens (DISTAGON T* 2.8/25 ZF from Carl Zeiss®), a minimal number of targets to be located in the part, and a software that registers the images and processes them to solve the inverse problem of a photogrammetric network. A specific procedure is used to take the multiview images but this point is described in the following chapter. The software automatically identifies the coded targets used to solve both, intrinsic and extrinsic orientation in the images. Then, it applies a scale to the scene according to the length to the detected physical artifact. The noncoded targets are considered and taken into consideration to define the approximated coordinate system according to the nominal specification. Once these steps are carried out, the results can be exported in file to use them afterwards.

In order to be able to use these results, a photogrammetric model (algorithm) was developed and programmed in Matlab. This model allows complementing different functions available in commercial software:

(1) Photogrammetric model inverse problem solving control

(2) Network design simulation

(3) Uncertainty assessment based on residuals

(4) 3D features spatial position determination based on geometric features

The photogrammetric model (see Figure 5) permits the input of the result of the data obtained in the previous step and its interpretation. This enables the user to take advantage of the prior exported data and to use it to determine the 3D of other features that are not measured with targets or adapters. The model is based on collinearity equations and the Brown model [17, 18] for camera distortion error estimation. Some other general references were also investigated to obtain a general overview of the current state of the art of close range photogrammetry [18–20].

These are the main equations that describe the mathematical model of the photogrammetric system:

$$\begin{aligned} x - x_0 &= -c\frac{m_{11}(X - X_0) + m_{21}(Y - Y_0) + m_{31}(Z - Z_0)}{m_{13}(X - X_0) + m_{23}(Y - Y_0) + m_{33}(Z - Z_0)} + \Delta x, \\ y - y_0 &= -c\frac{m_{12}(X - X_0) + m_{22}(Y - Y_0) + m_{32}(Z - Z_0)}{m_{13}(X - X_0) + m_{23}(Y - Y_0) + m_{33}(Z - Z_0)} + \Delta y. \end{aligned} \quad (1)$$

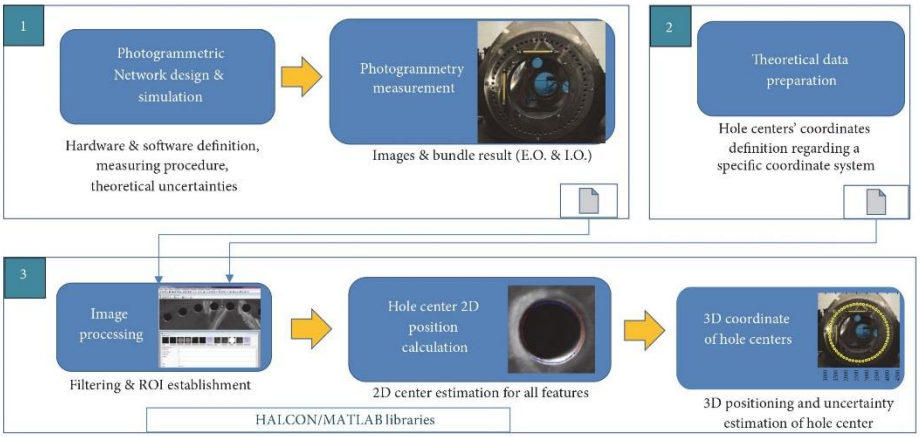

Figure 4: Flow chart of the developed solution.

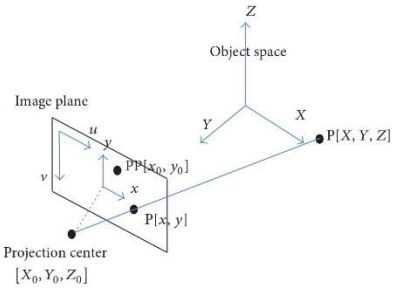

Figure 5: Collinearity projection model.

The parameters that compound the previous equations are the image coordinates $[x, y]$, the principal point coordinates $[x_0, y_0]$, the principal distance c, the rotation matrix components m_{ij}, the spatial coordinates $[X, Y, Z]$, the projection center coordinates $[X_0, Y_0, Z_0]$, and the optical distortions $[\Delta x, \Delta y]$.

Among the parameters that define the model, coordinates, spatial transformations, mechanical decentering, and optical distortions are considered. The bundle adjustment procedure is typically used to solve model parameters that comprise both extrinsic orientation and intrinsic one. The main optical aberrations are radial distortion, tangential distortion, shear distortion, and so forth.

The sum of all the distortion sources $(\Delta x, \Delta y)$ is corrected in the main equations (1). The photogrammetric model described has been used as the mathematical model of the described solution.

If a characteristic (e.g., the center) of these features is detected and measured in each image (nominal data is generated and used for this step), it is feasible to calculate the 3D position of those characteristics for the same reference frame considered in the industrial solution by means of the photogrammetric model. Most of the bibliographic references are based on geometric element direct determination [21], but the solution presented in this paper is based on image data adjustment. A short description of some approaches is presented in the next lines.

The first attempt was to fit geometric elements based on border points of the holes. For this aim, image processing is needed to identify and extract the points of the border of each hole in each image. The most common filters are Sobel or Canny [18] operators and they are applied after binarizing the image. The main drawback of this approach was the required time for all the images and features and the filtering parameter establishment due to nonhomogeneous image intensity distribution, so it was not considered any more as a suitable approach. Moreover, the fitting of the ellipses comprising the border points of the holes was not repetitive due to outliers (bezel points and noise), so nor was the accuracy obtained in this manner appropriate.

The following effort was focused on pattern matching approaches, where the features to be detected are searched on the images. Targeting this, a reference image (circle) is defined and then is employed as a pattern. However, the features seen in the images are not circles, so this reference image is not very representative of the features to be identified on the images and the trials were not robust. Because of this, more complex patterns need to be used. Considering this point and also that the image processing is highly time-consuming, this approach was also discarded.

This step was finally solved considering a new approach that is based on the photogrammetric model and nominal

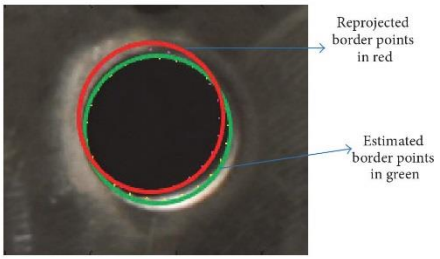

FIGURE 6: Nominal and estimated border points on the image feature.

geometric data previously determined that enables reprojecting and pointing on the images the nominal theoretical border points for each feature (see Figure 6). Based on this functionality, the following described image processing process flow was established.

The final image processing step (see Figure 7) was implemented in Matlab and it is based on the following processing flow (see process flow in Figure 4):

(i) Loading of images

(ii) TRITOP result importation

(iii) Nominal data importation

(iv) 3D data generation for the edge points of each hole from centers values

(v) For each image

  (a) Image adjustment (from RGB to grey data, edge filtering)

  (b) Region of interest (ROI) determination for each feature

  (c) Reprojection of edge points from 3D to 2D for each feature

  (d) Sum of the gradient of the evaluated ROI at these edge points for each feature

  (e) Maximization of this function to establish the correction value for the center image coordinates

  (f) Center image coordinate correction

  (g) Result data storage and exportation

This processing is mainly applied on nonoblique images to avoid eccentricity effects [22, 23] and to assure a proper accuracy for the determination of the hole center, distinguishing between bezel and hole diameter and, therefore, assessing the 3D position. So, although all images are necessary to solve a photogrammetric network, not all of the features are suitable for this image processing step nor for bundle adjustment step.

2.2. Measuring Procedure. The measuring procedure consists of a photogrammetry based measuring session from the point of view of feature acquisition and determination. This specification requires not only a photogrammetry based approach but also an acquisition process where the focusing and the contrast of the features to be measured are taken into account. With this aim, the combination between the image sensor and lens is studied so as to define the minimum focusing distance, the depth of field (dof), and the resolution on the features to be measured. Depending on this parameter and the working distance, the features to be determined are more accurately defined. It should be pointed out that, in order to get a more accurate intrinsic calibration, camera parameters remain fixed during the acquisition. The most critical one is the focal distance, but the shutter time and the aperture of the lens remain also fixed throughout the image acquisition process.

It is also important to consider the design of the image network to be taken according to accuracy aspects [24, 25] and measurand geometry and dimensions. In this case, about 60 holes located radially in 1200 mm diameter on a machined plane need to be measured. Although narrow views are preferable for feature measurement due to geometrical form deviations, wide angles (approximated to 90°) are suggested to solve the photogrammetric model and, at least, to obtain the same accuracy between XYZ coordinates according to the reference frame. So, there is a balance between accuracy requirements and feature oriented photogrammetric approaches for network design.

As a first step, this measuring development and procedure have been developed in laboratory conditions where lighting influences were under control in addition to part surface characteristics. Once this case study was solved, the second step consisted in real workshop conditions (see Figure 8) where these critical parameters were not so controlled. However, and in order to minimize these uncontrolled effects, some experimental tests were established beforehand. Also, the use of external lighting for workshop conditions was determined.

Taking into consideration that the execution time for the measuring is a critical factor on workshops measurements, this point was analyzed in the set-up of the system.

2.3. Industrialization. The previously defined procedure was modified to adapt it to real workshop conditions in relation to lighting condition, as well as to feature's real geometry. To minimize the effect of an unstable illumination, some fixed powerful light sources (see Figure 9) were used at the same base from which images were taken. The lighting for this approach is critical in order to set up and fix the image processing parameters for workshop conditions. For artificial targets, as the gradient change on the targets is assured whatever the lighting conditions are, the light sources are not necessary or at least are not indispensable.

Besides, a pointing angle of 30° was used to improve lighting path towards the surface of the part. This approach was previously established in lab using a sample to determine the most suitable lighting approach. The angle value employed for the experiments was selected taking into account the light incidence above the surface and the bezels (<45°) and also the

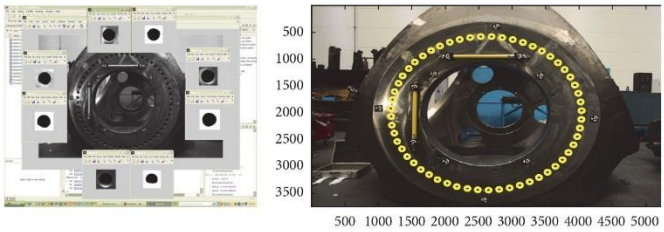

FIGURE 7: Image processing steps, from binarization to edge point determination and 3D positioning assessment.

FIGURE 8: From lab conditions to workshop ones.

FIGURE 9: External lighting orientation.

convergence angle between the cameras so as to get a proper accuracy for the spatial intersection of XY coordinates.

Another key point in carrying out these measurements is to study the optical parameters regarding the scene to be measured in relation to different measuring process parameters such as working distance, view angles, depth of focus, and resolution.

From the point of view of time saving, a minimum number of images were considered in data processing.

With the aim of estimating the approximated accuracy of the designed photogrammetric network, a photogrammetric model was used. This model allows for estimating the uncertainty for the positioning of the holes according to a specific photogrammetric intrinsic and extrinsic consideration. The uncertainty assessment is based on residuals analysis and determines the proportional relationship among the image data accuracy and the estimated spatial coordinates. The overall result is the uncertainty for each coordinate of the center of the holes. This estimation is useful to validate the photogrammetric network design for the real scene. The acceptance criteria between measuring uncertainty and manufacturing tolerance should be of at least 1/3 and 1/10 as recommended (ISO 17025 standard).

For this study, 12 images were considered with a working distance of 1.5 m.

Apart from the optical estimations of the measuring procedure, uncertainty estimation [26] was carried out with Spatial Analyzer® (SA) software considering a fixed position of laser-tracker and the holes center according to a reference frame defined in the center of all these holes. The objective of this simulation was to check if this kind of measurement can be considered as a reference for our solution. Monte-Carlo approach [27] was used to assess the uncertainty for each center position. A representation of this estimation is shown in Figure 10.

As a reference value for the comparison of obtained results, the same part was measured by means of laser-tracker taking care of accuracy aspects. The working distances, as well as tool calibration, were checked previously to minimize inaccuracies and to determine the center position of the holes

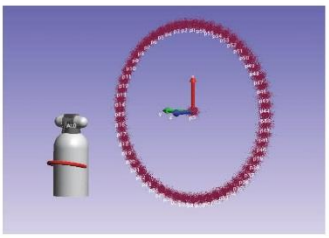

FIGURE 10: Uncertainty estimation for hole center positioning with a laser-tracker.

regarding the theoretical coordinate system defined in the nominal model.

The following results are the coordinate's difference between the reference values and the values obtained from the developed vision based system (see Figure 11). Both values were compared aiming to validate the result of the developed system. It must be pointed out that, in this manner, the traceability chain is assured at workshop conditions. Besides, these deviations are compared with the theoretical estimated uncertainty for the laser-tracker measurements. The common reference frame necessary for the comparison is defined in each system using the same geometries and elements.

3. Results and Discussion

The results of this research range from new uncertainty estimation functionalities to real case validation. In each of the stages, important findings for future measuring cases with even larger dimensions were found.

As a main result, it is established that the developed vision based system can measure multiple hole 3D position simultaneously without targets and with an accuracy of ±0.125 mm/m (confidence interval 2σ) for XY directions (see Figure 12). The stated accuracy is the difference between 2 measuring techniques that have their own coordinate system created by different approaches. Indeed, the state-of-the-art accuracy for photogrammetric approaches based on targets is 1 : 50000 (20 μm/m).

These results were demonstrated by means of a comparison between different measuring techniques and the above-mentioned procedures. A nominal definition of the features to be verified is previously required regarding a common coordinate system, which assures the comparison between methods. The laser-tracker approach is based on contact (reflector against surface) while photogrammetry is a noncontact procedure. Although similar areas or points haven been used to define the geometric elements that compound the coordinate systems, some differences are still possible. Besides, the residuals for the fitting of the projected points above the processed images are another source of error. This processing can be improved to adapt dynamically some image parameters for gaining robustness in this step but this tool has not been developed.

Moreover, for half of the holes (50%), the differences are less than 0.05 mm without taking into consideration the results for Z coordinate.

Another important result of this research turned out to be the development of an uncertainty estimation tool for close range photogrammetry [28–30] that allows the comparison of nominal accuracy with the verification tolerance ($U < T/3$), so as to check whether the photogrammetric set-up fulfills the accuracy requirements for the measurement. This new functionality will be improved in the future but currently, it permits this kind of accuracy estimation based on residuals (sensibility analysis) from the bundle adjustment solving step. Figure 13 shows the estimated uncertainty for each whole center depending on XYZ coordinates. This evaluation enables assessing the linear relationship between the inputs (image coordinates) to the photogrammetric model and outputs (results of XYZ coordinates).

The uncertainty for depth coordinate is larger (around ±0.35 mm) than for plane coordinates (X and Y), but in this type of verification this difference is not important because Z coordinate is not considered as a positioning result. So, for plane hole positioning center, the measuring procedure's uncertainty is ±0.15 mm (see Figure 13).

Another interesting result is the estimated uncertainty for the measurement carried out with the laser-tracker in a virtual and theoretical environment by means of SA software. This tool enables a priori estimation for the measuring process. In this case and to assure that the certified method is good enough for the comparison in Figure 12, the uncertainty of the reference process is also estimated. The results obtained range from 0.015 to 0.017 mm for all the center position (see Figure 14), so they are insignificant in comparison with the differences achieved between the results of both measuring methods. This means than in real measuring conditions there are more sources of error than the ones considered in simulation models.

Another key point of this study is the need to combine photogrammetric procedures with photography procedures so as to obtain results with enough accuracy. This interaction between these fields requires an advanced view of two worlds that is not obvious to a standard user. In workshop conditions, images with less than 30° angles were used to obtain the positioning values and reduce image distortion issues.

4. Conclusions and Future Work

It has been demonstrated that commercial photogrammetric results can be useful for further processing in relation to the results obtained in this study. Therefore, commercial devices capabilities currently in the market can be improved for future demanding tasks. The main drawback for noncontact approaches is the lack of control for lighting conditions. Normally the identification and processing of the features to be measured depend on lighting conditions and in workshop or outdoor environment, which is highly unstable factor. Future vision based developments will be more robust and smarter in this sense, but at the moment some limitations still exist.

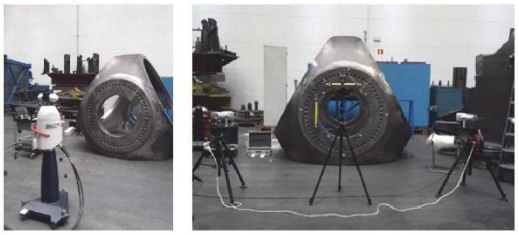

Figure 11: Laser-tracker and advanced photogrammetry based measuring approaches.

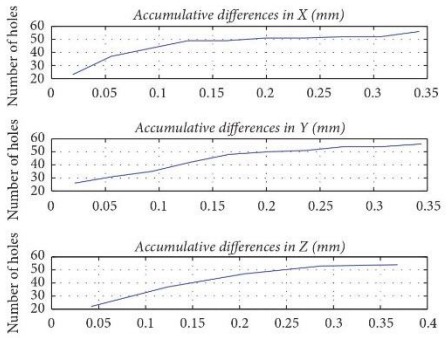

Figure 12: Deviations in *XYZ* coordinates for center position against reference measurements.

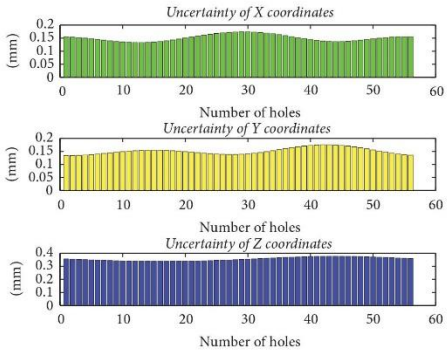

Figure 13: Estimated uncertainty for offline simulation of measurement.

The results obtained are suitable comparing to the specified accuracy and seem to be promising for further applications where the dimensions of the part are larger and actual certified procedures are hard to apply. In any case, the developed method is likely to be integrated as a graphical user interface (GUI) in order to make the most of it and use it for 3D measuring services in a flexible manner. Some programmed codes can also be improved for more efficient computing at this stage. More advanced and friendly simulation tools are also required to design properly the measuring procedure in the simulation field. Further integration stages (hardware and software) will provide new solutions for inline measuring tasks like the approach mentioned in [31].

Anyway, the results obtained are suitable enough for some sectors such as renewable energies, scientific and naval, where the developed tool can also be modified for other features and measurements. Accuracy is not greater due to the bevel in the entrance part of the holes. The adjustment algorithms of the center can be improved to become more robust in relation to this type of feature and others. The triangulation is not the optimum from photogrammetry side. That is why the accuracy of the obtained results is also conditioned in this sense. The comparison is also dependent on the alignment accuracy for the laser-tracker and TRITOP system.

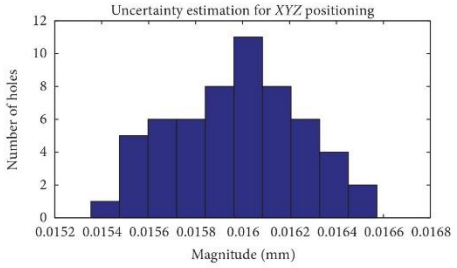

Figure 14: Uncertainty estimation for laser-tracker hole positioning measurement with SA software.

One of the main problems of the overall solution was to determine the image processing method. The first approach tried to define the border points of each hole and to fit these points to an ellipse. Aiming at this, several image filters were tested and geometric adjustment of ellipses was programmed. Nevertheless, the results were not repetitive nor accurate due to the bezel of each hole and also workshop

lighting variations. The pattern matching approach was also unsuccessful for this objective because of a lack of robust models of the features to be detected. Moreover, the approach was highly time-consuming for all the images and features. To solve these problems, the above described image processing approach was finally applied.

With the improvement of more powerful image identification algorithms and more realistic photogrammetric models, better results will be assessed in the future both for close range photogrammetry field and for other optical approaches for multiple scales.

Another improvement way is to work on the simulation side to understand and contrast the most correct procedures for the measurements. Some industrial software already offers this functionality for this task based on targets. In the future, this interesting field will be studied to assure, before the measurement is carried out, that the acceptance criteria of the part are achieved. This previous knowledge permits estimation of the uncertainty of the measuring procedure and is specially indicated for large volume metrology applications where verification and assembly tasks are critical.

Conflicts of Interest

The authors declare that they have no conflicts of interest.

Acknowledgments

The work described in this paper was carried out in collaboration with ETXETAR, S.A. Company in a Basque Project called DUOMO and funded by Business Development Basque Agency (SPRI).

References

[1] E. Savio, L. De Chiffre, and R. Schmitt, "Metrology of freeform shaped parts," *Annals of the CIRP*, vol. 56, no. 2, pp. 810–835, 2007.

[2] ASME, "Fundamentals of geometrid dimensioning & tolerancing (GD&T)," ASME Standard Y14.5-2009, 2009.

[3] ISO, "Geometrical product specifications (GPS)—geometrical tolerancing—tolerances of form, orientation, location and run-out," ISO Standard 1101:2017, 2017.

[4] JCGM, "Evaluation of measurement data—the role of measurement uncertainty inconformity assessment," JCGM Standard 106:2012, 2012.

[5] Case Study: Lakber Lakuntza, Leica Absolute Tracker AT901 for inspection of large-volume wind energy components, 2011, http://www.hexagonmetrology.com.ar/en/lakber-lakuntza_863.htm#.WPjwzmeluUk.

[6] Application Example 2009: Quality Control, Mobile Optical Coordinate Measuring Technology Used in Offshore Wind Turbines Setup, http://www.gom.com/fileadmin/user_upload/industries/offshore_windturbines_EN.pdf.

[7] G. Goch, W. Knapp, and F. Härtig, "Precision engineering for wind energy systems," *CIRP Annals—Manufacturing Technology*, vol. 61, no. 2, pp. 611–634, 2012.

[8] U. Mutilba and I. Del Rio, "Towards an effective dimensional verification of eolic casting," in *Proceedings of the 71st World Foundry Congress*, October 2014.

[9] "Evaluation of measurement data—an introduction to the Guide to the expression of uncertainty in measurement," JCGM 104:2009, 2009.

[10] Application report: Quality control of a large scale, http://www.aicon3d.com/fileadmin/user_upload/praxisberichte/en/pdf/Siemens_EN.pdf.

[11] W. T. Estler, K. L. Edmundson, G. N. Peggs, and D. H. Parker, "Large-scale metrology—an update," *CIRP Annals - Manufacturing Technology*, vol. 51, no. 2, pp. 587–609, 2002.

[12] W. Cuypers, N. Van Gestel, A. Voet, J.-P. Kruth, J. Mingneau, and P. Bleys, "Optical measurement techniques for mobile and large-scale dimensional metrology," *Optics and Lasers in Engineering*, vol. 47, no. 3-4, pp. 292–300, 2009.

[13] T. Brajlih, T. Tasic, I. Drstvensek et al., "Possibilities of using three-dimensional optical scanning in complex geometrical inspection," *Journal of Mechanical Engineering*, vol. 57, no. 11, pp. 826–833, 2011.

[14] R. H. Schmitt, M. Peterek, E. Morse et al., "Advances in large-scale metrology—review and future trends," *CIRP Annals—Manufacturing Technology*, vol. 65, no. 2, pp. 643–665, 2016.

[15] G. Giuseppe and R. Clement, *The Use of Self-identifying Targeting for Feature Based Measurement*, Coordinate Measuring System Committee, 2000.

[16] A. Zervos and C. Kjaer, "Pure Power, Wind energy Targets for 2020 and 2030," Tech. Rep., European Energy Association (EWEA), 2009.

[17] D. C. Brown, "Close-range CameraCalibration," *Photogrammetric Engineering*, p. 3718, 1971.

[18] T. Luhman, S. Robson, S. Kyle, and I. Harley, *Close range photogrammetry. principles, methods and applications*, Whittles Publishing, Rev Ed edition (2006) edition, 2006.

[19] T. Luhmann, "Close range photogrammetry for industrial applications," *ISPRS Journal of Photogrammetry and Remote Sensing*, vol. 65, no. 6, pp. 558–569, 2010.

[20] C. Fraser, "Advances in close-range photogrammetry," Photogrammetric week 2015.

[21] K. Andresen and Q. Yu, "Calculation of the geometric parameters of an ellipse in space by its edges in the images," *ISPRS Journal of Photogrammetry and Remote Sensing*, vol. 49, no. 2, pp. 33–37, 1994.

[22] T. Luhmann, "Eccentricity in images of circular and spherical targets and its impact on spatial intersection," *Photogrammetric Record*, vol. 29, no. 148, pp. 417–433, 2014.

[23] Z. Jiandong, Z. Liyan, and D. Xiaoyu, "Accurate 3D Target positioning in close range photogrammetry with implicit image correction," *Chinese Journal of Aeronautics*, vol. 22, no. 6, pp. 649–657, 2009.

[24] L. Jiansong, "Optimizing design and analysis of industrial photogrammetric network," *The International Archives of the Photogrammetry, Remote Sensing and Spatial Information Sciences*, vol. 37 part 5, 2008.

[25] E. Dall'Asta, K. Thoeni, M. Santise, G. Forlani, A. Giacomini, and R. Roncella, "Network design and quality checks in automatic orientation of close-range photogrammetric blocks," *Sensors*, vol. 15, no. 4, pp. 7985–8008, 2015.

[26] B. Muralikrishnan, S. Phillips, and D. Sawyer, "Laser trackers for large-scale dimensional metrology: a review," *Precision Engineering*, vol. 44, pp. 13–28, 2016.

[27] Z. Xusheng, Z. Lianyu, and T. Xiaojun, "Configuration optimization of laser tracker stations for large-scale components

in non-uniform temperature field using monte-carlo method," *Procedia CIRP*, vol. 56, pp. 261–266, 2016.

[28] T. Becker, M. Özkul, and U. Stilla, "Simulation of close-range photogrammetric systems for industrial surface inspection," *International Archives of the Photogrammetry, Remote Sensing and Spatial Information Sciences—ISPRS Archives*, vol. 38, Article ID 3W22, pp. 179–183, 2011.

[29] F. Buffa, A. Pinna, and G. Sanna, "A simulation tool assisting the design of a close range photogrammetry system for the sardinia radio telescope," *ISPRS Annals of Photogrammetry, Remote Sensing and Spatial Information Sciences*, vol. 3, no. 5, pp. 113–120, 2016.

[30] H. Hastedt, "Monte-carlo-simulation in close-range photogrammetry," *The International Archives of the Photogrammetry, Remote Sensing and Spatial Information Sciences*, vol. 34 part 30.

[31] A. Mendikute and A. Zatarain, "Automated raw part alignment by a novel machine vision approach," *Procedia Engineering*, vol. 63, pp. 812–820, 2013.

ARTICLE Nº2 (CASE STUDY2)

- Kortaberria, Gorka & Gomez-Acedo, Eneko & Molina, Jorge & Tellaeche, Alberto & Minguez, Rikardo. (2019). Theoretical accuracy assessment of model-based photogrammetric approach for pose estimation of cylindrical elements. Measurement Science and Technology. 10.1088/1361-6501/ab0b7d. →https://iopscience.iop.org/article/10.1088/1361-6501/ab0b7d/pdf

IOP Publishing
Meas. Sci. Technol. **30** (2019) 055003 (17pp)
Measurement Science and Technology
https://doi.org/10.1088/1361-6501/ab0b7d

Theoretical accuracy assessment of model-based photogrammetric approach for pose estimation of cylindrical elements

Gorka Kortaberria[1,4], Eneko Gomez-Acedo[1], Jorge Molina[2], Alberto Tellaeche[2] and Rikardo Minguez[3]

[1] Department of Mechanical Engineering, IK4-Tekniker, Eibar 20600, Spain
[2] Department of Smart and Autonomous Systems, IK4-Tekniker, Eibar 20600, Spain
[3] Department of Graphic Design and Engineering Projects, University of the Basque Country, Bilbao 48013, Spain

E-mail: eneko.gomez-acedo@tekniker.es (EG-A), jorge.molina@tekniker.es (JM), alberto.tellaeche@tekniker.es (AT), rikardo.minguez@ehu.eus and gorka.kortaberria@tekniker.es

Received 28 October 2018, revised 25 February 2019
Accepted for publication 28 February 2019
Published 4 April 2019

Abstract

In this research, a multi-view photogrammetric model was developed and tested in simulation in order to understand its capabilities for close-range photogrammetric applications. It was based on contour line detection and least squares geometrical fitting of a cylindrical geometry from multiple views. To feed and validate this model, synthetic data were created for several cylinders poses and camera network set-up. The simulation chain comprises three main stages: synthetic image creation, image data processing by means of shape-matching and cylinder pose estimation based on developed photogrammetric model. Beforehand, *a priori* data was theoretically established according to a common reference for both for intrinsic and extrinsic parameters of the cameras. The preliminary results highlight that the model is suitable for close-range photogrammetry and sensible to *a priori* known data as well as to image data quality. These results were compared against other validated geometrical methods to assure that the model is truthful. Preliminary results show that the accuracy of the model ranges between 1/1000 and 1/20 000 for multiple poses and cylinder dimensions. Moreover the simulation procedure has been enhanced with a Montecarlo approach to estimate more realistic pose uncertainties considering possible imaging error sources.

Keywords: model-based, simulation, cylinder pose, photogrammetry, contour lines, least square fitting, uncertainty

(Some figures may appear in colour only in the online journal)

1. Introduction

1.1. The context and limitations

The recovery of the 3D geometric information from 2D images is a fundamental problem in computer vision and photogrammetry fields. Recent reviews and advances in this field regarding this problem are presented in Luhmann *et al* (2013, 2006, 2016), Crc (2015) and Heipke *et al* (2016). Most of the approaches among multiple perspectives and features are based on collinearity equations and on a correspondence problem. Although these strategies are valid for most cases, sometimes they are not feasible. One of the main limitations of these methods is the preparation of the scene when the geometric elements to be measured are either large (>5 m), far away (>20 m) or hardly accessible. Harsh environments, such as those where elements to be measured are thermal emitting surfaces, are also challenging for traditional solutions as the location of artificial targets on the surface is not possible.

[4] Author to whom any correspondence should be addressed.

Occlusion problems for multi-view approaches is another limiting factor for target-based photogrammetry where line of sight is not guaranteed. Moreover, the measurement in solar plants environment suffer from poor object illumination and signalization problems as well as possible image recording difficulties due to air convection of hot surfaces. To tackle these drawbacks, model-based approaches are advisable in order to avoid scene preparation and to estimate the pose of the element of interest by means of geometric fitting. These kind of solutions are based on high quality detection of contour points that define the element or elements to be measured. Depending on this, high accuracies for 3D element verification, pose estimation or tracking can be obtained when the camera network employed assures image ray suitable convergence. One of the limitations corresponds to necessary approximated values of the element to be measured and previous camera network calibration solving (Fraser 2013, Fraser and Stamatopoulos 2014, Summan *et al* 2015, Luhmann *et al* 2016). The method can be used for several geometric components spatial determination such as lines, cylinders and circles.

1.2. Background

Pose estimation of geometric elements is a common requirement in 2D and 3D vision based applications, where different methods have been developed and studied to tackle this problem from different point of views. In the bibliography different methods (see figure 1) can be found such as pose orientation from known points (Oberkampf *et al* 1996, Triggs 1999, Zhi and Tang 2002, Xu and Liu 2013), pose estimation using shape-based 3D matching (Osada *et al* 2001, Rosenhahn *et al* 2006, Teck *et al* 2010, Yang *et al* 2016), pose estimation using surface-based 3D matching (Rabbani and Van Den Heuvel 2005, Su and Bethel 2010, Liu *et al* 2013, Paláncz *et al* 2016, Figueiredo *et al* 2017) and pose estimation based on model-based approaches. Pose estimation is required in motion applications as well as for measuring, bin-picking or even alignment tasks. The selection of the most suitable approach needs to consider multiple factors directly related to required measuring specifications. In this research the model-based approach has been selected as the accuracy, large working distance, round surface form, harsh measuring environment and high number of measuring perspectives are demanding requirements which other approaches do not fit.

This paper presents not only a novel photogrammetric simulation approach, but also a theoretical simulation chain to design a camera network that fulfills and enables one to guarantee that the measuring accuracy of the employed approach is under the application tolerance.

Thus, both aspects were analyzed by previous researches in order to provide a general overview in this field and to know more about the approaches followed in each case, as well as about the obtained results.

In order to evaluate if a photogrammetric procedures is fit to purpose, simulation based approaches permitting modelling testing and output result reliable quantification are required. Usually known as camera network design problem, this topic has been deeply studied in the following two main approaches, one of them uses mathematical models (Dunn 2007, Alsadik *et al* 2012, Dall'Asta *et al* 2015, El-hamrawy *et al* 2016, Tushev and Sukhovilov 2017) and the other uses synthetic data, following the 'design by simulation' concept (Olague and Mohr 2002, Becker *et al* 2011, Piatti and Lerma 2013).

Focused on the second method, which is similar to the simulation procedure described in this paper, Piatti and Lerma (2013) developed a virtual simulator that underpins the design of a photogrammetric measurement based on 3D scenes (Becker *et al* 2011) presents a free ray tracing software to build up a virtual close range photogrammetric sensor and simulate 3D scenes based on this simulation approach, and finally (Buffa *et al* 2016) presents a simulation study for a dimensional characterization of an antenna combining different tools.

Regarding simulation packages (software, libraries) for a photogrammetric network design and optimization based on nominal or synthetic data (images or geometrical information), there are few available options. The main ones are the combination of Spatial Analyzer© and VSTARS© inspection tools, academic softwares such as Phox© (Luhmann 2016) for photogrammetric design and parametric mathematical understanding, photogrammetric libraries integrated in computer vision Matlab© toolbox (Tushev and Sukhovilov 2017), opensource libraries (MICMAC©, APERO©, SFM©, GRAPHOS©) for dense point cloud reconstruction, etc.

The above-mentioned simulation alternatives and industrial photogrammetric solutions enable one to measure not only the spatial position of artificial targets or fixtures, but also the location of some natural features such as holes, lines (Gruen and Li 1991), pipes (Veldhuis and Vosselman 1998, Zhang *et al* 2017) or spheres in 3D. However, together with this objective, these alternatives need to triangulate these features from multiple perspectives with determined incidence angles. Therefore, the accuracy is reduced most cases and the correspondence problem must then be solved. A common approach is to use epipolar geometry to enhance stereo image matching strategies.

Previously mentioned approaches do not take into consideration the cases where the photogrammetric problem is solved by means of a minimization of the distance among image rays and the spatial geometric element to be fitted and measured. They offer the possibility to estimate the pose of a geometric element adjusting the 3D coordinates of the targets that define the object. Therefore, there is a lack of knowledge in this sense when this kind of ray projection based photogrammetric approaches are required. A general overview of this tracking 3D methods is described in Doignon (2007), where limitations and challenges are also mentioned.

In the literature, there are few references regarding photogrammetric approaches where the correspondence problem (Hilton 2005, Fraser *et al* 2010) is avoided. Most of the existing references are theoretical studies about the modelling and the problems derived from the geometrical determination of 3D elements such as lines, circles or cylinders. A survey and estimation approaches for these geometric elements is presented in Doignon (2007). However, compared to these

Pose estimation approaches	Scheme	Data type to be analyzed
Spatial resection with known points	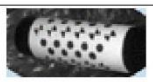	2D image data (known targets)
Shape-based 3D matching		2D image data (shape)
Surface-based 3D matching		3D point cloud (segmentation and fitting)
Model-based	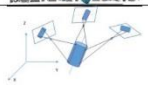	2D image data (contour points)

Figure 1. Review of cylinder pose estimation methods.

geometries, the literature regarding the pose estimation of cylindrical objects with constant radius, is somewhat sparse.

Moreover, although other geometrical features have been studied more in detail, there are two main classifications for the references based on single-view or multi-view approaches for cylinder pose estimation. In any of this cases, the obtained relative accuracy is not studied for large scale applications.

Both for single view (Shiu and Huang 1991b, Ferri *et al* 1993, Puech *et al* 1997, Penman and Alwesh 2006, Doignon and De Mathelin 2007, Liu and Hu 2014) approaches or multi-view ones (Houqin and Jianbo 2008, Becke 2015, Teney and Piater 2014, Becke and Schlegl 2015, Zhu *et al* 2015, Zhang *et al* 2017), cylinder pose estimation can be estimated based on several approaches or on a combination of them. Depending on the image data taken into consideration, only cylinder orientation in three degrees of freedom (dof) or five dof pose can be established employing the contour data corresponding to cylinder's circular borders. The combination of different contour data can tackle a more robust pose estimation combining both, orientation and position results.

On the one hand, there are different approaches for monocular camera methods such as probabilistic ones (Hanekr *et al* 1999), basic or more complex models depending on the dof number for the cylinder's pose (Huang *et al* 1996, Doignon and De Mathelin 2007), models considering different image data from shape matching outputs (Shiu and Huang 1991a) or cases where the geometrical dimensions of the element are known *a priori* (Huang *et al* 1996, Puech *et al* 1997, Renaud *et al* 2005, Liu and Hu 2014).

Apart from this, 3d circle pose estimation is solved in Shiu and Huang (1991a) and Andresen and Yu (1994) for the same approach where even the orientation is established by ellipse modelling and fitting approach.

On the other hand, there are multiple view approaches considering more complex and robust camera networks both for cylinder pose and 3D line detection.

For example, a canonical representation based software is presented in Navab and Appel (2006) for stereo or multi-views, theoretical preliminary modelling for pose estimation based on contour data and single or multi-view approaches in Becke (2015), semi-automatic linear feature extraction algorithm for estimation of 3D elements from multi-view approaches based on LSB-Snakes in Gruen and Li (1991), the reconstruction of straight and curved pipes from digital images with not corresponding points in Veldhuis and Vosselman (1998) and Zhang *et al* (2017), a least-squares method for locating a linear object by using its multiple parallel projections, etc…

As a summary of this literature compilation and analysis, the following list indicates the main difficulties and drawbacks that must be studied in detail so as to overcome them:

- In most cases, image noise is not taken into account in the simulation which is advisable for reliable model characterization
- The models are not applied for large-scale applications or case studies where the errors are amplified due to projection effects.
- Measuring solution validation against validated sources or tools is missing.
- Suitable feature point extraction is not usually available.
- Tools for accurate synthetic data creation (geometrical or image data) are not available.

1.3. The application

The research tends to enable an accuracy and robustness simulation of a model-based photogrammetric approach for a cylinder pose estimation when the element to be measured is hardly measurable with artificial targets (Knyaz 1998, Joon Ahn and Rauh 2001, Shortis *et al* 2004, Wijenayake *et al* 2014, Guo *et al* 2016). Thus, our approach to cylinder pose robust estimation differs from traditional approaches which

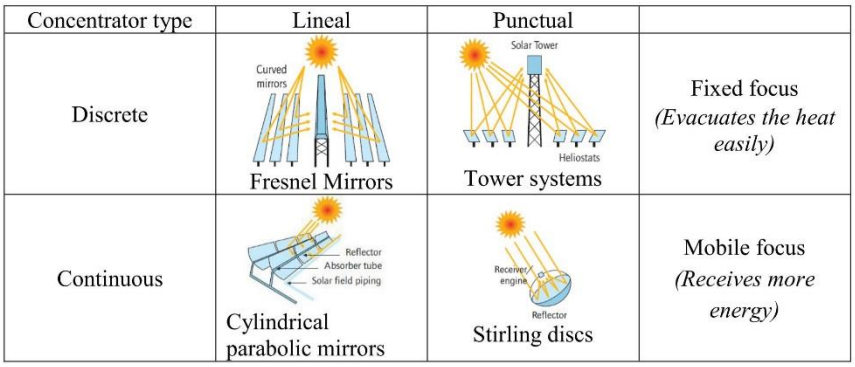

Figure 2. Review of concentration solar power (CSP) technology.

avoid the correspondence problem among images and multiple view perspectives.

The application is focused on thermal concentration applications, (see figure 2) where positioning a closed loop of the moving receivers is required for high energy efficiency performances. Traditional photogrammetric approaches (Shortis and Johnston 1996, Pappa *et al* 2001, Pottler *et al* 2005, Shortis *et al* 2008, Stynes and Ihas 2012, King *et al* 2013, Hafez *et al* 2017) are not suitable because of surface curvature and the impossibility to add distributed targets over the element due to high working temperatures and solar flux concentrations. Another disadvantage of traditional photogrammetric approaches is related to the high incidence angles that are required for planar targets in curved surface introducing target center measurement inaccuracies. In addition, the approach described in this article aims to develop more flexible photogrammetric solutions for 3D scenes than those offered by commercial solutions. Moreover, model-based methods are not integrated in these industrial software, which means that, in order to quantify the scope and design the best suitable measuring network considering the real scene requirements, it is necessary to carry out this modelling and test its performance.

1.4. Main objectives of the research

The objectives of the research are to develop, implement and validate a model-based photogrammetric simulation tool in order to assess the six dof positioning accuracy of a cylinder for a specific camera network and synthetic image data. Is it not an optimization procedure but a test and accuracy assessment approach for design purposes of this photogrammetric method. Therefore, the main error sources are studied, and the most suitable camera network is designed and stablished by means of developed simulation tools. The results of the research will enable one to quantify and determine the accuracy and suitability of this photogrammetric approach for large parts and working distances in harsh environments. Model testing will also describe the limitations for this photogrammetric approach offering the possibility to assess the cons and pros against traditional approaches.

2. Materials and methods

2.1. Description of the simulation method

The overall method comprises several tools, an implementation of a model (cost function), which enables the estimation of the five dof positioning of a cylinder based on contour points and a Montecarlo approachfor uncertainty assessment. The rotation of the cylinder around its axis is not controlled by the model. This model is fed with image data points extracted from synthetic images. The camera network (extrinsic orientation), the 3D scene and imaging parameters are established and the synthetic images are generated for each cylinder's spatial pose. For each cylinder pose, three images are generated for three camera views. These images are depict grey values ranging from 0 to 255 values simulating a 3507 × 2480 pixel camera and 6 mm principal distance lens. The pixel size is 2.8387 μm which is the scaling factor to convert pixel points to metric image points in mm. Afterwards, these images are processed with an image processing algorithm and data contour data points are obtained for each camera and pose with sub-pixel edge extraction methods. Eventually, these data points, camera network and an *a priori* geometry describing the 3D scene are imported in the photogrammetric model implemented in an engineering simulation environment. The model estimates for each image combination and fixed camera network, the real pose of the cylinder, minimizing the tangential distances among the light rays projected from image planes to the 3D geometry.

In order to obtain more realistic output results, the model has been improved with a Montecarlo simulation approach. Once the contour points are extracted from images, these pixel points are modified by random distribution error sources to evaluate their effect on the model's output. This process is repeated n times and the model output result is stored for statistical distribution analysis. The overall simulation workflow is presented below (see figure 3).

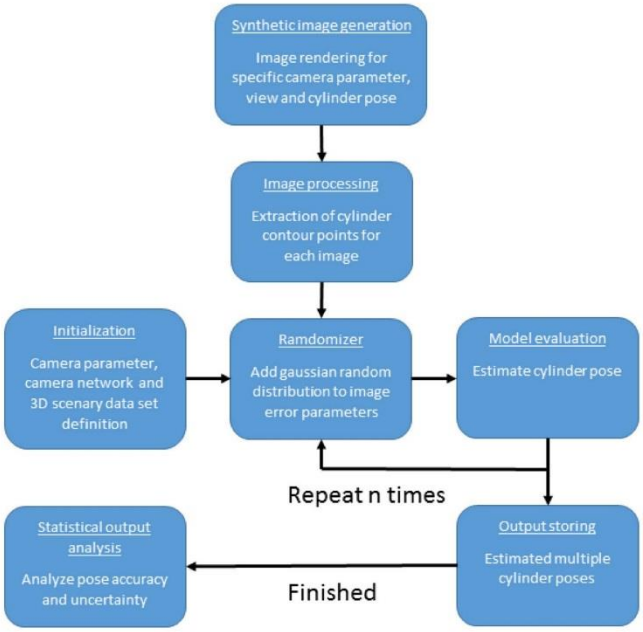

Figure 3. Simulation consecutive stages and overall process workflow.

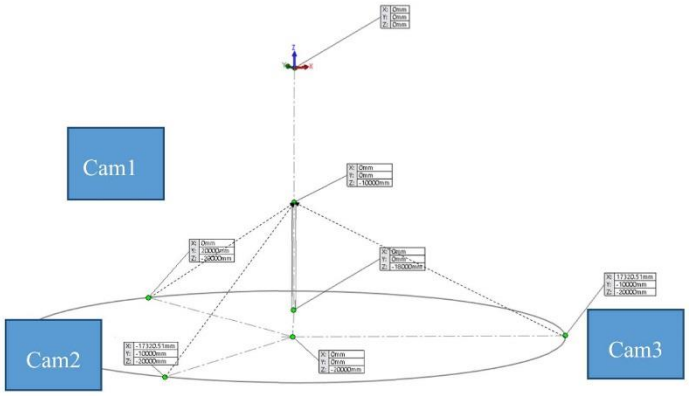

Figure 4. Cylinder vertical pose definition and camera network (extrinsic orientation) establishment.

2.2. Implementation and modelling

2.2.1. Synthetic data generation. In order to generate synthetic images, first of all the 3D scene is created 20 m away in radius from camera positions (see figure 4). In this case, 3D geometry comprises a cylinder of 8 m length and 250 mm diameter. This element is positioned and oriented according to a reference system simulating difference poses. For instance, vertical orientation and centered position (Pose1) or totally oblique ones (Poses 2 and 3). After the several poses are established, the camera views are added for the same reference system. These views (three cameras) are fixed and require identifying several parameters, such as the position, the pointing orientation, the principal distance and image sensor

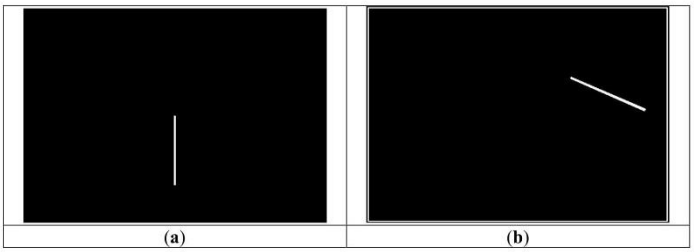

Figure 5. Synthetic images for cylinder's several poses from the same camera field of view (see camera 1 from figure 1. (a) Vertical pose of the cylinder. (b) Oblique pose of the cylinder.

dimensions. The field of view depends on the principal distance, lens aperture, selected camera model and therefore in sensors dimensions. Real illumination aspects affecting image generation as well as optical lens distortion are not considered in this step as the design environment is not prepared for this aim. However, imaging imperfections will be considered in Montecarlo simulation process as image noise error sources.

In the real application, object signalization limitations as well as image distortion effects will appear and directly affect the image data quality and therefore the performance of the model. While image distortion errors can be modelled, characterized by offline or self intrinsic calibration approaches (Fraser 2013, Luhmann *et al* 2016) and compensated as it is a systematic optical error source, object detection and contour point data extraction is a demanding requirement in high solar flux concentration applications (Lee *et al* 2013, Ruelas *et al* 2017). In order to minimize imaging errors and optimize image acquisition and processing steps, implemented cameras are expected to work in the infrared spectrum with dynamic range fitting which higlights the contrast between cylinder contour points and the background. In this manner, the shape-based matching process is simplified and optimized as the images contain less and more useful information speeding up image processing tasks.

Returning back to the image generation tool, once geometric parameters are settled (see figure 5), different cameras can be selected, and synthetic images are rendered (full grey level) and generated.

2.2.2. Image data processing. The employed image processing approach is based on shape matching methods that enable the finding and location of the objects of interest in an image. Within this aim, a suitable image pattern is required to define objects that are represented and recognized by their shape. There are multiple ways to determine or describe the shape of an object. In this paper, the shape is extracted by selecting all those points whose gradient exceeds a certain threshold. Typically, the points correspond to the contours of the object. The main image processing steps for previously generated synthetic images are described in the following workflow:

1. Image importation
2. Image pre-processing: a binarization on a greyscale image is applied to obtain a black and white image establishing a suitable threshold.

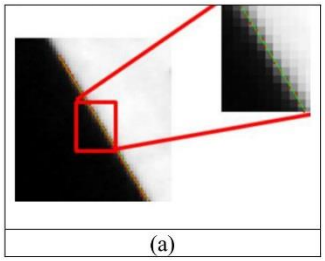

Figure 6. Sub-pixel edge location (red points) and line fitting (in green).

3. Shape based-matching (Harun and Sulaiman 2011): this is the most challenging phase of the overall image processing procedure because following tasks depend on its output. The shape based- matching algorithm tries to find the corresponding shape of an element comparing the image data against a trained pattern.. It does not use the gray values of pixels and their neighborhood as template but describes the model by the shapes of contours. This process is divided in two main steps. First of all, the shape-based pattern is defined in a sample image and trained to become the image pattern as robust as possible considering effects such as neighborhood points, contrast, noise, occlusions or even perspective changes (rotation, scale variation, etc). Secondly, this trained pattern is applied as an operator in an image where the object to be detected appears and the object and its region of interest (ROI) are determined correspondingly.
4. Edge data point extraction: Once the ROI of the object is restricted, edge extraction operators are applied to define the contour points of the shape (see figure 6). In order to speed up the subpixel-precise edge extraction, it is recommendable to apply it only to a reduced ROI. As accuracy is required for the vision based application, subpixel edge extraction operators are used (see figure 5). The main steps for image data extraction are: creation of sub-pixel contours by means of edge operators such as *threshold_sub_pix* and selection of relevant points where some of the segments are deleted, and others are combined to define the edge of interest. Usually a primitive

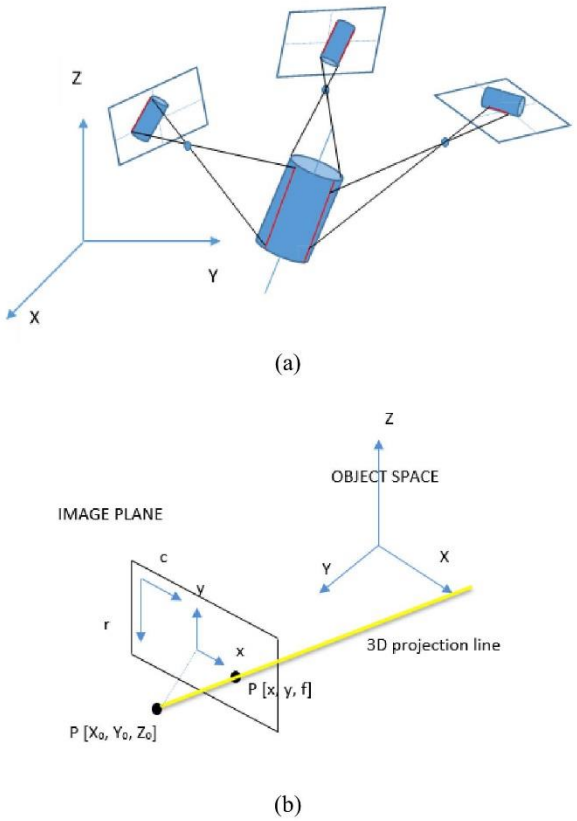

Figure 7. Edge method for cylinder pose estimation. (a) Multi-view 3D representation of the model (b) projection model from image plane to 3D space.

fitting step follows these previous steps, but in this case, is not necessary.

5. File creation for each image with contour point: finally, an Ascii file is created with these data for each image where the points corresponding to the contour points are described in row and columns in pixels units. These points do not consider image noise nor imaging parameter uncertainties.

2.2.3. Modelling. The core of this research is a photogrammetric model based on light ray projection from image planes to 3D space. Each image point and the projection center of each camera define a light ray that is tangent to the cylinder whose pose is to be found. Establishing the distances among the light rays and the geometric element and minimizing them enables to estimate the element's parameters.

The proposed methodology is not based on traditional approaches that employ artificial targets to measure a specific geometry. Usually, the 3D positions of these targets are obtained and then a least square algorithm is applied to estimate the most approximated element that fits with these 3D points. This common approach requires to assure the correspondence of the points enabling their triangulation, but this requirement is not always reached. When the element to be measured is, for example, a cylinder, the aforementioned approach is not the most suitable one. Thus, another approach is necessary to solve this limitation. The developed model for estimating the five dof positioning of a cylinder comprises an alternative approach based on Best-fit adjustment of a cylinder to measured 2D contour points in multiple images (see figure 7).

On the one hand, the inputs that feed this model are the contour points of each image, a camera network definition around those points, image parameters (principal distance and image scaling factor), image dimensions (pixel number) and an *a priori* cylinder pose (position, orientation) as well as dimensions (radius). On other hand, the output values are the real position and orientation (pose) of the cylinder related

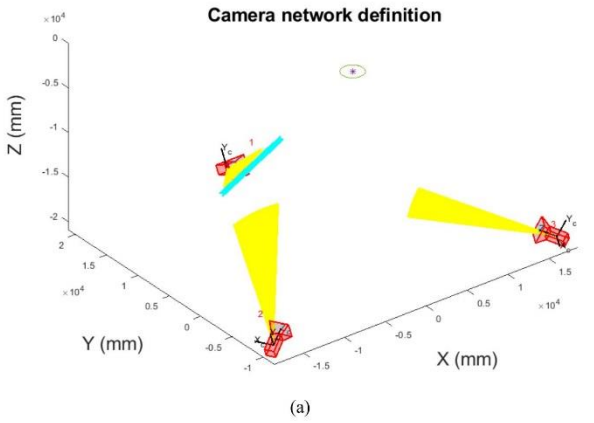

(a)

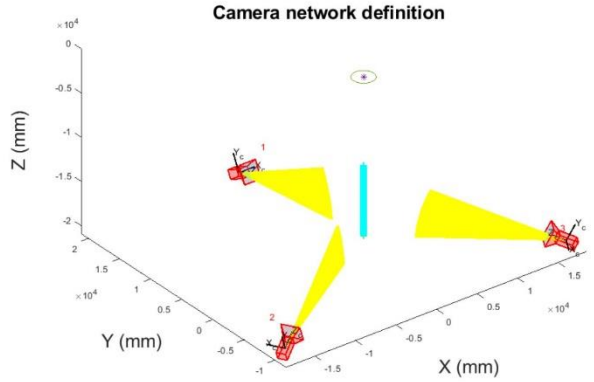

(b)

Figure 8. Photogrammetric model representation for several cylinder poses (in blue) and light rays (in yellow) pointing towards the primitive. (a) Oblique pose. (b) Vertical pose.

to a fixed coordinate system. Indeed, the pose of the cylinder is defined as 2 points P1 and P2 corresponding to the axis (see figure 10) for enabling an easier simulation result interpretation.

Model's performance is studied by means of inverse problem approaches which minimize the tangential distances among the light rays and the cylinder to be calculated. These rays are created for each image considering each image point ($Z = 0$) and the projection center (same for each image). The light rays are fitted to 3D lines that are defined in a common reference system shown in figure 3. In order to estimate the tangential distances for each ray and image, a 3D intersection function is employed. This function considers the estimation of the distances between each image ray (3D line) and cylinder axis and accordingly, estimating the tangential distances (see figure 8). The cylinder's pose is obtained by minimizing iteratively these distances.

In the following lines, a detailed mathematical description of the model is presented and the data flow is explained.

The starting point for the model are the image data of the contour points extracted from the synthetic images. For a specific cylinder pose, three files with image data are imported to the developed model. Each file corresponds to a camera and an interextrinsic orientation of this camera regarding to the absolute reference system.Besides, approximate values of the cylinder pose are required as input data.

This data in pixels (rc) is transformed and scaled (m) to metric data (mm) taking into account image's horizontal and verticals dimensions (dimHor and dimVert) and a rotation ($\alpha = 90°$) between coordinate systems. The data xy is in camera local coordinates. The applied plane transformation is,

$$x = m \cdot (R \cdot rc + T) \tag{1}$$

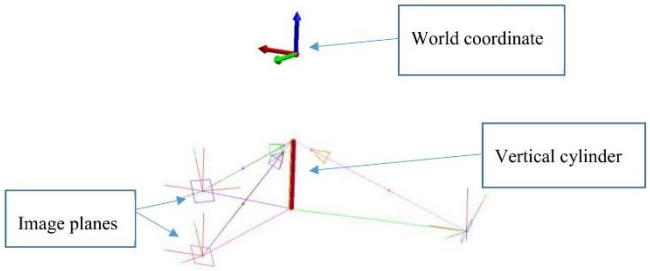

Figure 9. Definition of validation 3D pose and reference data processing with SA tool.

$$\begin{bmatrix} x \\ y \end{bmatrix} = m \cdot \left(\begin{bmatrix} \cos\propto & -\sin\propto \\ \sin\propto & \cos\propto \end{bmatrix} \cdot \begin{bmatrix} r \\ c \end{bmatrix} + \begin{bmatrix} \text{dimHor}/2 \\ \text{dimVert}/2 \end{bmatrix} \right). \tag{2}$$

Once each contour point is transformed for each image plane, a third coordinate is added to xy with the value of the focal distance (f). Thus, for each image point $x'y'z'$ coordinates are available in local coordinates.

$$\begin{bmatrix} x' \\ y' \\ z' \end{bmatrix} = \begin{bmatrix} x \\ y \\ f \end{bmatrix}. \tag{3}$$

After this transformation, another spatial transformation is required for each point to convert the $x'y'z'$ local coordinates to spatial XYZ coordinates corresponding to the main reference system. R (rotation matrix) and X_0 (translation vector) parameters define the extrinsic orientation and translation of the image plane (projection center) regarding to absolute reference system. These parameters are supposed to be known from previous calibration step.

$$X = X_0 + R^{-1} \cdot x' \tag{4}$$

$$\begin{bmatrix} X \\ Y \\ Z \end{bmatrix} = \begin{bmatrix} X_0 \\ Y_0 \\ Z_0 \end{bmatrix} + \begin{bmatrix} r_{11} & r_{21} & r_{31} \\ r_{12} & r_{22} & r_{32} \\ r_{13} & r_{23} & r_{33} \end{bmatrix} \cdot \begin{bmatrix} x' \\ y' \\ z' \end{bmatrix}. \tag{5}$$

With each transformed image point ($X_iY_iZ_i$) and the projection center point ($X_0Y_0Z_0$) of its corresponding camera, 3D lines are created (see figure 6). A straight line (X_{li}) between each transformed image point P_i (X_i, Y_i, Z_i) and P_0 (X_0, Y_0, Z_0) in parametric form is defined by:

$$X_{li} = X_i + t \cdot (X_0 - X_i) \tag{6}$$

$$\begin{bmatrix} X_{li} \\ Y_{li} \\ Z_{li} \end{bmatrix} = \begin{bmatrix} X_i \\ Y_i \\ Z_i \end{bmatrix} + t \cdot \begin{bmatrix} X_0 - X_i \\ Y_0 - Y_i \\ Z_0 Z_i \end{bmatrix} = \begin{bmatrix} X_i \\ Y_i \\ Z_i \end{bmatrix} + t \cdot \begin{bmatrix} a \\ b \\ c \end{bmatrix}. \tag{7}$$

Here P_i (X_i, Y_i, Z_i) is any image point corresponding to the line and the direction cosines are

$$\frac{X_0 - X_i}{d} = a \tag{8}$$

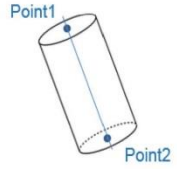

Figure 10. Cylinder pose definition based on two spatial points (P1, P2).

$$\frac{Y_0 - Y_i}{d} = b \tag{9}$$

$$\frac{Z_0 - Z_i}{d} = c. \tag{10}$$

$$\text{Where } d = \sqrt{(X_0 - X_i)^2 + (Y_0 - Y_i)^2 + (Z_0 - Z_i)^2}. \tag{11}$$

The following step is to estimate the intersection point between each line (X_{li}) and the approximated axis of the cylinder defined in the initialization. The intersection of two lines in 3D space it is only possible if they lay on a common plane. Otherwise, the lines are skew and the shortest distance between them is established. The intersection point is defined in the middle of a line that is perpendicular to both intersected lines and whose length is the minimized distance.

With each estimated intersection point, a distance d_i between this point and the cylinder axis is determined. These distance values (cost-function) for all image points are afterwards minimized to adjust the parameters of the cylinder by means of iterative Best-fit methods.

The distance d_i between 2 spatial lines defined by each transformed point P_i (X_i, X_i, Z_i) and a characteristic point P_C (X_c, Y_c, Z_c) corresponding to the cylinder axis with their respective direction cosines n_i (a_i, b_i, c_i) and n_c (a_c, b_c, c_c) is determined by

$$d_i = \frac{\pm \begin{vmatrix} X_i - X_c & Y_i - Y_c & Z_i - Z_c \\ a_i & b_i & c_i \\ a_c & b_c & c_c \end{vmatrix}}{\sqrt{a^2 + b^2 + c^2}} \tag{12}$$

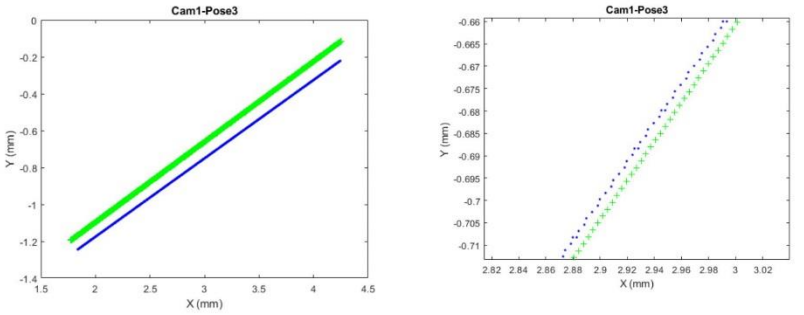

(a)

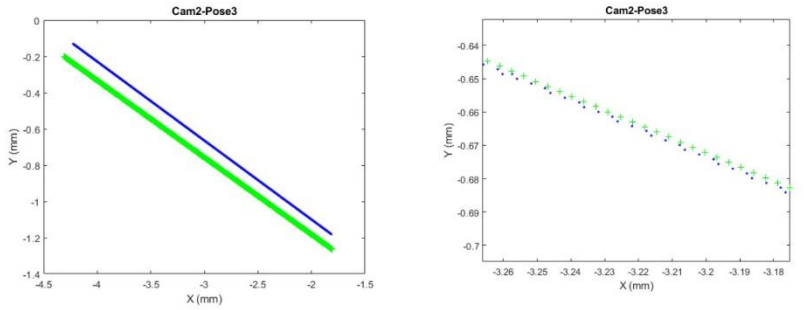

(b)

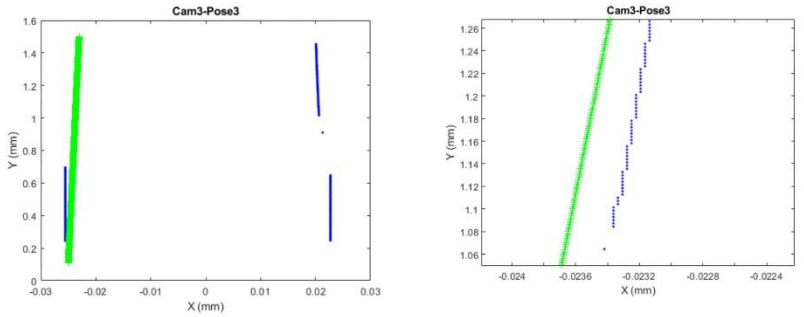

(c)

Figure 11. Qualitative comparison of reference (green) and synthetic (blue) image data for an oblique pose, each camera view and one side contour points. (a) Cam1-Pose3. (b) Cam2-Pose3. (c) Cam3-Pose3.

where,

$$a = \begin{vmatrix} a_i & b_i \\ a_c & b_c \end{vmatrix} \quad b = \begin{vmatrix} b_i & c_i \\ b_c & c_c \end{vmatrix} \quad c = \begin{vmatrix} c_i & a_i \\ c_c & a_c \end{vmatrix}. \tag{13}$$

The cylinder known radius (r) is subtracted to each estimated radial distance. The residual distance values among the image rays (3D lines) and the cylinder axis for all image points (i) and cameras (j) are minimized according to:

$$\sum_j \sum_i d_{ij}^2 - r = \min. \tag{14}$$

In order to solve this minimization problem, a linearization of the cost function is required for each parameter of the cylinder's model and each image point data which enables to construct the jacobian matrix (Kosmopoulos 2011, Afzal *et al* 2016, Hansen and Sutherland 2018) and estimate the corrections of model's parameters in each iteration. The convergence for the solver is obtained when the correction values (ΔP_c and Δn_c) of the element's geometric parameters are below a suitable threshold value.

The form of linearized equations follows

$$\frac{\partial d_{ij}}{\partial x} \cdot \Delta X_c + \frac{\partial d_{ij}}{\partial y} \cdot \Delta Y_c + \frac{\partial d_{ij}}{\partial z} \cdot \Delta Z_c + \frac{\partial d_{ij}}{\partial a} \cdot \Delta a_c + \frac{\partial d_{ij}}{\partial b} \cdot \Delta b_c + \frac{\partial d_{ij}}{\partial c} \cdot \Delta c_c = -d_{ij}. \tag{15}$$

The employed iterative method for minimization problem is not specified in detail as it is common issue in bibliographic references concerning inverse problems (Gao *et al* 2016, Nowak 2017, Ramm 2018) and it is out of the scope of this research.

2.3. Validation and testing

The validation of the implemented model is an important issue that ensures that the obtained results are accurate and meaningful, and therefore the conclusions in relation to these results can be considered truthful. For this purpose, a validated trigonometric approach was employed to check the partial data and results of the developed model. Once the model was approved, further tests were carried out to understand its scope concerning error sources and possible deviations between the theoretical model and the real scene. Moreover a Montecarlo simulation approach was established to estimate cylinder pose uncertainties and determine model's output distribution.

2.3.1. Validation of the developed model. The implementation of the developed model has been checked against an inspection tool called Spatial Analyzer© (hereafter SA) based on the same cylinder pose and camera network definition. This is a 3D inspection software that enables to reproduce the described photogrammetric approaches (see figure 9) from the point of view of pure trigonometry which permits to carry out 2D data validation and accuracy comparison in section 3.1 avoiding the part of image generation and data processing. Facing this objective, the SA interface is used to replicate the developed model in terms of camera network, cylinder pose definition and image ray composition from image planes towards tangential 3D points in the cylinder. Every data is referenced to the main world coordinate system.

Table 1. Quality analysis and differences between reference image data and synthetic data for an oblique pose.

Camera ID	Nominal (SA) FE (mm)	Synthetic FE (mm)	2D distance (mm)
1	0	0.10	0.05
2	0	0.10	0.05
3	0	0.06	0.14

The employed procedure and workflow for 3D scene definition and reference data extraction is the following one:

1. A cylinder is placed for a specific pose (position and orientation)
2. Local coordinate systems are defined corresponding to external camera orientation
3. Image planes are created in these coordinate systems
4. Projection centers are defined for each image plane
5. A plane is estimated that in tangential to the cylinder surface and passes through each projection center (3×)
6. Tangential points above the cylinder surface are estimated projecting the cylinder axis to previously created tangential planes
7. With each point and its corresponding projection center, 3D lines are created
8. The intersection of these lines with the image planes describes the image points

Thus, applying this methodology, reference data can be used to check the implemented model. Among this data, 3D tangential points and image points both in local and global coordinate system are obtained. The employed scaling factor to convert pixel points in image coordinates (metric values) is 2.8387.

2.3.2. Test for validation and comparison of results. The following chapters describe the tests and the targeted results for each test considering several aspects and parameters of the model. A symmetric camera network is studied which guarantees data redundancy and a proper visualization of the cylinder from different point of views. Asymmetric camera networks are not included in this paper, but asymmetry appears on 3D tangential point distribution all around the cylinder. First, a comparison among image data points comparing the values obtained from synthetic images and SA data is presented. Then, the accuracy of the developed model is analyzed based on image data and its inaccuracies, taking theoretically known pose values as *a priori* data. The model's robustness is tested with a deviation range of priori pose data to understand the dependency of the model on *a priori* known data values.

Table 2. Nominal and measured point comparison for all cylinder and pose case studies (Errors and uncertainties in mm).

		CS 1[a]		CS 2		CS 3		CS 4		CS 5	
POSE ID	Point ID	E_{xyz}	U_{xyz}	E_{xyz}	U_{xyz}	E_{xyz}	U_{xyz}	E_{xyz}	U_{xyz}	E_{xyz}	U_{xyz}
1	P1	0.28	0.26	2.93	0.26	0.59	0.25	0.60	0.25	0.05	0.09
	P2	1.27	0.34	1.42	0.35	0.71	0.30	1.58	0.43	0.77	0.23
2	P1	10.43	4.57	7.53	4.09	12.47	4.29	11.08	4.38	9.27	3.48
	P2	13.11	5.57	9.35	4.61	14.92	5.10	12.21	4.65	13.47	5.38
3	P1	8.57	4.63	7.68	3.51	6.52	2.98	6.43	4.03	9.81	3.50
	P2	11.77	5.77	9.92	4.87	8.56	3.22	8.69	4.77	17.83	4.80

[a] Case studies: 1 ($L = 8000$ mm and $D = 250$ mm), 2 ($L = 8000$ mm and $D = 500$ mm), 3 ($L = 8000$ mm and $D = 1000$ mm), 4 ($L = 4000$ mm and $D = 250$ mm), 5 ($L = 16\,000$ mm and $D = 250$ mm).

2.3.2.1.Comparison of synthetic image data and geometric data. Based on reference data obtained from the SA tool, a comparison among data types was carried out to verify and understand the differences between synthetic transformed image data (see equation (3)) applied to photogrammetric models and pure trigonometric precise data. In this manner, the effect of image to metric data transformation can be assessed and quantified.

This comparison can be established at two different stages of the model related with different data types. For instance, 2D image points can be compared with their corresponding 3D tangential points, but in this paper only 2D data are compared. The comparison comprises a qualitative and quantitative comparison between image data (see equation (2)) obtained with several cameras in their local coordinates (2D metric data). In the following chapter, 3D data resulting from the geometrical fitting are assessed to analyze their accuracy.

2.3.2.2. Accuracy of cylinder pose estimation model. After comparing the developed model against the reference 2D data and validating its performance, the accuracy for model parameters is assessed. This analysis is carried out on three poses of the cylinder for the different case studies, together with their respective synthetic data obtained from the procedure described in the process workflow (see figure 2). The aim of this test is to estimate pointing errors of the model by comparing the estimated cylinder parameters and the nominal values. Instead of comparing the obtained values of position and orientation with their nominals, two extreme points (P_1, P_2) of the cylinder (see figure 10) have been defined for each pose simulation case. The aim is to make easier the understanding of the results. Considering that extrinsic orientation of the camera network is precisely known and fixed, residuals are taken as model accuracy indicators.

Apart from mean positioning errors between estimated and nominal cylinder poses, *XYZ* coordinate uncertainties have been calculated for each cylinder point (P1 and P2) in order to understand the reliability of these results. This has been implemented by a Montecarlo simulation approach which enables to add image data and principal distance variations to the model. In this manner, the theoretical data is fitted to a more realistic scenario. The employed simulation parameter values are the following ones: image noise (0.5 pixels) and principal distance uncertainty ± 10 pixels. The convergence threshold values for this uncertainty assessment have been settled to 1 mm (average of residual tangential distances).

Moreover, cylinder dimensions (length and diameter) have been changed for each cylinder pose to check if this variation affects models accuracy. Lengths of 4, 8, 16 metres and diameters of 250, 500, 1000 mm have been tested as representative case studies.

2.3.2.3. Robustness of cylinder pose estimation model. Besides testing the accuracy of the model, its robustness is also tested. One of the requirements of this photogrammetric model is that approximated pose values of the cylinder are necessary to initialize it. Considering that real applications do not assure that the real pose and the nominal one are close to each other, this effect has been simulated and quantified to determine the model's robustness.

In this case, testing procedure consists in introducing initial errors for known poses and camera network to check the robustness and performance of the model. Errors ranging from 1 mm to 1000 mm are applied to *a priori* cylinder parameters (points P_1 and P_2 as in accuracy testing) and the model's response is studied for a 1 mm convergence threshold (which is the maximum value of correction parameter values). These errors are applied separately on each position coordinate (*XYZ*) and then combined for both points' coordinates (P_1 and P_2). Within this test a 8 m and 250 mm diameter cylinder case study has been studied.

Another interesting characteristic from the point of view of the model's robustness, is the minimum amount of image data required and their distribution along the contour lines of the cylinder. This aspect was also analysed when establishing the need for image data quality. The relationship between the model's input data and output data (pose estimation) was studied for the following cases and compared against full 2D data for pose 2:

- Continuous data taking into consideration only the contour points of one side (See case study B in table 3)
- Reduction of continuous image data points from 25% to 75% (See case studies C, D and E in table 3)
- 1/3th of image data for each camera view without correspondence for the same cylinder area (See case study F in table 3)

3. Results

The following results show the capabilities of the developed modelling from the point of view of accuracy and robustness, which are critical aspects for its characterization for future implementations in real applications.

3.1. Comparison of synthetic image data and geometric data

In order to validate and compare the quality of the image data when working with synthetic images in relation to reference data (SA), figure 11 presents, a qualitative comparison of image points on the left side, together with a detailed zoom on the right side. The represented case study corresponds to an oblique pose (pose 3) for a 8 m length and 250 of diameter cylinder. The comparison shows that the data obtained from 3D and transformed into 2D with SA is continuous and straight for contour points (green points) while the employed synthetic data present some imperfections. Regarding to synthetic data transformed to metric data (see equation (2)), the distribution of the points is not straight and even equidistant deviations are found compared against reference data (see zoom in right side for figure 11). Thus, it is obvious that synthetic data are not perfect and present some deviations derived/resulting from the rendering step and the edge point extraction approaches.

In order to analyze the deviation range numerically, in table 1 the error (FE) of each image data type and the 2D distance among fitted lines is shown for an oblique pose and 3 camera views. While the error form for SA reprojected image data is 0, the values for the synthetic are not negligible. These deviations are the main error sources that are conditioning 3D pose estimation accuracy analyzed in section 3.2.

In summary, it can be stated that the synthetic image data generation process is correctly implemented in the model and the procedure is accurate up to 0.14 mm for image coordinates corresponding to an oblique pose, which is the most critical case.

Although there is no way to guarantee/assure perfection, a possibility that could improve synthetic data accuracy is to use better rendering methods for image generation step. Thus, this error needs to be taken into account for these simulation procedures. Error minimization could be achieved by processing the input image data before the model feeding and then fitting these data as accurate contour 2D lines, but this approach would also introduce a systematic error for 3D distances estimated with the model.

3.2. Accuracy analysis of the model

The accuracy of the model has been established for all mentioned case studies (see section 2.3.2.2) and cylinder poses. Based on synthetic images, the image processing step, added imaging error sources and the previously described photogrammetric model (see section 2.2.3), the poses and uncertainties of the cylinder are estimated. In order to facilitate the comparison

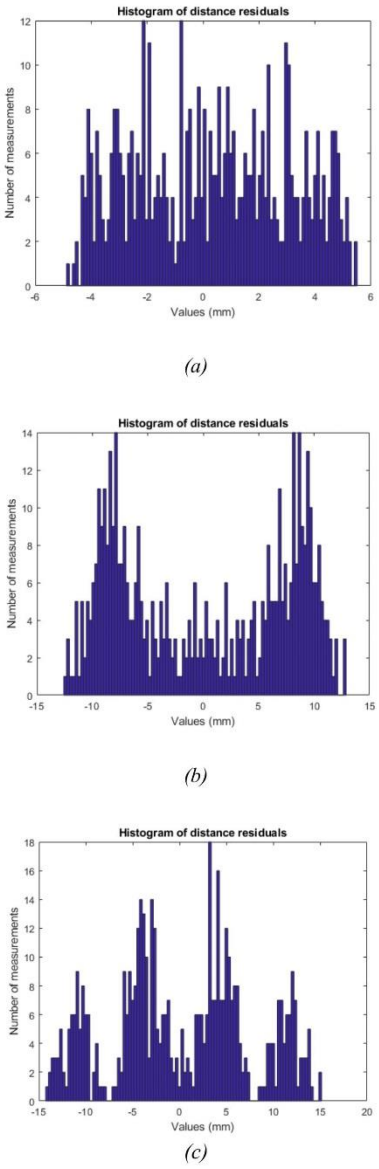

Figure 12. Histograms of distance residuals for estimated tangential points and cylinder axis for each nominal pose. (a) Pose1. (b) Pose2. (c) Pose3.

Table 3. Spatial positioning comparison for diverse 2D image data set. (A) Estimated values with both contour sides. (B) Estimated values with one contour side. (C) Estimate values with filtered contour points 25%. (D) Estimated values with filtered contour points 50%. (E) Estimated values with filtered contour points 75%. (F) Estimated values for not corresponding areas of the cylinder.

		Estimated coordinates (mm)			Differences (mm)		
Case study ID	Point ID	*X*	*Y*	*Z*	ΔX	ΔY	ΔZ
A	P1	−11 025.34	6355.53	−12 727.92	—	—	—
	P2	−6122.95	3529.23	−7072.95	—	—	—
B	P1	−11 018.88	6354.09	−12 727.92	6.46	1.44	0
	P2	−6126.19	3535.51	−7062.7	3.24	6.28	10.25
C	P1	−11 020.50	6353.43	−12 727.92	4.84	2.1	0
	P2	−6124.22	3535.31	−7063.59	1.27	6.08	9.36
D	P1	−11 019.48	6353.86	−12 727.92	5.86	1.67	0
	P2	−6124.72	3535.17	−7062.57	1.77	5.94	10.38
E	P1	−11 019.92	6353.95	−12 727.92	5.42	1.58	0
	P2	−6124.16	3535.12	−7063.49	1.21	5.89	9.46
F	P1	−11 009.31	6357.94	−12 727.92	16.03	2.41	0
	P2	−6139.51	3538.72	−7041.35	16.56	9.49	31.6

between obtained results and the nominal values, the pose is defined by means of two points (P1 and P2) that lay on the cylinder's axis and determine its length. This comparison is shown in table 2, where positioning errors (E_{xyz}) among nominal points and measured ones are presented as well as their uncertainty (U_{xyz}). For all the error values the mean differences are below 20 mm for working distances of 20 000 mm in radius (camera location) with uncertainties below ±5 mm. Therefore, the relative accuracy lays between 1/1000 and 1/20 000 for all case studies. Accuracy depends on the cylinder's pose and the image data quality mentioned in section 3.1, where deviations of tens of microns correspond to mm in 3D space due to projections effects. Moreover imaging error sources such as image noise and principal distance uncertainty add more error variability to image points. The more vertical the pose, the better results (ten times better for Pose1), because the contour points of the cylinder will be more accurately defined and detected. Although other rendering approaches were also employed for synthetic image generation, the results are similar, so the accuracy of the model is limited to this error source.

Besides, figure 12 presents a histogram for each pose, showing the residuals of the distances between the cylinder axis and the estimated 3D tangential points (see equation (12)) for case study1. As this figure shows, the residuals are not symmetric, and the differences tend to create groups which means that systematic errors are conditioning the results. This tendency is probably related to the deviations and the distribution of the image data points employed.

Although the range of the distance residual values for each pose corresponds to even tens of mm, the average values are similar to the absolute deviations of the points P1 and P2 analyzed in table 1.

3.3. Robustness analysis of the model

One aspect and limitation of the photogrammetric model is the need to know *a priori* data close to cylinder's pose. However, this requirement is not always assured with enough accuracy, therefore, it is important to establish the robustness of the model regarding this aspect. Aiming at this, the model has been tested with *a priori* pose data with known *XYZ* deviations for P1 and P2 points and the fitting result was assessed. The expected result is the nominal pose correcting these initial deviations. After testing, the model for oblique and vertical poses for all case studies, the following can be stated:

- For *XY* position deviations, the residuals of points that define the cylinder pose are less than 1 mm for large working distances.
- For *Z* deviations, the model converges but the result is not robust because a reference along the axis is missing.
- Robustness does not depend on the cylinder pose; deviations are similar in both cases.
- The model depends on *a priori* pose knowledge, but the real position can deviate even few meters from supposed known values.

In order to analyze the image data effect on the cylinder pose fitting result, several cases were assessed changing both the number of points and its distribution along the contour points of the cylinder. As an example of this evaluation, table 3 presents the results for the cases presented in section 2.3.2.3 for the camera pose number 2 and cylinder dimensions of CS1. These tables present point coordinates P1 and P2, and the differences between them can be established taking them as a reference for case study A.

For any of the cases presented, the differences among each approach are not higher than 10 mm, except for the case where the image points for each camera view are not correspondent (See case study *F*). For this exception, the deviations for both *XY* and *Z* directions are higher because of a worse conditioned image data point distribution.

4. Discussion and conclusions

Results highlight that the theoretical model is suitable for close-range photogrammetric pose estimation and sensible

to *a priori* known data and image data quality. Therefore, it could be used with design purposes in order to fulfill measuring system requirements and select a suitable and affordable approach. In this research a symmetric camera network has been employed considering that is a rather realistic approach for real implementation. Other effects such as receiver deformation, camera network instabilities or computational efficiencies are not taken into account in this research. However, real scenery image data quality and disturbances due to high energy concentration effects as well as imaging parameter uncertainties are considered in the simulation process. The real materialization of the simulated photogrammetric approach will consider intrinsic and extrinsic calibration methods, referencing methods and cylinder pose estimation testing against certified measuring procedures. Thus experimental tests will be carried out once the overall procedure is established and every tool is prepared. The obtained results will be correlated with the model's performance.

With these preliminary results, it can be concluded that the model is accurate, and that this simulation procedure enables the obtaining of cylinder pose values with relative low deviations so that the suitability of tracking application requirements can be assessed. The relative accuracy of the model falls between 1/1000 and 1/20 000 with uncertainties of ±5 mm for all case studies and poses. In the future, further synthetic data generation procedures and tools will be studied to speed up the simulation procedure and steps as they are time-consuming tasks.

The model is conditioned to initial *a priori* pose values that are not always known or provided, so it would be preferable to improve the independency of the model in this sense. Nevertheless, in some applications this fact does not constitute a limitation. For example, in a positioning control loop, the position previous to the one that is to be estimated is always known and it is very similar.

The robustness of the model is strong for the cylinder's axis orientation but weaker for spatial position determination. In order to improve this functionality and therefore, the response of the model, a model-based 3D circle estimation approach is required so as to combine it with the procedure presented in this paper. Higher model performance for five dof accurate pose estimation could be achieved with a combination of both approaches

According to the image data point number and distribution, it has been demonstrated that the model is robust when the image data is well distributed along the cylinder. Besides, in order to improve the computation time of the model, high data filtering is possible, thus assuring the same accuracy level.

Acknowledgments

This research is supported by the Basque business development agency and MOSAIC project funded by the European Union's Horizon 2020 research and innovation programme.

Author contributions

EG-A designed the 3D scene poses in SW© and created the synthetic images, JM processed the images and created the data files, GK developed the photogrammetric model and simulated its capabilities, AT and RM reviewed the overall concept, GK also wrote the paper and all co-authors checked it considering their contribution and expertise.

Conflicts of interest

The authors declare no conflict of interest.

ORCID iDs

Gorka Kortaberria https://orcid.org/0000-0001-9487-7425

References

Andresen K and Qifeng Yu 1994 Calculation of the geometric parameters of an ellipse in space by its edges in the images *ISPRS J. Photogramm. Remote Sens.* **49** 33–7

Afzal M, Arteaga I L and Kari L 2016 An analytical calculation of the Jacobian matrix for 3D friction contact model applied to turbine blade shroud contact *Comput. Struct.* **177** 204–17

Alsadik B S, Gerke M and Vosselman G 2012 Optimal camera network design for 3D modeling of cultural heritage *ISPRS Ann. Photogramm. Remote Sens. Spatial Inf. Sci.* **I-3** 7–12

Becke M and Schlegl T 2015 Least squares pose estimation of cylinder axes from multiple views using contour line features *IECON 2015—41st Annual Conf. of the IEEE Industrial Electronics Society* vol 3 pp 1855–61

Becke M 2015 On modeling and least squares fitting of cylinders from single and multiple views using contour line features, Eds H Liu, N Kubota, X Zhu, R Dillmann and D Zhou *Intelligent Robotics and Applications*: ICIRA 2015 vol 9246 (Cham: Springer) pp 812–23

Becker T A, Özkul M A and Stilla U B 2011 Simulation of close-range photogrammetric systems for industrial surface inspection *Int. Arch. Photogramm. Remote Sens. Spatial Inf. Sci.* **38** 179–83

Buffa F, Pinna A and Sanna G 2016 A simulation tool assisting the design of a close range photogrammetry system for the sardinia radio telescope *ISPRS Ann. Photogramm. Remote Sens. Spatial Inf. Sci.* **III-5** 113–20

Crc C F 2015 Advances in close-range photogrammetry Prof. Clive Fraser Evolution 1: Film to Digital Evolution 2: Manual to Automatic Image Meas. and Orientation Evolution 3: Manual Feature Extraction and Graphical Output to Automatic 3D Point Cloud Generation pp 7–11

Dall'Asta E, Thoeni K, Santise M, Forlani G, Giacomini A and Roncella R 2015 Network design and quality checks in automatic orientation of close-range photogrammetric blocks *Sensors* **15** 7985–8008

Doignon C 2007 An Introduction to model-based pose estimation and 3D tracking techniques *Reconstruction, Pose Estimation and Tracking* ed Rustam Stolkin (Vienna: I-Tech) pp 1–530

Doignon C and De Mathelin M 2007 A degenerate conic-based method for a direct fitting and 3D pose of cylinders with a single perspective view *Proc. IEEE Int. Conf. on Robotics and Automation* pp 4220–5

Dunn E 2007 Development of a practical photogrammetric network design using evolutionary computing *Photogramm. Rec.* **22** 22–38

El-hamrawy S, El-din Fawzy H and Al-Tobgy M 2016 Optimum design for close range photogrammetry network using particle swarm optimization technique *IOSR J. Mech. Civ. Eng.* **13** 17–23

Ferri M, Mangili F and Viano G 1993 Projective pose estimation of linear and quadratic primitives in monocular computer vision *CVGIP Image Underst.* **58** 66–84

Figueiredo R, Moreno P and Bernardino A 2017 Robust cylinder detection and pose estimation using 3D point cloud information *IEEE Int. Conf. on Autonomous Robot Systems and Competitions* pp 234–9

Fraser C, Jazayeri I and Cronk S 2010 A feature-based matching strategy for automated 3D model reconstruction in multi-image close-range photogrammetry *American Society for Photogrammetry and Remote Sensing Annual Conf. 2010: Opportunities for Emerging Geospatial Technologies* vol 1 pp 175–83 (www.scopus.com/inward/record.uri?eid=2-s2.0-84868587896&partnerID=40&md5=3dc2d82cad7d24d8dce587cd23e2798f)

Fraser C and Stamatopoulos C 2014 Automated target-free camera calibration *Proc. of the ASPRS 2014 Annual Conf.* vol II-5 (https://doi.org/10.5194/isprsannals-II-5-339-2014)

Fraser C S 2013 Automatic camera calibration in close range photogrammetry *Photogramm. Eng. Remote Sens.* **79** 381–8

Gao W, Leng J and Zhou X 2016 Iterative minimization algorithm for efficient calculations of transition states *J. Comput. Phys.* **309** 69–87

Guo X, Chen Y, Wang C, Cheng M, Wen C and Yu J 2016 Automatic shape-based target extraction for close-range photogrammetry *Int. Arch. Photogramm. Remote Sens. Spatial Inf. Sci.* **XLI-B1** 583–7

Gruen A and Li H 1991 Extraction of 3D linear features from multiple images by LSB-snakes *Proc. SPIE* **3072** 119–30

Hafez A Z, Soliman A, El-metwally K A and Ismail I M 2017 Design analysis factors and specifications of solar dish technologies for different systems and applications *Renew. Sustain. Energy Rev.* **67** 1019–36

Hanekr R, Navabi N and Appelt M 1999 Yet another method *Proc. 1999 IEEE Computer Society Conf. on Computer Vision and Pattern Recognition* vol 2 pp 544–50

Hansen M A and Sutherland J C 2018 On the consistency of state vectors and Jacobian matrices *Combust. Flame* **193** 257–71

Harun M H and Sulaiman M 2011 Shape-based matching : application of edge detection using Harris point shape-based matching: application of edge detection using Harris point *Int. Conf. Robot. Autom. Syst.* (https://doi.org/10.13140/RG.2.1.2151.2808)

Heipke C, Madden M, Li Z and Dowman I 2016 Theme issue 'state-of-the-art in photogrammetry, remote sensing and spatial information science' *ISPRS J. Photogramm. Remote Sens.* **115** 1–2

Hilton A 2005 Scene modelling from sparse 3D data *Image Vis. Comput.* **23** 900–20

Houqin B and Jianbo S 2008 Feature matching based on geometric constraints in weakly calibrated stereo views of curved scenes *J. Syst. Eng. Electron.* **19** 562–70

Huang J B, Chen Z and Chia T L 1996 Pose determination of a cylinder using reprojection transformation *Pattern Recognit. Lett.* **17** 1089–99

Joon Ahn S and Rauh W 2001 Circular coded target for automation of optical 3D—Measurement and camera calibration *Int. J. Pattern Recognit. Artif. Intell.* **15** 905–19

King P, Comley P and Sansom C 2013 Parabolic trough surface form mapping using photogrammetry and its validation with a large coordinate measuring machine *Energy Procedia* **49** 118–25

Knyaz V A 1998 Non contact 3D model reconstruction using coded targets *Int. Conf. Graphicon*

Kosmopoulos D I 2011 Robust Jacobian matrix estimation for image-based visual servoing *Robot. Comput.-Integr. Manuf.* **27** 82–7

Lee C D, Huang H C and Yeh H Y 2013 The development of sun-tracking system using image processing *Sensors* **13** 5448–59

Liu C and Hu W 2014 Relative pose estimation for cylinder-shaped spacecrafts using single image *IEEE Trans. Aerosp. Electron. Syst.* **50** 3036–56

Liu Y J, Zhang J B, Hou J C, Ren J C and Tang W Q 2013 Cylinder detection in large-scale point cloud of pipeline plant *IEEE Trans. Vis. Comput. Graphics* **19** 1700–7

Luhmann T 2016 Learning photogrammetry with interactive software Tool PhoX *Int. Arch. Photogramm. Remote Sens. Spatial Inf. Sci.* **41** 39–44

Luhmann T, Fraser C and Maas H G 2016 Sensor modelling and camera calibration for close-range photogrammetry *ISPRS J. Photogramm. Remote Sens.* **115** 37–46

Luhmann T, Robson S, Kyle S and Boehm J 2013 *Close-Range Photogrammetry and 3D Imaging. Close-Range Photogrammetry and 3D Imaging* 2nd edn (Berlin: De Gruyter) (https://doi.org/10.1515/9783110302783)

Luhmann T, Robson S, Kyle S and Harley I 2006 *Close Range Photogrammetry: Principles, Methods and Applications. LibTuDelftC* 1st edn (Dunbeath: Whittles Publishing)

Navab N and Appel M 2006 Canonical representation and multi-view geometry of cylinders *Int. J. Comput. Vis.* **70** 133–49

Nowak I 2017 Bayesian approach applied for thermoacoustic inverse problem *Energy* **141** 2519–27

Oberkampf D, DeMenthon D F and Davis L S 1996 Iterative pose estimation using coplanar feature points *Comput. Vis. Image Underst.* **63** 495–511

Olague G and Mohr R 2002 Optimal camera placement for accurate reconstruction *Pattern Recognit.* **35** 927–44

Osada R, Funkhouser T, Chazelle B and Dobkin D 2001 Matching 3D models with shape distribution *Shape Modeling and Applications, SMI 2001 Int. Conf.* pp 154–66

Paláncz B, Awange J L, Somogyi A, Rehány N, Lovas T, Molnár B and Fukuda Y 2016 A robust cylindrical fitting to point cloud data *Aust. J. Earth Sci.* **63** 665–73

Pappa R S, Giersch L R and Quagliaroli J M 2001 Photogrammetry of a 5 m inflatable space antenna with consumer-grade digital cameras *Exp. Tech.* **25** 21–9

Penman D W and Alwesh N S 2006 3D pose estimation of symmetrical objects of unknown shape *Image Vis. Comput.* **24** 447–54

Piatti E J and Lerma J L 2013 Virtual worlds for photogrammetric image-based simulation and learning *Photogramm. Rec.* **28** 27–42

Pottler K, Lüpfert E, Johnston G H G and Shortis M R 2005 Photogrammetry: a powerful tool for geometric analysis of solar concentrators and their components *J. Sol. Energy Eng.* **127** 94

Puech W, Chassery J-M and Pitas I 1997 Cylindrical surface localization in monocular vision vol 18 pp 711–22

Rabbani T and Van Den Heuvel F 2005 Efficient hough transform for automatic detection of cylinders in point clouds *ISPRS Workshop on Laser Scanning* vol 3 pp 60–5

Ramm A G 2018 Inverse problem of potential theory *Appl. Math. Lett.* **77** 1–5

Renaud P, Andreff N, Philippe M and Gogu G 2005 Kinematic calibration of parallel mechanisms: a novel approach using legs observation *IEEE Trans. Robot.* **21** 529–38

Rosenhahn B, Brox T, Cremers D and Seidel H P 2006 A comparison of shape matching methods for contour based pose estimation *Lecture Notes in Computer Science (Including Subseries Lecture Notes in Artificial Intelligence and Lecture Notes in Bioinformatics* vol 4040) (LNCS) Eds R Reulke *et al* (Berlin: Springer) pp 263–76

Ruelas A, Velázquez N, Villa-Angulo C, Acuña A, Rosales P and Suastegui J 2017 A solar position sensor based on image vision *Sensors* **17** 1–13

Shiu Y C and Huang C 1991a Pose determination of circular cylinders using elliptical aiid side projections pp 265–8

Shiu Y C and Huang C 1991b Locating cylindrical objects from perspective projections *Proc. of the IEEE 1991 National Aerospace and Electronics Conf. NAECON 1991* (https://doi.org/10.1109/NAECON.1991.165892)

Shortis M R and Johnston G H G 1996 Photogrammetry: an available surface characterization tool for solar concentrators, {P}art {I}: measurement of surface *J. Sol. Energy Eng.* **118** 146–50

Shortis M R, Johnston G H G, Pottler K, Lüpfert E and Commission V 2008 Photogrammetric analysis of solar collectors *Int. Arch. Photogramm. Remote Sens. Spatial Inf. Sci.* **37** 81–8

Shortis M R, Seager J W, Robson S and Harvey E S 2004 Automatic recognition of coded targets based on a hough transform and segment matching *Electronic Imaging. Videometrics VII* p 5013

Stynes J K and Ihas B 2012 Slope error measurement tool for solar parabolic trough collectors preprint Pix 16560 (https://doi.org/10.1115/1.3035811)

Su Y-T and Bethel J 2010 Detection and robust estimation of cylinder features in point clouds *ASPRS* vol 2, pp 887–93

Summan R, Pierce S G, Macleod C N, Dobie G, Gears T, Lester W, Pritchett P and Smyth P 2015 Spatial calibration of large volume photogrammetry based metrology systems *Measurement* **68** 189–200

Teck L W, Sulaiman M, Shah H N M and Omar R 2010 Implementation of shape—based matching vision system in flexible manufacturing system *J. Eng. Sci. Technol. Rev.* **3** 128–35

Teney D and Piater J 2014 Multiview feature distributions for object detection and continuous pose estimation *Comput. Vis. Image Understand.* **125** 265–82

Triggs B 1999 Camera pose and calibration from 4 or 5 known 3D points *Proc. of the 7th IEEE Int. Conf. on Computer Vision* vol 1 pp 278–84

Tushev S and Sukhovilov B 2017 Photogrammetric system accuracy estimation by simulation modelling *2017 Int. Conf. on Industrial Engineering, Applications and Manufacturing (ICIEAM)* pp 1–6

Veldhuis H and Vosselman G 1998 The 3D reconstruction of straight and curved pipes using digital line photogrammetry *ISPRS J. Photogramm. Remote Sens.* **53** 6–16

Wijenayake U, Choi S I and Park S Y 2014 Automatic detection and decoding of photogrammetric coded targets *13th Int. Conf. on Electronics, Information, and Communication, ICEIC 2014—Proc.* pp 1–2

Xu S and Liu M 2013 Feature selection and pose estimation from known planar objects using monocular vision *2013 IEEE Int. Conf. on Robotics and Biomimetics (ROBIO)* pp 922–7

Yang C, Feinen C, Tiebe O, Shirahama K and Grzegorzek M 2016 Shape-based object matching using interesting points and high-order graphs *Pattern Recognit. Lett.* **83** 251–60

Zhang T, Liu J, Liu S, Tang C and Jin P 2017 A 3D reconstruction method for pipeline inspection based on multi-vision *Measurement* **98** 35–48

Zhi L and Tang J 2002 A complete linear 4-point algorithm for camera pose determination *AMSS Acad. Sin.* **21** 239–49

Zhu Z, Stamatopoulos C and Fraser C S 2015 Accurate and occlusion-robust multi-view stereo *ISPRS J. Photogramm. Remote Sens.* **109** 47–61

ARTICLE Nº3 (CASE STUDY3)

- Kortaberria, Gorka & Mutilba, Unai & Goez-Acedo, Eneko & Tellaeche, Alberto & Minguez, Rikardo. (2018). Accuracy Evaluation of Dense Matching Techniques for Casting Part Dimensional Verification. Sensors. 18. 3074. 10.3390/s18093074. →https://www.mdpi.com/1424-8220/18/9/3074

sensors

MDPI

Article

Accuracy Evaluation of Dense Matching Techniques for Casting Part Dimensional Verification

Gorka Kortaberria [1,*], Unai Mutilba [1], Eneko Gomez-Acedo [1], Alberto Tellaeche [2] and Rikardo Minguez [3]

[1] Department of Mechanical Engineering, IK4-Tekniker, 20600 Eibar, Spain; unai.mutilba@tekniker.es (U.M.); eneko.gomez-acedo@tekniker.es (E.G.-A.)
[2] Department of Smart and Autonomous Systems, IK4-Tekniker, 20600 Eibar, Spain; alberto.tellaeche@tekniker.es
[3] Department of Graphic Design and Engineering Projects, University of the Basque Country, 48013 Bilbao, Spain; rikardo.minguez@ehu.eus
* Correspondence: gorka.kortaberria@tekniker.es; Tel.: +34-636-987-081

Received: 3 August 2018; Accepted: 12 September 2018; Published: 13 September 2018

Abstract: Product optimization for casting and post-casting manufacturing processes is becoming compulsory to compete in the current global manufacturing scenario. Casting design, simulation and verification tools are becoming crucial for eliminating oversized dimensions without affecting the casting component functionality. Thus, material and production costs decrease to maintain the foundry process profitable on the large-scale component supplier market. New measurement methods, such as dense matching techniques, rely on surface texture of casting parts to enable the 3D dense reconstruction of surface points without the need of an active light source as usually applied with 3D scanning optical sensors. This paper presents the accuracy evaluation of dense matching based approaches for casting part verification. It compares the accuracy obtained by dense matching technique with already certified and validated optical measuring methods. This uncertainty evaluation exercise considers both artificial targets and key natural points to quantify the possibilities and scope of each approximation. Obtained results, for both lab and workshop conditions, show that this image data processing procedure is fit for purpose to fulfill the required measurement tolerances for casting part manufacturing processes.

Keywords: point cloud; uncertainty; dense matching; photogrammetry; inspection; multi-view stereo; structure from motion

1. Introduction

The present study was focused on the quality assurance requirements and measurement procedures of the foundry-based manufacturing processes and can also be applied to other similar manufacturing processes such as the forge, where manufacturing tolerances may be similar. Nowadays, large scale raw component suppliers are requesting the optimization of their productive processes to compete with lower cost manufacturers worldwide. This optimization demands more efficient and profitable manufacturing methods to control the stability of the processes through procedures that guarantee the quality of the products. Following this objective, a key stage in the manufacture value chain of wind components is the casting phase. Here, the pre-form of the parts that are subsequently machined is generated to obtain their definitive functionality at the operational level. Therefore, casting parts should ensure a minimum oversize that ensures that material exists in those areas of the piece to be machined. Simulation tools such as Computer Aided Design (CAD) software and Finite Element Analysis (FEA) software are employed targeting this aim. Nevertheless, realistic models of

the casting process are hardly established due to the complexity of the manufacturing process and the understanding of the involved parameters. Thus, part inspection becomes crucial to verify that the manufacturing process accuracy is under manufacturing tolerances and these results are also used to adjust simulation models as well as to compensate the pattern's design and size. In this scenario, casting quality characterization encompasses five main categories: casting finishing, dimensional accuracy, mechanical properties, chemical composition and casting soundness. All aspects are crucial to assure that the part meets customer's specifications and non-destructive testing methods (visual inspection, measuring machines, magnetic particle inspection, ultrasonic testing, etc.) are usually applied for their characterization.

An accurate dimensional inspection is commonly applied for First Article Inspection (FAI) or even for serial production control, where commonly part-to-CAD analysis and/or geometrical analysis according to ISO 8062-3 Standard is required for manufactured parts conformity assessment.

Either the casting manufacturing processes or the measurement procedures and technologies have evolved to speed up the result obtaining process to feed faster the production quality control stage. Thus, currently, a clear tendency aims to integrate in-situ measurements during the manufacturing process to substitute final closeout inspections. However, total time consumption for part inspection should be tackled to offer a rapid response. Here, two stages can be clearly distinguished: the acquisition and the processing of the measures.

Nowadays, technologies applied in the verification process do not allow a total automation of the inspection stage for several main reasons: the dimensions of the pieces, the multiple stations (positions) of the inspection systems as well as their lack of autonomy. Therefore, there is a latent opportunity in terms of improving existing procedures to reduce inspection times. In this scenario, the present paper highlights dense matching techniques to solve the aforementioned problem.

1.1. Background

The state of the art of 3D measuring technologies and methodologies for casting part verification have substantially been developed in the last few years, offering faster, more complete and more automatic approaches. The evolution of measurement methodologies is closely related to the employed measurement technologies and the output data that they provide. To understand the portfolio of common measuring technologies for medium to large scales components [1–3] an overview is presented in Figure 1, where an evolution from contact to non-contact approaches is presented and also a data processing procedures evolution is shown. The difference and the use of each measuring technology depends on the measurement case study and the dimensional analysis required in each case. Therefore, the selection of the most appropriate technology depends on the measurable requirements such as: measuring uncertainty, point resolution, type of processing, measuring scale, part accessibility, etc.

Traditionally, casting part dimensional verification has been executed by handheld manual instruments such as calipers, calibrated fixtures or measuring tapes. However, these devices do not allow verifying the main dimensions of large parts which leads to partial verification with low process quality confidence. To overcome this limitation, large Coordinate Measuring Machines (CMM) and Portable Coordinate Measuring Machines (PCMM) were developed many years ago pushed by large part manufacturers. CMMs are the most accurate approach but they require bringing the part to the machine which is time-consuming and sometimes an unaffordable option due to part dimensions. PCMMs aim to cover this physical limitation. Nowadays, many kinds of systems and brands exist [4,5]. A review of 3D measuring systems is also presented related to manufacturing verification needs in several scales and suitability of measuring devices and techniques is studied for 3D parts.

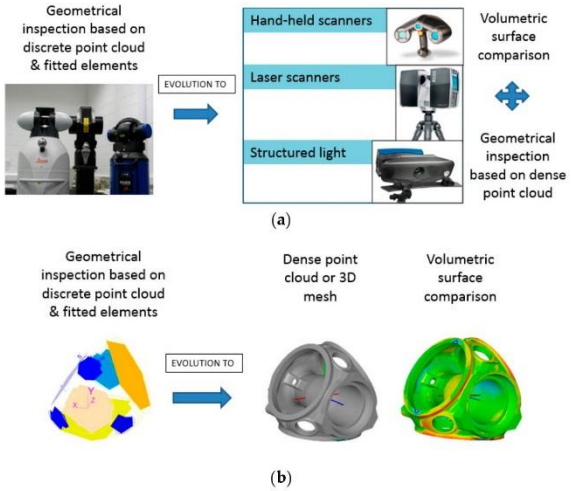

Figure 1. Evolution of measuring technology approaches for casting part dimensional verification: (**a**) data acquisition technologies; and (**b**) data processing schemes.

Laser tracker technology was the pioneer in volumetric eolic component verification (Figure 2). Its parametric modeling is mentioned in [6,7], whereas a general review of its performance and applicability is presented in [8]. It has been widely used for machined component inspection for almost 20 years, thus its application to casting part inspection is imposed by machining companies in the eolic component manufacturing chain. It offers the possibility to quantify and verify the overall dimensions of the part with high accuracy requirements as well as allows verifying the accuracy performance of other measuring or manufacturing means [9–12]. Recent laser-tracker developments include hand-held accessories to scan the part surface without contact by means of real-time tracking of a laser-triangulation sensor or probe and even highly automated scanning robotic approaches. Compared to initial laser tracker technology that only offers the possibility to measure a discrete point cloud touching the part surface with a calibrated retroreflector, automatic eolic component inspection procedures come closer to the goal of surface scanning.

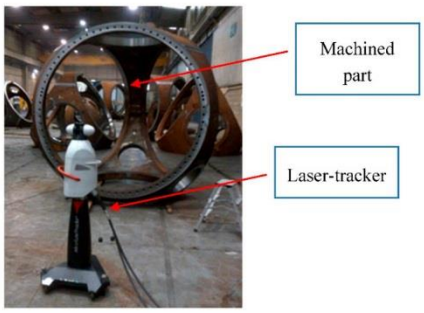

Figure 2. Laser-tracker technology for machined part dimensional inspection.

Conventional shape and dimensional analysis of casting components with tactile coordinate measuring systems has some limitations, such as: discrete point measurement strategy, lack of free-form

shape information and time consumption for volumetric component measurement. In the last few years, 3D optical scanners [5] are replacing laser trackers as the most used measuring equipment for the dimensional quality control assessment of machined and casting parts. Modeling and calibration issues are mentioned in [13–16], whereas some examples of application are studied in [17,18] and even accuracy performance is determined for lighting conditions in [19]. Although their accuracy is still a bit lower (±30 μm/m) than laser-tracker technologies (±15 + 6 μm/m) for high accuracy applications, casting part verification methodologies have been adapted to these technologies as they offer a volumetric view of the part compared to its nominal CAD definition. Optical scanners such as laser-triangulation sensors [20], structured light sensors (Figure 3), or even Time Of Flight (TOF) based laser- scanners [21,22] have the ability to measure dense point clouds that are used to analyze the oversized material distribution or carry out reverse engineering tasks. They capture more detailed and easily interpretable quality information of an object with significantly shorter measuring times and accuracies ranging from 0.05 mm to 2–3 mm for large parts (several meters) which assures post-machining steps. Many technology suppliers already offer this kind of equipment as an alternative to tactile approaches.

Figure 3. Scanning of casting part by means of structure light scanner and reference targets.

The main drawbacks of these optical systems are data acquisition time and part accessibility. As the part is usually bigger than the field of view (FOV) of the measuring system and the required point cloud resolution is quite demanding, the scanning system needs to be located in several positions around the part to scan every surface point. This means that each device location should be accurately aligned to previous locations with common references to reconstruct the 3D point cloud in a common coordinate system. However, these partial alignments add inaccuracy to overall point clouds as a residual error is carried out each time that can suppose a non-continuous point cloud, especially for round parts. Besides, this working procedure forces to see common reference targets among different consecutive scanner locations, which makes the measuring procedure a time consuming and restricted method. Currently, to tackle and enhance the accuracy of device location alignment stage, structured light based scanners are combined with photogrammetric approaches which guarantee higher accuracy referencing points. This method comprises two measuring systems and therefore steps. First, a photogrammetric approach is used to measure some dot targets all around the part and these artificial targets are used as a reference for the subsequent scanning step. The points are identified and used as tie points for each partial scanning, enabling to fuse all 3D data in a common reference system. Moreover, the accuracy is improved as the output of the previous photogrammetric step is more precise than locating the scanners in multiple locations and applying consecutive point cloud fusions which leads to overall 3D point cloud inaccuracies. Besides, using previously calibrated dot targets as a reference enables taking partial scans all around the part without having to assure a consecutive overlapping among each scan and consequently offering a more flexible measuring procedure. Another possibility to improve data acquisition time is to use robotic measuring cells. Nevertheless, this approach is nowadays oriented to other manufacturing sectors where required investment can ensure a fast-economic return.

X-ray computed tomography (CT) is a new technology that offers not only the output of 3D point cloud of the surface but also the inner 3D structure for material integrity checking. However, this technology is currently limited to 1 m range due to required installation costs and X-ray source power. Some references regarding to technique description, modeling, accuracy and applicability are mentioned in [22–25].

Dense matching techniques are the development of vision-based systems to measure dense 3D point cloud from imagery data. It comprises two main stages (see Figure 4) to reconstruct the dense point cloud: camera network calibration and dense image matching based on previously estimated photogrammetric results. In the literature, network orientation is also referred to as a structure from motion technique [26–29]. It targets going beyond traditional photogrammetric solutions improving image processing algorithms for textured surface reconstruction. Therefore, it requires texturized surfaces which means that non-homogeneous images are needed to feed and solve feature-based matching problem [30], stereo pair triangulation and multi-view bundle block adjustment [31–34].

On the one hand, the photogrammetric stage allows sorting out the bundle adjustment of the photogrammetric model the results of which are: 3D point coordinates (XYZ) by means of multi-view triangulation, self-camera calibration (intrinsic parameters) and orientation and position of the images (extrinsic calibration) according to the main coordinate system. These output values are afterwards the input data for dense matching approaches [35]. The photogrammetric stage can be carried out with coded targets [36] as well as based on natural tie points [37].

On the other hand, dense matching techniques [38–40] accomplish 3D dense point cloud reconstruction from oriented images and considering known camera intrinsic parameters. Tie points are combined in a bundle block adjustment, resulting in the 3D coordinates of all tie points and, more importantly, the position and orientation of each image. If these parameters are previously and accurately estimated, the expected results for dense matching approaches are supposed to be more precise. An accuracy study of this reconstruction method and algorithms is presented in [41,42]. Matching techniques [43,44] are usually applied in two steps (see Figure 4) to obtain at first sparse matching points (few key points) and then to use them as input for dense matching and triangulation (dense point cloud reconstruction). Matching algorithms are based on known relative orientations among images and image-pair searching schemes. For each image pixel on a reference image, a corresponding point is established in other images and views by means of pixel-based matching algorithm [38–40]. Once the dense correspondence is solved, stereo or multi-view triangulation [45] is enabled and determined, which offers 3D colorized dense point clouds from epipolar images and constraints [41–44]. Most e approaches are based on the minimization of cost functions that consider the degree of the similarity among pixels and includes constraints to consider possible errors in the matching process as well as geometric discontinuity changes.

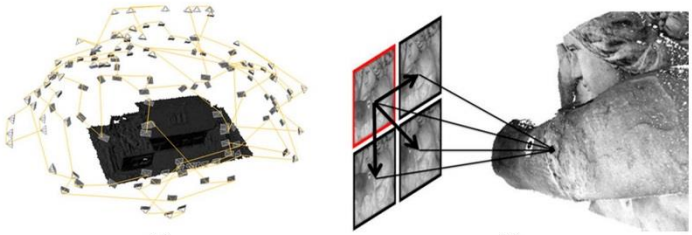

(a) (b)

Figure 4. Dense reconstruction workflow among multiple views: (**a**) photogrammetric step; and (**b**) dense matching approach.

An increasing number of software solutions for the automatic or semi-automatic generation of textured dense 3D point clouds images have recently appeared in the market [46–48].

iWitnessPRO-Agilis© photogrammetric software has evolved to dense reconstruction capabilities. It combines a photogrammetric library (Australis©) and the SURE© tool from the Institute For Photogrammetry at the University of Stuttgart to enable 3D point cloud reconstruction with different camera network calibration approaches (semi-automatic, automatic with coded target, and targetless orientation by means of feature-based matching) [49,50].

1.2. Motivation

Although dense matching photogrammetric based applications are extending more and more into industrial applications, the casting part verification with these novel photogrammetric methods has not been studied before. Most applications target cultural heritage, aerial topography or satellite surveying/mapping applications, but not industrial applications. Thus far, these approaches have not been studied from the point of view of accuracy and traceability, because there is not much information in the current literature [51,52]. It is within this context that this paper aims to provide an approach to assess the accuracy of dense matching techniques from a metrological point of view. Therefore, the approach adopted here is based on established and certified measuring approaches whose accuracy is already known and is used as a reference.

Considering that usually employed certified methods combine photogrammetry with further scanning processes aiming to increase point cloud accuracy and surface continuity, this study established the scope of dense matching techniques as an alternative verification approach employing a unique hand-held industrial camera. If the imagery data from photogrammetric approaches are also suitable to obtain dense point clouds, there is no need to scan the part after the photogrammetric stage has been carried out, which would considerably shorten the overall measuring time and reduce the cost of the measuring solution and technology.

The reduction of the measuring process duration would enable lower cost measuring services and faster feedback for casting part manufacturers to improve the process quality control for high value parts.

1.3. Objectives

The objectives of this research were to understand the accuracy assessment and measuring process requirements for dense matching photogrammetric techniques focused on the verification of medium to large casting parts. One remarkable aspect, in addition to sufficient accuracy to fulfill the manufacturing tolerances, is the time consumption required to carry out the dimensional verification of the parts. To consider this novel method as a suitable procedure, the overall process should reduce time consumption at least during the image data acquisition stage. This point led to carrying out a comparison of automated reconstruction approaches based on coded-targets or target-free schemas. Other factors such as adaptability of the process for different part dimensions and part complexity were also considered in this research.

Targeting the above-mentioned goals, a certified method for 3D verification was considered as a reference to quantify, determine and compare the achieved results between both measuring procedures and therefore to validate the studied approach.

Apart from these objectives, this study also focusede on the adaptability and improvement of dense matching techniques for the case presented, assessing the pros and cons of this method against current state of art approaches.

2. Materials and Methods

2.1. Measurement Method

Dense photogrammetry is an image processing technique based on 2D images to obtain 3D information based on the texturing of the surface to be measured. The multiple images that ensure high overlapping areas are processed with a photogrammetric analysis software to obtain a dense

point cloud. The software employed in this research is called iWitnessPRO-Agilis©. This software is a photogrammetric tool (iWitnessPro©) enhanced with dense matching capabilities (SURE© tool) to construct dense point cloud estimation based on image data.

To execute dense photogrammetry, it is necessary to have a part with well-conditioned surface texture such as casting or forged parts. Without this texture, the dense reconstruction of the surface by means of image processing is not possible. Homogeneously texturized parts, such as machined components, cannot be measured with this method.

This research aimed to allow as automatic as possible data processing, thus, in addition to the textured surface, coded targets were placed on the measurand to facilitate this aim. The approach considering only natural key points (feature-based matching-approach) is offered by the software but the processing requires users few controls such as data scaling. The location of coded targets are recommendable to solve with precision the following aspects: the calibration of the camera itself (intrinsic parameters), the external orientation (extrinsic parameter) of each image obtained and the spatial XYZ coordinates of each target whose center is to be determined. The technique also allows sorting the photogrammetric problem out without coded targets if the part offers characteristic geometric elements that can be discerned in several images as reference unequivocal points. However, it is expected that the accuracy is reduced if the use of targets is avoided, thus advantages and disadvantages of each approach should be considered. To automate the processing of the images, it is necessary for the software to independently calculate the external orientation, internal and scaling of the images, in addition to executing the dense reconstruction from these known data. To guarantee this result, the software performs two main stages. First, the photogrammetry is solved and then the dense matching technique is applied to obtain dense point clouds. This dense matching technique employs photogrammetric results to establish the correspondence among images based on image neighborhood data (average pixel values) and define the surface points by means of a combination of multi-stereo pairs and their triangulation for all the images. The overall workflow that comprises both processing stages is shown in Figure 5.

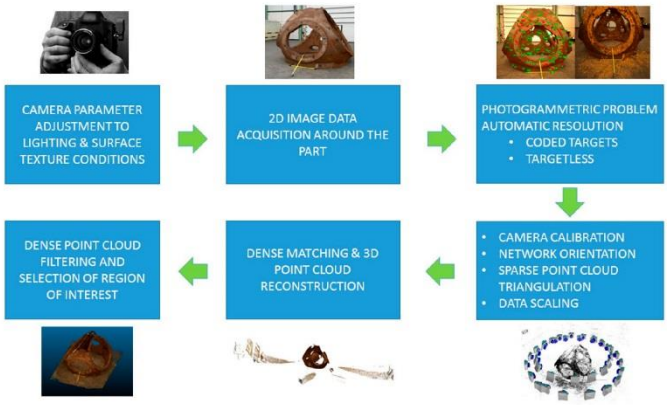

Figure 5. Dense matching process detailed workflow for shop-floor case study.

To guarantee accurate results, both photogrammetric and photography requirements have to be considered. If only photogrammetric camera set-ups are used, the surface points are not well focused, and the dense matching is not working. Therefore, a balance between both fields should be considered when image acquisition is carried out. A more detailed definition of the measuring process and the data processing follows these steps and scheme:

1. Preparation of the cast part with targets (if necessary) and a calibrated length bar
2. Adjustment of the camera and lens to measure the measuring scenario
3. Image acquisition process with fixed camera settings
4. Data processing
   (a) Photogrammetry with coded targets or targetless approaches
   (b) Dense matching
5. Dense point cloud filtering and refinement

In each step, multiple aspects should be analyzed before the measurement to assure that the overall measurement workflow will be successful. The most critical ones are listed below:

- Camera and lenses adjustment: It defines the resolution, the depth of field, exposition time, lenses aperture, the contrast of surface tie points, etc.
- Image network design: Minimum overlapping among images both for photogrammetry and dense matching reconstruction is necessary to detect coded targets, key points or unique surface points.
- Camera self-calibration: Intrinsic parameters (focal length, principal point, optical distortions, etc.) are determined for each measurement as camera internal parameters are not temporally stable.

Thus, the edge-cutting method presented in this research requires a good combination of these influencing factors to obtain suitable results. In the following paragraphs, a detailed description of employed adjustments are defined for the developed measuring method.

2.1.1. Preparation of the Scene

The criteria for the placement of the coded targets (based on dot distribution) are the following:

- Minimum five common targets between different images
- Robustness is improved if there are eight or more targets
- Size of the target should ensure an approximate image size of 10 pixels
- Image processing module of the software cannot detect another type of coding, which is the reason to use this type of targets. They can be white on black or red on black.

In addition to the targets, it is necessary to locate on the scene to be measured a calibrated length bar (see Figure 6) that establishes the scale of the acquired images. If there is more than one artifact, the scaling is performed with the average value adjusted for both measurements. It is interesting for the scaling to be automatic to use a bar with encoded targets so that the software in question (iWitnessPRO-Agilis©) knows the points to which the scaling corresponds. It is necessary to make this definition in the software at least once.

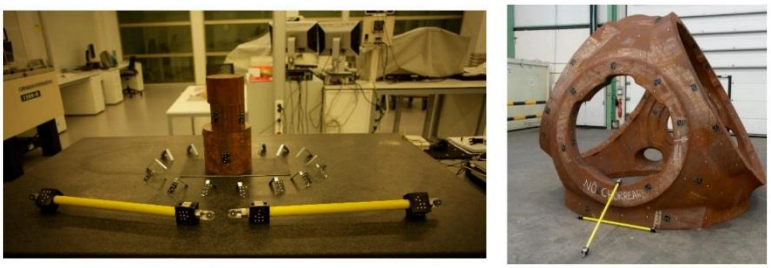

(a) (b)

Figure 6. Coded targets and calibrated scale bar located around the textured part: (**a**) lab testing; and (**b**) shop-floor testing.

2.1.2. Camera Adjustment

Once the scene is prepared, it is necessary to adjust the camera parameters to the lighting conditions of the room where the images are taken. Normally, in a photogrammetric process, the camera adjustment is set on the targets to be measured (maximum aperture and a zoom of 10×), but in a dense matching it is also necessary to consider a good contrast on surface points to be scanned. Therefore, when adjusting the camera, a compromise should be found between the coded targets and the surface texture to be measured. The main parameters to be adjusted are:

- Working distance
- The aperture
- Flash intensity (if required)
- Depth of field

These parameters should be kept constant for the entire measurement to solve the photogrammetric bundle adjustment.

The identification of the camera with the software is automatic and therefore the parameters related to the sensor (resolution and image dimension) are determined automatically. However, it is necessary to verify these parameters and change them if necessary. In this study, a Canon EOS-1Ds Mark III camera was used with 25 mm focal length lenses.

2.1.3. Acquisition of Images

When it comes to image acquisition process, it is necessary to consider what is intended to be measured both with photogrammetry and dense matching techniques. Therefore, in addition to photogrammetric aspects, a proper contrast and triangulation of surface points should be guaranteed. For this, it is necessary to reach a compromise between a good angle of triangulation and an excessive change of perspective between consecutive images. Thus, high angular views should be avoided and angles ranging from 60° to 110° are recommended. Depending on the relative angle between pairs of images, the accuracy of the photogrammetric or dense reconstruction stage will be reinforced.

In addition to triangulation, it is important to take care of the internal calibration aspect, for which it is necessary to acquire rotated images on the image plane. Normally, 4 × 90° rotated images are acquired, respectively, at the beginning of the measurement. The same criteria of acquiring rotated images during the measurement is strongly recommended to enhance camera self-calibration.

In this study, the images were taken around the part following the clockwise criteria and combining different height and view angles for each image acquisition position (see Figure 7).

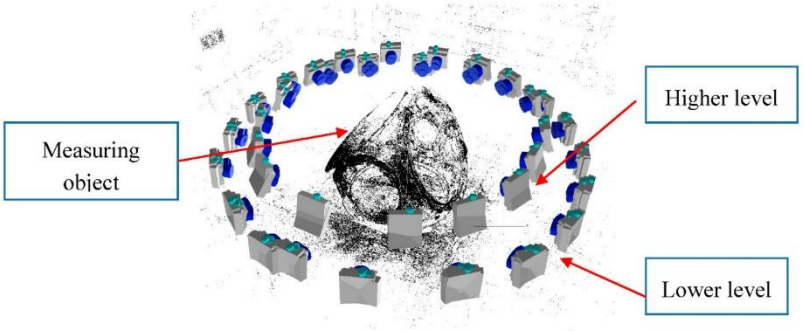

Figure 7. Camera shooting technique around the part.

2.1.4. Image Data Processing

Once the images are acquired, the processing of the photogrammetry and dense matching is carried out in two steps. The bundle adjustment is automatically solved if coded targets are employed for determination of image orientation and scaling, while the processing is more manual when natural key points are determined from imagery. The second step, named dense matching, is supposed to be automatic, but depending on the image data casuistic, few parameters should be fitted, such as: density of point cloud, image-pair combinations, pixel point neighborhood size, etc.

The extension of the generated file format for dense point cloud is "las" extension, therefore CloudCompare© software is used to visualize the point cloud and to convert it to more traditional "ascii" format files as well as to select the region of interest (ROI) of the dense point cloud. These files are afterwards used for the comparison of measured against reference data.

Photogrammetric Processing

• *Based on coded targets*

This is the most common method to solve the bundle adjustment in industrial photogrammetric systems as the automation level is high. Only preliminary image processing parameters need to be adjusted to assure solving intrinsic orientation, extrinsic orientation and coordinates of 3D point of interest at the same time without knowing a priori values of these parameters.

The coded targets enable the automatic referencing between image pairs and among every image rejecting outliers and obtaining more robust image correspondence as the point identification is unequivocal. Moreover, the 3D scene scaling is carried out, automatically identifying the coded targets that correspond to the calibrated length bar (see Figure 8). The main drawback of this approach is the preparation of the scene with the artificial targets and the assuring of a minimum number of common points among images.

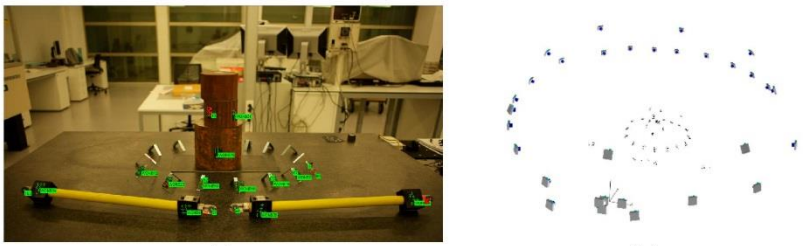

(**a**) (**b**)

Figure 8. Automated orientation in lab: (**a**) coded target image identification (in green); and (**b**) sparse triangulation of coded targets and camera network determination.

• *Based on Feature Based Matching (FBM)*

It is a different photogrammetric processing approach to estimate the extrinsic calibration of images. Instead of using artificial coded targets, natural key features are identified in the images and the correspondence among the multiple stereo pairs is estimated by means of image matching techniques. Approximately 50,000 feature points are used in each image. After establishing the tie points among the images, the relative orientation between image pairs is determined and the absolute orientation considering the first image as a reference. Finally, a bundle adjustment (minimum convergence of three image rays) approach is applied to refine and improve the extrinsic calibration of the camera network.

Once the camera network is defined, 3D scene scaling is established, which is necessary to obtain a metric 3D point cloud. This step is manually executed by choosing an image pair where the

calibrated length bar is seen. Based on manual target centroiding identification and epipolar image correspondence, the image points corresponding to the artifact were selected and applied to a known calibrated distance (see Figure 9).

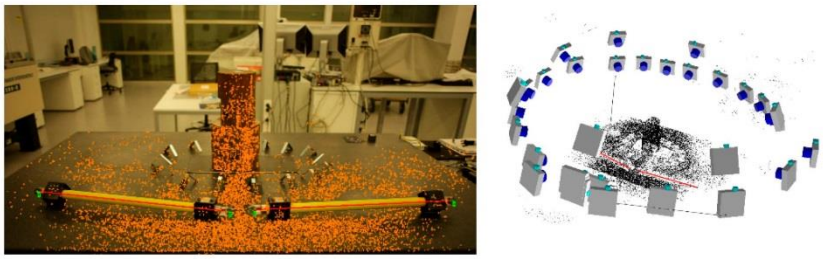

(**a**) (**b**)

Figure 9. Targetless orientation in lab: (**a**) tie point image identification (in orange) and length bar definition (in red); and (**b**) sparse triangulation of feature points and camera network determination.

Dense Matching Reconstruction

The dense matching reconstruction is performed by means of SURE© software, which is a tool for photogrammetric surface reconstruction from imagery. It is a software solution for multi-view stereo, which enables the derivation of dense point clouds from a given set of images and known orientations (see Figure 10). Nearly one 3D point can be obtained corresponding to each image pixel with the highest resolution.

(**a**) (**b**)

Figure 10. Dense matching schema for shop-floor case study: (**a**) structure from motion; and (**b**) dense 3D colorized point cloud without filtering.

The input to SURE is a set of images and the corresponding interior and exterior orientations (structure from motion approach), whereas the output information of the software is dense point clouds or depth images. It is a multi-stereo solution, so single stereo models (using two images) are processed and subsequently fused. It automatically analyzes the block configuration to find suitable stereo models to match in several steps (coarse methods for stereo pair selection and accurate methods for dense stereo 3D reconstruction). During the 3D reconstruction step, the disparity information from multiple images is fused and 3D points or depth images are computed. By exploiting the redundancy of multiple stereo pairs and combinations, blunder and outliers are filtered or rejected. In this research, the full resolution of the camera (21 Megapixels) was used and a point was triangulated as minimum with a stereo pair.

2.2. Validation Procedure for Accuracy Assessment

The validation of the presented methodology was performed by means of a "two-step" measuring procedure combining an optical 3D scanner (ATOS IIe©, Braunschweig, Germany) based on structured light with an optical portable CMM (TRITOP©, Braunschweig, Germany) based on photogrammetry, which assures high accuracy reference data used for the comparisons presented in this research. The fusion of these technologies enables obtaining higher accuracy point cloud data (grown truth) for medium to large dimension parts and a more flexible scanning procedure.

First, a photogrammetric procedure was applied to measure the XYZ coordinates of all the targets placed in the measuring scenario (see Figure 11a). This was accomplished by TRITOP system employing the ring coded targets, a high-tech industrial camera (see Figure 11b), and advanced photogrammetric software to solve the bundle adjustment problem. Dot type coded targets were used as fiducial references for the subsequent scanning stage as the TRITOP system considers these targets as non-coded targets. Each partial scan was referenced by means of these fiducials to a common reference system defined by previously executed photogrammetric stage. The targets based on dot type codification were also used for the automated orientation case study in further analysis presented in this paper. Therefore, both types of coded targets (see Figure 11a) were placed in similar locations to guarantee that the photogrammetric problem can be solved and the reachable accuracy is practically the same

(**a**) (**b**) (**c**)

Figure 11. Measuring method for reference data determination in lab: (**a**) scene preparation with coded targets (ring and dot type) and scale bar; (**b**) photogrammetric camera (TRITOP©); and (**c**) structured light 3D scanner (ATOS IIe©).

Once that photogrammetry was solved, a dense 3D scanning measurement of the part was executed with the available structured light 3D scanner (see Figure 11c) using the dot type fiducials coded as references for the partial alignment of each scan. Known fringe patterns were projected onto the surface of the object and recorded by two cameras, based on the stereo camera principle. As the beam paths of both cameras and the projector were calibrated in advance (extrinsic calibration), 3D surface points from three different ray intersections could be calculated. The number of scans depended on the part surface complexity and required detail. Every partial scan was transformed to a common coordinate system employing as a reference the points that were measured before with the photogrammetric method. Once the part was totally scanned, the point cloud was transformed to a continuous mesh by means of Delaunay triangulation approaches [53–56].

3. Results

The following content presents the results of the comparison of the studied dense matching approaches against photogrammetrically referenced structured light 3D scanner for both lab and shop-floor lighting conditions. Moreover, for each different case study, the photogrammetric

orientation problem was solved considering artificial coded targets or natural key features employing the same acquired image dataset.

One of the main differences between using the artificial coded targets or natural key features is the processing time and the automation level for photogrammetric model solving. Whereas the artificial coded target approach is totally automatic for camera network orientation estimation and scaling, the feature based targetless orientation approach requires a specific feature identification image parameter adjustment as well as manual 3D point cloud scaling. The processing time takes twice as long as using coded targets and increases exponentially with the number of images, feature point number and camera resolution. Coded target employment is a method to optimize this step, from the point of view of robustness and computing cost. The highest processing time is for dense matching reconstruction which takes several hours to obtain a full resolution 3D point cloud. The obtained accuracy is shown and discussed below for each case study.

To compare and assess the accuracy of the novel methodology, free 3D inspection software was used (GOM Inspect©, Braunschweig, Germany). The employed method for any comparison was the following one:

1. Import both meshes: the reference data measured by GOM© systems and the one achieved by dense photogrammetry.
2. Perform raw alignment between meshes with six nearly common points on the surface.
3. Perform best-fit alignment for accurate registration considering the reference data as nominal mesh.
4. Compare the 3D color map between aligned meshes and analyze deviations among measured points.
5. Perform statistical evaluation of achieved deviations with histograms (2σ).

In the case of camera network estimation by means of FBM, as this method offers rather high number of 3D points within the photogrammetric stage, the surface comparison is presented both for sparse point cloud and dense point cloud case studies. Although other alignment methods (geometric, datum-based, and 3-2-1) are available, best-fit approach has been chosen as it estimates the minimum average oversize that ensures that material exists in those areas of the piece to be machined. Moreover, it has been considered as a more statistical alignment method for the comparison as it gives the same weight to all surface points instead of fitting some geometric elements and taking them as a reference to define the coordinate system.

3.1. Lab Tests for Medium Size Parts

3.1.1. Orientation Based on Artificial Targets

The first test was performed in lab conditions with stable lighting and environmental conditions. The part used for the experiment was an assembly of three rusted cylinders of Ø 50 mm × 500 mm in height with stochastic surface texture, as shown in Figure 12. After reference data acquisition (32 images), the overall dense photogrammetry was applied following the measuring procedure described in Section 2. The acquired images were initially used to solve the photogrammetry by means of coded-targets and then the dense point cloud reconstruction was established with high resolution.

The relative accuracy of the photogrammetry was 1/80,000 mm (RMS) and the camera self-calibration was accurately established. Regarding the surface data comparison, the deviations fell into ± 0.2 mm (2σ), as shown in Figure 12a and its histogram. The obtained dense point cloud contained 10.5 million points (see Figure 12b), and coded targets were placed on lacking areas for determination of orientation. The higher deviation was found in edge points as the triangulation and the definition of the averaged points for dense matching is more challenging in these areas.

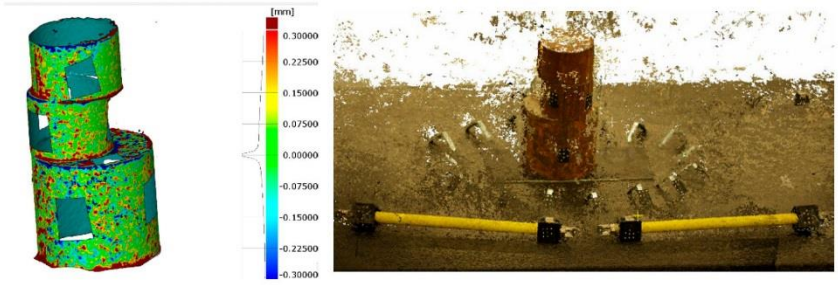

(**a**) (**b**)

Figure 12. 3D representation of measured part in lab environment with coded target orientation approach: (**a**) surface point comparison against reference mesh; and (**b**) dense point cloud with color and texture information (full resolution).

3.1.2. Targetless Orientation Based on Feature Based Matching

The second test for lab conditions was performed on feature-based matching for camera network orientation establishment. The same pictures as in Section 3.1.1 were used but coded-targets were not employed to define the absolute orientation of the images. Once the photogrammetric part was solved, the data were scaled (sparse point cloud) and afterwards dense matching was done to obtain dense point cloud.

The relative accuracy of the photogrammetry was 1/27,000 mm (RMS). Camera calibration was considered the same as obtained in the previous analysis due to higher accuracy assurance and convergence difficulties with self-calibration attempts. Regarding the surface data comparison, the deviations fell into ±0.4 mm (2σ), as shown in Figure 13a (sparse point cloud), and ±0.8 mm (2σ), as shown in Figure 13b (dense point cloud). The obtained dense point cloud contained 0.2 million points (see Figure 13b) with empty gaps were coded targets were placed. Again, the higher deviations were found in edge points and a difference of 200% was obtained comparing dense point cloud and sparse one.

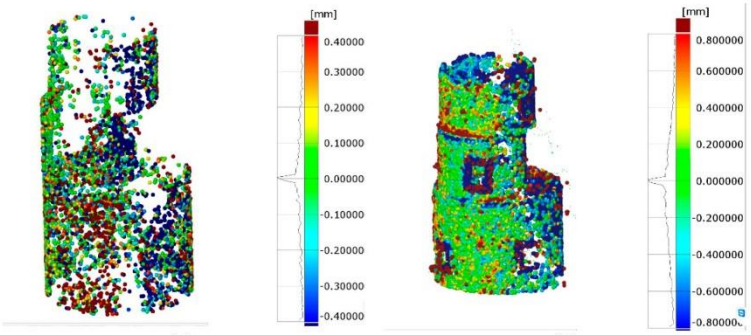

(**a**) (**b**)

Figure 13. 3D representation of measured part in lab environment with targetless orientation approach: (**a**) surface point comparison against reference mesh with sparse point cloud; and (**b**) surface point comparison against reference mesh with dense point cloud (quarter resolution).

3.2. Workshop Tests for Large Parts

3.2.1. Orientation Based on Artificial Targets

The preliminary test executed in workshop conditions did not assure stable lighting or proper accessibility to every part surface. The part used for the experiment was a casting eolic hub of 2500 mm × 2500 mm × 1500 mm with stochastic surface texture, as shown in Figure 14. After reference data acquisition (150 images), the dense photogrammetric was applied following the measuring procedure described in Section 5. The acquired images were initially used to solve the photogrammetry with coded-targets as in lab tests and then the dense point cloud reconstruction was determined.

The relative accuracy of the photogrammetry was 1/157,000 mm (RMS) and the camera self-calibration was accurately established. Regarding the surface data comparison, the deviations fell into ±3 mm (2σ), as shown in Figure 14a and its histogram. The obtained point cloud contained 2 million point with 0.2 mm resolution (see Figure 14b). The highest deviations were found in edge points, as occurred for lab results. The overall surface of the part was not scanned but most of the surfaces were measured, as shown in Figure 14b. To complete the scanning of every surface of the part, another part location is necessary, enabling the non-accessible surfaces to be measured. This requirement is usual for traditional measuring procedures but in this test a unique part location was applied and considered as enough for comparison.

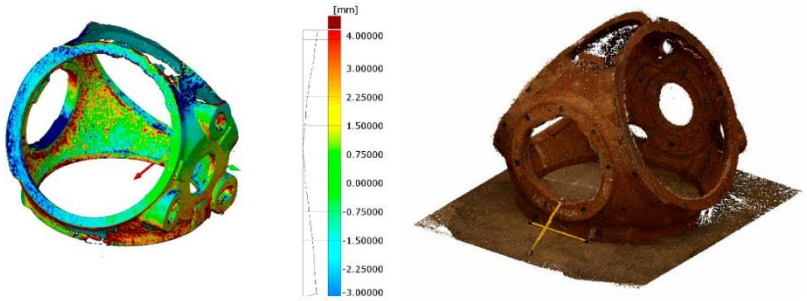

Figure 14. 3D representation of measured part in shop-floor environment: (**a**) surface point comparison against reference mesh; and (**b**) dense point cloud with color and texture information (full resolution).

3.2.2. Targetless Orientation Based on Feature Based Matching

The second test for workshop conditions was performed on feature-based matching for camera network orientation establishment. The same pictures as in Section 3.2.1 were used but coded-targets were not employed to define the absolute orientation of the images. Once the photogrammetric part was solved, the data were scaled (sparse point cloud) and afterwards dense matching was carried out to obtain dense point cloud.

The relative accuracy of the photogrammetry was 1/38,500 mm (RMS). Camera calibration was considered the one obtained in the previous analysis due to higher accuracy assurance and convergence difficulties with self-calibration attempts. Regarding the surface data comparison, the deviations fell into ±3 mm (2σ), as shown in Figure 15a (sparse point cloud), and ±6 mm (2σ), as shown in Figure 15b (dense point cloud). The obtained dense point cloud contained 0.5 million points (see Figure 15b) with lacking areas at the upper part of the measurand. Again, the higher deviations were found in edge points and a difference of 200% was obtained comparing dense point cloud and sparse one.

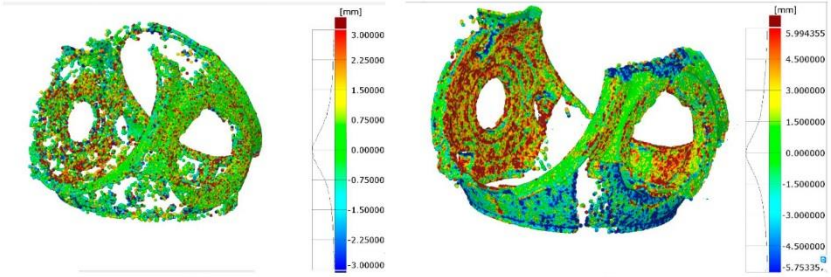

Figure 15. 3D representation of measured part in shop-floor environment with targetless orientation approach: (**a**) surface point comparison against reference mesh with sparse point cloud; and (**b**) surface point comparison against reference mesh with dense point cloud (quarter resolution).

4. Discussion

The trend in casting part dimensional inspection is to use smarter systems and procedures to speed up the measuring process assuring the acceptance criteria of the manufactured parts. Traditionally, measuring devices such as laser trackers or 3D optical scanners are used for FAI inspection or serial quality control. Time of flight based 3D laser scanners are also a recent alternative for 3D information acquisition of casting parts with uncertainties of about ±0.5 mm/m. Nevertheless, these devices do not allow automatic measurements because the measuring system has to be located and adjusted manually in different positions around the part. Partial measurements are placed in a unique coordinate system with the location of common artificial targets around the part.

Apart from this, other objectives such as improvement of the 3D point cloud processing step, automation of the measuring process, reduction of acquisition cost of the measuring devices, and robustness of the measuring process are also desired. This research was focused on studying the capabilities and scope of dense matching techniques and their suitability to be applied to casting part verification, where the manufacturing tolerances are not as tight as with machined parts. A comparison of dense matching approaches with traditional verification approaches is shown in Table 1 as a summary and overall overview of measuring alternatives' pros and cons. The relative accuracy is compared taking into account only lab conditions and current standards as specifications of currently employed systems are defined in this environment.

Table 1. Summary and comparison of measuring techniques for casting part verification.

Measuring Device (PCMM)	Relative Accuracy (μm/m)	Surface Comparison	Accessibility	Scalability	Environmental Conditions	Ease of Use	Degree of Automation
Laser-tracker (ASME B89.4.19-2006)	±15 + 6 (MPE)	Low	Low	Low	Air flow stability required	High	Low
3D scanner (VDI 2634 BLATT 3)	±30	High	Low	Low	Laser stability	High	Low
Dense photogrammetry (Orientation with coded-targets)	1/80,000 (RMS)	High	High	High	Lighting stability required	Low	High
Dense photogrammetry (Targetless orientation)	1/27,000 (RMS)	High	High	High	Lighting stability required	Low	Medium to low

The main advantages of studied methods as follows: fast acquisition time, high accessibility to multiple surfaces, high resolution (one point per pixel), high level of automation, and scalability to parts dimensions. The disadvantages are as follows: lower precision than other measuring techniques,

the results contain points with noise, data are missing in the obtained point cloud depending on employed resolution and the extent is unknown until overall processing is carried out, high processing time, and expert user is required to ensure an accurate result in non-stable lighting environments.

Another important aspect related to this novel method is the low cost of the whole system comprising both the hardware and the software as well as the flexibility of the system for different scenarios and measuring scales. Moreover, the automation is feasible with a fixed multi-camera network set-up or CNC positioning systems enabling the possibility to develop inspection cells for manufacturing quality control. Currently, one important limitation to completely automatize the solution, is the offline processing step and high computation time for PCs. However, this drawback is day by day improving as the technology is constantly developing and smarter algorithms are being developed. Thus, in few years this limitation will be overcome and even real-time dense matching will be possible. Other aspects to be improved in further developments are the robustness of the technique from the point of view of rejection of outliers and data filtering to extract accurate results as well as development of standards and guidelines based on this technology.

Currently, advanced users are required to apply the measuring process described in this paper, but controlling lighting conditions can reduce this requirement and make more useful this procedure to all photogrammetric users. This way, this procedure could be offered as an alternative service for medium and large casting parts instead of applying other 3D approaches.

In relation to accuracy, dense matching techniques seem to be a suitable measuring procedure for casting part verification as they enable obtaining dense point cloud with accurate enough accuracy (lower than manufacturing tolerance) for part shape and dimension verification. The estimated relative accuracy (RMS) of the measured 3D point coordinates is determined as the ratio of the estimated point standard error over the effective maximum diameter of the object point array along with the corresponding proportional accuracy. Coded-target based approach is the most accurate approach. The grade of tolerances for casting is mentioned in ISO 8062-3:2007 Standard. This part of ISO 8062 defines a system of tolerance grades and machining allowance grades for cast metals and their alloys. It applies to both general dimensional and general geometrical tolerances, although this study was focused mainly on general dimensional verification. As a reference, for a common tolerance grade 12, tolerances of ±10 mm and ±17 mm are required for the dimensions of the parts analyzed in this study. Thus, obtained accuracies are fit to purpose considering these manufacturing tolerances.

A more detailed comparison of analyzed dense matching case studies is presented in Table 2, where obtained accuracy as well as required time for different measuring steps is shown as a summary of the results obtained in this research.

Table 2. Summary and comparison of dense matching techniques for lab and shop-floor environments.

Test Type	Point Number (million)	Relative Accuracy (mm/m)	Measuring Time (min)	Processing Time (min)		Manufacturing Tolerance Grade 12 (mm)	Deviations (2σ)	
				a	b		Sparse (mm)	Dense (mm)
Lab test 1	10.5	1/80,000	5	5	120 to 180	±10	-	±0.2
Lab test 2	0.2	1/27,000		12			±0.4	±0.8
Shop-floor test 1	2	1/157,000	15	10	>300	±17	-	±3
Shop-floor test 1	0.5	1/38,500		20			±3	±6

a: Orientation stage; b: Dense reconstruction.

The relative accuracy (proportional RMS) for automated orientation based on coded-targets is 3–4 times higher compared with feature based matching approaches, for both lab and shop-floor case studies, whereas the deviations against traceable measuring methods are approximately twice lower. This difference is mainly due to the referencing step during the photogrammetric problem which is directly influenced by the accuracy of identification of key points for referencing. Whereas the automated orientation method employs the centroiding tool to estimate the center of the high-contrast elliptical targets with an accuracy of 0.03–0.1 pixels, targetless orientation approach uses less accurate (0.1–0.5 pixel) point identification methods, which leads to lower reconstructed point cloud accuracy

and point cloud density. The final accuracy of 3D dense point cloud is a direct function of the referencing accuracy, so the more precise the point marking and referencing approach, the better the triangulation and the higher the point quantity of the reconstructed point cloud.

Higher image number and perspectives could also improve the triangulation of each reconstructed point and therefore the relative accuracy for both cases, but it will complicate the data processing phase, thus a compromise between accurate photogrammetry and suitable dense matching needs to be found. The number of reconstructed points totally depends on this balance as a more demanding point triangulation limit gives a lower density point cloud and vice versa. In this research, a minimum intersection of three viewpoints was required to estimate a 3D point. As the camera network orientation for targetless case is less accurate than the one with coded targets, the same parameterization for the point triangulation step gives lower dense point cloud and some missing areas.

The measuring time depends on the preparation of the scene and camera set-up as well as in the size of the part to be measured. However, comparing to other measuring methods, it is fast as only images of the part need to be taken from different perspectives and heights. One of the drawbacks of dense matching techniques is the data processing step once the images have been taken. Whereas photogrammetric problem estimation is affordable from the point of view of time compared to industrial solutions, dense matching step takes much time and PC memory, which makes it more difficult to process the same imagery with different image processing parameterization.

5. Conclusions

Edge-cutting dimensional verification technologies ensure a reliable dimensional assessment of casting parts to check if they fulfill the required conformity assessment. Low enough measuring uncertainties guarantee a proper part inspection, machining process and therefore an overall manufacturing process efficiency.

3D PCMMs are being used more and more nowadays for inspection tasks with advanced probes for data acquisition improvement, but they still require to be moved around the part which takes a long time for data acquisition. Besides, depending on part shape and dimensions, these techniques are hardly applicable to quality control requirements. Dense matching techniques based on imagery data seem to be an affordable alternative to these measuring techniques as they enable faster data acquisition schemas with rich data information. The processing of these data permits reconstructing dense point cloud with high relative accuracy. Therefore, volumetric surface data are estimated which enables surface data comparison against nominal CAD data.

However, this study should be complemented with other accuracy evaluation methods and applications where dense matching techniques are used for verification of textured industrial parts. Currently, few studies are contained in the literature from the metrological point of view that tackle measuring procedure uncertainty or traceability of these measuring techniques. For example, another procedure to establish the measuring accuracy could be to manufacture a calibrated part and use it as a known reference or to characterize each influence error to estimate the measuring uncertainty applying the "error propagation law" as it is carried out for calibration and adjustment of other metrological complex devices. The efficiency of data processing also needs improvement by utilizing parallel processing and hierarchical optimization techniques to quicken result procurement.

Author Contributions: E.G.-A. was in charge of the project and conceived the main objectives; U.M. and G.K. designed and performed the experiments; G.K. analyzed and processed the data; A.T. and R.M. reviewed the overall concept; G.K. wrote the paper; and all co-authors checked it considering their contribution and expertise.

Funding: This research was partially funded by ESTRATEUS project (Reference IE14-396).given are accurate and use the standard spelling of funding agency names at https://search.crossref.org/funding, any errors may affect your future funding.

Acknowledgments: This research was supported by the Basque business development agency and is the output of ESTRATEUS project (Reference IE14-396) where novel manufacturing and measuring methods were studied as strategic lines for Basque industry development.

Conflicts of Interest: The authors declare no conflict of interest.

References

1. Cuypers, W.; van Gestel, N.; Voet, A.; Kruth, J.; Mingneau, J.; Bleys, P. Optical measurement techniques for mobile and large-scale dimensional metrology. *Opt. Lasers Eng.* **2009**, *47*, 292–300. [CrossRef]
2. Schmitt, R.H.; Peterek, M.; Morse, E.; Knapp, W.; Galetto, M.; Härtig, F.; Goch, G.; Hughes, B.; Forbes, A.; Estler, W.T. Advances in Large-Scale Metrology—Review and future trends. *CIRP Ann. Manuf. Technol.* **2016**, *65*, 643–665. [CrossRef]
3. Muelaner, J.E.; Maropoulos, P.G. Large volume metrology technologies for the light controlled factory. *Procedia CIRP* **2014**, *25*, 169–176. [CrossRef]
4. Goch, G.; Knapp, W.; Ha, F. Precision engineering for wind energy systems. *CIRP Ann. Manuf. Technol.* **2012**, *61*, 611–634. [CrossRef]
5. Savio, E.; de Chiffre, L.; Schmitt, R. Metrology of freeform shaped parts. *CIRP Ann. Manuf. Technol.* **2007**, *56*, 810–835. [CrossRef]
6. Conte, J.; Santolaria, J.; Majarena, A.C.; Acero, R. Modelling, kinematic parameter identification and sensitivity analysis of a Laser Tracker having the beam source in the rotating head. *Meas. J. Int. Meas. Confed.* **2016**, *89*, 261–272. [CrossRef]
7. Conte, J.; Santolaria, J.; Majarena, A.C.; Brau, A.; Aguilar, J.J. Identification and kinematic calculation of Laser Tracker errors. *Procedia Eng.* **2013**, *63*, 379–387. [CrossRef]
8. Muralikrishnan, B.; Phillips, S.; Sawyer, D. Laser trackers for large-scale dimensional metrology: A review. *Precis. Eng.* **2015**, *44*, 13–28. [CrossRef]
9. Aguado, S.; Santolaria, J.; Aguilar, J.; Samper, D.; Velazquez, J. Improving the Accuracy of a Machine Tool with Three Linear Axes using a Laser Tracker as Measurement System. *Procedia Eng.* **2015**, *132*, 756–763. [CrossRef]
10. Nubiola, A.; Bonev, I.A. Absolute calibration of an ABB IRB 1600 robot using a laser tracker. *Robot. Comput. Integr. Manuf.* **2013**, *29*, 236–245. [CrossRef]
11. Aguado, S.; Samper, D.; Santolaria, J.; Aguilar, J.J. Machine tool rotary axis compensation trough volumetric verification using laser tracker. *Procedia Eng.* **2013**, *63*, 582–590. [CrossRef]
12. Acero, R.; Brau, A.; Santolaria, J.; Pueo, M. Verification of an articulated arm coordinate measuring machine using a laser tracker as reference equipment and an indexed metrology platform. *Meas. J. Int. Meas. Confed.* **2015**, *69*, 52–63. [CrossRef]
13. Babu, M.; Franciosa, P.; Ceglarek, D. Adaptive Measurement and Modelling Methodology for In-Line 3D Surface Metrology Scanners. *Procedia CIRP* **2017**, *60*, 26–31. [CrossRef]
14. Mahmoud, D.; Khalil, A.; Younes, M. A single scan longitudinal calibration technique for fringe projection profilometry. *Optik* **2018**, *166*, 270–277. [CrossRef]
15. Cuesta, E.; Suarez-Mendez, J.M.; Martinez-Pellitero, S.; Barreiro, J.; Alvarez, B.J.; Zapico, P. Metrological evaluation of Structured Light 3D scanning system with an optical feature-based gauge. *Procedia Manuf.* **2017**, *13*, 526–533. [CrossRef]
16. Vagovský, J.; Buranský, I.; Görög, A. Evaluation of measuring capability of the optical 3D scanner. *Procedia Eng.* **2015**, *100*, 1198–1206. [CrossRef]
17. He, W.; Zhong, K.; Li, Z.; Meng, X.; Cheng, X.; Liu, X. Accurate calibration method for blade 3D shape metrology system integrated by fringe projection profilometry and conoscopic holography. *Opt. Lasers Eng.* **2018**, *110*, 253–261. [CrossRef]
18. Garmendia, I.; Leunda, J.; Pujana, J.; Lamikiz, A. In-process height control during laser metal deposition based on structured light 3D scanning. *Procedia CIRP* **2018**, *68*, 375–380. [CrossRef]
19. Li, F.; Stoddart, D.; Zwierzak, I. A Performance Test for a Fringe Projection Scanner in Various Ambient Light Conditions. *Procedia CIRP* **2017**, *62*, 400–404. [CrossRef]
20. Genta, G.; Minetola, P.; Barbato, G. Calibration procedure for a laser triangulation scanner with uncertainty evaluation. *Opt. Lasers Eng.* **2016**, *86*, 11–19. [CrossRef]
21. Isa, M.A.; Lazoglu, I. Design and analysis of a 3D laser scanner. *Meas. J. Int. Meas. Confed.* **2017**, *111*, 122–133. [CrossRef]

22. Herráez, J.; Martínez, J.C.; Coll, E.; Martín, M.T.; Rodríguez, J. 3D modeling by means of videogrammetry and laser scanners for reverse engineering. *Meas. J. Int. Meas. Confed.* **2016**, *87*, 216–227. [CrossRef]
23. Dosta, M.; Bröckel, U.; Gilson, L.; Kozhar, S.; Auernhammer, G.K.; Heinrich, S. Application of micro computed tomography for adjustment of model parameters for discrete element method. *Chem. Eng. Res. Des.* **2018**, *135*, 121–128. [CrossRef]
24. Sarment, D. Cone Beam Computed Tomography. *Dent. Clin. NA* **2015**, *62*, 3–6. [CrossRef]
25. Hermanek, P.; Carmignato, S. Porosity measurements by X-ray computed tomography: Accuracy evaluation using a calibrated object. *Precis. Eng.* **2017**, *49*, 377–387. [CrossRef]
26. Peterson, E.B.; Klein, M.; Stewart, R.L. *Whitepaper on Structure from Motion (SfM) Photogrammetry: Constructing Three Dimensional Models from Photography*; Technical Report ST-2015-3835-1; U.S. Bureau of Reclamation: Washington, DC, USA, 2015.
27. Toldo, R.; Gherardi, R.; Farenzena, M.; Fusiello, A. Hierarchical structure-and-motion recovery from uncalibrated images. *Comput. Vis. Image Underst.* **2015**, *140*, 127–143. [CrossRef]
28. Brito, J.H. Autocalibration for Structure from Motion. *Comput. Vis. Image Underst.* **2017**, *157*, 240–254. [CrossRef]
29. Westoby, M.J.; Brasington, J.; Glasser, N.F.; Hambrey, M.J.; Reynolds, J.M. "Structure-from-Motion" photogrammetry: A low-cost, effective tool for geoscience applications. *Geomorphology* **2012**, *179*, 300–314. [CrossRef]
30. Fraser, C.; Jazayeri, I.; Cronk, S. A feature-based matching strategy for automated 3D model reconstruction in multi-image close-range photogrammetry. In Proceedings of the American Society for Photogrammetry and Remote Sensing Annual Conference 2010: Opportunities for Emerging Geospatial Technologies, San Diego, CA, USA, 26–30 April 2010; Volume 1, pp. 175–183. Available online: https://www.scopus.com/inward/record.uri?eid=2-s2.0-84868587896&partnerID=40&md5=3dc2d82cad7d24d8dce587cd23e2798f (accessed on 5 January 2018).
31. Moons, T.; Vergauwen, M.; van Gool, L. 3D Reconstruction from Multiple Images. 2008. Available online: https://www.researchgate.net/publication/265190880_3D_reconstruction_from_multiple_images (accessed on 5 January 2018).
32. Elnima, E.E. A solution for exterior and relative orientation in photogrammetry, a genetic evolution approach. *J. King Saud Univ. Eng. Sci.* **2015**, *27*, 108–113. [CrossRef]
33. Jazayeri, I.; Fraser, C.; Cronk, S. Automated 3D object reconstruction via multi-image close-range photogrammetry. In *International Archives of Photogrammetry, Remote Sensing and Spatial Information Sciences, Proceedings of the ISPRS Commission V Mid-Term Symposium 'Close Range Image Measurement Techniques', Newcastle upon Tyne, UK, 21–24 June 2010*; Volume XXXVIII, pp. 3–8. Available online: http://www.isprs.org/proceedings/XXXVIII/part5/papers/107.pdf (accessed on 5 January 2018).
34. Zhu, Z.; Stamatopoulos, C.; Fraser, C.S. Accurate and occlusion-robust multi-view stereo. *ISPRS J. Photogramm. Remote Sens.* **2015**, *109*, 47–61. [CrossRef]
35. Hernandez, M.; Hassner, T.; Choi, J.; Medioni, G. Accurate 3D face reconstruction via prior constrained structure from motion. *Comput. Graph.* **2017**, *66*, 14–22. [CrossRef]
36. Giuseppe, G.; Clement, R. The Use of Self-Identifying Targeting for Feature Based Measurement. 2000. Available online: http://www.geodetic.com/f.ashx/papers/Release-The-Use-of-Self-identifying-Targeting-for-Feature-Based-Measurement.pdf (accessed on 22 January 2018).
37. Stamatopoulos, C.; Fraser, C.S. Automated Target-Free Network Orienation and Camera Calibration. *ISPRS Ann. Photogramm. Remote Sens. Spat. Inf. Sci. II* **2014**, *5*, 339–346. [CrossRef]
38. Remondino, F.; Spera, M.G.; Nocerino, E.; Menna, F.; Nex, F. State of the art in high density image matching. *Photogramm. Rec.* **2014**, *29*, 144–166. [CrossRef]
39. Haala, N. The Landscape of Dense Image Matching Algorithms, Photogramm. *Week* **2013**, *2013*, 271–284. Available online: http://www.ifp.uni-stuttgart.de/publications/phowo13/index.en.html (accessed on 22 January 2018).
40. Haala, N. Multiray Photogrammetry and Dense Image Matching, Photogramm. *Week* **2011**, *11*, 185–195. [CrossRef]
41. Re, C.; Robson, S.; Roncella, R.; Hess, M. Metric Accuracy Evaluation of Dense Matching Algorithms in Archeological Applications. *Geoinform. FCE CTU* **2011**, *6*, 275–282. [CrossRef]

42. Toschi, I.; Capra, A.; de Luca, L.; Beraldin, J.-A.; Cournoyer, L. On the evaluation of photogrammetric methods for dense 3D surface reconstruction in a metrological context. *ISPRS Ann. Photogramm. Remote Sens. Spat. Inf. Sci. II* **2014**, *5*, 371–378. [CrossRef]
43. Shi, J.; Wang, X. A local feature with multiple line descriptors and its speeded-up matching algorithm. *Comput. Vis. Image Underst.* **2017**, *162*, 57–70. [CrossRef]
44. Gesto-Diaz, M.; Tombari, F.; Gonzalez-Aguilera, D.; Lopez-Fernandez, L.; Rodriguez-Gonzalvez, P. Feature matching evaluation for multimodal correspondence. *ISPRS J. Photogramm. Remote Sens.* **2017**, *129*, 179–188. [CrossRef]
45. Wenzel, K.; Rothermel, M.; Fritsch, D.; Haala, N. Image Acquisition and Model Selection for Multi-View Stereo. In Proceedings of the 3D-ARCH 2013–3D Virtual Reconstruction and Visualization of Complex Architectures, Trento, Italy, 25–26 February 2013.
46. Robian, A.; Rani, M.R.M.; Ma'Arof, I. Manual and automatic technique needs in producing 3D modelling within PhotoModeler scanner: A preliminary study. In Proceedings of the 2016 7th IEEE Control and System Graduate Research Colloquium (ICSGRC), Shah Alam, Malaysia, 8 August 2016; pp. 181–186. [CrossRef]
47. Jaud, M.; Passot, S.; le Bivic, R.; Delacourt, C.; Grandjean, P.; le Dantec, N. Assessing the accuracy of high resolution digital surface models computed by PhotoScan®and MicMac®in sub-optimal survey conditions. *Remote Sens.* **2016**, *8*, 465. [CrossRef]
48. Jebur, A.; Abed, F.; Mohammed, M. Assessing the performance of commercial Agisoft PhotoScan software to deliver reliable data for accurate 3D modelling. In Proceedings of the 3rd International Conference on Buildings, Construction and Environmental Engineering, Sharm el-Sheikh, Egypt, 23–25 October 2017. [CrossRef]
49. Remondino, F.; Nocerino, E.; Toschi, I.; Menna, F. A critical review of automated photogrammetric processing of large datasets. In Proceedings of the 26th International CIPA Symposium–Digital Workflows for Heritage Conservation, Ottawa, ON, Canada, 28 August–1 September 2017; pp. 591–599. [CrossRef]
50. Fraser, C. *Advances in Close-Range Photogrammetry*; Photogrammetric Week: Belin/Offenbach, German, 2015; pp. 257–268.
51. Remondino, F.; Spera, M.G.; Nocerino, E.; Menna, F.; Nex, F.; Gonizzi-Barsanti, S. Dense image matching: Comparisons and analyses. In Proceedings of the 2013 Digital Heritage International Congress (DigitalHeritage), Marseille, France, 28 October–1 November 2013; pp. 47–54. [CrossRef]
52. Mousavi, V.; Khosravi, M.; Ahmadi, M.; Noori, N.; Haghshenas, S.; Hosseininaveh, A.; Varshosaz, M. The performance evaluation of multi-image 3D reconstruction software with different sensors. *Meas. J. Int. Meas. Confed.* **2018**, *120*, 1–10. [CrossRef]
53. Lo, S.H. Parallel Delaunay triangulation in three dimensions. *Comput. Methods Appl. Mech. Eng.* **2012**, *237–240*, 88–106. [CrossRef]
54. Lee, D.T.; Schachter, B.J. Two algorithms for constructing a Delaunay triangulation. *Int. J. Comput. Inf. Sci.* **1980**, *9*, 219–242. [CrossRef]
55. Aichholzer, O.; Fabila-Monroy, R.; Hackl, T.; van Kreveld, M.; Pilz, A.; Ramos, P.; Vogtenhuber, B. Blocking Delaunay triangulations. *Comput. Geom. Theory Appl.* **2013**, *46*, 154–159. [CrossRef] [PubMed]
56. Devillers, O.; Teillaud, M. Perturbations for Delaunay and weighted Delaunay 3D triangulations. *Comput. Geom. Theory Appl.* **2011**, *44*, 160–168. [CrossRef]

Further interesting information regarding to photogrammetric fundamentals and industrial solution providers is presented as follows, as well as reference associations and peer-reviewed journals:

- GOM optical systems→ https://www.gom.com/3d-software/gom-system-software/tritop-professional.html
- Photogrammetric basis (VSTARS)→ https://www.geodetic.com/basics-of-photogrammetry/
- PHOTOMETRIX 3D scanning solutions→ https://iwitnessphoto.com/
- HEXAGON solution→ https://www.hexagonmi.com/products/photogrammetry/dpa-industrial
- Industrial photogrammetric software comparison → https://en.wikipedia.org/wiki/Comparison_of_photogrammetry_software
- Interesting hardware and software information→ http://www.photogrammetry.com/index.htm
- Camera calibration toolbox→ http://metrovisionlab.unizar.es/
- International photogrammetric associations→
    - https://www.isprs.org/
    - https://www.asprs.org/
    - https://www.rspsoc.org.uk/
- Photogrammetry related journals→
    - https://www.journals.elsevier.com/isprs-journal-of-photogrammetry-and-remote-sensing
    - https://onlinelibrary.wiley.com/journal/14779730
    - https://www.asprs.org/asprs-publications/pers
    - https://www.jstage.jst.go.jp/browse/jsprs
    - https://www.schweizerbart.de/journals/pfg